

Some aspects of
SWITCHING AMPLIFIERS
and their
PERFORMANCE

by

A. A. Grainger, B. E. (Hons.)

This thesis is submitted in fulfilment of
the requirements for the degree of

Doctor of Philosophy

in the Faculty of Electrical Engineering

UNIVERSITY OF TASMANIA

HOBART

February 1977

I agree that, if this thesis is
accepted for a degree of the
University of Tasmania, it may
then be available for loan and
copying.

(signed) *A. A. Grainger*

date . *29 April 1977*

Acknowledgements and Claim of Originality.

I acknowledge the help and support of the many people who made this thesis possible, encouraged and guided its development and participated in its final presentation.

In particular I thank my parents for their considerable assistance, the Commonwealth of Australia for the scholarship financially supporting this research, the staff and students of the University for their interest, my supervisor, Mr. P.A. Watt, and the head of the Department of Electrical Engineering, Professor C.H. Miller for their patience, guidance and helpful suggestions, Helen and Graham Brennen who typed and proof-read the original draft, and Irene Zorko who typed the many modifications and corrections for this draft.

* * * * *

Except as stated herein this thesis contains no material which has been accepted for the award of any other degree or diploma in any university, and to the best of my belief and knowledge this thesis contains no copy or paraphrase of material previously published or written by another except where due reference is made in the thesis text.

A. N. Tranger

Thesis Outline

Chapter I examines current usage and existing theory of switching amplifiers. Areas where existing or potential usage extend beyond published theory are defined, the most important area being the lack of adequate switching wave descriptions. The work aimed at redressing the imbalance between theory and practice is described and its relationship to the thesis outlined.

In Chapter II the steps necessary to form a switching wave description are outlined. The amplifier features incorporated include details of the encoder, the switch array, and the control signals which flow between encoder and switch array. The input-output characteristic and other design features are combined with the requirements of the encoder and switch array to define restrictions on the switch control signals and the switching wave.

In Chapter III detailed switching waveform descriptions are derived for waves controlled by natural samplers, modified natural samplers, and regular samplers. The low frequency components of the descriptions are used to define the sampling wave shapes needed to achieve specific input-output characteristics for amplifiers with both d.c. and a.c. supply waveforms. A modified natural sampler is described which permits compensation for arbitrary supply waveform perturbations. The high frequency components of the waveforms are an important by-product of the method of derivation.

In Chapter IV the fidelity of information transfer through switching amplifiers is examined. The waveform descriptions are used to evaluate the spectrum of passband noise for natural and regular sampling control with both d.c. and a.c. supplies. The inter-relationship between signal quality, bandwidth, and sampling rate is derived for each amplifier, and comparisons are made between amplifiers.

Chapter V provides a basis for the analysis of the low frequency performance of switching amplifiers embedded in feedback networks. The application of the analysis to amplifiers using any form of natural sampling is demonstrated and the extension to regular sampling outlined. The method described also provides criteria not previously described elsewhere.

Chapter VI deals with the class of self-oscillating encoders based on a linear filter feedback path and a comparator with hysteresis. The performance limits of the simplest system are described. A method for predicting the d.c. input-output characteristic of all such encoders is presented and its application to two particular encoders discussed.

Chapter VII describes a switching amplifier from the point of view of energy flow from source to load. The restrictions on amplifier structure and performance imposed by this view, and by real components, are outlined and some of the limits imposed by present hardware briefly discussed. An equivalent circuit for the energy flow path incorporates many of the features discussed.

Chapter VIII is a review of the material presented in previous chapters. Emphasis is on presenting the design tools which result from the attitudes and methods incorporated within the thesis. The chapter concludes with a brief look at those areas where theory or practice remains inadequate, thus providing direction for further research.

CONTENTS

1	AN INTRODUCTION	1-00
1.1	The Research Area	1-02
1.2	Switching Waveform Practice & Terminology	1-05
1.3	Switching Waveform Literature	1-11
1.4	Research Activity	1-22
1.5	Thesis Content	1-34
2	DESCRIBING THE SWITCHING WAVE	2-00
2.1	Switch Arrays	2-01
2.1.1	Operating Restrictions placed on an Array	2-01
2.1.2	Equivalence of Simple and Complex Arrays	2-01
2.2	Switch Control Unit	2-02
2.3	State Function for Switches	2-03
2.4	The Voltage formed at a Node of Switches	2-04
2.5	Linear Amplification	2-06
2.6	Minimisation of Error Energy	2-08
2.7	Summary	2-07
3	SYNTHESIS OF WAVEFORM DESCRIPTIONS	3-00
3.1	Waveform Synthesis by Natural Sampling	3-02
3.1.1	A Mathematical Description	3-02
3.1.2	Node Voltage Components	3-05
3.1.3	Assembly of Node Components	3-12
3.1.4	A Switching Wave with Two Arbitrary Levels	3-15
3.1.5	Multi-D.C.-Level Switching Waves	3-18
3.2	Waveform Synthesis by Regular Sampling	3-23
3.2.1	The Coder Law	3-23
3.2.2	The Relationship to Natural Sampling	3-23
3.2.3	The Modulator Nonlinearity	3-25
3.2.4	The Generation and Assembly of Switching Waves	3-28
3.3	Review	3-31
4	HIGH FREQUENCY COMPONENTS OF PERIODIC WAVES	4-00
4.1	Waves with D.C. Control Signals	4-05
4.1.1	D.C. Levelled Waves	4-07
4.1.2	A.C. Levelled Waves	4-13
4.1.3	An Asymptotic Waveform	4-24
4.1.4	Harmonic Cancellation	4-26
4.2	The Harmonic Sidebands of Switching Waves	4-29
4.2.1	The Spectrum of Phase Modulation	4-32
4.2.2	Sidebands of Switching Waves	4-42
4.2.3	More Complex Switching Waves	4-47
4.2.4	The Ideal Filter Assumption	4-60
4.3	The Subharmonic Gain	4-65
4.3.1	The Subharmonic Case	4-67
4.3.2	Natural Sampling	4-71

5	FEEDBACK WITH NATURAL SAMPLING	5-00
5.1	Low Frequency Characteristics	5-02
5.1.1	The Model	5-03
5.1.2	The Amplifier Characteristic	5-06
5.1.3	Limits of the Computational Model	5-11
5.1.4	Double Sampling, Multiple Sampling	5-13
5.2	A.C. Control Signal Performance	5-14
5.2.1	Aspects of A.C. Models	5-15
5.3	Summary	5-18
6	SELF OSCILLATING ENCODERS	6-00
6.0	Operation of the Constant Area Encoder	6-01
6.1	Experimental Performance	6-02
6.2	Matching Theory and Observation	6-04
6.3	Other Self-Oscillating Switch Controllers	6-05
7	ENERGY FLOW PATH IDEALS, STRUCTURES AND LIMITS	7-00
7.1	Non-Disipative Energy Transfer	7-01
7.1.1	Filter Elements	7-01
7.1.2	Current and Voltage Analogues	7-02
7.1.3	Reversible Power Flow	7-03
7.1.4	Supply Filtering	7-04
7.1.5	The Equivalent Circuit	7-05
7.1.6	Circulation of Supply Energy	7-06
7.2	Switch Array and Circuit Forms	7-10
7.2.1	A Classification for Switches	7-10
7.2.2	Combinations of Switches	7-11
7.2.3	Minimum Switch Requirements of Common Circuits	7-13
7.2.4	Pairing Complementary Unidirectional Amplifiers	7-17
7.2.5	Combinations of Switching Amplifiers	7-18
7.3	Filter and Switch Performance	7-20
7.3.1	Filters	7-20
7.3.2	Switches	7-26
7.3.3	Modifications for the Equivalent Circuit	7-32
7.4	Summary	7-33
8	A PERSPECTIVE	8-00
8.1	The d.c. input-output of Natural Sampling	8-01
8.2	The a.c. input-output of Natural Sampling	8-02
8.3	The spectrum of waves - Natural Sampling	8-03
8.4	Optimisation of sampling wave shape	8-04
8.5	The asynchronous Natural Sampler	8-05
8.6	Waves with many levels - Phased addition	8-07
8.7	Waves with many levels - Quantizer method	8-08
8.8	Regular Sampling	8-09
8.9	Natural Sampling with feedback	8-11
8.10	Self Oscillating Encoders	8-13
8.11	Equivalent Circuits	8-15
8.12	Areas for further research	8-16

CHAPTER I : AN INTRODUCTION

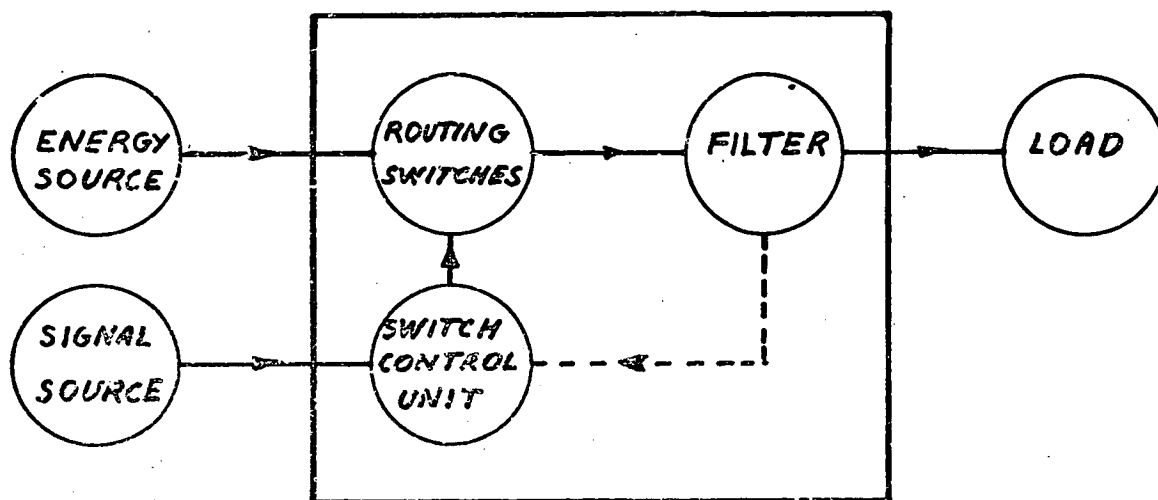
- 1.1 The Research Area
 - 1.1.1 Attractions of Switching Amplifiers
 - 1.1.2 Principle of Operation
 - 1.1.3 Limitations
 - 1.1.4 Research Area Selections
- 1.2 Switching Waveform Practice and Terminology
 - 1.2.1 Background of Waveform Synthesis
 - 1.2.2 Control of the Switching Wave
 - 1.2.3 Common Switch and Filter Arrangements
- 1.3 Switching Waveform Literature
 - 1.3.1 Linear Natural Sampling
 - 1.3.2 Linear Regular Sampling
 - 1.3.3 Non-linear Control of Waves with Two D.C. Levels
 - 1.3.4 Control of Waves with Many D.C. Levels
 - 1.3.5 Control of Waves with A.C. Levels
 - 1.3.6 Note about Non-linear Control
 - 1.3.7 Natural Sampling in the presence of Feedback
 - 1.3.8 Self Oscillating Encoders
- 1.4 Research Activity
 - 1.4.1 Natural Sampling
 - 1.4.2 Modified Natural Sampling
 - 1.4.3 A Special Form of Natural Sampling
 - 1.4.4 Regular Sampling
 - 1.4.5 Feedback Amplifiers
 - 1.4.6 Self Oscillating Encoders
- 1.5 Thesis Content

CHAPTER 1.

AN INTRODUCTION

Chapter 1 reviews current literature on switching amplifiers and allied topics. The incomplete and often inadequate past treatment in this area has prompted further research in an attempt to bridge the gap between theory and practice, and to extend the range of useful design criteria.

In section 1.1 a survey of switching amplifier attractions, potential usage, and limitations indicates the need for additional research in the area of information transfer from input signal to switching wave. Common switching waves and the terminology used throughout the thesis are presented in section 1.2. This background information is used in the literature survey of section 1.3 to pinpoint those areas where descriptions of existing waveforms are inadequate or non-existent. The research activities initiated by the omissions of existing waveform descriptions are indicated in section 1.4. Section 1.5 contains a brief outline of the relationship between the research and the contents of the thesis.



BLOCK OUTLINE OF SWITCHING AMPLIFIER

DIAGRAM 1-12

1.1. The Research Area

1.1.1. Attractions of Switching Amplifiers.

As a device for power control the switching amplifier has one major advantage over conventional amplifiers, namely its potential efficiency. A conventional amplifier uses its active devices (valves, transistors, etc.) as complements to the load in the power circuit. The resulting dissipation of power in these active devices is of the same order of magnitude as that in the load. Control of the energy flow by this method is inherently inefficient. A switching amplifier uses its active devices as switches. These, and a filter, are in series with the load in the power circuit. Since ideal switches and filters are lossless, the potential efficiency of this form of amplifier is very high. In practice, efficiencies as high as 99% have been attained.

This high efficiency has an important corollary, namely that a given active device can control a much larger energy flow when used in a switching amplifier than the same device when used in a conventional amplifier. This is possible only because the switch losses are very much less than the total energy flow.

1.1.2. Principle of Operation.

It is convenient to regard any amplifier as involving two flow paths: an energy flow path and an information flow path. Signals in the information flow path control the energy transmitted by the energy flow path. In a switching amplifier the flow paths meet at the switch array which forms the heart of the amplifier. The confluence of the flow paths is apparent in diagram 1.1.2 which also indicates the interconnections between the major subsections of an idealised switching amplifier. Note that the energy flows from the source

(supply) to the energy sink (load) via the switch array and output filter. Information abstracted from the control signal by the encoder flows to the switch array where it is impressed upon the energy flow. As already indicated the controlled energy flow generated by the switch array then passes through the filter to the load.

From the control signal the encoder generates switch control signals which determine the duration of closure of the elements of the switch array. This enables the interaction of the switch array with the supply to create a switching wave, the spectrum of which will be determined in the first instance by the switch control signal and ultimately by the control signal processed by the encoder. The control signal defines the amplifier output, since this output is determined by the spectrum of the switching wave and the frequency response of the filter.

The above description of a switching amplifier has been deliberately phrased in general terms because in theory the principle of synthesising and filtering a switching wave can be applied to the control of any energy flow. In practice, the application may be limited by the availability of appropriate switches and filters.

While this discussion is confined to electronic amplifiers, it is possible to envisage analogous mechanical systems which embody this method of achieving an amplifier (see for example, appendix A 1.1.2.).

1.1.3. Limitations

The encoder, the switch array, and the output filter each impose limitations on the performance of the

complete amplifier. The encoder circuitry imposes mutually dependent limits on the ratio of bandwidth to switching wave frequency and on the quality of reproduction of the amplifier. The switch array limits the efficiency, maximum frequency, and power control capacity of the switching wave. The output filter imposes mutually dependent limits on the mass*, efficiency and power transfer capacity.

If these limits are traced to their sources they are found to arise from the properties of individual components and from the organisation of these components relative to one another. In a switch array or output filter the optimum organisations of components are well defined so that improvements to these subsections must await developments in the fields of semi-conductor or electro-magnetic materials. In the encoder, limitations imposed by component technology are minimal. Existing hardware is sufficiently fast and powerful to implement all the known encoding techniques without significantly limiting amplifier performance. The limits imposed by encoders are those of the encoding method employed, not those of the components. Thus the performance limits of existing amplifiers can be traced to component technology in the switch array and filter, and to the encoding methods used to control the switching wave.

1.1.4. Research Area Selection.

The surplus capacity of encoder components gives this subsection the potential to be more complex. This tempts one to look for new encoder techniques, ones which increase the bandwidth or output signal quality attainable with present day switch and filter

* physical mass of the filter assembly.

components. However not enough is known about many waveforms to clearly establish the limits of their encoding techniques. This makes it difficult to compare existing encoder limitations and thus to assess the value of new encoding techniques. Accordingly, the primary aim of the research was to generate descriptions of all existing switching waves, descriptions which enable encoder techniques to be compared and thus characterised. A secondary aim was to use any increases in understanding of encoding techniques to form and evaluate new encoding methods.

The remainder of chapter I is concerned with establishing the extent of existing waveform descriptions and the consequent direction of the work presented in this thesis.

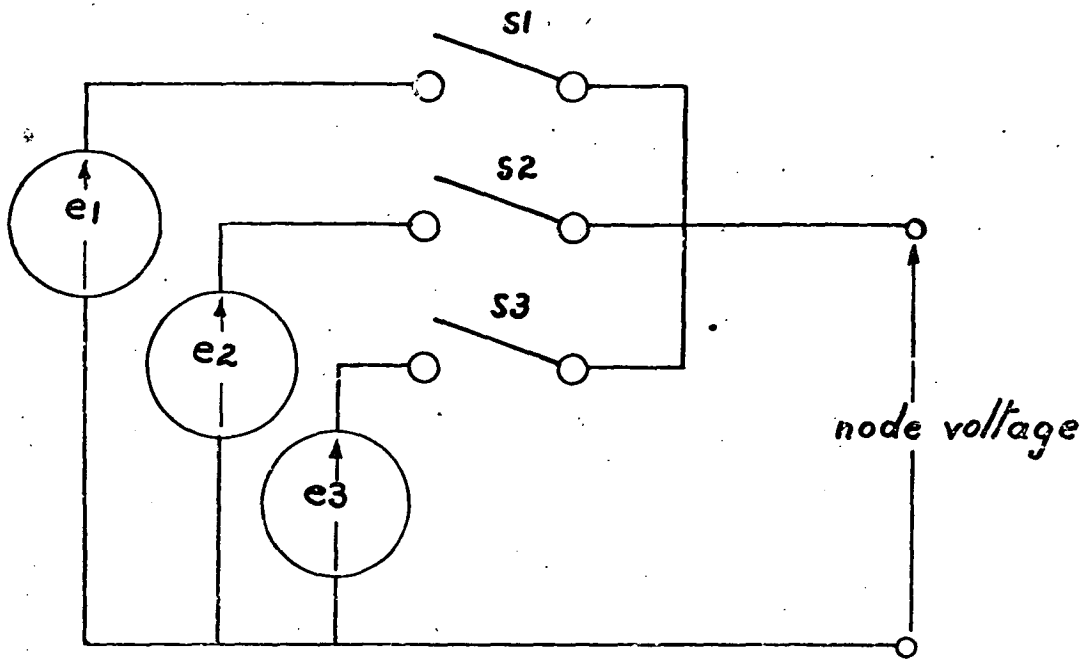
1.2. Switching Waveform Terminology and Practice.

1.2.1. Background of Waveform Synthesis.

The way a switching wave is synthesised determines many of the important characteristics of the performance of the switching amplifier. This passage is intended to provide a background where each of the important classifications of switching waves are discussed briefly. The aim is to give the reader an intuitive grasp of the essential feature of all switching waves, that is their ability to provide a component, suitable as an amplifier output signal, and separable from other components by the filter.

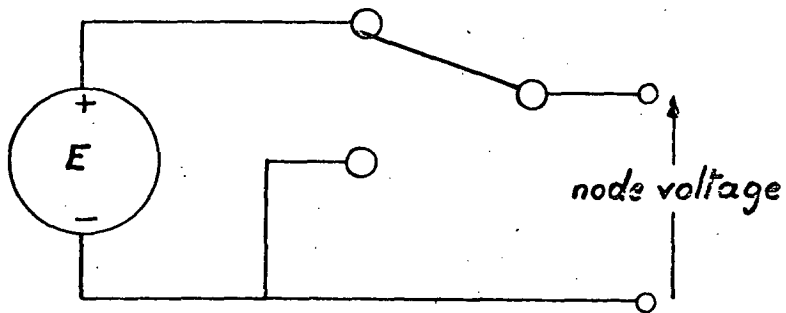
Terminology

The switching wave, applied to the filter, may be either a voltage or current wave. This depends upon the type of energy source used. Since voltage sources are more common than current sources the more common switching waves are voltage waves. For this



FORMING A NODE VOLTAGE

D 1.2.1



A SIMPLE SWITCH ARRAY

D1.2.1.1a

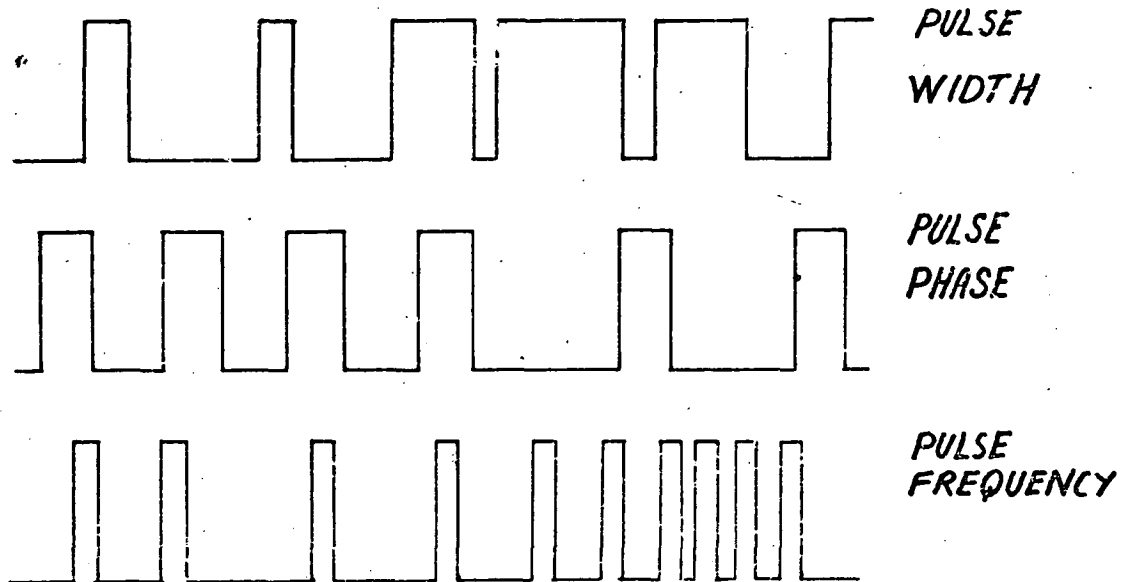
reason there are many parts of the text where the word voltage may be replaced by the word current with no loss of meaning. Due to the analogy between electrical and mechanical systems these words may even be replaced by force and velocity since what is really discussed is the generation and processing of signals.

Mechanics

There is no unique way to synthesise a given type of voltage wave using voltage sources and switches, however, to illustrate the following discussion it is helpful to have one means as an aid to understanding. Diagram D 1.2.1 shows an arrangement of switches and supplies suitable for this purpose. The operation of the circuit is as follows. At any instant only one switch is closed so that the voltage wave at the node traces the associated supply voltage. By connecting the node to each supply in turn a switching wave with three levels is formed. This type of structure may be extended to any number of supplies greater than one. The supply voltage waveforms define the switching wave during the intervals between steps. These waveform "levels" are important features of the switching wave and are used to classify switching waves.

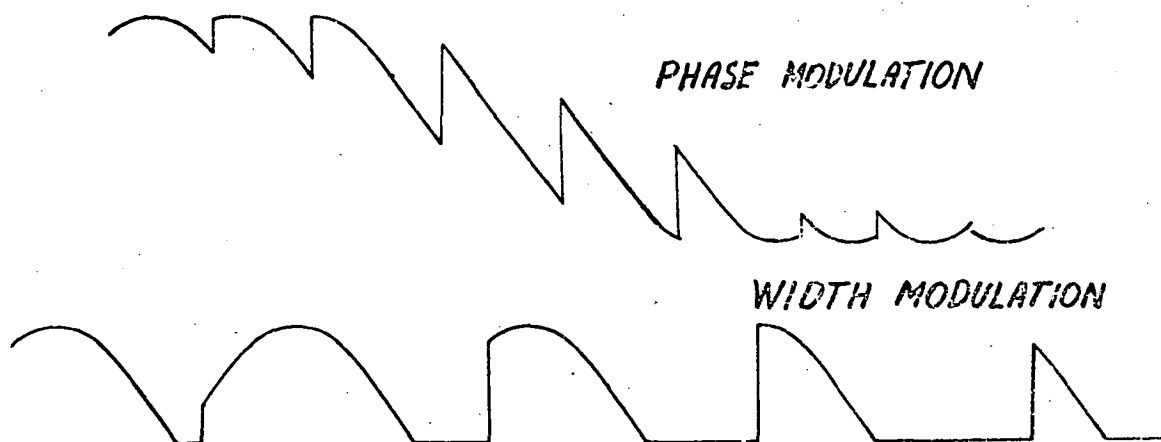
1.2.1.1. D.C. Levelled Waves.

The d.c. levelled switching wave produced by the supply and switch array of diagram D 1.2.1.1a has levels of zero and E. A wave produced by this array has an average or d.c. component with value dependent on the proportions of a waveform cycle. The component is a fraction of E corresponding to the fraction of time for which the switching wave has the level E. This component has all the desirable characteristics of an output component since it can be filtered from



D.C. MODULATION FORMS

D 1.2.1.1b



A.C. MODULATION FORMS

D 1.2.1.2a

the remainder of the wave by a low pass filter, and can be controlled by the waveform proportions.

There are many possible ways of arranging the control of waveform proportions but relatively few are commonly used and have distinctive names. The dominant characteristics of these are listed below and illustrated by diagram D 1.2.1.1b.

Pulse width modulation has a waveform with constant frequency. The average output is proportional to the pulse width.

Pulse frequency modulation has a waveform frequency proportional to output component. The width of pulses is constant.

Pulse phase modulation is similar to pulse frequency modulation but since the average frequency is constant it is incapable of generating a d.c. output component.

The best known asynchronous system, other than pulse frequency modulation, has several names including Constant Area Sampler and PDM/PFM due to its independent use by a number of researchers.

1.2.1.2. A.C. Levelled Waves

The most common a.c. levelled waves have two or more symmetrically phased supplies of constant frequency. These are synchronously modulated by either pulse phase or pulse width modulation to produce switching waves with d.c. components controlled by the phase of the switching instants relative to the phase of the supplies. Diagram D 1.2.1.2a illustrates the two types of modulation for the two supply case.

Other possible forms of modulation of a.c.



Modified Delta Modulation



Modified Pulse width Modulation

SUB-SUPPLY FREQUENCY MODULATIONS

D 1.2.1.2b

supplies include those shown in diagram D 1.2.1.2b. These forms are not considered in the thesis.

1.2.2. Control of the Switching Wave.

The switching wave is cyclic. The positions of the steps relative to one another during each cycle control the output component. To control the switching wave the input signal, or a signal derived from the input signal, is sampled at least once per switching wave cycle. The signal level at the sampling instant controls the position of one or more steps of the cycle. In this way the amplifier input signal controls the relative phase of each of the steps during each cycle of the switching wave.

Three basic classes of sampling are employed. The two better known, natural and regular sampling, generate fixed frequency waves, the third, an unnamed class, generates variable frequency switching waves.

For regular sampling the phase of the sampling instant is fixed. The value of the sample controls the phase difference, or time delay, between the sampling point and the step or steps of the switching waves.

A switching wave step, controlled by natural sampling, occurs at the instant the input signal satisfies a periodically varying condition. That is the step and sample occur at the same instant.

The third unnamed class of sampling is used by f.m. coders, constant area samplers and other similar asynchronous coders. In essence steps in the switching wave occur when a signal derived from both coder input and coder output satisfies some condition. For example, the constant area sampler has positive steps when the integral of the difference between input and output

signal reaches a minimum critical value, and negative steps when the integral reaches a maximum critical value.

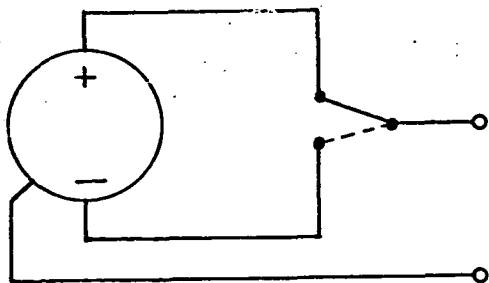
This short introduction to waveform synthesis has outlined the common switching waves and some of the control techniques used with them. The waveforms discussed should be considered as examples of a much wider class of switching waves since they do not include waveforms associated with many d.c. supplies or a.c. supplies with asymmetrical phases or d.c. components, or other variants of the simplest supply waveforms. Associated with variants of supply waveforms are modifications to the basic control techniques. The discussion has ignored these and a whole class of switching waves where the amplifier input is used to control not the d.c. component of the switching wave but one of the various harmonics of the switching wave cycle frequency.

1.2.3. Common Switch and Filter Arrangements.

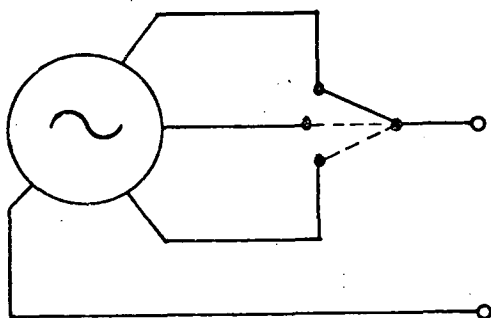
Common switching amplifiers use only a few switch array structures and a limited number of combinations of switch arrays and filters. These are outlined briefly below.

1.2.3.1. Basic D.C. Supplied Array.

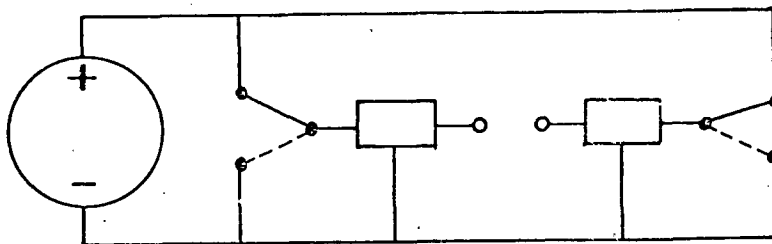
Two switches are used with two supplies, one of which may be zero, to produce a switching wave with characteristics matching those of the waveforms of diagram D 1.2.1.1b. The voltage range of the low frequency component of the wave may be varied from one supply voltage to the other. The first and other harmonics may be varied in amplitude, phase, and frequency. A convenient representation of the circuit is shown in diagram D 1.2.3.1. The switches are



D1.2.3.1



D1.2.3.2



D1.2.3.3

COMMON CIRCUIT ARRANGEMENTS

usually combinations of transistors and diodes, or thyristors with associated forced commutation networks. Valves have been used.

1.2.3.2. Basic A.C. Supplied Array.

Symmetrical phases of a single frequency sine-wave voltage source are usually used in conjunction with a switch structure corresponding to diagram D 1.2.1. Two, three, six and twelve phase systems are used in conjunction with thyristor switches to produce waveforms similar to those of diagram D 1.2.1.2a. Natural and forced commutation are both employed. Diagram D 1.2.3.2 shows a convenient representation of the circuit.

1.2.3.3. Combined Structures.

Series Connection

D.C. supplied arrays are often paired in the manner shown in diagram D 1.2.3.3. This bridge circuit is a form of series connection which doubles the output range but requires no extra supplies. By suitable phasing of the switching waves produced at the nodes this arrangement can produce waves with three levels across the output terminals of the array. The frequency of this wave is twice the cycle frequency of any switch in the system.

The same procedure may be used with a.c. supplied amplifiers though this is less common. The major disadvantage is that the output of the amplifier is floating with respect to the supply sources.

Series connections of more than two units are rare since the supply sources can no longer be common and care must be taken to ensure that reverse voltages on switches cannot occur.

Parallel Connection

The terminals of independent arrays cannot be directly connected in parallel since each array would be short circuited by the others. After individual filtering switching amplifier outputs may be paralleled provided the outputs are similar in the filter passband regions of their spectrum. Provision must usually be made to prevent excessive circulatory currents between the amplifiers. Paralleling of amplifier outputs is used to increase output current, to reduce filter size by harmonic cancellation, and to provide bidirectional output current from pairs of complementary amplifiers each capable of unidirectional current output.

Provided measures are taken to limit circulatory currents any number of amplifiers may be paralleled.

1.3. Switching Waveform Literature.

Descriptions of the waveforms within a switching amplifier are important for optimising the amplifier design. For this reason these waveforms have a central role in switching amplifier theory. The following review of the literature concerning these waveforms is intended to demonstrate how this role has developed in the past. It also defines the limitations of present waveform descriptions and indicates areas where future development is needed. The latter aspect leads naturally to an outline of the material embodied by this thesis.

1.3.1. Linear Natural Samplers

Three authors ^{1, 2, 3} have produced descriptions of a wave with two d.c. levels for which the steps between these levels are controlled by "linear" natural sampling. The word linear is used here to indicate that

sampling waves employed by this encoder are periodic waves composed of two ramps, that is the sampling waves are piecewise linear. These authors appear to have developed their descriptions independently and consequently there is considerable variation in their approach to describing switching waveforms.

Bennet¹ formulated his description first as a double fourier series each coefficient being a double fourier integral with one integral having special integration limits, limits embodying the modulating signal as a sinewave function of time. This formulation is very abrupt and does not show how the modulation process and the waveform description are related to one another.

Fitch² and Kretzmer³ based their initial development of descriptions on the conditions prevailing at the sampling instant, that is the instant at which a switching wave step is formed. Fitch used this information to formulate a similar double fourier series to that of Bennet. In contrast Kretzmer matched the conditions for a step in the switching wave with the conditions for a step in a periodic ramp, periodic with respect to an index which was a function of time rather than time itself. The matching process enabled this function to be determined in terms of the modulating signal so that by adding two opposite polarity ramps, one with positive steps the other with negative steps, a complete description of the switching wave was synthesised. This description incorporated the modulation as an arbitrary non-periodic function of time. Although this description can be generated by the approaches used by Bennet and Fitch this potential is camouflaged by their early adoption of periodic sinusoidal modulations.

Thus while Bennet was able to demonstrate a freedom from harmonic distortion and Fitch a freedom from intermodulation products Kretzmer was able to demonstrate the modulator linearity for any input signal.

The waveforms actually used in class D amplifiers employing "linear" natural sampling are good approximations to those described by the similar expressions developed by Bennet, Fitch and Kretzmer. Consequently they have been widely used as a basis for switching amplifier design and for comparison with other amplifiers.

The class D amplifiers designed by Miller⁴ and later by Bell and Sergeant⁵ used these descriptions as the basis for the choice of sampling wave and for the design of the output filter.

The descriptions allowed these designers to make necessary compromises between parameters such as amplifier bandwidth, amplifier output stage losses, amplifier sideband noise, and sampling rate. The design processes used by these authors can be applied to any switching amplifier design but accurate algebraic descriptions of the switching wave or equivalent bodies of experimental measurements are essential.

1.3.2. Linear Regular Sampling.

Before continuing this review of natural sampling with the topic of "nonlinear" sampling waves, mention must be made of "linear" regular sampling. Black⁶, in his book "Modulation Theory", published a description, attributed to Bennet, of a two levelled wave employing regular rather than natural sampling. As for his description of the wave produced by the

natural sampler the modulation described is sinusoidal. This description appears to be the only one in the literature. It can be employed in the same manner as those of natural sampling to yield the important design interrelationships employed by Miller⁴ and Bell and Sergeant⁵.

1.3.3. Non-Linear Control of Switching

Waves with two D.C. Levels.

Brit⁷ pointed out that class D amplifiers need not be confined to triangular or ramp sampling waveforms but can employ other periodic waveforms to give non-linear input-output characteristics. The same point is made by Turnbull and Townsend⁸ in a more general discussion. Neither of these papers attempt to describe the associated switching waves in a manner corresponding to the earlier descriptions of Bennet, Fitch, or Kretzmer.

1.3.4. Control of Waves with many D.C. Levels.

Switching waves with more than two d.c. levels may be produced by several means. Pitman, Ravas, and Briggs⁹ used the paralleled outputs of several amplifiers with staggered phasing of the associated switching waves to produce an amplifier with a virtual multilevelled wave. The multilevelled switching wave has also arisen in the field of positional sensor arrays possessing quantizer like input-output characteristics. McVey¹⁰ and Chen¹¹ have investigated the linearisation of such detectors by perturbing the input signal to the array with both sinusoidal and triangular vibrations. The electrical analogue is natural sampling with a quantizer as the switch control characteristic. The induction motor drives described by Pollack¹² employ multilevel waves controlled by natural sampling.

Of the multilevelled waves controlled by natural sampling, all but those of McVey and Chen use linear sampling waves and can also be synthesised by adding together a number of two levelled waves with separate but phase related natural samplers. Consequently, their switching wave descriptions can also be formed by adding the descriptions of their component waveforms. Although Pitman, Ravas, and Briggs obviously appreciated this they do not appear to have used such a synthesised description to estimate the undesirable passband components of the switching wave. The quantizer generated waves are not described in the switching amplifier literature.

1.3.5. Control of Waves with A.C. Levels.

The principles of cyclo-converters and controlled rectifiers were established very early but widespread recognition of these as amplifiers was inhibited until the advent of semiconductor switches. Milnes¹³ foreshadowed the current development as early as 1965. McVey and Russel¹⁴ investigated power supplies based upon a thyristor-switched sinusoidal supply and a nonlinear, natural sampling, controller. Barton and Birch¹⁵ described an impressive linear amplifier using natural sampling to control a thyristor array. Malensini¹⁶ developed a simple but effective generator of sampling waves suitable for the linear control of all the thyristor generated sine-levelled switching waves. Evans¹⁷ carried this process further to a fully protected linear amplifier similar in scale to that of Barton and Birch.

1.3.6. Note about Nonlinear Control.

The rapid practical development of the useage of nonlinear sampling waves has proceeded solely on the basis of the d.c. input-output characteristic. By correlating the d.c. component of the switching wave with the phase angle of the steps in the wave the shape of sampling wave required to give a linear characteristic is easily established. However this approach cannot predict the a.c. input-output characteristic or the magnitude of switching frequency sidebands. In this area practical amplifiers outstrip the theory of switching waves.

1.3.7. Natural Sampling in the Presence of Feedback.

Switching amplifiers are well suited to power amplification and this may be expected in such roles as motor drives and regulated power supplies. Many of these roles require the amplifier to form part of a feedback loop (pathway). These situations introduce a fundamental difference between conventional and switching amplifiers for it is impossible to apply directly the normal rules of feedback to switching amplifiers.

For both natural and regular sampling the difficulty arises because the feedback signal to the switching amplifier input contains components at the same frequency as the sampling wave. These components, which come from the switching amplifier output, effectively change the shape of the sampling wave and thus change the input-output characteristic of the switching amplifier. The resultant changes in loop gain and linearity make feedback calculations of system stability and accuracy both interactive with loop gain, and signal dependent, and so vastly more complex than normal feedback computations.

The situation is complex for purely d.c. loop signals but this complexity is magnified when a.c. signals are considered for then each harmonic of the switching wave becomes split into many sidebands each of which is filtered differently so that the effective sampling wave becomes even more signal dependent and thus less amenable to accurate description. The situation can be further complicated by the phenomenon known as subharmonic instability.

If the signal frequency is an integral sub-multiple of the sampling frequency then two sidebands of each switching wave harmonic will match the input signal in frequency. The relative phasing of these components, which is set by the phasing of the input signal with the sampling wave(s), controls the effective input signal and thus the nominal amplifier gain at these frequencies. This results in the amplifier possessing a range of phase and gain values at each subharmonic frequency thereby complicating the concepts underlying the principles of feedback to a higher degree.

Despite the fundamental role played by feedback ripple in changing the low frequency input-output characteristic of a switching amplifier, this aspect of feedback is not discussed in the literature. The nearest approach is made by Fallside¹⁸ in a paper concerning the half subharmonic instability of a thyristor amplifier.

In the establishment of an instability bound the analysis includes the input signal components due to feedback of the switching wave. Despite this no mention is made of the change in the input-output characteristic even though the analysis appears to be

calculating the slope of this characteristic in order to establish the stability criterion. The omission of this topic from the literature is difficult to comprehend since any experimental measurement of the input-output characteristic of the amplifier, after it is included in a feedback loop, will reveal the change in characteristics produced by the feedback ripple. One would expect these measurements to have been made by many designers checking the accuracy of their calculations.

The several papers concerning subharmonic instability indicate a greater awareness of this aspect of the performance of feedback loops containing switching amplifiers. Fallside¹⁸ has investigated the subharmonic stability of natural samplers used with controlled rectifiers in power supplies. This paper is concerned with the onset of instability. A later paper by Fallside and Farmer¹⁹ concerns the use of describing functions as a means of predicting the onset and limit cycles of subharmonic oscillations. Furmage²⁶ has examined equivalent aspects of the class D amplifier using similar approaches to the problem. All these analyses are of necessity approximate and the accuracy of predictions is not high so that critical designs must be tested experimentally rather than relying upon theoretical analyses. In spite of these limitations, the results are useful since they can predict the direction of trends towards or away from stable operation and can thus yield useful qualitative information.

1.3.8. Self Oscillating Encoders

All the encoders discussed here are used to control waves with two d.c. levels. The output switch positions are determined by a level detector, usually a

schmitt trigger though under certain conditions a comparator with zero hysteresis may be used. The level detector is provided with a signal representing the error between the outputs of two linear filters, one fed by the input signal and the other fed by the amplifier output. This structure is arranged so that any change in the error beyond one bound of level detector will cause the output to change state and so eventually cause the error to move towards the opposite bound of the level detector. When the error reaches this bound the process is reversed and the resulting oscillation forms a switching wave. The error between the filtered switching wave and the filtered input signal is thus confined to within a definite error range and so the switching wave is forced to adjust to a match with the input signal.

The most convenient way to classify these encoders is on the basis of the type of filter used to provide the switching wave component of the error signal. This same filter is usually used for the input signal as well. The actual matching of input signal and switching wave is then made at the filter input. The following reviews of the various papers in this field are classified by the type of filter used.

Shaefer²⁰ investigated the encoder employing an integrator as the filter element. His interest arose from considerations of the use of pulsed jets in the attitude control systems of space vehicles and resulted in his comparison of the above system with other forms of switching wave. Among the desirable aspects of the encoder he included: finite output stage bandwidth, low complexity, and excellent input-output linearity for d.c. signals. His analysis included a computation of the

parabolic relationship between d.c. input signal level and oscillation frequency. He concluded that this encoder is preferable to both pulse width and pulse frequency modulation on the grounds of output signal quality after filtering, and output stage bandwidth requirements associated with the output signal range.

The encoder examined by Bose²¹ employed a filter consisting of a single pole lowpass filter cascaded with a fixed delay. This examination yielded information concerning the d.c. input-output characteristic and the relationship between input signal and oscillation frequency.

Turnbull and Townsend²² described the operation and also reported on the measured performance of several self-oscillating encoders with simple R.C. feedback filters. They concluded that this form of encoder had less sideband noise in the passband than equivalent pulse width encoders. Das and Sharma²³ investigated the performance of these encoders with first and second order R.C. filters, mainly with a view to its use as an alternative to delta modulation in communications systems. These authors have called the encoder a "Rectangular Wave Modulator".

The encoder employing an integrator as the feedback filter can also be realised using saturable core magnetic devices. This form of the encoder utilises the fact that the volt seconds required to move between saturation flux density in one sense to saturation flux density in the other sense is constant just as the volt seconds required to move the integrator output across the hysteresis range of the level detector is constant. The core is thus used as both integrator and

level detector. This approach has been employed by Jackson and Weed²⁴ and later by Yu and Wilson²⁵. The latter authors have attempted to analyse the a.c. modulation characteristics of the waveforms, in particular the variation of mean switching frequency with the amplitude of a sinewave a.c. input signal.

These authors and Shaefer²⁰ have all emphasised the constancy of the volt seconds per half cycle and this feature has thus given rise to the name "constant area sampler" for this encoder.

Although many of these authors have considered the problem of describing the waveforms produced by self oscillating encoders none of the encoder outputs have been described for a.c. input signals. Computations of oscillation frequency and output waveform proportions have been described for d.c. input signals but only for the constant area encoder and the encoder described by Bose²¹. Yu and Wilson²⁵ attempted to evaluate the mean oscillation of the constant area encoder for a sinewave input signal but were forced to make approximations which effectively reduced their analysis to the evaluation of the mean square value of a sinewave, and their analysis is valid only for very low frequencies.

For self oscillating encoders all filter designs and associated estimations of signal quality and bandwidth have had to rely on experimental measurement. There are no switching wave descriptions analogous to those for linear natural samplers.

RESEARCH TOPICS AND THEIR CHRONOLOGY

Topic	Number	Activity	Relative order and duration
Natural Sampling without feedback	1.11	Experimental confirmation of Fitch's theory	***
	1.12	Development of computer programs to evaluate switching wave spectra for linear sampling	***
	1.21	Development of a theory for nonlinear sampling waves	*****
	1.22	Experimental measurements of input output relationships produced by nonlinear sampling	****
	1.31	Development of methods for generating theoretical descriptions of multilevel waveforms	*****
	1.32	Development of computer programs to evaluate the spectra of sine levelled waveforms	****
	1.33	Experimental measurements of sine levelled waves	***
	1.41	Development of concept of modified natural sampling	***
	1.42	Formulation of theory for modified natural sampling	***
	1.43	Experimental measurements of waveforms of modified sampler	***
	1.51	Development of descriptions for waves in quantizer sampler	*****
Regular Sampling without feedback	2.1	Experimental confirmation of Bennett's theory	***
	2.21	Development of theory applicable to all forms of regular sampler	*****
	2.22	Development of computer program to evaluate waveform spectra	*****
	2.23	Experimental measurements of waves controlled by regular sampling	****
Feedback Amplifiers	3.1	Experimental trials with a simple natural sampling amplifier	**
	3.21	Development of programs to evaluate describing functions for linear samplers	****
	3.22	Experimental measurements of describing function boundaries	*
	3.31	Development of theory for d.c. input-output relationships	*****
	3.32	Development of computer programs to evaluate input-output relationships	*****
	3.33	Experimental measurements of input-output relationships	*****
Self Oscillating encoders	4.1	Experimental trials with the encoder with integral feedback	**
	4.21	Development of model to describe the d.c. characteristics	*****
	4.22	Experimental measurements of selected amplifier waveforms	***

FIGURE D 1.4

1.4. The Research Activity upon which the Thesis is Based.

Figure D 1.4 indicates the research areas, the nature of the research activities, and the time sequence of these activities. The earliest activity is to the left, the latest to the right. The following passage relates the sequence of motivations which prompted these activities. It also indicates the coupling between these activities and the material presented in later chapters. This passage is followed by an outline of the reasons for the existing structure of the thesis.

1.4.1. Natural Sampling.

Research began with a series of experimental measurements 1.1* intended to test the range of validity of the waveform descriptions proposed by Fitch². This starting point was chosen as a consequence of the use of these descriptions by Miller and by Bell and Sergeant⁵. Their design procedures, based upon such descriptions, appeared to provide a firm foundation upon which all the various switching amplifiers could be designed in principle.

The starting point for the extension of existing techniques was the evaluation of waveform descriptions for all these amplifiers. The first essential step in this direction is to examine the existing descriptions, their method of formation, their ranges of validity, and their useful prediction capacity.

The initial experimental measurements indicated that the range of validity of these descriptions was not appreciably limited by any physical aspect of the switching amplifier apart from effects associated with its output impedance and its

* These numbers refer to figure D 1.4.

finite speed of commutation from one level to another. Furthermore, these limitations are readily compensated by simple parasitic calculations. The real limit in the usefulness of the descriptions lay with the difficulty of using them to evaluate the sidebands associated with non-sinusoidal control signals. Bessel functions can be used to evaluate their amplitude and phase for sinusoidal control signals but other signals possess no equivalent source of tabulated data.

While it would be very useful to be able to predict the energy distribution in the sidebands for any control signal, this is not feasible. However it is possible to evaluate the magnitude and phase of sidebands associated with periodic control signals. This information was expected to increase a designers ability to predict output signal quality since existing data did not indicate whether design for sinusoidal control signals was conservative or not. Accordingly, research activity 1.12 was commenced.

The theoretical background, numerical computation techniques, numerical results and some conclusions regarding the relationships between signal to noise ratio and amplifier bandwidth associated with this research are presented throughout sections 4.2 to 4.2.4 of the thesis. As far as the existing waveform descriptions were concerned their ability to predict the switching wave spectrum associated with non-sinusoidal periodic control signals was confirmed by the close match between predictions based on computed results and the final measurements of research activity 1.11. The range of these measurements is outlined in appendix E under section numbers 1.1 and 1.2.

The objects of activities 1.11 and 1.12 having been achieved, they constitute the foundations upon which subsequent work proceeded. The next stage in developing the general design approach was a theoretical one. Previous descriptions of switching waves were confined to linear samplers, that is samplers employing triangular or ramp waveforms. Many practical encoders employ non-linear sampling waves or non-ideal linear sampling waves. Only the d.c. input-output relationship and the harmonics associated with d.c. control signals could be adequately described by existing methods. No methods existed which were applicable to forming suitable descriptions of these waves for a.c. control signals. Activity 1.2 concerned a generalisation of Fitch's² approach to include the shape of the sampling wave. This was found to be feasible. The approach and its use are outlined in chapter 3, sections 3.1.1 and 3.1.2 and in appendix A, sections 3.1.1a and 3.1.2a. The activity 1.22, experimental measurements of input-output relationships for non-linear sampling waves, consisted of measurements similar to those described for linear sampling waves but were far fewer in number. They applied only to sinusoidal sampling waves and sampling waves produced by the low pass filtering of square waves. The consistency of these measurements with the predictions of the theory was excellent.

The third phase of research activities concerning natural sampling was motivated by the inadequacies of the existing descriptions of switching waves with more than two levels. Although d.c. levelled waves are occasionally used, the bulk of multi-

levelled waves are based upon a.c. supplied switch arrays. The encoders controlling such waveforms can produce a linear amplifier characteristic if the sampling wave is non-linear and if the sampling period matches the supply period or an integral subdivision or product of the supply period. These encoders are used in practice but no complete descriptions of their waves have been found in the literature.

The simple approach outlined in chapter 2, section 2.4 is a convenient way of demonstrating a general method for synthesising the description of such waves. It relates the final description to the encoder generated signals which define the state of the array. This approach can be used in conjunction with the previously generated descriptions of encoder outputs to synthesise complete waveform descriptions. The composite method is described in chapter 3, section 3.1.2. Examples of its use occur in section 3.1.3 and in appendix A 3.1.3.

The major reason for activity 1.3 1 was the generation of descriptions for the sine-levelled waves of thyristor amplifiers. These descriptions form the basis of any assessment of output signal quality and the establishment of output filter design parameters. Before such activities can take place however it is necessary to establish the optimum shape of the sampling waves and then to evaluate the magnitude of the switching wave sidebands. Procedures for the first of these tasks are outlined in chapter 3, section 3.1.3. The second task, evaluation of the sidebands, is subject to the same difficulties as the analogous task for a linear, two levelled wave with d.c. levels. The same approach can be used for evaluating the sidebands associated with periodic input signals. In this case

only the sidebands associated with sinewave control signals were evaluated. Results of these evaluations are presented as part of the material constituting chapter 4, section 4.2.3.3. The evaluations were checked by the experimental measurements outlined in appendix E 2.2. The good correlation between theory and experiment indicated the approach used to be accurate and thus enabled it to be used as a substitute for the trial and error designs of the past.

The above research on natural sampling thus concludes the development of ways to generate descriptions for all switching waves controlled by this technique. It also enabled descriptions to be formed for waves not yet used but differing only in supply waveform or number of levels. These activities, especially the work on non-linear sampling waves, prompted a search for a more ideal sampling process than natural sampling. This led to a separate research activity, 1.4 of diagram D 1.4.

1.4.2. Modified Natural Sampling.

The natural sampler employs a sampling wave shape which is explicitly defined, at design time, by the input-output characteristic and the supply waveforms. These aspects are touched upon in chapter 3, section 3.1.3. If the supply waveform is subject to variations of any kind then the input-output relationship of the working amplifier will also change. It has no means of compensating for supply waveform changes except by means of matching changes in the sampling waveform. This essential relationship was appreciated early on but a proper definition of the necessary linkage between sampling wave shape and supply wave shape was delayed until the completion of activity 1.3.

The other aspect of the use of natural sampling to control a switching wave with a.c. levels, concerns the ratio of sampling wave frequency to supply wave frequency. Conventional samplers are constrained to have this ratio as a small integer. This constraint restricts the amplifier bandwidth to a frequency close to the supply frequency. A more ideal control technique would sample at a much higher frequency and so expand the amplifier bandwidth accordingly.

The key part of such an encoder would be the mechanism whereby the sampling wave shape is continuously varied to compensate for supply waveform variations over the sampling period. Activity 1.4 2 consisted of a trial and error search for such a mechanism. The second trial was successful in producing a technique which appeared to have the necessary properties. This encoder is described in chapter 3, sections 3.1.4.1 and 3.1.4.2. An algebraic investigation of the encoder input-output properties is outlined in appendix A 3.1.4. The subsequent experimental checks of this theory were not completed prior to the writing of the thesis. Those tests which were carried out are described in appendix E3. They suggest that the approach is valid and should be investigated further.

1.4.3. A Special Form of Natural Sampling.

The final activity concerning natural sampling, activity 1.5, was prompted by the paper by Chen¹⁰ concerning the linearisation of a quantizer input-output relationship by means of a sinewave input signal perturbation. The situation was recognised as a special form of natural sampler and since it was amenable to the existing algebraic approach this encoder was examined

with a view to fitting it into the existing pattern of natural samplers. A theoretical investigation of the properties required of a perturbation to produce a linear amplifier is outlined in appendix A 3.1.5a. Other aspects of this encoder are investigated in A 3.1.5b, c, and d. Section 3.1.5 of chapter 3 introduces the subject and outlines the most important aspects discussed in the appendix.

No experimental verification of these waveform descriptions was attempted due to the great similarity with the more usual varieties of natural sampler. One small difference is remarked upon in section 4.1.1.2 of chapter 4. It is interesting to note that a later paper¹¹ on this subject indicated that the unit amplitude triangular perturbation yields a linear input-output characteristic. This is one of the solutions yielded by the analysis mentioned above, and is a well known result for simpler encoders.

1.4.4. Regular Sampling.

The general principles used to form descriptions for waves controlled by natural sampling can also be used to form descriptions of equivalent waveforms controlled by regular sampling. This fact prompted the activities of section 2 of figure D 1.4. The same goals and methods were employed as those for natural sampling.

The first activity, 2.1, was an experimental confirmation of the linear sampler output waveform description attributed to Bennet⁶. The description given is not accompanied by an explanation of its derivation and is confined to a wave formed by a

"linear" sampler when the control signal is a sinewave. The accuracy of this description was checked, by the experiment outlined in appendix E 6, and found to be an accurate description. Thus the existing descriptions formed a basis against which subsequent work could be compared and checked.

Activity 2.2 1 was concerned with forming a description of the regular sampler output when the input signal was an arbitrary waveform and the sampling waves were chosen to produce any form in input-output characteristic. The approach employed is described in concept in chapter 3, section 3.2.2, and is illustrated graphically in figure D 3.2.2. The corresponding algebraic result was derived with some difficulty and is subject to the constraint that the control signal be periodic.

The algebraic description was used as the basis of a computer program to evaluate the waveform spectra of an encoder output when the encoder input is a bandlimited periodic control signal. This program, C 2.2.1, was used to produce estimates of signal and sideband components of the encoder output for several simple periodic waveforms. These were experimentally checked by measurements analogous to those outlined in E 6.0. In addition, the algebraic solution was used directly to estimate the distortion and intermodulation for a pair of sinewave input signals. This was carried out algebraically in the manner outlined in appendix A 3.2.3 and is described in section 3.2.3. These results were checked by the measurements outlined in appendix E 6.

These simple applications of the derived theory do not test its full range of validity. It was

not considered worthwhile to do so because regular sampling has many disadvantages when compared to natural sampling and its practical uses are usually confined to simple situations similar to those examined above. The validity of the theory for these examples nevertheless indicates the range of validity is probably as wide as any future useage is likely to require.

1.4.5. Feedback Amplifiers.

As figure D 1.4 indicates, the first experiments concerning feedback around a switching amplifier occurred at about the time of the development of the theory for non-linear natural sampling. This preliminary investigation concerned a high gain amplifier employing "linear" natural sampling. The feedback employed produced an open loop gain corresponding to a high gain low pass filter. Under these conditions the sampling rate was observed to double and it was obvious that normal conditions for operation of the sampler did not prevail. At this point the experiment was abandoned in favour of experiments confirming the validity of the newly developed theory for non-linear natural samplers. The experimental situation was not investigated again until after the conclusion of measurements validating the theoretical analysis of regular sampling. Other aspects of this work were investigated in the interim period.

A colleague, Furmage²⁶, undertook an investigation of the behaviour of class D amplifiers when operating within a feedback loop as part of his honours project. This work was based upon the

investigation of a similar situation, one involving thyristor amplifiers by Fallside¹⁸. One line of this investigation concerned the use of describing functions as a means of detailing the apparent behaviour of the amplifier near subharmonic frequencies. These were evaluated by vector summation of the sidebands which coincide at the input signal frequency whenever this is a subharmonic of the sampling rate. Furmage was inhibited in his work by a time limit and was forced to evaluate many describing functions by hand calculation based upon approximations which limited the accuracy of his estimates. Before continuing my own investigations into this situation I resolved to evaluate the subharmonic gain functions by modifying the existing computer programs for estimating sideband amplitudes. This constituted activity 3.2 1. These programs, C 3.1 and C 3.2, evaluated the subharmonic gain functions for both regular and natural sampling. The results produced by these programs and the computing techniques employed are described in section 4.3 of chapter 4.

The computational activity was completed before the experimental investigation constituting activity 3.2 2 commenced. When this activity did commence it immediately became apparent that the whole basis of the sideband evaluation and thus the subharmonic gain was invalidated by the occurrence of gross changes in the conditions within the sampler itself. The complexity of the situation, already briefly described in preface to the literature survey on this topic, halted all further investigation of this topic while the isolation of basic parameters was considered.

The first outcome of this re-appraisal of the problem was a model for the changes which occur in the d.c. input-output characteristic of a natural sampler placed within a feedback loop. This model is described in chapter 5, section 5.1. The evaluation of the d.c. input-output characteristic is based upon the assumption that all the waveforms within the amplifier are periodic and have the same period, that of the sampling waves. Subject to this restriction the model is potentially applicable to the prediction of the d.c. input-output characteristic and the phase relationships between waveforms. Confirmation of the model accuracy was obtained by comparing computed input-output relationships, evaluated by programs C 4.1 and C 4.2, with the experimental measurements outlined in appendix E 4.1 and E 4.2 respectively. The algebraic solutions used as examples in section 5.1 were also used to test the model accuracy.

The method used to evaluate the d.c. input-output characteristic cannot be applied directly to evaluate the a.c. input-output characteristic since it relies upon the feedback ripple possessing a periodic waveform. It is conceivable that the method could be extended to subharmonic situations such as those encountered in practice. When this was attempted no method was found for solving the static equations defining the situation. Attempts to predict the position of the stability boundary between normal and subharmonic conditions were also made but these were not successful. These unsuccessful attempts to predict the a.c. characteristics of amplifiers influenced by feedback constituted activity 3.4. The general problem is briefly discussed in section 5.2, chapter 5.

1.4.6. Self Oscillating Encoders

There are close ties between amplifiers with feedback and self-oscillating encoders. The successful prediction of the d.c. input-output characteristics of the former prompted an attempt to apply the same approach to self-oscillating encoders. Prior to this attempt some preliminary investigations of the integral feedback self-oscillating encoder had been completed. These investigations constituted activity 4.1. The aim of these investigations was to gain familiarity with these encoders and to confirm the basic features as described by Shaeffer²⁰ and others. These measurements and their analysis are described in sections 6.1 and 6.2 (chapter 6) respectively. The main result of this early activity was an evaluation of the conditions for the onset of phaselocking and a subsequent theoretical derivation for this condition. For the integral encoder it is relatively easy to predict that the d.c. input-output encoder has a linear characteristic and that the oscillation frequency is a parabolic function of the d.c. input signal. The more complex encoders are not so easily predicted in their behaviour.

Activity 4.2 was an attempt to produce a single approach applicable to the analysis of all members of this class of encoder. The goal of the approach was the prediction of the d.c. input-output characteristic and the variation of oscillator frequency with d.c. input signal. The result of the attempt is the theory outlined in appendix A section 6.3. This theory yields two equations which must be solved to evaluate first the oscillation frequency and subsequently the d.c. input-output characteristic.

To verify the accuracy of this theory two specific examples were considered, the integral feedback filter, and the lowpass high Q, feedback filter. The theoretical predictions are evaluated in appendix A section 6.3b. The experimental measurements performed earlier for the integral filter were correctly deduced. The high Q filter system was experimentally measured after the analysis. These measurements and the accuracy of the predicted characteristic are discussed in appendix E 5. This successful development of a theory for self-oscillating encoder characteristics concluded the experimental investigations upon which this thesis is based.

1.5. Thesis Content.

From the references to the thesis body made in the chronological description of research activities, it will be apparent that this thesis contains much more than a description of this activity. In an attempt to introduce more cohesion into the diverse and fragmentary literature concerning the choice and design of switching waves, and the design of the amplifiers employing and controlling these waves, many attitudes and ideals have been included with the intention of guiding the designer away from undesirable or unfortunate design parameters and towards the best hardware attainable with whatever technology is available. These attitudes and ideals have been incorporated into a logical progression of the subject through a range of subtopics starting with encoders at the start of Chapter II and finishing with equivalent circuits at the end of Chapter VII. Although the progression is not complete and emphasis is placed

unequally on the various subtopics, it is hoped that the existence of the thesis will stimulate others in this area.

CHAPTER I REFERENCES

<u>Number</u>	<u>Surname</u>	<u>Source of Publication Details</u> <u>(Appendix R Location)</u>
1	Bennet "New Results in the Calculation of Modulation Products" Bell System Tech. Journal Vol. 12 April 1933 PP 228-243	2.1
2	E. Fitch "The Spectrum of Modulated Pulses" J. IEE Vol. 94 PT 3A 1947 PP 556-564	2.2
3	E.R. Kretzmer "Distortion in Pulse Duration Modulation" Proc. IRE Vol. 35 November 1947 PP 1230-1235	2.3
4	C.H. Miller "High Efficiency Amplification Using Width Modulated Pulses" Proc. IREE (Australia) Vol. May 1964 PP 314-323	2.11

<u>Number</u>	<u>Surname</u>	<u>Source of Publication Details</u> <u>(Appendix R Location)</u>
5	E.C. Bell, T. Sergeant "Distortion and Power Output of P.D. Modulated Amp." Electronic Engineering Vol. 37 August 1965 PP 540-542	2.14
6	H.S. Black "Modulation Theory" N.J.: Van Nostrand 1953 PP 263-281	1.2.1
7	D.R. Brit "Modulated Pulse Audio Frequency Amplifiers" Wireless World Vol. 69 No. 2 February 1963 PP 76-83	2.9
8	G.F. Turnbull, J.M. Townsend "A Feedback Pulse Width Modulated Audio Amp." Wireless World Vol. 71 No. 4 April 1965 PP 160-168	2.13

<u>Number</u>	<u>Surname</u>	<u>Source of Publication Details</u> <u>(Appendix R Location)</u>
9	P.F. Pitman, R.J. Ravas, R.W. Briggs "Staggered Phase Technique" Electrotechnology Vol. 83 No. 6 June 1968 PP 55-58	2.28
10	E.S. McVey, P.F. Chen "Improvements of Position and Velocity Detecting Accuracy by Signal Perturbation" IEEE Trans Vol. IECI-16 July 1969 PP 94-98	2.39
11	P.F. Chen "Optimal Signal Perturbation Waveform for Sensing Arrays" IEEE Trans Vol. IM-19 May 1970 PP 135-139	2.42
12	J.J. Pollack "Advanced Pulse Width Modulator Inverter Techniques" IEEE Trans IA-8 March/April 1972 PP 145-154	2.48

<u>Number</u>	<u>Surname</u>	<u>Source of Publication Details</u> (Appendix R Location)
13	A.G. Milnes "Transistor Power Amplifiers with Switched mode of Operation" Trans.AIEE Vol. 75 Pt. 1. 1956 PP 368-372	2.5.
14	E.S. McVey, R.E. Russel "The Design of a Simple Single Phase SCR Regulator" IEEE Internat.Con. Rec. IGA-8 March 1966 PP 68-73	2.19
15	T.H. Barton, R.S. Birch "A 5kw Low Frequency Power Amplifier ..." IEEE Internat.Con. Rec. PT 9-12 No. 10 PP 146-153	2.33
16	L. Malesini "Improved Delay Circuit for Thyristor Linear Power Control" Electronic Engineering January 1969 PP 84-89	2.31

<u>Number</u>	<u>Surname</u>	<u>Source of Publication Details</u> <u>(Appendix R Location)</u>
17	F.J. Evans "A Linear Thyristor Power Stage with Self Limiting Firing Circuits" IEEE Trans Vol. IECI-17 No. 1 February 1970 PP 25-33	2.41
18	F. Fallside, A.R. Farmer "Ripple Instability in Closed Loop Control Systems" Proc. IEE Vol. 114 March 1967 PP 139-152	2.23
19	F. Fallside "Ripple Instability in Closed-loop Pulse Modulation Systems including Inverter Drives" Proc. IEEE Vol. 115 1968 PP 55-58	2.27
20	R.A. Schaefer "A New Pulse Modulator for Accurate d.c. Amplification ..." IRE Trans on Instrumentation September 1962 PP 34-47	2.8

<u>Number</u>	<u>Surname</u>	<u>Source of Publication Details</u> (Appendix R Location)
21	A.G. Bose "A Two State Modulation System" Electrotechnology Vol. 74 No. 2 August 1964 PP 42-47	2.12
22	G.F. Turnbull, J.M. Townsend "Efficiency Considerations in a Class D Amp." Wireless World Vol. 73 No. 4,5 April, May 1967 P 154, P 214	2.24
23	J. Das, P.D. Sharma "Rectangular Wave Modulation - A P.L.M.- FM System" Electronic Letters Vol. 2 No. 1 January 1966 PP 7-9	2.15
24	S.P. Jackson, H.R. Weed "The Differential Saturable Transformer as the Basic Component of a Controlled High- Efficiency Power Supply" IEEE Internat.Con. Rec. IGA-2 No. 5 September/October 1966 PP 378-383	2.18

<u>Number</u>	<u>Surname</u>	<u>Source of Publication Details</u> <u>(Appendix R. Location)</u>
25	Yuan Yu, T.G. Wilson, Et Al "Static d.c. to Sinusoid a.c. Inverter....."	2.25
	IEEE Trans Mag-3 No. 3 September 1967 PP 250-256	
26	S.G. Furnage "Subharmonic Instability in Closed Loop Control Systems with Pulse Width Modulation"	1.3.1
	Honours Thesis in Electrical Engineering, Uni. Tas. March 1969	

CHAPTER II : DESCRIBING THE SWITCHING WAVE

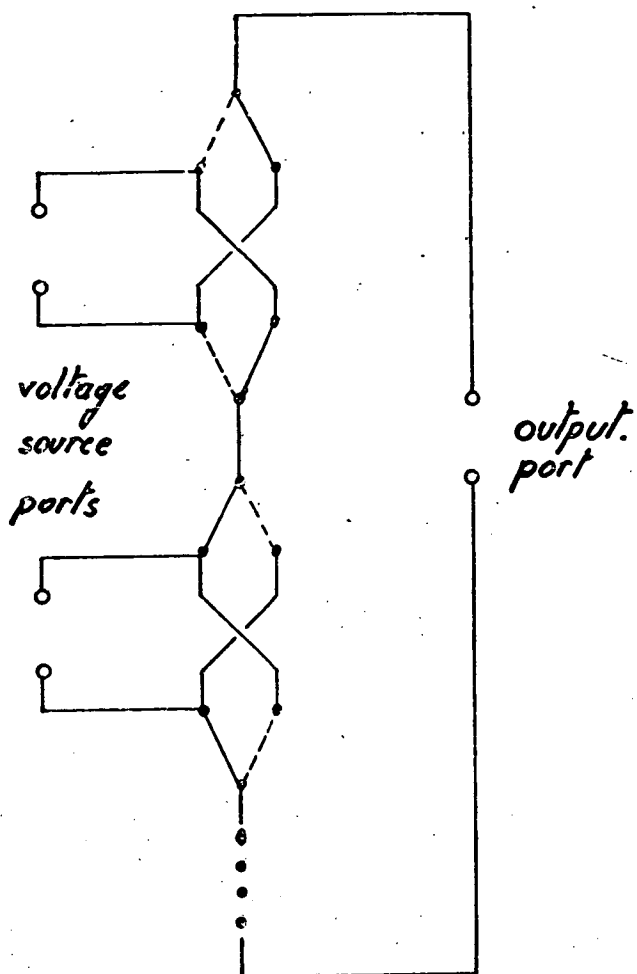
- 2.1 The Switch Array
- 2.1.1 The Operating Restrictions on a Switch Array
- 2.1.2 The Equivalence of a Complex Array and a Simple Array
- 2.2 The Switch Control Unit
- 2.3 State Function for Switches
- 2.4 The Voltage Formed at a Node of Switches
 - The limitations of Voltages formed at a Node of Switches
- 2.5 Linear Amplification
- 2.6 Minimisation of Switching Wave Energy
- 2.7 Summary

Chapter II

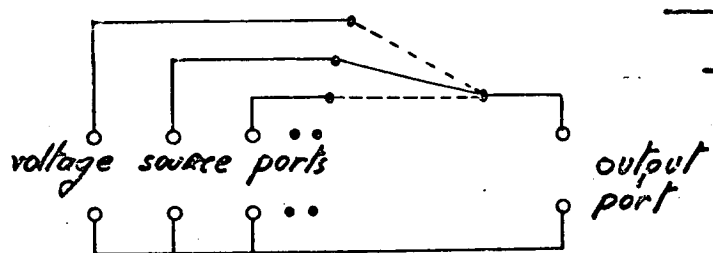
Describing a Switching Wave and its Control Functions.

In this chapter the switching wave of an amplifier is described in terms of the switching wave levels and the control functions which select the levels. The description is used to discuss encoder independent features of the wave including: output signal bounds, allocation of a dynamic range to each control function, and the concept of minimum energy waveforms. In later chapters where control functions are derived for specific encoders the encoder independent features above help define the output requirements of the individual encoders.

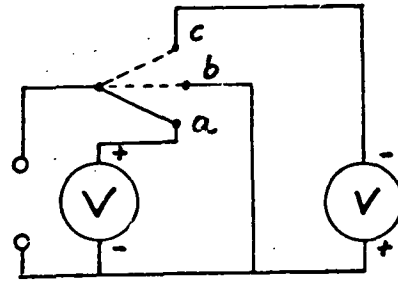
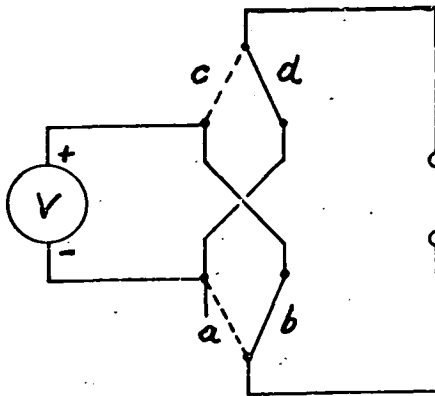
Aspects of switch array topology, switch control unit operation, and the switch control functions themselves, which must be introduced or defined before a switching wave can be described are incorporated into sections 2.1, 2.2, and 2.3 respectively. Section 2.4 deals with the switching wave description and the associated output signal dynamic range. The allocation of a dynamic range to each switch control signal and the introduction of the concept of minimum energy waveforms constitute sections 2.5 and 2.6 respectively.



Complex Array
D2.1.2a



Simple Array
D2.1.2b



Output Voltage		+V	0	-V
Array Switches	Simple	a	b	c
Closed	Complex	$a \neq c$	$a \neq d$ or $b \neq c$	$b \neq d$

Equivalent Simple & Complex Arrays

D 2.1.2c

2.1 Switch Arrays.

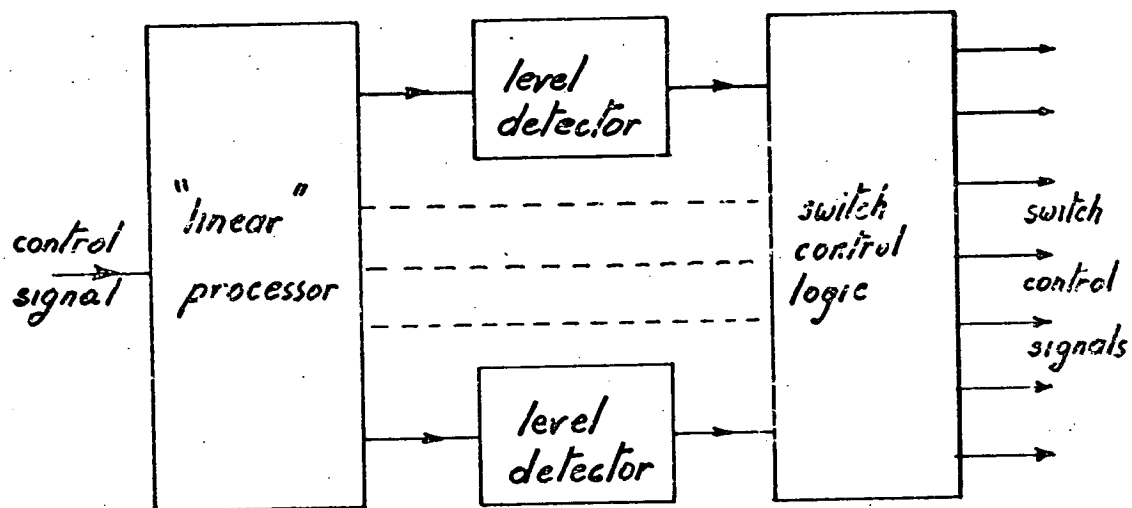
2.1.1 The Operating Restrictions placed on a Switch Array

The switch array links the supply voltages, forming the switching wave, to a common port. The array may be regarded as a multiport network with many input ports and a single output port. The array must satisfy two important conditions. These are, first, the output voltage must be defined by the switches and the supply voltages, second, the supply voltages must not be short-circuited. These conditions are satisfied if the only complete circuit within the network connects one or more of the input ports in series with the output port.

2.1.2 The Equivalence of a Complex Array and a Simple Array

The most flexible form of switch array allows any one of a number of floating supply voltages to be added, subtracted, or omitted from a series circuit which includes the output port. Diagram D 2.1.2a illustrates such an array. This array is capable of combining N supply voltages by means of $4N$ switches to produce 3^N voltages at the output port. This may be compared to the simple array shown in diagram D 2.1.2b, where N supplies are connected by N switches to provide N voltages at the output port. These two arrays represent extreme forms of switch arrays. There are many intermediate forms such as series connections of simple arrays and series parallel connections of bridge and simple arrays.

By drawing a chart similar to that in diagram D 2.1.2c the switch states of a complex array may be specified in terms of those of a simple array. This equivalence between complex and simple arrays is due to the one to one correspondence between output voltages and switch closures for a simple array. Since this equivalence is basic, and the one to one correspondence of switch closures and output state is convenient for discussion purposes, simple arrays will be used to illustrate the following discussions of waveforms.



THE SWITCH CONTROL UNIT

D 2.2

2.2 The Switch Control Unit

The switches of an amplifier are operated by the switch control unit according to rule from the input signal. The input signal is converted to a number of switch control signals by the following sequence. First the amplifier input signal is presented to one or more coders. Each coder converts the input signal, which may have any level within a particular range, to a signal which may take one of two definite levels. These binary coder outputs are then combined by a logic unit to produce the control signals for each switch in the amplifier array.

A coder may be subdivided into two parts. The first modifies the input signal but retains the analogue form, while the second converts this analogue signal to a binary signal. The form of modification employed depends upon the method of coding used. For example, the input signal may be added to the signal from a local oscillator if natural sampling is employed or it may be sampled and held prior to the same process if regular sampling is employed. The analogue to binary conversion is accomplished with a level detector such as a comparator or a schmitt trigger.

The structure of the logic unit is determined by the type of coder used and by the form of the switch array. An amplifier with two switches and a single coder will only need one coder output and the inverse of this to control the switches. By comparison an amplifier with three supply voltages connected in the most flexible way possible, may require five coders as inputs to the logic unit which generates the twelve switch control signals so that all twenty seven possible output voltages can be produced.

Very efficient use of coders will result in complex logic units especially if the more flexible forms of switch array are used. The minimum number of coder outputs necessary to control an array may be found since each output voltage produced by an array corresponds to a

particular set of switch states. The minimum number of binary signals, that is coder outputs, necessary to control a switch array with m states or output levels is the smallest integer greater than $\log_2 (m-1)$. This formula is illustrated for the previous example.

In practice small numbers of output levels of a switch array are usually required and a simple but inefficient system is used with one coder per switch array state.

2.3 State Function for Switches

An ideal switch has only two states, zero impedance and zero conductance. Any real switch, electronic or mechanical, is non-ideal in that it has a range of states from near zero impedance to near zero conductance. In order to describe the basic waveforms of switching amplifiers it is convenient to use ideal switches as a first approximation to real switches and then to detail the relatively minor adjustments to the idealised situation to describe the action of real switches.

In order to describe the condition of an ideal switch a state function is now defined. A switch has a state described by the state function, $g(t)$, defined by

$$g(t) = 1 \text{ if the switch conducts at time } t \\ 0 \text{ if the switch insulates at time } t$$

This function can be described* by two variables, $\theta_1(t)$ and $\theta_2(t)$ associated with the changes of switch state. If the switch changes from insulation to conduction when $\left(\frac{\theta_1(t)}{2\pi}\right)$ increases through an integer or $\left(\frac{\theta_2(t)}{2\pi}\right)$ decreases through an integer value and $\left(\frac{\theta_2(t)}{2\pi}\right)$ changes from conduction to insulation for the opposite rates of change of these variables through integer values then $g(t)$ is described by the equation below.

$$g(t) = \left(\frac{\theta_1(t) - \theta_2(t)}{2\pi}\right) + \sum_{n=1}^{n=\infty} \frac{1}{n\pi} (\sin(n\theta_1(t)) - \sin(n\theta_2(t)))$$

*See Appendix A 2.3.

The variables $\theta_1(t)$ and $\theta_2(t)$ are sufficiently restricted by the inequality

$$0 < \theta_1(t) - \theta_2(t) < 2\pi$$

The state function and restriction of variables are derived and discussed in appendix A 2.3.

2.4 The Voltage Formed at a Node of Switches

A group of m switches connect m voltage sources to a node. If all the switches are off the node voltage is defined by the load. If more than one switch is on then two or more voltage sources are connected together and the voltage at the node is undefined. Only when a single switch is conducting is the node voltage defined. Let the state function of the i^{th} switch be $g_i(t)$, then the requirement that only one switch conducts at any time is described by

$$\sum_{i=1}^{i=m} g_i(t) = 1$$

For a real node with real switches difficulty in changing switch states occurs and the restriction used is usually

$$\sum_{i=1}^{i=m} g_i(t) = \begin{cases} 1 & \text{when no switch is changing state} \\ 0 & \text{when a switch is changing state} \end{cases}.$$

This restriction is applied to prevent high switch currents during transitions between states should two switches conduct at the same time.

The voltage formed at the node may now be described in terms of each supply voltage $V_i(t)$ and the switch state functions $g_i(t)$. The component of the node voltage due to the i^{th} switch, V_{ni} , is zero when the switch is open and the supply voltage, $V_i(t)$, when the switch is closed. Thus if the switch state function is $g_i(t)$ the node voltage component is

$$V_{ni}(t) = V_i(t) \cdot g_i(t)$$

The complete node voltage, V_n , is formed by summing all the component voltages.

$$V_n(t) = \sum_{i=1}^{i=m} V_i(t) \cdot g_i(t)$$

The Limitations of Voltages Produced at a Node of Switches

The instantaneous value of the node voltage is limited to the range between two voltages $V_{\max}(t)$ and $V_{\min}(t)$ where $V_{\max}(t)$ is the maximum voltage of the m supply voltages at time t and $V_{\min}(t)$ is the minimum voltage of the m supply voltages. The expression $V_{\min}(t) \leq V_n(t) \leq V_{\max}(t)$ describing this limitation is derived in appendix A 2.4.

The range of values of d.c. component is frequently used to describe the range of output voltage at a node. The d.c. component is subject to a restriction which applies whenever the component approaches either of the supply voltage limits. This restriction is independent of the way in which the switching wave is formed because it is due to the spectrum of the switching wave envelope. Consider a d.c. component which approaches the upper supply voltage limit, $V_{\max}(t)$. If the d.c. component exceeds the minimum value of $V_{\max}(t)$ then the switching wave proportions cannot be adjusted to maintain the average value of the d.c. component without causing the switching wave to have a component with frequency matching the frequency of $V_{\max}(t)$. The precise restriction is derived in appendix A 2.4.1. The d.c. component of the switching wave can of course rise to the average value of $V_{\max}(t)$ but only if the spectrum of the switching wave contains components matching in frequency those of $V_{\max}(t)$.

Similar restrictions apply for a.c. components of the node voltage. Provided the sum of the a.c. and d.c. components lie between the minimum value of $V_{\max}(t)$ and the maximum value of $V_{\min}(t)$ then no restrictions need be placed on the remaining terms of the node voltage, however if the a.c. component exceed these limits then harmonics of the component modulated in amplitude by the associated bound are required for the node voltage to remain within the prescribed bounds. Again the contribution of each harmonic is not explicitly defined although a minimum supply frequency harmonic may be specified which is sufficient for

node voltage to remain within the specified limits. The limiting amplitude of the sinewave component is obtained when the node voltage switches between $V_{\max}(t)$ and $V_{\min}(t)$ once each half cycle of the frequency of interest. When this limiting value is reached the amplitudes of each harmonic of the sinewave component and of the supply voltages as well as the intermodulation components are known.

In switching amplifiers producing single frequency or narrow bandwidth outputs near a single fixed frequency the generation of harmonics in the output is not very important since they may be filtered from the amplifier output. In most switching amplifiers however generation of harmonics is undesirable. Thus most switching amplifiers produce output components of the switching wave with amplitudes in the range between the minimum value of $V_{\max}(t)$ and the maximum value of $V_{\min}(t)$ to avoid having supply frequency components of the switching wave while amplifiers with less constraint on output components at supply frequency limit the output voltage between the average value of $V_{\max}(t)$ and the average value of $V_{\min}(t)$ to avoid the presence of signal frequency harmonics.

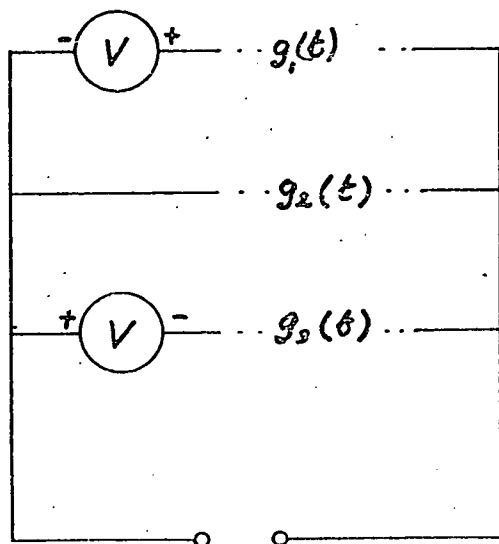
2.5 Linear Amplification

The node voltage, V_n , is synthesised in such a way that one component, $V_n]_0$, is linearly related to the amplifier input so that the amplifier output may be formed by filtering the node voltage. A node of m switches with state functions, g_i , and associated supply voltages, V_i , has node voltage

$$V_n = \sum_{i=1}^{i=m} V_i \cdot g_i$$

The node voltage component related to the input signal $e(t)$ is described by

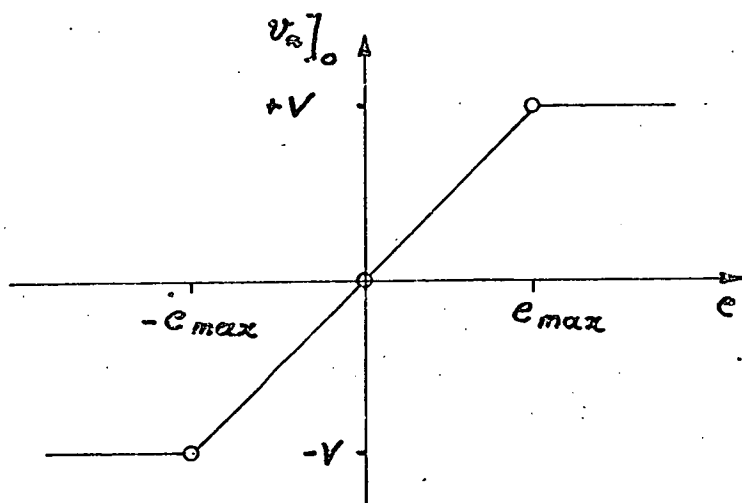
$$V_n]_0 = K e(t)$$



$$g_1(t) \Big|_0 = \begin{cases} 1 & e < -e_{\max} \\ e/e_{\max} & 0 < e < e_{\max} \\ 0 & 0 \geq e \end{cases}$$

$$g_3(t) \Big|_0 = \begin{cases} 1 & e < -e_{\max} \\ -e/e_{\max} & 0 > e > -e_{\max} \\ 0 & e > 0 \end{cases}$$

$$g_2(t) = 1 - g_1(t) - g_3(t)$$



Piecewise Linearity with Three Supply Array

D 2.5

This relationship may be ensured if the component of $V_n]_0$ due to each switch, $V_{ni}]_0$, is of the form

$$V_{ni}]_0 = K_i e(t) + C_i \quad \text{where}$$

$i=m$

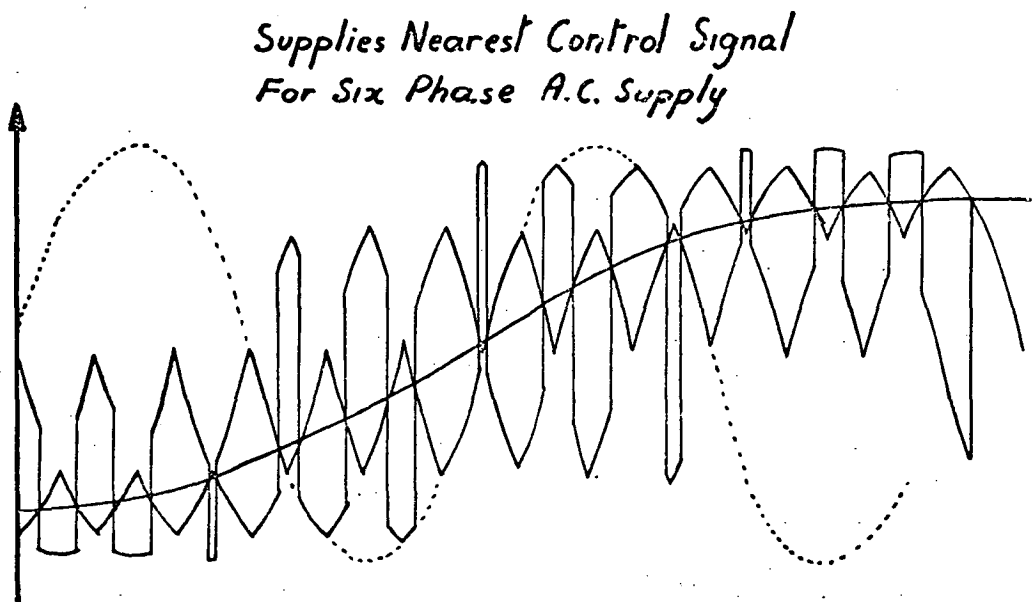
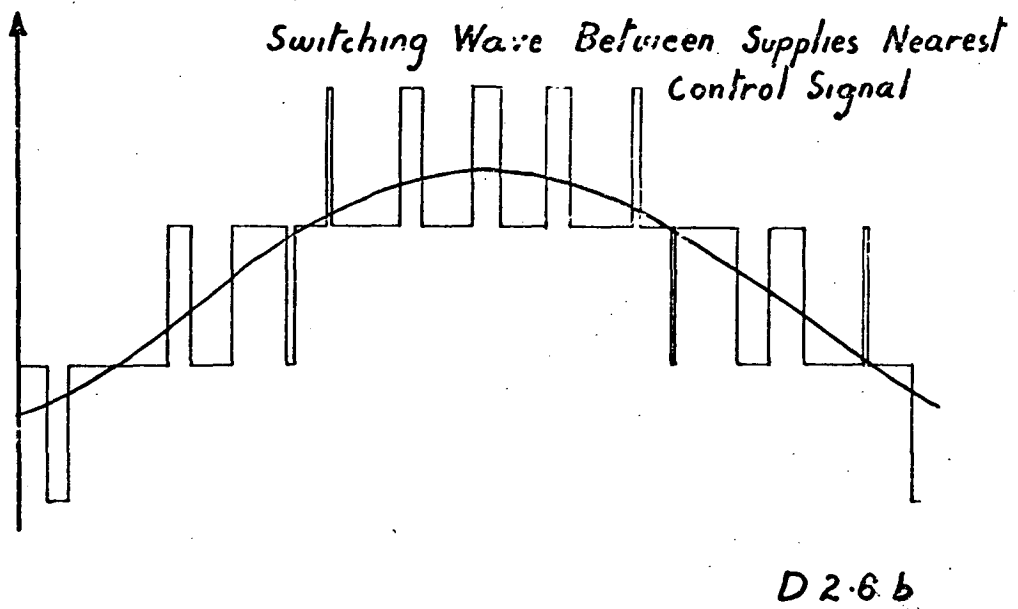
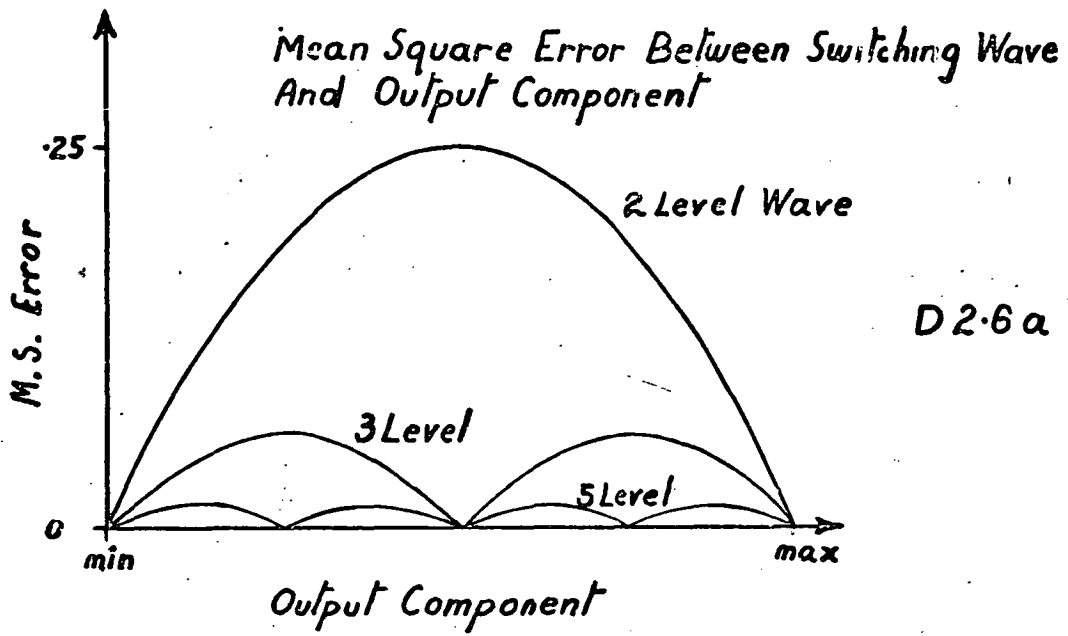
$$\sum_{i=1}^m C_i = 0$$

This is a sufficient rather than a necessary condition for linear amplification. However, of the many ways in which linear amplification is achieved the method of making each component a linear function of the input is one of the simplest and is widely used. The most common extension of this method uses components due to separate switches for different ranges. The node voltage due to a particular switch is of the form

$$V_{ni}]_0 = \begin{cases} K_i \cdot a_1 + C_i & \text{for } e(t) < a_1 \\ K_i \cdot e(t) + C_i & \text{for } a_1 < e(t) < a_2 \\ K_i \cdot a_2 + C_i & \text{for } e(t) > a_2 \end{cases}$$

The sum of two or more such individual switch components with complementary limits and the same value of K_i produce a node voltage component which obeys the linearity condition. The major advantage of such a scheme is to reduce the size of step in the switching waveform so that filtering of the node voltage is less difficult.

As an example consider the switch and supply array of diagram D 2.5. In this example $g_1(t)$ and $g_2(t)$ control the output for positive input signals while $g_2(t)$ and $g_3(t)$ control the output for negative inputs. The resulting amplifier is linear over the range of outputs $-V < V_n]_0 < +V$ with a gain $\frac{V}{e_{\max}}$. The size of switching steps is half that of a single amplifier operating from $+V$ and $-V$ and has maximum R.M.S. ripple on the output component on either side of zero output rather than at zero output. Against these advantages are the disadvantages of twice the complexity and the need for balanced gains and accurate fitting of limits of the active ranges of each amplifier half.



2.6 Minimisation of Switching Wave Energy

By providing N equally spaced d.c. levels for a waveform, rather than three as in the previous example, the voltage error between the waveform and the desired output may be reduced to the fraction, $1/(N-1)$, of that for a waveform with two levels. At each output level corresponding to a waveform level the error signal is zero. Diagram D 2.6a shows the variation of error with output voltage. When N is odd one of the waveform levels will correspond to the centre of the output range giving a zero of error voltage at the zero of output.

The method of generating an output level, by switching between the nearest waveform levels above and below the target, minimises the mean square error of the output waveform. This is demonstrated, in appendix A.2.6. to be true of both d.c. and a.c. waveform levels. Examples of a three level waveform with d.c. levels and a six level waveform with a.c. levels are shown in diagram D 2.6b.

The waveform with d.c. levels is similar to a quantizer output when a small perturbation is added to the input signal. The waveform with a.c. levels is similar in some respects to the waveform produced by a cycloconverter.

2.7 Summary

The switching wave may be described as a sum of components each due to a particular waveform level and an associated binary control signal. Each binary control signal corresponds to a particular set of switch states of the switch array and is defined by a boolean function of the outputs of one or more level detectors. Each level detector is provided with a modified form of the input or control signal, the form of modification being dependent on the type of switching wave to be produced, the switch array, the logic function, and the form of level detection employed.

The switching wave is restricted to a range of levels between the instantaneous maximum and instantaneous minimum of the waveform levels possible. The switching waveform will contain components with frequencies corresponding to these levels if the output component of the waveform exceeds the range between the minimum of the former and the maximum of the latter. Should the output component of the waveform exceed the range between mean values of the above levels then the switching wave will contain components at the harmonics of the output component frequency.

There are two commonly used restrictions giving linear amplification. The first kind requires that each component of the waveform contribute to the output an amount proportional to the control signal. This method is most suitable for waveforms with a.c. levels. The second kind requires that the contributions be proportional over a limited range of output component levels and a constant contribution outside this range. This method is readily applied to waveforms with d.c. levels. Although other techniques are possible the methods used depend on the situation and cannot be described in a general manner.

Minimisation of the error between the switching wave and the output component may be achieved by switching between the nearest levels above and below that of the output component. This minimisation is not usually regarded as a restriction since it may conflict with other requirements. It is regarded more as an ideal since it minimises some of the filter requirements for steady state outputs.

References

S. B. Dewan, M. D. Kankam "A Method for Harmonic Analysis
of Cycloconverters"

IEEE Trans IGA-6 No. 5

September 1970 PP 455-462

R. H. Masterman "Cyclo Converter Amplifier"

Electronics Letters

Vol. 5 No. 14

July 1969 PP 306-308

CHAPTER III : SYNTHESIS OF WAVEFORM DESCRIPTIONS

- 3.0 Introduction**
- 3.1 Waveform Synthesis by Natural Sampling**
 - 3.1.1 A Mathematical Description of Natural Sampling**
 - 3.1.2 Node Voltage Components Produced by Natural Sampling**
 - 3.1.2.1 from dc Supply Voltages**
 - 3.1.2.2 from ac Supply Voltages**
 - 3.1.3 Assembly of Node Components**
 - 3.1.4 A New form of Encoder**
 - 3.1.4.1 A Switching Wave with Two Arbitrary Levels**
 - 3.1.4.2 Supply Waveform Rejection for Complex Waveforms**
 - 3.1.5 Multi-dc-Level Switching Waves**
 - 3.1.5.1 Linearly and Perturbation Amplitude**
 - 3.1.5.2 Sensitivity to Perturbation Amplitude**
 - 3.1.5.3 Output Waveforms with Natural Sampling**
- 3.2 Waveform Synthesis by Regular Sampling**
 - 3.2.1 The Coder Law**
 - 3.2.2 The Relationship to Natural Sampling**
 - An example of regular sampling**
 - 3.2.3 The Modulator Nonlinearity**
 - Regular Sampling with Combined Inputs**
 - Two Step Modulation**
 - 3.2.4 The Generation and Assembly of Switching Waves**
 - Features of Regular Sampling**
- 3.3 Review of Chapter**

Chapter III.

Synthesis of Waveform Descriptions for
Waves Controlled by Four Encoders
Employing Periodic Sampling.

3.0 Introduction

The need for switching wave descriptions was established in Chapter I, and a method for synthesising these was outlined in Chapter II. The synthesis method is based upon a knowledge of the switch array geometry, the switching wave levels, the linkage between encoder outputs and the switches of the array, the tactics used to achieve linearity over a wide signal range, and the input-output properties of the encoders. This chapter is concerned with the application of the method to describe switching waves controlled by four types of encoders: those using natural sampling, a modification of natural sampling, a special form of natural sampling, and regular sampling. In order to implement each synthesis the encoder input-output characteristic is derived in its most general form, that is with the input signal as an arbitrary function of time. It is this feature which enables the theory presented here to be set apart from that presented in the literature.

The chapter is divided into two major parts, one concerned with natural sampling and its progeny, the other concerned with regular sampling. That dealing with natural sampling is subdivided into three sections the details of which are outlined below.

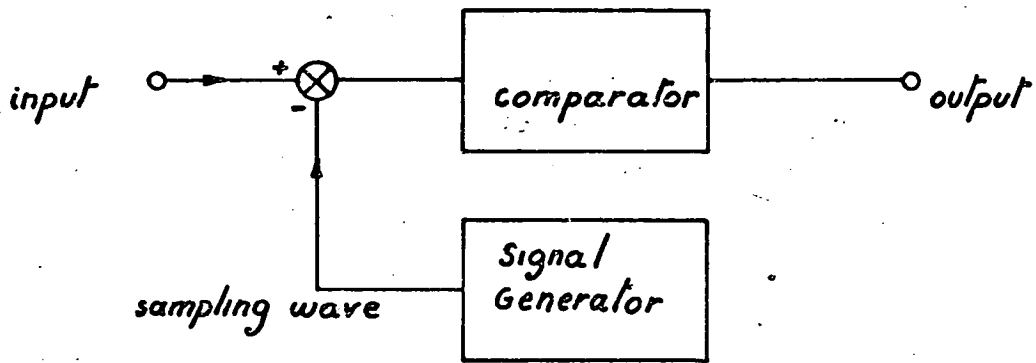
The first section deals with natural sampling as it is applied to waves with d.c. levels and to waves with periodic a.c. levels of constant waveform and having periods matching the sampling period.

The second section deals with a new form of encoder, one where the shapes of the sampling waves are continuously adjusted to compensate automatically for changes in the levels of the switching wave.

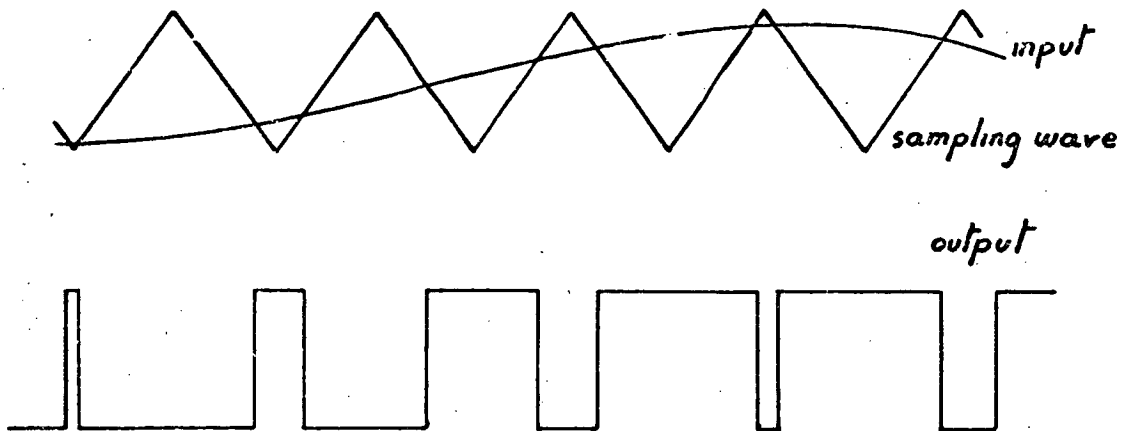
The third section deals with the control of switching waves employing many equally spaced levels by means of a variant of natural sampling where the analogue to digital interface is a quantiser and the sampling wave is a perturbation of the input signal.

The second part, concerning regular sampling, parallels the first section of the first part in that it considers the control of waves with either d.c. levels or periodic, fixed waveform, a.c. levels commensurate with the sampling wave.

The discussions associated with each encoder differ in structure since most of the methods and principles involved are common to all and need only be discussed in detail for the first. Consequently the largest section concerns the application of natural sampling to the control of d.c. and a.c. levelled waves. This section is structured with three subdivisions, namely, the encoder input-output relationship, the control of the waveform contribution of an individual waveform level, and the assembly of waveform components to achieve a linear amplifier. The structure thus mirrors the steps for synthesising waveform descriptions. The second and third encoders are more specific and material related to them does not need this ordering. Discussion of the fourth encoder, that employing regular sampling, follows the pattern of the first encoder discussion, that is, it mirrors the steps of the waveform description synthesis. The most important feature of each encoder analysis, the derivation of the encoder input-output characteristic is essentially algebraic and is thus confined to appendix A.



A Natural Sampler



A NATURAL SAMPLER AND TYPICAL WAVEFORMS

3.1 Waveform Synthesis by Natural Sampling

A natural sampler is a coder. The output is a state function formed by rule from two or three input signals. One input, the signal to be sampled, is compared to periodic sampling waveforms present at the other two inputs. Each of the sampling waveforms influences the output during consecutive intervals of the period. During each interval the output state is determined by the sign of the difference between the associated sampling wave and the input signal. Transitions from one state to another occur when changes in polarity of the difference occur. The sampling waves have slope of constant sign over their respective sampling intervals and may be the two slopes of a single waveform or single slopes of separate waveforms.

A typical example of natural sampling is shown in diagram D 3.1. The input waveform is compared to a triangular wave. The positive slopes of the triangular wave determine when negative changes in the output state predominate while negative slopes of the triangular wave determine when positive steps in the output predominate. In this example the width of the state function waveform between steps indicates the value of the input to the sampler and thus conveys information describing the input signal.

Another form of natural sampling can produce an output with pulses of nominally constant width but with variable phase. The information describing the input signal is contained in the phase of the pulse relative to the sampling waveforms rather than in the width of the pulse.

3.1.1 A Mathematical Description of Natural Sampling

An input signal, $e_{in}(t)$, and monotonic sampling waves, $S_1(ft)$ and $S_2(ft)$, are used in a natural sampler. An error signal $E_K(t)$ is produced by the difference between $e_{in}(t)$ and $S_K(ft)$ where $K = 1, 2$. ($K = 2$ when $\frac{dS_K(ft)}{dt} > 0$)

Thus

$$E_K(t) = e_{in}(t) - S_K(ft) \quad K = 1, 2$$

A change in output from one state to another takes place when the error signal is zero. The direction of the change of state is indicated by $\frac{dE(t)}{dt}$] $E(t) = 0$. The sign, P, of the direction of change in output is given by $P = \text{sign} \left\{ \alpha_K \frac{dE_K(t)}{dt} \right\}$] $E_K(t) = 0$ } $K = 1, 2$,

where $\alpha_1 = -\alpha_2 = 1$ for pulse phase modulated signals and $\alpha_1 = \alpha_2 = 1$ for pulse width modulated signals.

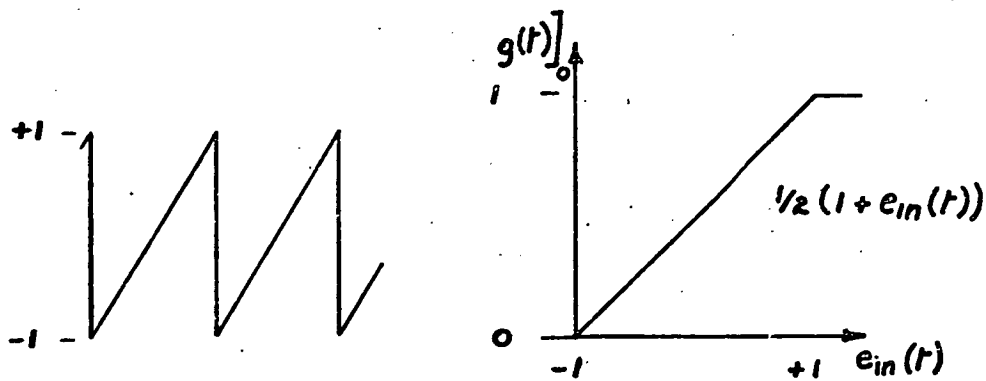
It is shown in appendix A 3.1.1 that a state function $g(t)$ of the form below has the desired properties for a natural sampler.

$$g(t) = S_2^{-1} [e(t)] - S_1^{-1} [e(t)] + \sum_{n=1}^{\infty} \frac{1}{n\pi} \left\{ \sin 2\pi n (ft - S_1^{-1} [e(t)]) - \sin 2\pi n (ft - S_2^{-1} [e(t)]) \right\}$$

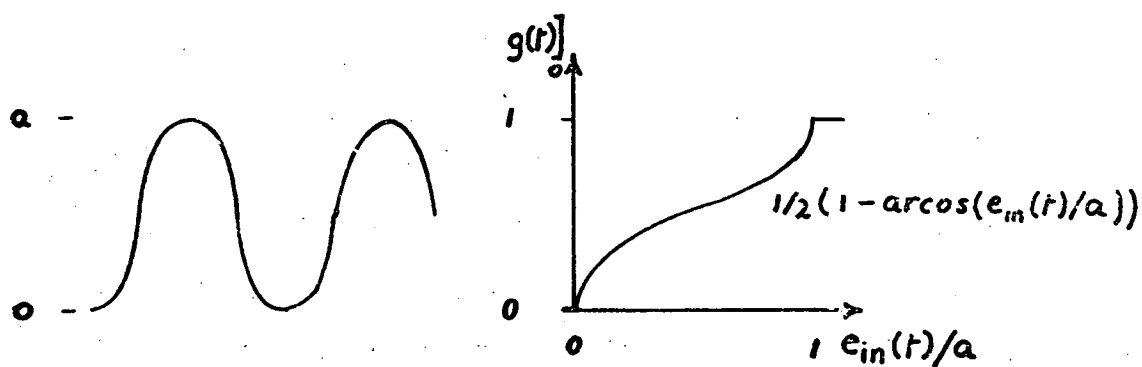
where $S_K^{-1} [x] = \frac{\phi}{2\pi}$ is the inverse function of $S_K(\phi) = x$. In the derivation of this expression some restrictions on the form of the sampling waves and the range of inputs which may be modulated are necessary.

The sampling waves must have constant polarity of slope for the range of input signals to be coded. This is necessary since the inverse functions cannot be adequately defined otherwise. Also over the range of input signals to be coded the sampling waves must not intersect one another. These restrictions are derived in appendix A 3.1.1a.

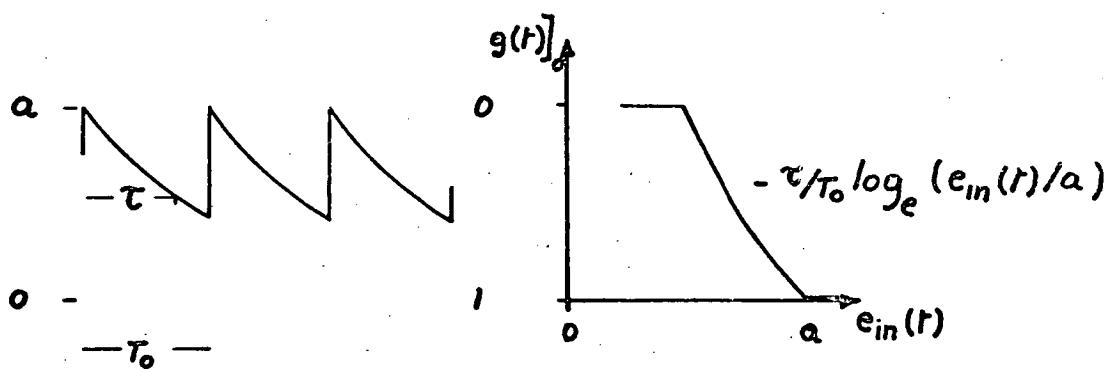
The component of the state function described by $S_1^{-1} [e(t)] - S_2^{-1} [e(t)]$ is the only component of the state function independent of the sampling frequency. The component has a simple functional relationship between its amplitude and the amplitude of the input signal. The form of this relationship depends on the spacing of the sampling waves for a given amplitude of both. For pure phase



Linear



Cosine



Exponential

SAMPLING WAVES AND TRANSFER FUNCTIONS

modulation the component is fixed and does not vary with the input signal. For pulse width modulation the transfer function between input and component amplitude has a fixed part and a part with constant polarity of slope. Typical examples of sampling waveforms and transfer functions are shown in diagram D 3.1.1 where $g(t)]_0$ denotes the component $S_1^{-1}[e(t)] - S_2^{-1}[e(t)]$.

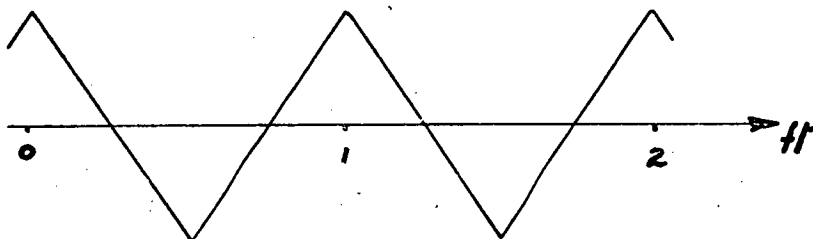
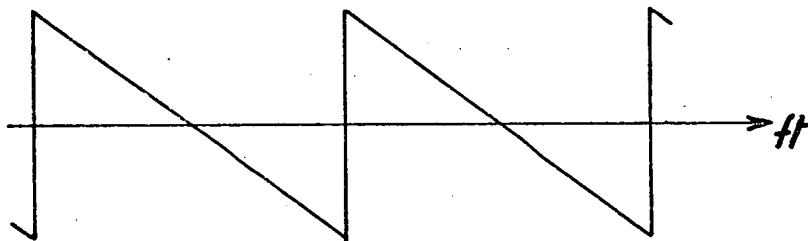
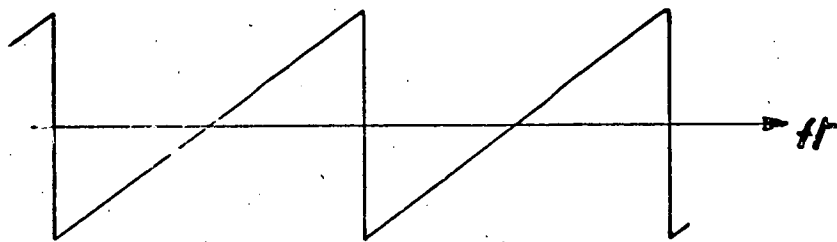
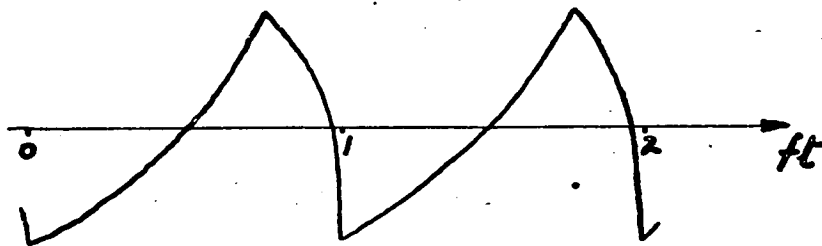
The other components of the coder output waveform are sidebands of the frequency of the sampling wave and its harmonics. Natural sampling of both pulse phase and pulse width types produce sidebands due to phase modulation. The modulation angle θ is related to the input by the equation

$$\theta = 2\pi n S_K^{-1}[e(t)]$$

where n is the number of the sampling wave frequency harmonic. When θ and $e(t)$ are linearly related the sidebands may be described in terms of harmonics of the input frequency but this is difficult for inputs other than sinewaves. When $S_K(ft)$ is not linear the sidebands are very difficult to describe in terms of harmonics of the input signal.

One indication of the bandwidth of the sidebands of a phase modulated signal is provided by the instantaneous frequency of the modulating signal. The instantaneous frequency is given by

$$\begin{aligned} f_i &= \frac{d}{dt} (2\pi n (ft - S_1^{-1}[e(t)])) \\ &= 2\pi n (f - \frac{d S_1^{-1}[e(t)]}{dt}) \\ &= 2\pi n (f - \frac{d S_1^{-1}[e(t)]}{d e(t)} \cdot \frac{d e(t)}{dt}) \\ &= 2\pi n (f - f \frac{e'(t)}{S_1'(ft)}) \Big|_{S_1(ft) = e(t)}. \end{aligned}$$



EXAMPLES OF SAMPLING WAVEFORMS FOR LINEAR
TRANSFER FUNCTIONS

D 3.1.2a

When this is zero the slope of the sampling wave and the input signal are the same. This criterion of equal slopes of input and sampling wave is useful for comparison of different natural samplers but is of little use in filter design for the switching waves produced by switches controlled by natural sampling.

3.1.2 Node Voltage Components Produced by Switches Controlled by Natural Sampling D.C. Supply Voltage.

A d.c. supply voltage, V_i , when modulated by a switch state function, $g_i(t)$, produced by natural sampling, with sampling waves $S_1(ft)$ and $S_2(ft)$, gives a node voltage component $V_{ni}(t)$ described by

$$V_{ni}(t) = V_i \left\{ S_2^{-1} [e(t)] - S_1^{-1} [e(t)] + \sum_{n=1}^{\infty} \frac{1}{n\pi} (\sin 2\pi n (ft - S_1^{-1} [e(t)]) - \sin 2\pi n (ft - S_2^{-1} [e(t)])) \right\}$$

Provided $e(t)$ lies between the maxima of the sampling waves and the minima of the sampling waves the terms $V_{ni}(t)$, $V_{ni}]_0$, corresponding to the input signal are described by

$$V_{ni}]_0 = (S_2^{-1} [e(t)] - S_1^{-1} [e(t)]) V_i.$$

Thus the requirement for linearity imposes the restriction on $S_1(ft)$ and $S_2(ft)$ defined by

$$V_i (S_2^{-1} [e(t)] - S_1^{-1} [e(t)]) = K_i e(t) + C_i$$

or

$$S_2^{-1} [e(t)] - S_1^{-1} [e(t)] = K_i \left(\frac{e(t)}{V_i} \right) + \left(\frac{C_i}{V_i} \right)$$

If the form of either $S_1(ft)$ or $S_2(ft)$ is chosen then the form of the other is determined by the expression. Several forms of sampling waves are shown in diagram D 3.1.2a. The last three are commonly used waveforms. The first waveform is to demonstrate the arbitrary nature of waveforms which may be chosen to satisfy the linearity conditions.

The two higher frequency components of V_{ni} centered about the fundamental and harmonics of the sampling wave frequency are influenced by the shape of the sampling waves. Since the filtering of the switching wave must suppress these components as strongly as possible, the distribution of energy in the sidebands of the sampling wave frequency is important. The choice of sampling wave shape is thus influenced by this criterion after the condition for linearity is satisfied.

In order to choose a "best" sampling wave the instantaneous frequency criterion referred to earlier may be used. This expression would give the highest instantaneous frequency to a sampling waveform with maximum slope since this would allow the greatest band width of input signal before the instantaneous frequency of the sidebands becomes zero. This would suggest that a symmetrical triangular wave sampling is the best form of sampling wave.

A.C. Supply Voltages

When supply voltages other than d.c. are used two distinct switch state functions may be used. If the repetition rate of the supply voltage and the switch state function are the same then their frequencies are said to be commensurate otherwise they are non commensurate. When non commensurate switching is used with natural samplers as coders, difference frequencies are produced in the output. This is usually undesirable and a modified form of natural sampling which reduces these difference frequencies is normally employed instead of natural sampling. The most common situation is that where commensurate natural sampling is used.

Commensurate switch control for linear amplification based on natural sampling may take two forms. The first, in which variable pulse width switch state functions are used, is analogous to the method used for d.c. signals. The second method is based on nominally constant

width pulses whose phase, relative to the supply voltage, is varied to change the output component. To produce linear amplification the relationships between the wave shape of the supply voltage $V_i(t)$ and the sampling waves $S_{K_i}(ft)$ may be determined explicitly.

It is shown in appendix A 3.1.2b that a switch state function, $g_i(t)$, defined by sampling waves $S_1(ft)$ and $S_2(ft)$ and a control voltage, $e(t)$, may be used to modulate a supply voltage, $V_i(ft)$, so that the node voltage component $V_{ni}]_0$ obeys the linearity equation

$$V_{ni}]_0 = K_i e(t) + C_i$$

provided
$$\int_{ft=0}^{ft=x} V_i(ft) d(ft) = \frac{S_1(x) - B_1}{A_1} = \frac{S_2(x) - B_2}{A_2}$$

where

$$0 < x < 1$$

and

$$K_i = \left[\frac{1}{A_1} - \frac{1}{A_2} \right], \quad \frac{B_1}{A_1} - \frac{B_2}{A_2} = C_i$$

This solution suggests that the shape of the sampling wave be determined from the integral of the supply voltage waveshape. **Because** the definition of $S_K(ft)$ requires that the slope is monotonic over the sampling interval the supply voltage zeros of amplitude will determine these interval limits since the slopes will be zero when the supply voltage is zero. If the waveform has more than one pair of zeros per period then there will be more than one pair of sampling waves per period. Each pair may be considered as belonging to a separate natural sampler. The state function formed to control the switch is then the sum of the state function outputs of the natural samplers.

The output of each coder is associated with the interval between two consecutive zeros of the supply voltage. Between each pair of zeros the integral of the supply voltage waveshape will have monotonic slopes of opposite polarity of slope. This means that the sampling

wave co-efficients A_1 and A_2 will have the same sign for pulse width modulation but opposite sign for pulse phase modulation.

For given values of A_1 and A_2 the maximum output range is available when both extremes of the range are set by the amplitude of a single sampling wave. This can be arranged by suitable choice of B_1 and B_2 .

The difference between consecutive maxima and minima of the integral of the supply voltage will not be equal if the waveform contains a d.c. component over the interval. The larger difference is referred to as D_2 and the smaller as D_1 below. The variable α defined by

$$\alpha = \left| \frac{D_1}{D_2} \right| \text{ is by the definition of } D_1 \text{ and } D_2$$

restricted to the range $0 \leq \alpha \leq 1$. The maximum range of input Δe_{in} is described by

$$\begin{aligned} \Delta e_{in} &= \text{max.value of } \left\{ \begin{array}{l} (\text{min.value of } |A_1 D_1| \text{ and } |A_3 D_2|) \text{ and} \\ (\text{min.value of } |A_1 D_2| \text{ and } |A_2 D_2|) \end{array} \right\} \\ &= |A_2 D_2| \times \left(\text{max.value of } \left\{ \begin{array}{l} (\text{min.value of } |B| \text{ and } 1) \text{ and} \\ (\text{min.value of } |B| \text{ and } \alpha) \end{array} \right\} \right) \\ \text{where } B &= \frac{A_1}{A_2} \\ &= |A_2 D_2| \cdot \left\{ \begin{array}{ll} 1 & \text{if } |B| > \frac{1}{\alpha} \\ \alpha |B| & \text{if } 1 < |B| < \frac{1}{\alpha} \\ \alpha & \text{if } \alpha < |B| < 1 \\ |B| & \text{if } |B| < \alpha \end{array} \right\} \end{aligned}$$

The maximum value of input range and the value of K_i determines the output range. By suitable choice of A_1 and A_2 the maximum output range for a given situation may be determined from

$$\Delta V_{ni}]_0 \text{ maximum} = \Delta e_{in} \times \left| \frac{1}{A_2} - \frac{1}{A_1} \right|$$

The maximum output from pulse width and pulse phase modulations for different situations are tabulated below.

Restriction on $\frac{A_1}{A_2}$ relative to $\frac{D_1}{D_2}$	Condition for, an maximum output range with expression for Ki.					
	Pulse Width Modulation			Pulse Phase Modulation		
	Condition	Output	Ki	Condition	Output	Ki
$\left \frac{A_1}{A_2} \right > \left \frac{D_2}{D_1} \right $	$\frac{A_2}{A_1} = 0$	$ D_2 $	$\frac{1}{A_2}$	$\frac{A_1}{A_2} = \frac{D_2}{D_1}$	$ D_2 + D_1 $	$\frac{-1}{A_1} \left[\frac{ D_2 + D_1 }{ D_1 } \right]$
$1 < \left \frac{A_1}{A_2} \right < \left \frac{D_2}{D_1} \right $	$\frac{A_2}{A_1} = \left \frac{D_1}{D_2} \right $	$ D_2 - D_1 $	$\frac{1}{A_2} \left[\frac{1 + D_1}{D_2} \right]$	$\frac{A_1}{A_2} = \frac{D_2}{D_1}$	$ D_2 + D_1 $	$\frac{-1}{A_1} \left[\frac{ D_2 + D_1 }{ D_1 } \right]$
$\left \frac{D_1}{D_2} \right < \left \frac{A_1}{A_2} \right < 1$	$\frac{A_1}{A_2} = \left \frac{D_1}{D_2} \right $	$ D_2 - D_1 $	$\frac{1}{A_1} \left[\frac{-D_1}{D_2} - 1 \right]$	$\frac{A_2}{A_1} = \frac{D_2}{D_1}$	$ D_2 + D_1 $	$\frac{1}{A_1} \left[\frac{ D_2 + D_1 }{ D_2 } \right]$
$\left \frac{A_1}{A_2} \right < \left \frac{D_1}{D_2} \right $	$\frac{A_1}{A_2} = 0$	$ D_2 $	$\frac{1}{A_1} \left[-1 \right]$	$\frac{A_1}{A_2} = \frac{D_1}{D_2}$	$ D_2 + D_1 $	$\frac{1}{A_1} \left[\frac{ D_2 + D_1 }{ D_2 } \right]$

Because D_1 and D_2 are normalised changes in the integral of the supply voltage they represent minimum and maximum average values for the positive and negative portions of the supply voltage. The maximum range of output for Pulse Width Modulation is thus only half that for Pulse Phase Modulation for a pure a.c. supply. For a supply voltage which equals but does not cross zero at some point in its cycle the two techniques give the same output range and have the same sampling waveforms. For supply voltages of constant polarity the restrictions used to obtain the sampling wave intervals and ranges do not apply since the slope of the integral will have constant polarity. For this case maximum output range for pulse width modulation is the maximum possible. Pulse phase modulation for maximum output is a limiting case of the possible forms of Pulse Width Modulation.

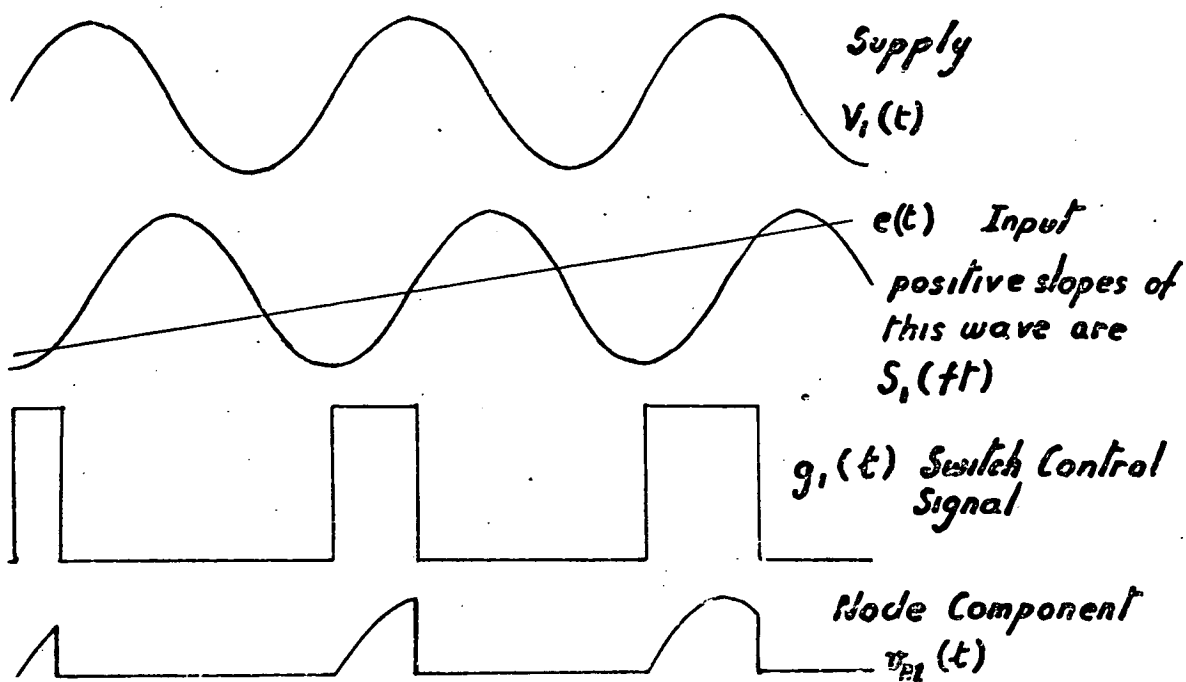
From the discussion above it is apparent that pulse width modulation is best suited for constant polarity supply voltages while Pulse Phase Modulation is best suited for supply voltages with alternating polarity.

There is a second method for choosing sampling waveforms for pure phase modulation. The switch state function for pure phase modulation is described by $g(t)$ where

$$g(t) = \alpha + \sum_{n=1}^{n=\infty} \frac{1}{n\pi} \left\{ \sin 2\pi n(ft - S_1^{-1}[e(t)]) - \sin 2\pi n(ft - S_2^{-1}[e(t)]) \right\}$$

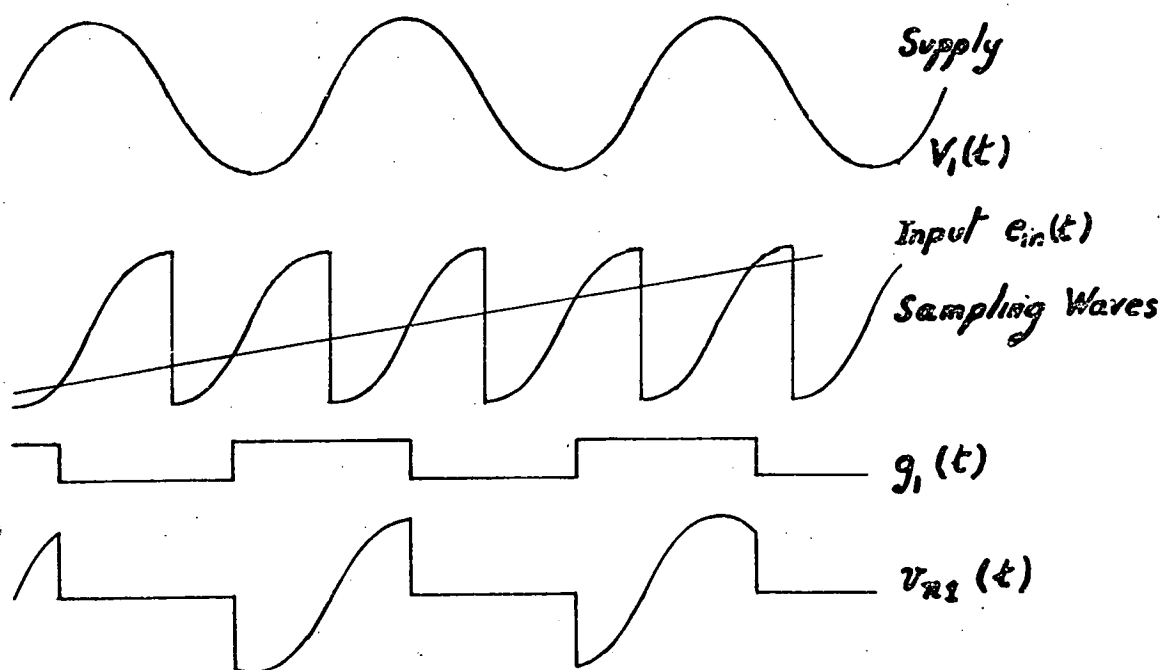
where $S_2^{-1}[e(t)] - S_1^{-1}[e(t)] = \alpha$

The restriction on $S_1(ft)$ and $S_2(ft)$ to have identical waveforms shifted in time by $(\frac{\alpha}{f})$ defines a sampling waveform derived from the supply voltage waveform but transformed in a different manner to an integral. If the supply voltage is described by $V_i(ft) = a_0 + \sum_{n=1}^{n=\infty} a_n \cdot \sin [2\pi n ft + \phi_n]$, then the



A NODE COMPONENT FORMED BY
PULSE WIDTH MODULATION

D 3-1-2 b



A NODE COMPONENT FORMED BY PULSE PHASE
MODULATION

D 3-1-2 c

sampling waves which produce a node voltage according to the linearity condition,

$$V_{ni}]_0 = K_i \cdot e(t) + C_i, \text{ are described by}$$

$$S_K(ft) \text{ where } S_K(ft) = \left(\frac{-1}{K_i}\right)^K \left\{ \alpha \cdot a_{0-C_i} + \sum_{n=1}^{n=\infty} \frac{a_n}{n\pi} \cdot \left\{ \sin \left(2\pi n(ft + (-1)^{K+1} \frac{\alpha}{2} + \phi_n \right) \right\} \cdot \sin n\pi\alpha \right\} \text{ for } K=1 \text{ and } 2.$$

The harmonic amplitudes of the supply voltage are transformed in a similar manner to integration but apart from a shift in time their phase is not altered. ($S_2(ft)$ is the negative slope of the above waveform). As an example consider a supply voltage $V_i(ft) = \sin(2\pi ft)$. Then

$$S_K(x) = \frac{A_K}{2\pi} \left[1 - \cos 2\pi x \right] + B_i \quad 0 < x < 1$$

Now $S_1(x)$ has a negative slope while $S_2(x)$ has a positive slope if pulse width modulation is used. If $S_2(x)$ is the sampling wave for $0 < x < \frac{1}{2}$ and $S_2(x)$ is the sampling wave for $\frac{1}{2} < x < 1$ then A_1 and A_2 are positive. To produce a node component $V_{ni}]_0$ of the form

$$V_{ni}]_0 = e(t) \text{ the values of } A_1, A_2, B_1, \text{ and } B_2 \text{ are related by}$$

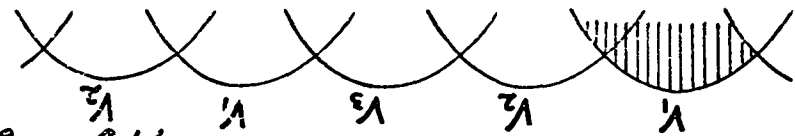
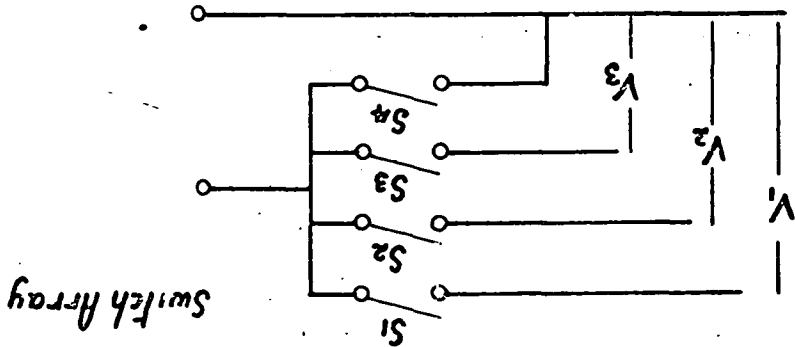
$$\frac{1}{A_2} - \frac{1}{A_1} = 1 \text{ and } \frac{B_1}{A_1} = \frac{B_2}{A_2}$$

For maximum output

with $A_2 = 1$ and $B_2 = 0$, then $A_1 = \infty$ and $B_1 = 0$.

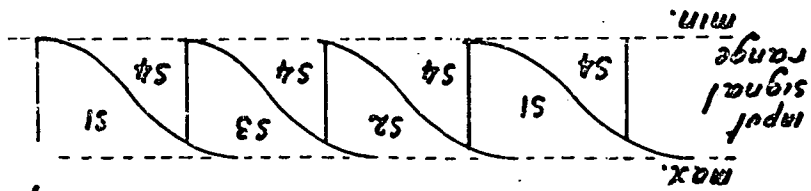
An input variation from $0 \rightarrow \frac{1}{\pi}$ will produce a change in output from $0 \rightarrow \frac{1}{\pi}$. This can be seen in diagram D 3.1.2b, where supply voltage, sampling waves, switch state function and node voltage are shown for an input in the centre of the range.

The solution above is optimum for pulse width modulation. The equivalent pulse phase modulation



Supply Voltage Waveforms

Sampling Wave Diagram



EXAMPLE OF SAMPLING WAVE DIAGRAM

system has $A_1 = A_2 = \frac{1}{2\pi}$, $B_1 = B_2 = 0$. The input variation from $-\frac{1}{\pi}$ to $+\frac{1}{\pi}$ will produce a change in output component from $-\frac{1}{\pi}$ to $+\frac{1}{\pi}$. The corresponding waveforms to those for the example above form diagram D 3.1.2c.

3.1.3 Assembly of Node Components Linearly Dependent on the Input Signal

A total node voltage is formed by summing the components. A convenient method for visualizing the node voltage component contributions, when natural sampling is used, is a diagram showing all the sampling waves for one period of a wave. An example of such a diagram for the situation with three symmetrical supply voltages is diagram D 3.1.3a. (The situation shown is typical of thyristor arrays for unidirectional current output). Each area of the diagram is labeled with the conducting switch. For any pair of parameters, input voltage and phase angle, one and only one switch should be on. This is the original restriction on the different switch states. In terms of the diagram this means that between the input voltage limits the sampling waves should not cross nor should any area represent no switch connected to the node. The supply voltages and resultant node voltage are shown for an input signal over one period of the sampling waves.

The diagram above shows one period of each of the sampling waves. In theory it is possible that sampling waves be harmonics of a fundamental frequency. Although such a case does not occur commonly the sampling waves forming the diagram could be drawn and the diagram would represent several periods of all except the lowest frequency sampling wave or waves.

For the example shown above the sampling waveshapes were determined by the integral of the

effective supply voltage waveshape for each switch. The shaded area of the supply voltage indicates the effective value. This was dictated by the turning off characteristics of thyristors. Notice that each node component is formed by a combination of pulse width and pulse phase modulations, as a result of this limitation.

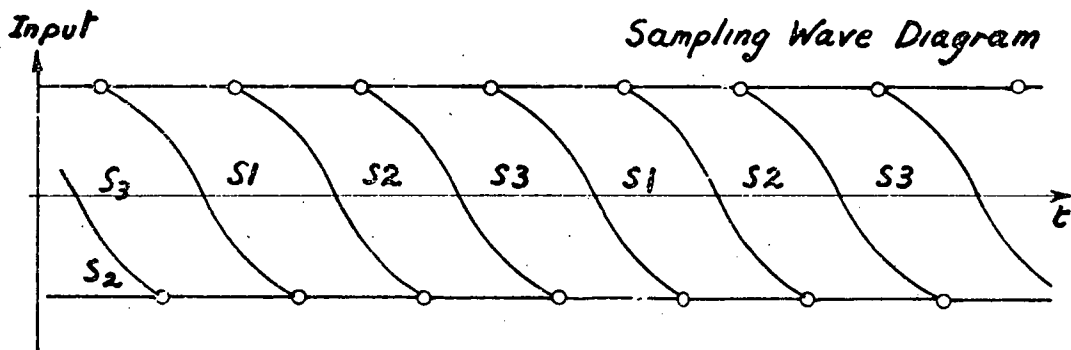
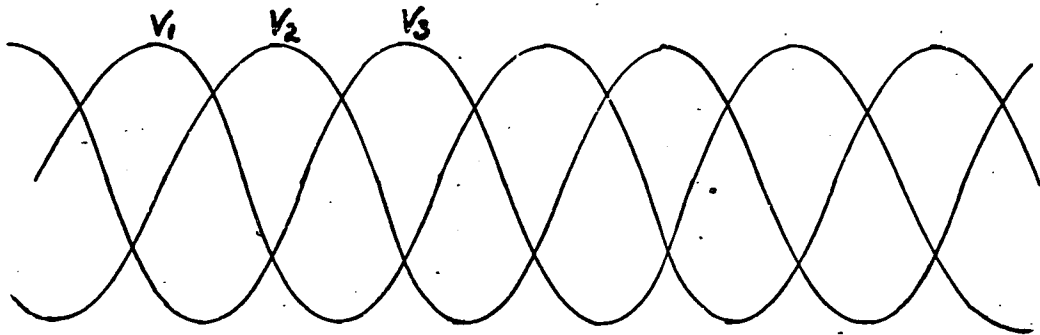
If it is desired to obtain a maximum range of output from a switching amplifier, for a given set of supply voltages, then some of the supply voltages may not be needed. This is illustrated for the case where each node voltage component is linearly related to the input signal by the following argument.

The maximum output voltage at a node is obtained when the node voltage is equal to $V_{\max}(t)$, the maximum of the supply voltages. Similarly the output voltage is minimum when the node voltage is equal to $V_{\min}(t)$, the minimum of the supply voltages. These two limiting node voltages define the limiting values of each node voltage component. If a supply voltage is not connected by a switch to the node at either of these limits then the contribution of that voltage to the node voltage is zero for maximum and minimum input signals. Since the mean voltage due to any component is linearly related to the input voltage this implies that such a supply voltage contributes nothing to the mean node voltage for any input value.

This has important consequences for switching amplifiers operating from d.c. supplies. If more than two supply voltages are available then for maximum output range of the amplifier only the two extreme voltages should be connected to the node if each supply and switch contributes linearly to the output voltage.

For switching amplifiers with a.c. supply voltages the situation is not so simple; however if a

Supply Voltage Waveforms



S_1 , S_2 , and S_3 are the switches conducting.

A SAMPLING WAVE DIAGRAM FOR MAXIMUM OUTPUT RANGE

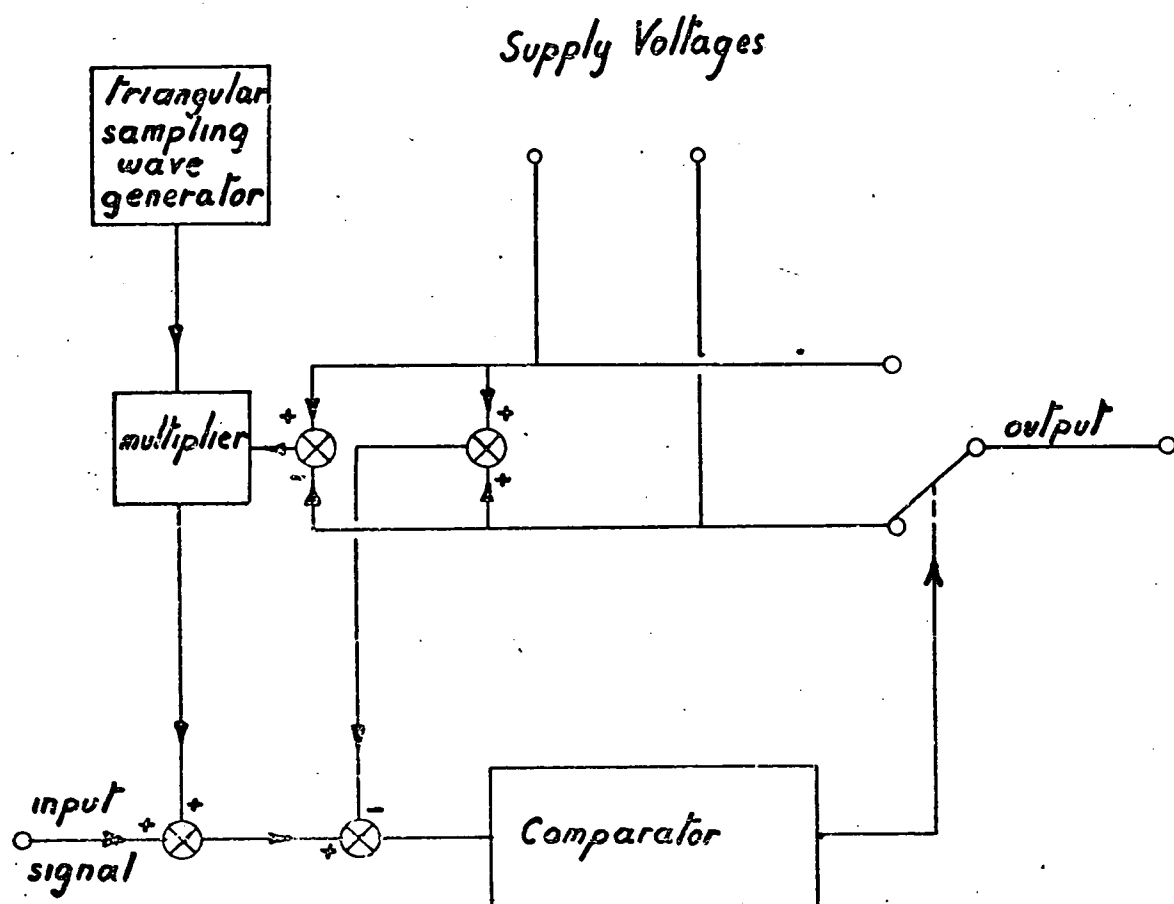
D 3.1.36

supply voltage does not form part of the envelope of the supply voltage waveforms then it may be replaced, with no effect on the output voltage range by a switch to the zero voltage supply.

If maximum output voltage range of a switching amplifier is used as a design criterion then because this defines the contribution of each switch at two input signal levels the sampling waveforms for each switch are defined by the linearity condition. An example of this method of choosing sampling waveforms is shown in diagram D 3.1.3b. In this example the sampling waves are those for natural phase modulation so that the limits are symmetrical except for a phase shift. Because of the supply voltage symmetry all sampling waves are the same shape differing only in phase.

In some situations symmetry of sampling waves does not occur and since sampling waves for each switch cannot cross this may sometimes restrict the output range by requiring switches other than those connecting supply voltages forming the envelope to be closed. Other conditions may arise when sampling waves would be required to cross each other. In this situation a dead band between sampling waves is achieved by earthing the node over a narrow band of the diagram.

When a switching amplifier output is not required to vary over a maximum output range the restrictions on sampling waveforms are not sufficient to produce a unique solution. The final switching waveform is then determined by the switch characteristics or by minimisation of undesired output components in the switching wave.



SELF ADAPTING AMPLIFIER

D 3.1.4

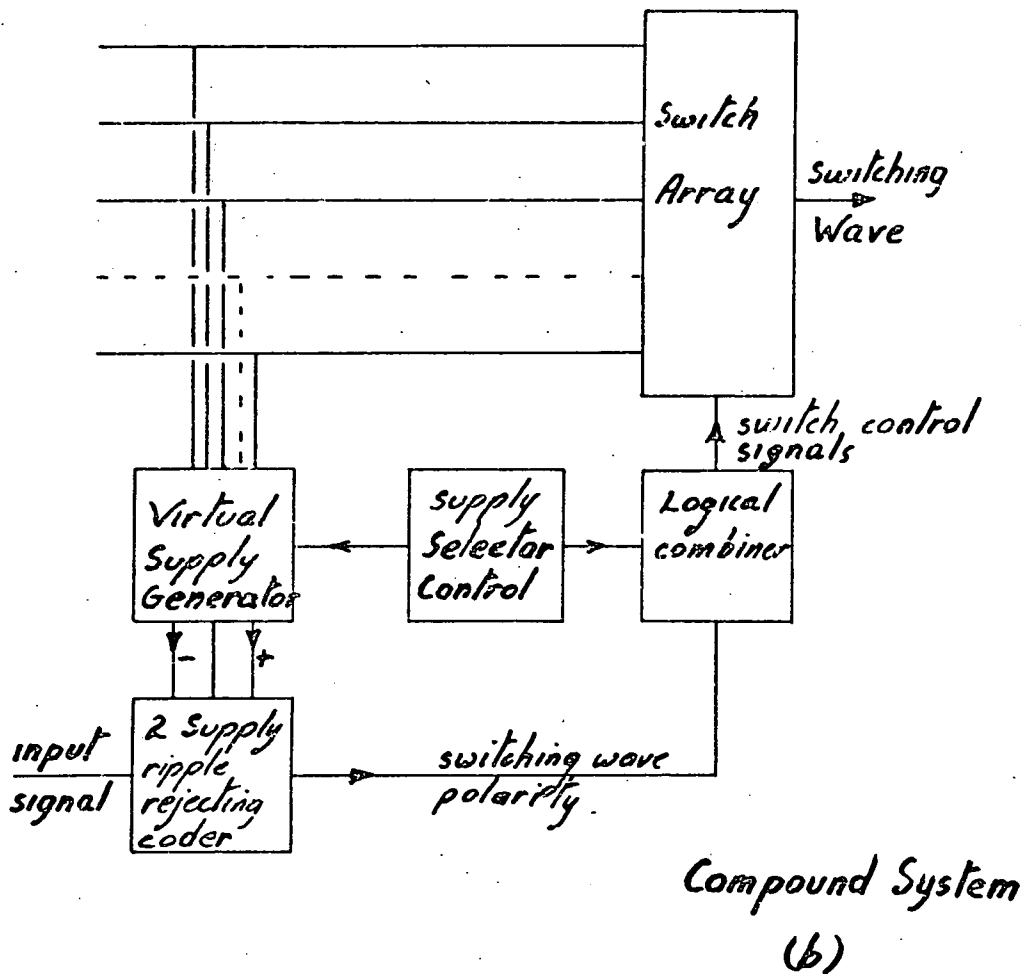
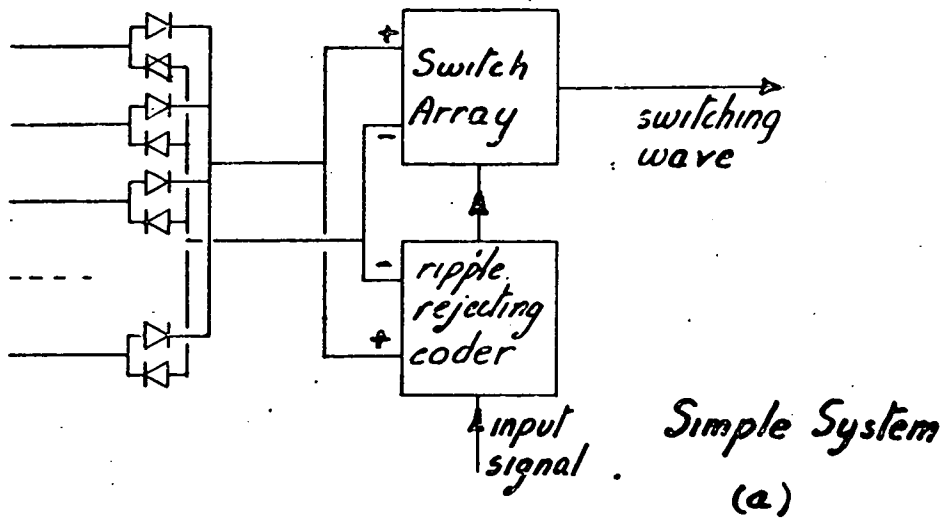
3.1.4 A New Form of Encoder

3.1.4.1 A Switching Wave with Two Arbitrary Levels

The natural sampling discussed previously was based on sampling rates commensurate with the frequencies of any a.c. components of the waveform levels. The following version of a switching wave controlled by natural sampling relies on these frequencies being separated. The method is subject to the usual restrictions outlined in a previous chapter but within these is capable of providing linear amplification with arbitrary waveform levels.

It is shown in appendix A 3.1.4 that two waveform levels, not having components commensurate with the sampling frequency, may be used to provide linear amplification. A linear natural sampler, intended to control the switching between two equal d.c. levels of opposite sign is modified so that, first, the sampling waveforms are amplitude modulated by the difference in the waveform levels, and second, a component equal to the average of the two levels is subtracted from the input signal. The block diagram D 3.1.4 illustrates the case where the sampling waves are opposite slopes of a triangular wave.

An intuitive model is easily formed by realising that the amplitude of the output is directly modulated by the supplies and the modulation of the sampling wave cancels this. The mean value of the output is then corrected by subtracting the mean of the levels from the input signal.



Ripple Rejecting Systems

D3-1-4-16

3.1.4.2 Supply Waveform Rejection for Complex Waveforms

The two supply amplifiers just outlined may be considered as a second amplifier part which follows a first part. The role of the first part is to select supply waveforms according to some set rule. This is easily envisaged for the case where a rectifier is used to provide the two supply amplifier. The rule in this case is simply that the positive inner amplifier supply is the largest of the available supplies and the negative supply the smallest. The resulting switching wave has levels at each of these inner supply waveforms.

This simple picture is the basis for the amplifier shown in diagram D 3.1.4.1b. Rather than form the supply waveforms for the inner amplifier supplies as outlined in figure 3.1.4.1a it is necessary only to produce waveforms for the coder part of the inner amplifier. A single switch array may then be instructed by the coder and virtual supply encoder to select the appropriate supply for the switching wave. This approach minimises the number of power switching devices required. (It should be appreciated that the use of a simple rectifier supply is not efficient nor approximately ideal when it may be called upon to provide the reactive currents present at a switch array.)

This class of amplifier has a number of freedoms from supply waveform imposed restrictions common to other switching wave generating systems. The major freedom is the choice of effective supply levels. This class of amplifier could for instance produce the minimum energy waveform discussed in section 2.6. This is not feasible by any other method.

The second important freedom is that of

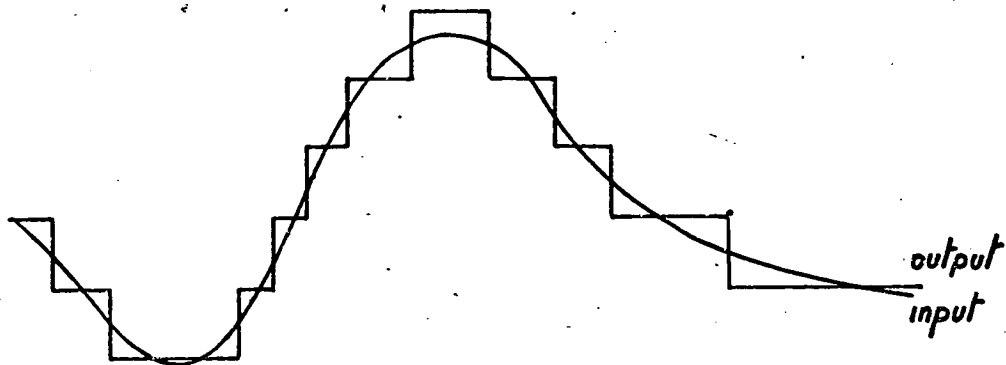
sampling frequency choice. Since the sampling frequency is not restricted to the supply frequency or a harmonic of this frequency, as it is for commensurate sampling, the maximum feasible switching rate may be chosen to minimise filter size and maximise amplifier bandwidth.

There are of course a number of disadvantages or rather limitations. The main such is the arbitrary frequency of switch control signals to any one switch. In some circumstances, such as those where minimum energy waveforms are involved, two opposing control signals may be issued to the same element of the switch array with negligible time separations. This is very often an undesirable feature.

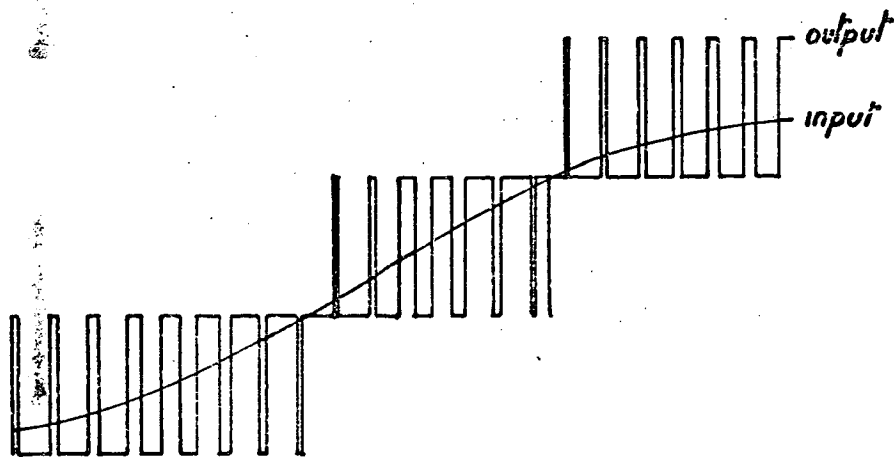
A second limitation in many circumstances is the need for symmetrical bi-directional switch elements.

There is also a cost imposed by added circuit complexity since either analogue signal selection and switching or paralleled input coders with digital signal selection are necessary for the selection of the virtual supplies, and more complex gating is required for the generation of the switch control signal.

The technique has the same rejection of supply waveform changes as the two supply case, namely, rejection of supply waveform amplitude changes, to the point where limiting occurs, rejection of supply waveform frequency changes, and independence to a large degree from supply wave shape changes.



Input and Output Waveforms of a Quantizer



Input and Output Waveforms of a switching Amplifier
based on Natural Sampling

D 3.1.5a

3.1.5 Multi - d.c. - level Switching Waves

A coder and switch array produce a switching wave which is a quantised version of the input signal. This multi level switching wave differs from the input signal by an error signal. If this error is used to control a two level switching amplifier with a linear characteristic then the sum of the two output signals will be a switching wave with a linear relationship between its low frequency component and the input signal. Such a switching wave may in fact be produced by a single switching amplifier by a suitable choice of coders and switch control logic, but the visualization of two separate amplifiers is convenient for the design and understanding of such waveforms. Some examples are shown in diagram D 3.1.5a.

The switching waves produced by quantizer and complete amplifier differ in output spectrums. In the former case the error between the output and the input consists of components with frequencies of d.c. the input signal frequency, and the harmonics of this frequency. In the latter case the error signal consists of components with frequencies at the sampling frequency of the second amplifier, the harmonics of this frequency, and at sidebands of these frequencies due to harmonics of the input signal. In the latter case the separation in frequency of the output desired and the error waveform enables filtering to be used whereas in the former case this is not feasible.

The descriptions of the methods used to produce the waveform and of the type of the waveform spectrum have not included any specification of the type of switching amplifier used to modify the quantizer error. Although any amplifier with a linear characteristic may be used, those most commonly employed are based on natural

sampling. This is due to the simplicity of converting a quantizing coder to a natural sampler; all that is required is that the input signal have a suitable sampling wave added to it.

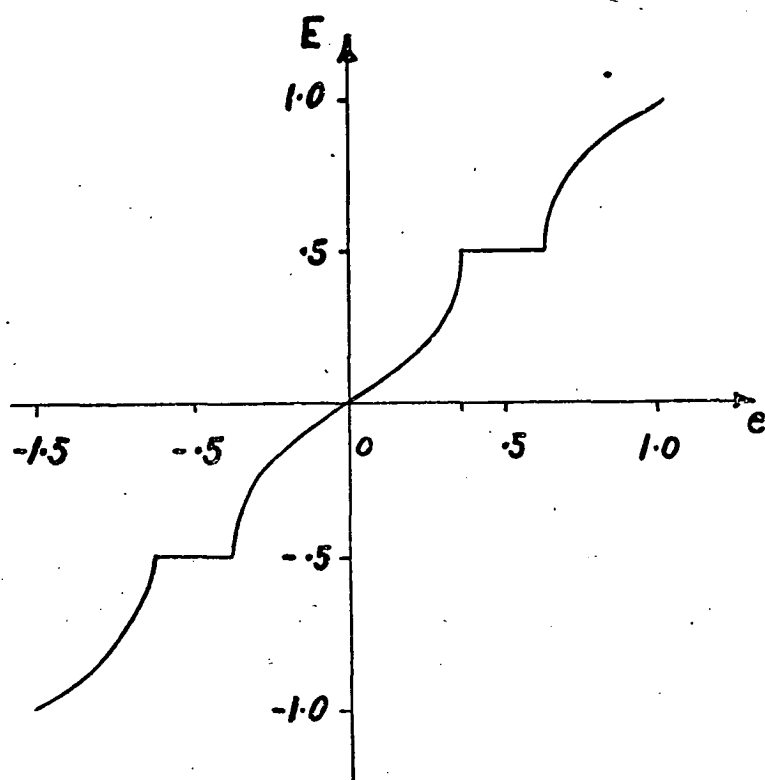
In appendix A 3.1.5a the conditions for a perturbation signal added to the input signal of a quantizer to give a linear characteristic are derived. The perturbation signal must have the following characteristics. First, it must have a linear probability distribution between maximum and minimum amplitudes. Second, it must have maxima and minima which differ by one or more steps of the quantizer input. Third, it must have zero d.c. component. Finally, it must have a lowest frequency component such that sidebands due to harmonics of the highest input frequency are of greater frequency than the input signal.

Although these requirements of the perturbation signal do not define a waveform they are adequate for the purpose of deciding whether a particular waveform is suitable. It is conceivable that a noise signal could satisfy all the requirements but this would not give natural sampling since the waveform is not periodic. Waveforms such as the triangular and sawtooth shapes with suitable amplitudes will give natural sampling and also satisfy the requirements.

Linearity and Perturbation Properties

The requirements of sampling waves just dealt with may be understood with the aid of the following description of the relationship between the probability distribution of perturbation amplitude and the transfer characteristic of the system. In appendix A 3.1.5b the low frequency components of the sampling wave are shown to be described by

$$E = e + (\frac{1}{2} - l - p_{\max}) - \sum_{m=0}^{m=k-1} P(m-l) + C$$



AMPLIFIER CHARACTERISTIC WITH SINEWAVE
PERTURBATION

D3.1.5 b

where these symbols have the following meanings:

e is the input signal normalised at one unit per quantizer step;

p_{\max} is the maximum value of the normalised perturbation signal;

k is the integer less than or equal to the minimum value of the perturbation signal;

ℓ is a variable such that

$$-p_{\max} < e - E_n = \ell < 1 - p_{\max} \text{ for } E_n \text{ an integer;}$$

$P(x)$ is the probability that the perturbation signal is less than x ;

C is a constant equal to the sum of the average of the perturbation waveform and the average of $k \cdot P(x)$ over the range of x such that

$$p_{\max} - k < x < p_{\max}.$$

To illustrate these parameters and their use consider a sinewave perturbation with amplitude, a , less than half a quantizer step. The probability that the perturbation is less than x is

$$P(x) = \begin{cases} 1 & \text{if } x < a \\ 1/2 + \frac{\arcsin(x/a)}{\pi} & \text{if } -a \leq x \leq a \\ 0 & \text{if } -a < x \end{cases}$$

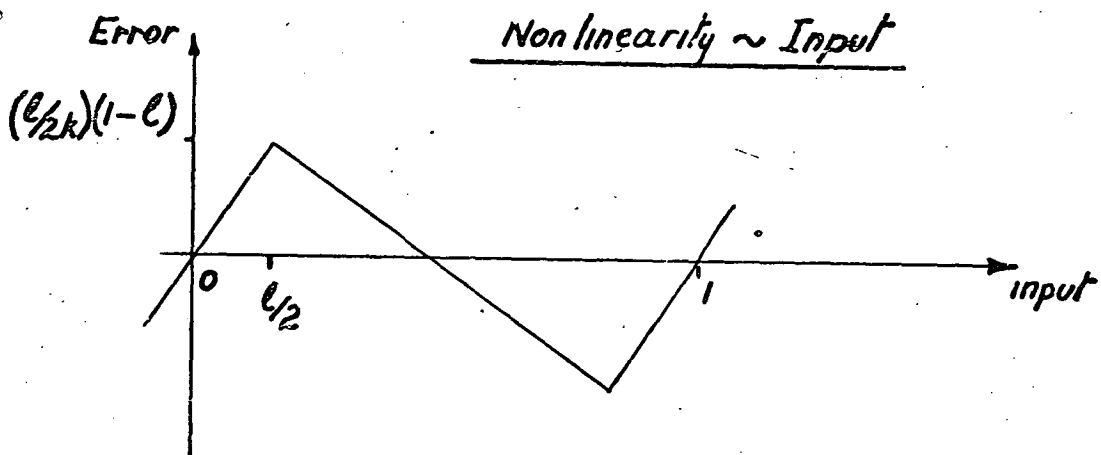
The other parameters are:

$$p_{\max} = C = a; \quad k = 0.$$

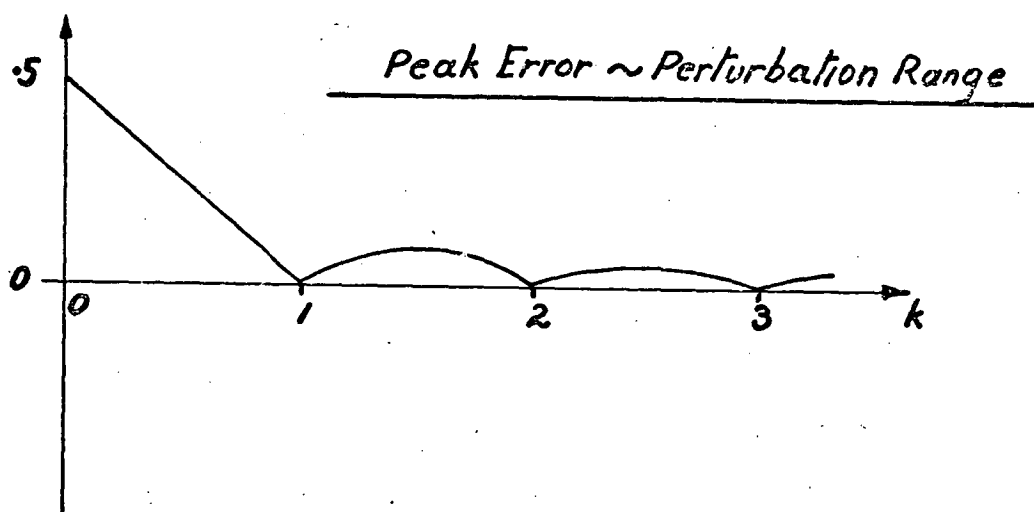
The characteristic is

$$E = E_n + 1/2 - P(-\ell).$$

Diagram D.3.1.5b shows how the requirements for the perturbation apply by illustrating the characteristic for a case where some are invalid. The perturbation peak to peak amplitude controls the width of the flat regions corresponding to the original quantizer characteristics. A peak to peak amplitude equal to an integer multiple of one quantizer step eliminates these



D 3.1.5c



D 3.1.5d

regions. The probability distribution of amplitude controls the shape of the characteristic. A linear distribution gives a linear characteristic.

The Sensitivity to Perturbation Amplitude

When a perturbation with a linear amplitude distribution is used it is important to maintain the peak to peak amplitude near an integer multiple of one quantizer step. The form of the nonlinearity when the perturbation peak to peak amplitude is not the above is examined in appendix A 3.1.5c. Diagram D 3.1.5c illustrates the deviation.

The deviation is a periodic triangular wave with respect to e . The amplitude of the wave as a function of perturbation peak to peak amplitude, k , is shown in diagram D 3.1.5d. The function shown has minima at integer values of k . The slope of the function on either side of an integer value of k is a measure of the sensitivity of linearity to perturbation amplitude. If this slope is normalised with respect to the perturbation amplitude the peak nonlinearity as a function of percentage change in perturbation amplitude is obtained. The relationship is

$$\text{peak error} = (1/2), |\Delta k/k|$$

This sensitivity indicates that peak error near an integer value of k is half the percentage deviation of k from an integer value.

Output Waveforms with Natural Sampling

The complete description of the switching waves produced by ramp and symmetrical triangular sampling waves satisfying the linearity conditions are derived in appendix A 3.1.5d. The expressions are valid for sampling waves with peak to peak amplitudes of k quantizer steps for k an integer. The expressions

for the perturbation and associated output waveforms are given by:

$$p(t) = -k \sum_{n=1}^{\infty} \frac{\sin(n(wpt - \pi))}{(n\pi)},$$

$$e_o = e + \sum_{n=1}^{\infty} \left[\frac{\sin(n(kwpt + 2\pi e)) - k \sin(n(wpt - \pi))}{(n\pi)} \right],$$

$$p(t) = -k \sum_{n=1,3}^{\infty} \frac{4 \cos(mwpt)}{(n\pi)^2},$$

$$e_o = e + \sum_{n=1}^{\infty} \frac{2 \sin(\pi n(e + \frac{1}{2})) \cos(nwpt)}{(n\pi)}, \quad \text{if } k=1.$$

or

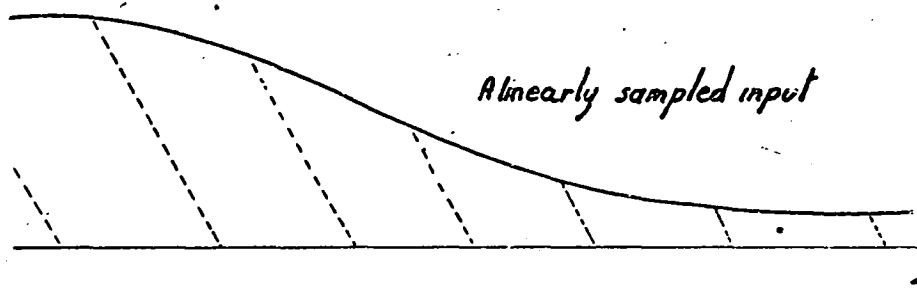
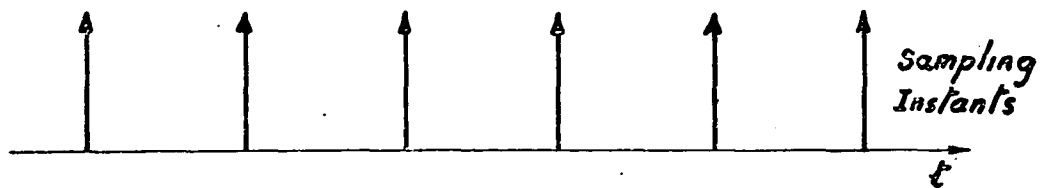
$$e_o = e + \sum_{m=2,4}^{\infty} \left[\frac{2 \sin(m\pi(e + \frac{k}{2})) \cos(mkwpt)}{(m\pi)} \right]$$

$$+ \sum_{m=1,3}^{\infty} \left[\frac{2 \sin((\frac{m\pi}{k})(e + \frac{1}{2})) \cdot (\sin(\frac{m\pi}{2}) / \sin(\frac{m\pi}{2k}))}{(m\pi)} \right]$$

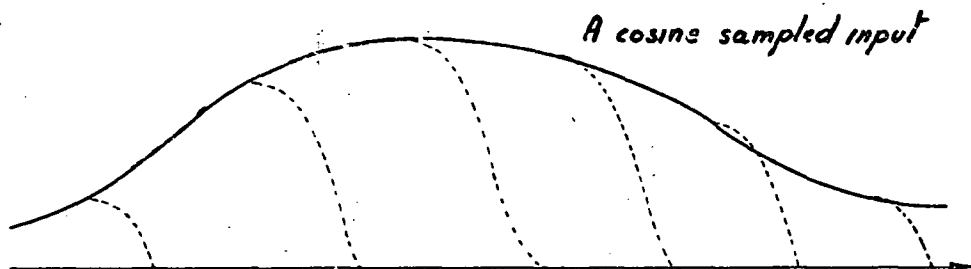
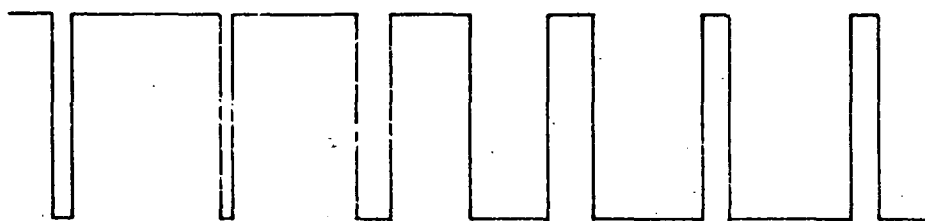
$$\cdot \cos(mwpt) / (m\pi).$$

for all values of k .

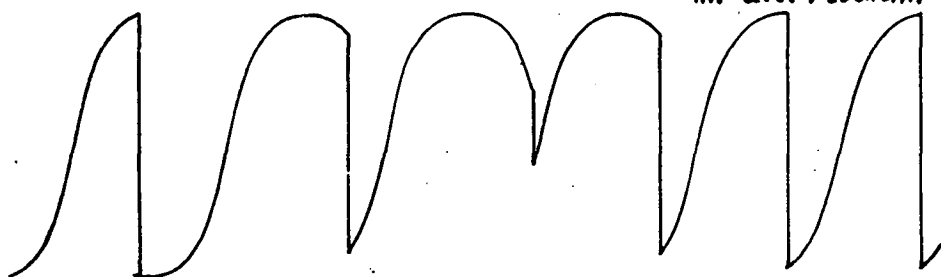
The first pair describe the waveform of a ramp and associated switching wave, the second a symmetrical triangular wave. For k equal to unity both expressions are identical to those for a normal, two level, d.c. supplied, switching amplifier using the same form of sampling wave.



The resultant switching wave



An a.c. resultant waveform



EXAMPLES OF REGULAR SAMPLING

D 3.2.1

3.2 Waveform Synthesis by Regular Sampling

3.2.1 The Coder Law

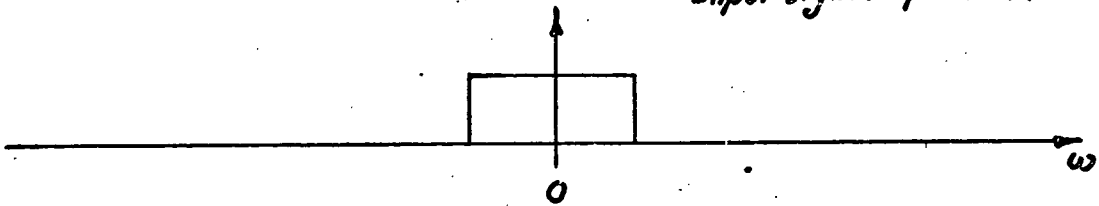
The coder controlling a step between two levels of a switching wave is said to employ regular sampling if a periodic sample of the input signal determines the position of the step relative to the sampling instant. In a simple case the step may lag the sampling instant by a time proportional to the input signal amplitude at the sampling instant. In a more complex situation the time between the sampling and the step change may be a nonlinear function of the input signal value at the sampling instant. Examples are shown in diagram D 3.2.1.

3.2.2 The Relationship to Natural Sampling

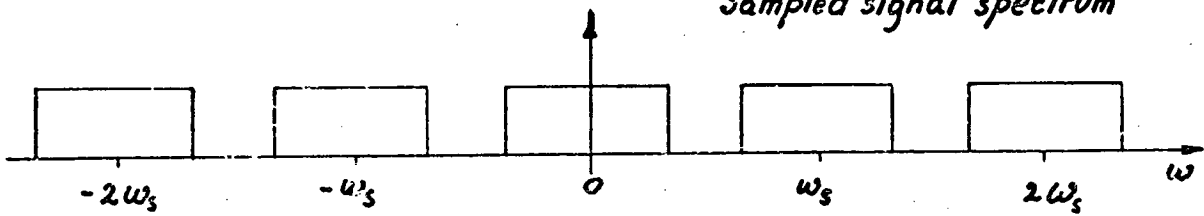
A coder using natural sampling will produce the same output as one using regular sampling if the natural sampler is provided with the input signal to the regular sampler after this has been sampled and held at the same instants the regular sampler does this. This relationship between the two forms of coding enables some relationships between the forms of output to be deduced.

In natural sampling the coder output contains terms with frequencies corresponding to the input signal and others with frequencies which are sidebands of carriers at the sampling frequency and its harmonics. The sideband components are due to a modified form of phase modulation of the carrier components by the input signal. Now if the input signal of a regular sampler is a sinewave then the corresponding input to a natural sampler would be a sinewave subjected to sampling and holding at the sampling frequency of the natural sampler. This input signal will contain components at frequencies other than the basic frequency of the sinewave. The other frequencies correspond to filtered sidebands of the

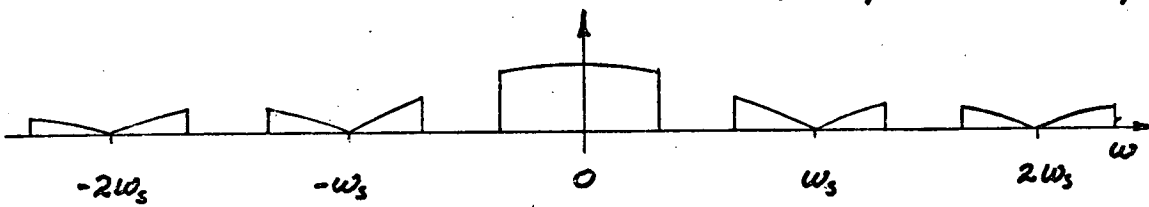
Input signal spectrum



Sampled signal spectrum



Modulus of sampled and held spectrum



THE SPECTRAL TRANSFORMATION OF SAMPLING AND
HOLDING A SIGNAL

D. 3.2.2

sampling frequency where the sidebands are the same as those for amplitude modulation and the filter has a $\text{sine}(x)/x$ frequency characteristic with a delay in time as the phase characteristic. A representation of an input signal before and after sampling and holding is shown in diagram D 3.2.2.

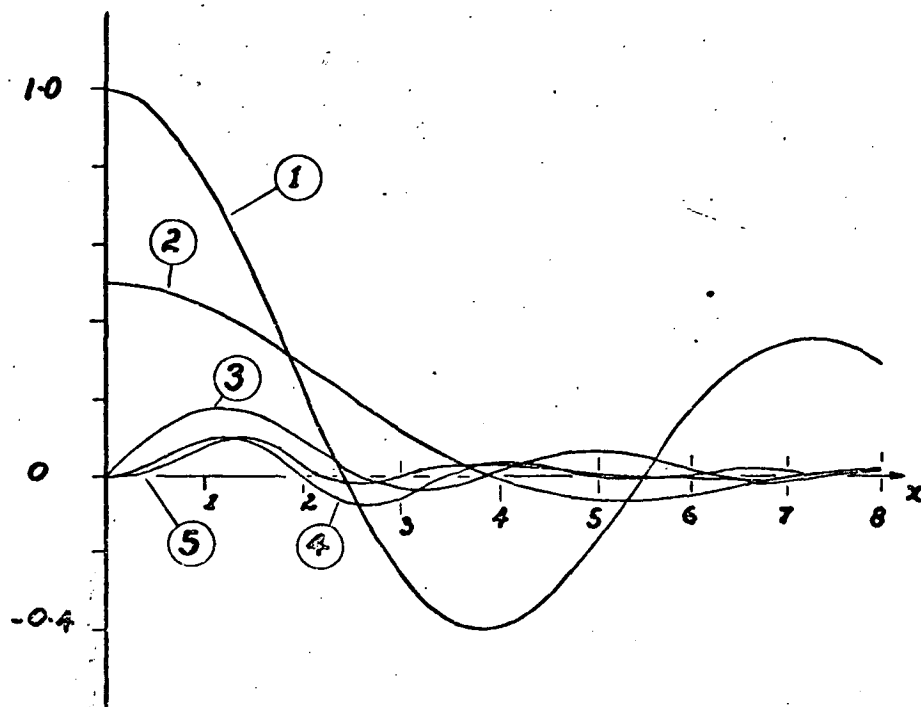
A natural sampler with this form of input will produce in the output signal components, due to the sidebands in the input, with frequencies corresponding to the input signal and its harmonics. This is equivalent to distortion of the input signal. Due to the nulls in the $\text{sine}(x)/x$ characteristic of the sample and hold process the distortion is small for low frequency input signals. This is consistent with the expected result that d.c. signals must remain undistorted.

This difference between natural and regular sampling, whereby the former generates signals which are essentially distortionless and the latter signals with distortion, is the most fundamental one. In most other respects the two forms of sampling are very similar. They both produce phase modulated signals to form sidebands of the sampling frequency harmonics and both may be used with a wide range of supply voltages to produce linear d.c. characteristics for switching amplifiers.

An example of Regular Sampling

The general expression for a coder step produced by regular sampling is derived in appendix A 3.2.2. In order to illustrate the use of this expression the following example is also developed.

A switching waveform, with d.c. levels of plus and minus one unit, has steps displaced in phase relative to the sampling instants by angles defined by the equations



LEGEND

1	Fundamental	$J_0(x)$
2	First Harmonic	$J_1(x)/x$
3	Second Harmonic	$J_2(2 \cdot x)/(2 \cdot x)$
4	Third Harmonic	$J_3(3 \cdot x)/(3 \cdot x)$
5	Fourth Harmonic	$J_4(4 \cdot x)/(4 \cdot x)$

FUNCTIONS ASSOCIATED WITH REGULAR SAMPLING

D 3.2.3

$\phi_p = 0$ and $\phi_n = \pi(1 + a \cdot \sin(w_m t_s))$.

ϕ_p and ϕ_n are phases for the positive and negative steps respectively. The expression for the switching wave is

$$E = \sum_{q=1}^{q=\infty} 2a J_q(\pi a q w_m / w_s) \sin(q w_m (t - \frac{\pi}{w_s})) / (\pi a q w_m / w_s) \\ - \sum_{n=1}^{n=\infty} \left\{ 2 \sin(N(w_s t - \pi)) J_0(Na\pi) / (\pi N) - 2 \sin(N w_s t) / N\pi \right\} \\ - \sum_{n=1}^{n=\infty} \sum_{q=1}^{q=\infty} 2a \left(\frac{J_q(\pi a (N + q w_m / w_s))}{(\pi a (N + q w_m / w_s))} \right) \sin(N(w_s t + \pi) + q w_m (t - \frac{\pi}{w_s}))$$

The low frequency terms, the first group in the expression, correspond to the input signal and are the output component of the waveform. The second group have frequencies corresponding to the sampling rate and its harmonics. The last group have frequencies separated from the frequencies of the second group by multiples of the modulation frequency. This group are modulation sidebands of the second group.

3.2.3 The Modulator Nonlinearity

The nonlinearity of the modulator may be gauged with the aid of diagram D 3.2.3. The amplitudes, normalised with respect to a , of each of the first four harmonics are shown as functions of $\pi a w_m / w_s$. The values of a and w_m / w_s are both less than unity due to the modulator characteristics so that the index, $\pi a w_m / w_s$, has a range from zero to π .

For small values of the index, where a or w_m / w_s is small, the distortion is very low. If both a and w_m / w_s are half their maximum values then the second and third harmonic amplitudes are one third and one sixth respectively of the desired output. The amplitude of the fundamental is also reduced by seven percent. As the input signal is increased further in either amplitude or

frequency the relative amplitudes of the distortion components increase rapidly. At an index of 4.5 the energy of the fundamental equals the sum of the energies of the harmonics. The maximum energy of the distortion terms is approximately one fifth of the fundamental at an index of 1.4.

For a single sinewave input the distortion is worst when the frequency is near half the sampling frequency and the amplitude is the maximum possible without modulator saturation. For very low frequencies or very small amplitudes the distortion is negligible.

Regular Sampling with Combined Inputs

The expression for a waveform with a control signal given by

$\phi(t) = \pi(1 + a \sin w_a t + b \sin w_b t)$ is calculated in appendix A 3.2.3. The terms corresponding to the input signal are given by the expression below.

$$E = \sum_{m=-\infty}^{\infty} \sum_{r=-\infty}^{\infty} \left(\frac{J_r \left(\pi a \left(\frac{r w_a + m w_b}{w_s} \right) \right)}{\frac{\pi (r w_a + m w_b)}{w_s}} \right) J_m \left(\pi b \left(\frac{r w_a + m w_b}{w_s} \right) \right).$$

$$j e^{j (r w_a + m w_b) (t - \frac{\pi}{w_s})}.$$

The terms giving the fundamental components of the output signal correspond to the cases when $m=0$, $r=1, -1$ and $r=0$, $m=1, -1$.

These are

$$a \cdot \left(\frac{2 J_1 \left(\pi a \frac{w_a}{w_s} \right)}{\pi a \left(\frac{w_a}{w_s} \right)} \right) J_0 \left(\pi b \frac{w_a}{w_s} \right) \sin \left(w_a \left(t - \frac{\pi}{w_s} \right) \right) \quad \text{and}$$

$$b \cdot \left(\frac{2 J_1 \left(\pi b \frac{w_b}{w_s} \right)}{\pi b \left(\frac{w_b}{w_s} \right)} \right) J_0 \left(\pi a \frac{w_b}{w_s} \right) \sin \left(w_b \left(t - \frac{\pi}{w_s} \right) \right).$$

When both a and b are small these terms are near their values for a linear modulator since $J_0(x)$ and $\frac{2J_1(x)}{x}$

both tend to unity as x approaches unity. If either a or b is increased the value of the other decreases due to the J_0 term. The sum and difference frequency terms are given by

$$\begin{aligned}
 & a.b. \frac{\pi(w_a + w_b)/w_s}{2} \left(\frac{2J_1(\pi a(w_a + w_b)/w_s)}{\pi a(w_a + w_b)/w_s} \cdot \frac{2J_1(\pi b(w_a + w_b)/w_s)}{\pi b(w_a + w_b)/w_s} \right) \\
 & \quad \cdot \sin((w_a + w_b)(t - \pi/w_s)) , \quad \text{and} \\
 & -a.b. \frac{\pi(w_a - w_b)/w_s}{2} \left(\frac{2J_1(\pi a(w_a - w_b)/w_s)}{\pi a(w_a - w_b)/w_s} \cdot \frac{2J_1(\pi b(w_a - w_b)/w_s)}{\pi b(w_a - w_b)/w_s} \right) \\
 & \quad \sin((w_a - w_b)(t - \pi/w_s)) .
 \end{aligned}$$

As the indices of the Bessel functions become small these terms become asymptotic to the first group in their list of products. The higher order harmonics and intermodulation terms converge more rapidly than the terms so far discussed so that for small signals the output may be approximated by the expression

$$\begin{aligned}
 E = & a \sin(w_a(t - \pi/w_s)) + b \sin(w_b(t - \pi/w_s)) \\
 & + a.b. \pi/2 \left\{ (w_a + w_b)/w_s \sin((w_a + w_b)(t - \pi/w_s)) \right. \\
 & \quad \left. - (w_a - w_b)/w_s \sin((w_a - w_b)(t - \pi/w_s)) \right\}
 \end{aligned}$$

Two Step Modulation

The output waveform of the examples is modulated only on the negative going step. As a consequence to obtain maximum and minimum output the phase of the step must be varied by π in each direction from a mean phase of π relative to the sampling instant. The mean phase controls the delay of the modulator so

that in the examples given this was half the switching wave period.

By modulating both steps of the waveform the modulation index for a given output is halved as is the delay of the modulator. The maximum nonlinearity of the modulator is reduced by much more than this factor. The effects of modulating both edges of the waveform rather than one are similar to those obtained by doubling the sampling frequency which is what in effect has been done.

The worst distortion with symmetrical double edge modulated regular sampling with d.c. waveform levels occurs when the modulation index is that for full unsaturated output amplitude. If the maximum input frequency is taken as half the repetition frequency of the switching wave then the largest component of the error is the second harmonic which is one sixth of the output. The other harmonics are much smaller than this component.

3.2.4 The Generation and Assembly of Switching Waves

Regular and Natural sampling produce identical coder outputs when the control signal is d.c. Thus for d.c. control signals the techniques used to give switching amplifiers using natural sampling linear characteristics will also give those using regular sampling a linear characteristic. The distortion due to regular sampling of a.c. control signals cannot be cancelled by a coder modification. This is only feasible if the frequency dependence of the distorted signal may be cancelled by means of a filter since it is possible to cancel distortion which is purely amplitude dependent by adjusting the sampling waveshape.

The methods used to assemble switching wave components controlled by natural samplers may not be sufficiently restrictive for regular sampling when a.c.

signals are to be processed. Where two or more samples per period are used to control adjacent waveform level segments whose turn on and turn off phase ranges may overlap, it is possible for a rapidly changing signal to cause the level, normally second to turn on, to turn on before the other. This situation is likely to arise with multi phase a.c. level waveforms using phase modulation. Situations involving switching sequences, based on order of turn on or on memory, may require some additional logic for switch control to prevent such situations causing failure. The possibility may also be avoided by filtering the input signal so that rates of change greater than the critical value are prevented from occurring.

The Features of Regular Sampling

The examples have illustrated the two main features of the low frequency components of a linearly controlled regular sampler.

First, the output signal is nonlinearly related to the input signal. The nonlinearity is not a one to one relationship between instantaneous values of input and output but depends on the input signal spectrum, in particular on the ratio of input signal component frequencies to the sampling frequency for a given step. For small values of input signal amplitude and or frequency the nonlinearity is negligible. d.c. input signals are reproduced undistorted.

Second, the output signal is delayed relative to the input signal. The magnitude of the delay is dependent on the mean period between the taking of a sample and the forming of a step. If the sampler produces a symmetrical switching wave for zero input and has a maximum range of positive and negative output levels then

the delay is half the sampling period for single edge modulation and one quarter the sampling period for symmetrical double edge modulation when the input signal is sinusoidal. For an input signal with a.c. and d.c. components the delay is dependent on the d.c. level for single edged modulation but not for double edged modulation.

3.3 Review

The switching wave of an amplifier controlled by natural sampling may be described by a low frequency component, a fundamental component with frequency matching the sampling rate, and an infinite set of components with frequencies at harmonics of the fundamental. Each of these components have magnitudes and, in the latter cases, phases which are mathematical functions of the input signal. The form of this function for a given amplitude or harmonic phase is determined by the shapes of both the sampling waves in the encoder controlling the switches, and the energy source waveforms.

Linear amplification requires the low frequency component of the switching wave to be a linear function of the control signal. For a given supply waveform this requirement restricts the range of possible sampling waveforms by imposing relationships between the shapes of the waveforms controlling each switching wave step. In some circumstances the shape of these sampling waves is uniquely defined by this restriction, in others, design criteria such as output range or sideband minimisation, are needed to completely define the waveforms.

Although it is not discussed here it should be appreciated that similar techniques to those used for the definition of sampling wave shapes for linear amplification can be used to define these shapes for linear modulators. The basic requirements are that the magnitude of a given harmonic be a linear function of the input signal, and the phase have constant value. These two requirements are sufficient, in most cases, to completely specify the sampling waves.

By modifying the shape of the sampling wave it is possible to produce switching waves with output

independent of supply ripple superimposed upon d.c. supplies. The technique may be applicable to waves with more than two levels though this is not discussed.

Switching waves with many equally spaced levels are produced by quantizers and sensor arrays as well as by switching amplifiers. Natural sampling may be used to linearise a quantizer characteristic. The low frequency component of the quantizer output is related to the input signal by the probability distribution of the perturbation used as a sampling signal. A linear characteristic is produced when the distribution is linear and the peak to peak amplitude is a multiple of one step size. Characteristics with periodic deviations from linearity can be predicted when these aspects of sampling wave are not satisfied.

If a natural sampler is used to encode a signal which is itself produced by sampling and holding the amplifier input signal then the encoded signal is identical to that produced by regular sampling. The description of waveforms due to regular sampling is achieved using this model of the process. The switching waves of natural and regular sampling are identical for d.c. control signals and identical techniques may be used to achieve linear amplifier characteristics.

The major difference between natural and regular sampling is the nonlinearity and intermodulation of the output of a regular sampler when a.c. control signals are used. The index of this distortion is the product of modulation amplitude and control signal frequency measured relative to the sampling rate. For low frequencies the distortion signal is proportional to control signal frequency and amplitude with a value of about -25db. at an index of 0.2.

References

T. H. Barton, R. S. Birch "A 5kw Low Frequency Power Amplifier"

IEEE Internat. Con. Rec. PT 9-12 No. 10 PP 146-153

Bennet "New Results in the Calculation of Modulation Products"

Bell System Tech. Jrnl. Vol. 12 April 1933

PP 228-243

H. S. Black "Modulation Theory"

N. J. Van Nostrand 1953 PP 263-281

P. F. Chen "Optimal Signal Perturbation Waveform for Sensing Arrays"

IEEE Trans Vol. IM-19 May 1970 PP 135-139

S. B. Dewan, M. D. Kankam "A Method for Harmonic Analysis of Cycloconverters"

IEEE Trans IGA-6 No. 5 September 1970 PP 455-462

E. Fitch "The Spectrum of Modulated Pulses"

J. IEE Vol. 94 PT 3A 1947 PP 556-564

E. R. Kretzmer "Distortion in Pulse Duration Modulation"

Proc. IRE Vol. 35 November 1947 PP 1230-1235

L. Malesini "Improved Delay Circuit for Thyristor Linear Power Control"

Electronic Engineering January 1969 PP 84-89

E. S. McVey, P. F. Chen "Improvement of Position and Velocity Detecting Accuracy by Signal Perturbation"
IEEE Trans Vol. IECI-16 July 1969 PP 94-98

B. Mokrytzki "Pulse Width Modulated Inverters for A.C. Motor Drives"
IEEE Internat. Con. Rec. IGA-8 March 1966 PP 8-23

E. A. Parrish, J. W. Stoughton "Achieving Improved Position Detection Using a Modified Triangular Perturbation Signal"
IEEE Trans IM-21 No. 1
February 1972

P. F. Pitman, R. J. Ravas, R. W. Briggs "Staggered Phase Technique"
Electrotechnology Vol. 83 No. 6 June 1968 PP 55-58

CHAPTER IV

THE HIGH FREQUENCY COMPONENTS OF PERIODIC

SWITCHING WAVES

4.0 The High Frequency Components of Periodic Switching Waves

A switching amplifier controlled by natural sampling may be designed so that the low frequency component of the switching wave is an accurately magnified version of the input signal. In addition to this signal the switching wave has components with frequencies at the fundamental and harmonics of the sampling rate. Each such harmonic component has an amplitude and phase which is a function of the input signal. It is these modulated harmonics of the switching wave which must be rejected by the output filter.

Each modulated harmonic is composed of a large number of unmodulated sidebands. These sidebands are separated from the nominal harmonic frequency by a multiple of the modulation frequency, that is the control signal frequency. Some of these sidebands have frequencies within the amplifier passband, others are incompletely rejected because the filter is not ideal. These unrejected and partially rejected sidebands form a noise signal at the amplifier output. The magnitude and type of noise vary with the switching wave, the filter, the control signal components, and the ratio of passband width to sampling frequency. This chapter examines these features of the sidebands and places upper bounds on the noise to signal ratio of a number of switching waves in terms of the parameters outlined above.

The sidebands of the switching wave may have frequencies which are identical with the control signal or its harmonics. In such circumstances there is an apparent distortion of the amplifier output. This distortion differs from that caused by nonlinearity and is similar in some respects to that due to regular

sampling. It is sensitive to the relative phase of control and sampling signals. This distortion is discussed under the heading of subharmonic gain.

CHAPTER IV : SWITCHING WAVE SPECTRA

4.0

Introduction

4.1

Spectra of waves with d.c. control signals

4.1.1

Switching waves with d.c. levels

4.1.1.1

Waves with two levels

4.1.1.2

Multi-Level waves

4.1.2

A.C. waveform levels

4.1.2.1

Harmonic cancellation

4.1.2.2

Some thyristor generated waves

4.1.3

The asymptotic waveform

4.1.4

Harmonic cancellation

Summary of harmonic characteristics

4.2

Spectra of waves with a.c. control signals

4.2.1

The spectrum of phase modulation

4.2.1.1

A single periodic modulation

4.2.1.2

Multiple periodic modulations

4.2.1.3

Energy distribution descriptions

4.2.1.4

Numerical evaluation of sideband amplitudes

4.2.1.5

Limitations of numerical processes

Outline of computation sequence

4.2.2

The sidebands of switching waves

4.2.2.1

Switching wave components within the passband

4.2.2.2

Passband energy estimation by contour map

4.2.2.3

Passband energy variation with modulation amplitude

4.2.2.4

Passband energy variation with bandwidth & input frequency

Maximum passband energy

4.2.2.5

Multi-Level waveforms

4.2.2.6

Non-sinusoidal control signals

4.2.3

More complex switching waves

4.2.3.1

Sideband energy

4.2.3.2

Multi-phase waves with unclamped sinewave levels

4.2.3.3

Sidebands of sinewave levelled waves

4.2.3.4

Worst sideband conditions

4.2.3.5

Maximum passband noise

4.2.3.6

Comparing a.c. and d.c. levelled waves

4.2.4

The ideal filter assumption

4.2.4.1

Filtering of a two level wave with one modulated edge

4.2.5

Summary

4.3

Subharmonic Gain

4.3.1

The subharmonic case

4.3.1.1

Computation of distortion

4.3.1.2

Visualisation

4.3.1.3

Subharmonic gain

4.3.2

Subharmonics of natural sampling

4.3.2.1

Single edged modulation

The second subharmonic

Other subharmonics

4.3.2.2

Symmetrical modulation

4.3.3

Conclusion

Outline

This chapter has three broad divisions.

The first of these deals with the functions which modulate the harmonics of a number of common switching waves. The second examines the sidebands of these harmonics when periodic control signals are used. The third describes the subharmonic gain and its computation. These divisions are now outlined in more detail.

By specifying the shape and phase of the waveform levels and the modulation laws governing the turn on and turn off of each of the levels the particular expressions describing some common switching waves are formed. These examples include expressions for both d.c. and a.c. levelled waveforms. The variation of harmonic amplitude with both harmonic number and output component are discussed and comparisons are made of maximum harmonic amplitudes, maximum output components, and ratios of these. To summarise these features use is made of energy component diagrams which enable visual comparisons of total harmonic energy, total waveform energy, and individual harmonic energy for a full range of output components. In the case of a.c. levelled waveforms where very complex functions may occur this information is supplemented by tables.

Since the simplest switching wave has sidebands produced by pure phase modulation the second division commences with a brief description of the theory, graphical description, and numerical calculation of sidebands due to phase modulation. This information is used to illustrate, by graphical means, the computation of passband noise energy and to demonstrate the variation of this noise with the amplitude and frequency of the sinewave control signal, and with the ratio of passband width to sampling frequency.

An ideal bandpass filter is assumed. From this background material graphs of minimum signal to noise ratio, as a function of the modulation parameters, are derived and described. The methods are then extended to include multi-level waveforms, nonsinusoidal inputs, and d.c. levelled waves with two modulated steps. a.c. levelled waves have more complex descriptions and graphical methods of passband noise calculation are not adequate. Graphs based on computed sidebands are presented and their features compared with similar graphs for d.c. levelled waves. These graphs are all based on an ideal bandpass filter which rejects all sidebands except those in the passband. A short description is given of the use of nonideal filters of various orders to illustrate the relationship between the ideal and actual signal to noise ratios.

The third division is concerned with the apparent amplifier gain when a harmonic of a sinewave control signal has a frequency coincident with the sampling frequency. Expressions for the subharmonic gain vector are derived and numerical computation methods outlined. Graphs based on computed information are used to demonstrate the characteristics of this vector for two levelled switching waves with single and double edged modulation.

4.1 Spectra of Waves with d.c. Control Signals.

It is shown in appendix A 4 that the switching waveform produced by natural sampling has the form of the expression

$$E = a_0 + \sum_{r=1}^{\infty} a_r \cos(rw_s t) + b_r \sin(rw_s t), \text{ where}$$

$$a_0 = \sum_{i=1}^I \frac{1}{2\pi} \int_{A_i}^{B_i} V_{si}(w_s t) dw_s t, \text{ and}$$

$$a_r + jb_r = \frac{1}{\pi} \sum_{i=1}^I \int_{A_i}^{B_i} V_{si}(w_s t) \cdot e^{jr w_s t} dw_s t.$$

The suffix, i , denotes the i^{th} level of the I waveform levels. A and B are functions of the controlling signal, e , and of the sampling waves, $S_A(w_s t)$ and $S_B(w_s t)$, where S_{Ai} controls the instant of switching to the i^{th} level and S_{Bi} controls the instant of switching from this level. The relationships between S_A and S_B , and, A and B , are

$$S_A^{-1}(e) = A(e) \text{ and } S_B^{-1}(e) = B(e).$$

The coefficients of the Fourier series, a_0 , a_r , b_r , are functions of the control signal, e . The previous chapter examined the methods by which a_0 could be a linear function of e . This imposed restrictions on the sampling waveshapes and the ranges of the functions A and B . These restrictions result in some restrictions on the characteristics of the relationships between a_r and b_r with e . These relationships are now examined in greater detail.

The Fourier series coefficients, a_0 , a_r , and b_r , are described by integrals of products involving as one factor the waveform level waveshapes. These may be

replaced by appropriate Fourier series of the form

$$V_{si}(w_s t) = \sum_{h=0}^{h=H} a(h,i) \cos(hw_s t + \phi(h,i)).$$

The expression for the total switching wave then becomes

$$\begin{aligned} E = & \sum_{i=1}^{i=I} \sum_{h=0}^{h=H} a(h,i) \left[\sin(h\theta + \phi(h,i)) \right]_{\theta=A_i}^{\theta=B_i} / (2\pi h) \\ & + \sum_{r=1}^{r=\infty} \sum_{i=1}^{i=I} \sum_{h=0}^{h=H} \sum_{s=\pm 1} \bar{a}(h,i) \left[\sin(r(w_s t - \theta) \right. \\ & \left. + s(h\theta + \phi(h,i))) \right]_{\theta=A_i}^{\theta=B_i} / (2\pi(s h - r)). \end{aligned}$$

As an example consider the familiar situation where two d.c. supplies of equal but opposite magnitude are used in conjunction with complementary control functions. The appropriate variables for the expression above in this case are

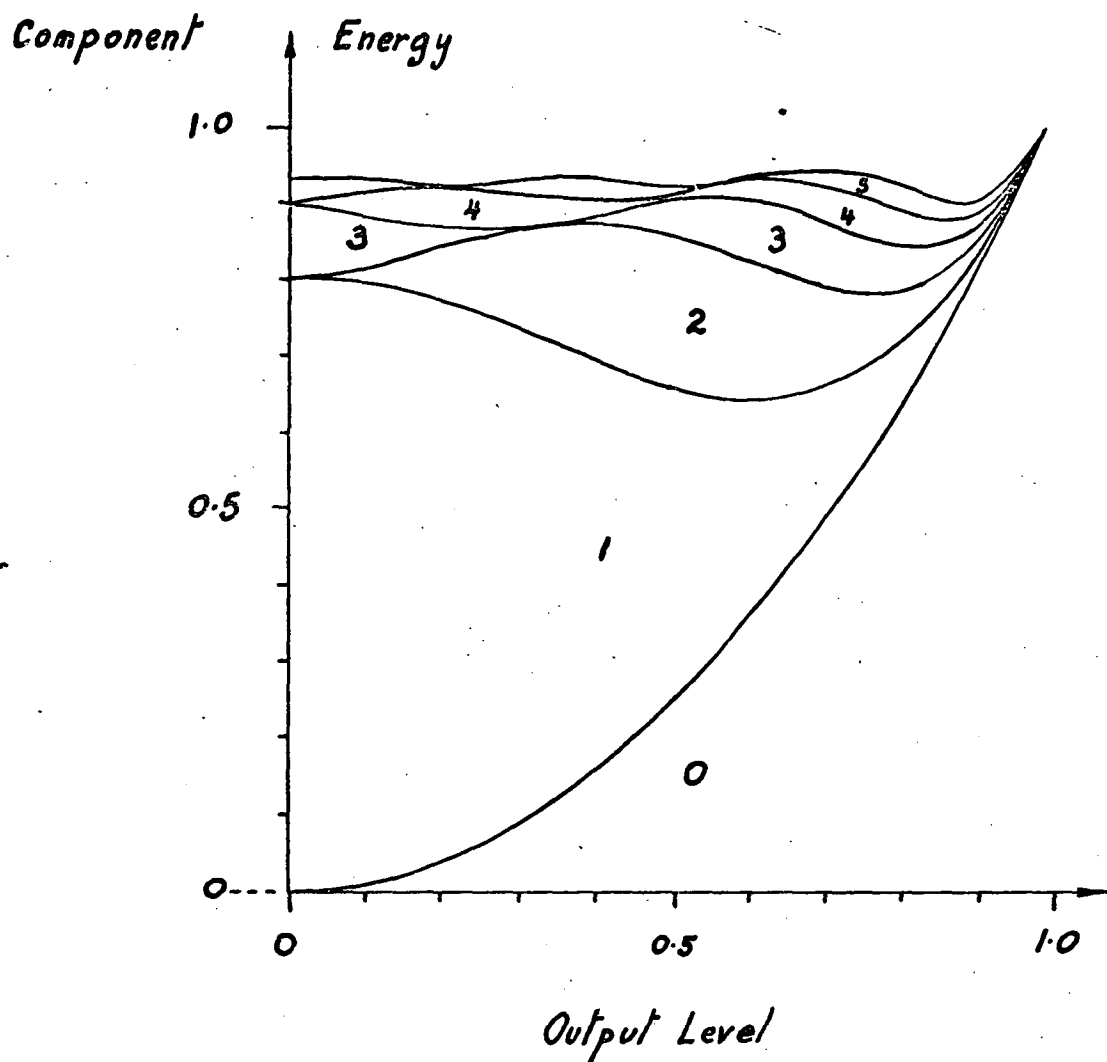
$$a(h,1) = -a(h,2) = \begin{cases} 1 & h=0 \\ 0 & h \neq 0 \end{cases},$$

$$\phi(h,i) = 0,$$

$$A = A_1 = B_2 - 2\pi, B = B_1 = A_2, H = 0, \text{ and } I = 2.$$

The low frequency component is the limit as h tends to zero of the expression above. Thus

$$\begin{aligned} E_0 &= (1. \left[\theta \right]_{\theta=A}^{\theta=B} - 1. \left[\theta \right]_{\theta=B}^{\theta=A+2\pi}) / 2\pi \\ &= (B-A)/\pi - 1. \end{aligned}$$



CONTRIBUTION OF EACH HARMONIC TO WAVE ENERGY

D 4-1-1

The r^{th} harmonic is evaluated more directly and is given by

$$ER = \frac{1}{r} \left[2 \sin(r(w_s t - \theta)) \right]_{\theta=A}^{\theta=B} / (-2r\pi) - \frac{1}{r} \left[2 \sin(r(w_s t - \theta)) \right]_{\theta=B}^{\theta=A+2\pi} / (-2\pi r).$$

$$= 2. (\sin(r(w_s t - A)) - \sin(r(w_s t - B))) / (\pi r).$$

4.1.1 Switching Waves with d.c. Levels

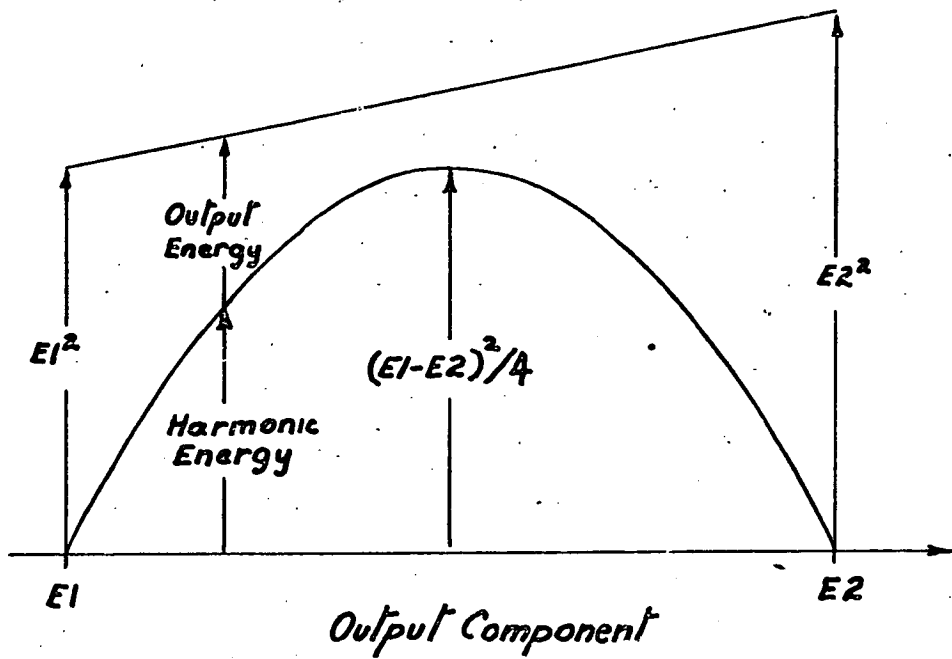
4.1.1.1 Waves with Two Levels

For switching waves with d.c. levels there is a close link between the amplitude of a given harmonic and the output or low frequency component, EO. This is illustrated for the example above by the following sequence of manipulations.

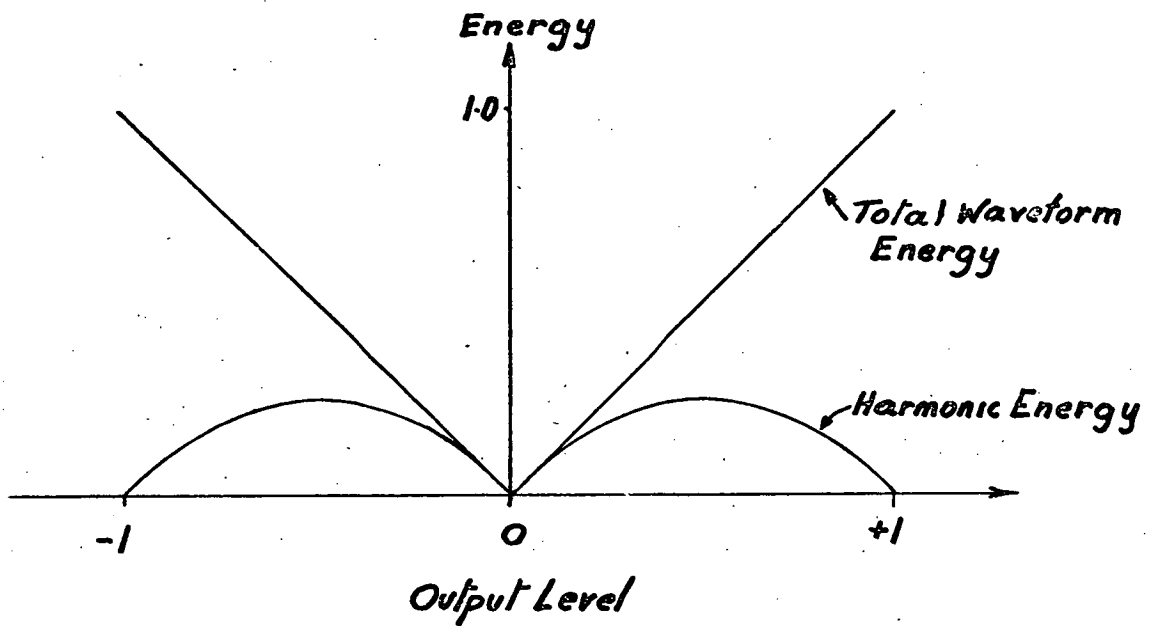
$$\begin{aligned} ER &= 4. \sin(r/2(w_s t - A - w_s t + B)) \cos(r(w_s t - A + w_s t - B)/2) / (\pi r) \\ &= 4. \sin(r(B - A)/2) \cos(r(w_s t - (B + A)/2)) / (\pi r) \\ &= 4. \sin(r\pi(EO + 1)/2) \cos(r(w_s t - (B + A)/2)) / (\pi r). \end{aligned}$$

Thus a variation of EO from the lower limit of -1 to the upper limit of +1 causes the r^{th} harmonic to vary sinusoidally in amplitude, with a peak value of $4/r\pi$, through r half cycles.

The amplitudes of all harmonics are zero when the output is at either the maximum or minimum value, that is when the output is the same value as a waveform level. The odd harmonics have maxima at zero output.



D 4.1.1.2 a



WAVEFORM ENERGY COMPONENTS

D 4.1.1.2 b

Diagram D 4.1.1.1 shows the contributions of each harmonic to the total energy of the switching wave. The features mentioned above are very prominent. In addition it is easy to compare the relative amplitudes of the different components in a physical rather than a mathematical sense. Notice that the total energy of the wave is fixed at unity for this example.

4.1.1.2 Multi Level Waves

The introductory example has some features in common with those multi level switching waveforms where switching is restricted to those levels adjacent to the output component value. These waveforms were described in chapter II as minimum energy waveforms. For output components between two waveform levels, E_1 and E_2 , the energy description is of the form shown in diagram D 4.1.1.2a, where only the total waveform energy, and the sum of the harmonic energies are shown. The total waveform energy varies linearly with output level over the range of output between E_1 and E_2 . The parabolic variation of total harmonic energy with output corresponds directly to that of the introductory example. The proportions of the total harmonic energy contributed by the individual harmonics are also the same as those for the introductory example.

A switching waveform with the three levels $+1$, 0 , and -1 , has two intervals of the form described above thus giving the energy components shown in diagram D 4.1.1.2b. This particular example has no switching wave at zero output. This may be a desirable feature of switching waves where zero output is common since power consumption is zero and output ripple of the amplifier is zero. Other switching waves with an even number of intervals between waveform levels may also

have this characteristic.

If the range of the output component is fixed but the number of waveform levels is increased then the energy of the switching wave, as a function of output component, is a series of chords around the parabola of the output component energy. The points on the parabola corresponding to the ends of chords are levels of the waveform where there is no energy in the harmonics of the switching wave. The total energy of the harmonics has a value equal to the difference between chord and parabola and is thus parabolic. For waveform levels separated by equal intervals the maximum value of each harmonic is inversely proportional to the number of intervals. Notice that the number of cycles of each harmonic as the output component is varied over the full range is proportional to the number of intervals.

There are two simple methods for generating minimum energy multi-level waveforms with equal intervals between levels. The first is to sum a number of two level waveforms similar to the introductory waveform. If each waveform has the same control signal and an identical waveform as the others except that the phases of the waveforms are uniformly spread over one period then a multi-level waveform with minimum energy is generated. If the number of waveforms summed is n then the total waveform produced will have $n+1$ levels.

The second method is based on the quantizer system described in chapter III. The switching wave produced by a quantizer, when the input signal is perturbed by a suitable signal with a peak to peak amplitude of one quantizer input step, is a minimum energy waveform. The waveforms produced by this method

differ from those of the first method, when both the positive and negative going steps are modulated, but are the same when only one step is modulated. The difference is a sudden jump in the phase of the two steps as the waveform average passes through a waveform level. In the first case the phases of the individual steps are continuous functions of the average waveform level. When only one step of the waveform is modulated the phase jump is one period and is thus not noticeable. A second difference in the two waveforms is their frequency scales. The frequency of the waveform produced by summing n waveforms is n times the frequency of the individual waveforms while the frequency of the quantizer produced waveform is the frequency of the perturbation signal.

The increase in effective switching frequency produced by the summing of a number of waveforms is one way of overcoming switching speed limitations encountered in high power switching devices. In this case summing is often achieved by paralleling separate switching amplifiers at their filter outputs. This enables the same d.c. supply rails to be used for all amplifiers and also allows all control circuits to be at similar voltage levels. A quantizer type structure does not have these properties.

All d.c. levelled, minimum energy, switching waves have the same relationship between normalised harmonic energies and normalised output. Thus, for a given output and the adjacent waveform levels, the values of each harmonic amplitude are defined. This is a direct consequence of the restrictions placed on the switching wave by the minimum energy requirement.

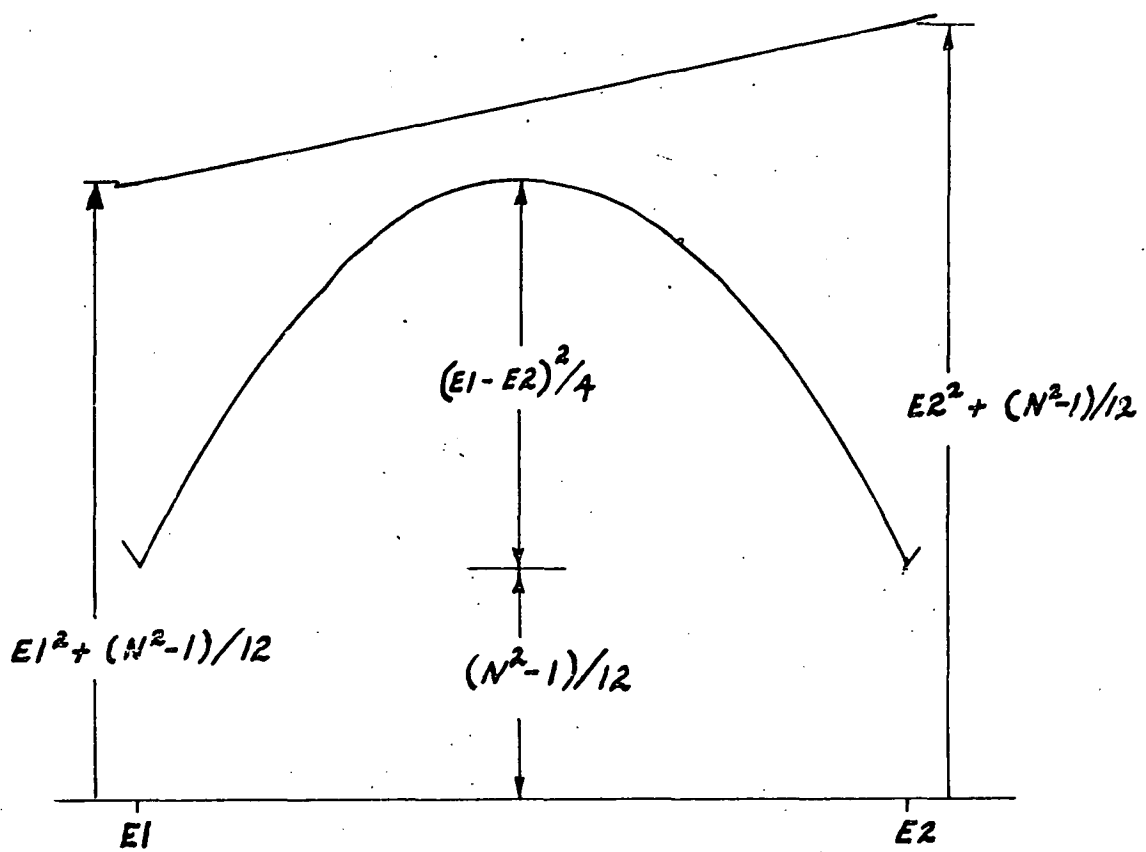
By ignoring this requirement it is possible to generate switching waveforms with different relationships between harmonic energies. The aim of choosing a non minimum waveform is usually to minimise filtering requirements, that is, to reduce the contribution of the lower harmonic energies. This reduction is at the expense of the higher harmonic energies which must increase by the decrease in lower harmonic energy and the increase in total waveform energy above the minimum level.

It is shown in appendix A 4.1.1.2a that one non minimum energy switching wave is produced by adding a number of two level waveforms subject to the same conditions as those for the minimum energy waveform excepting that the phasing of the components is uniformly distributed over only one half period. This results in the cancellation of all even harmonics and results in modified co-efficients for the remaining harmonics. The expression obtained when R two level unit energy waveforms are added is below.

$$E = \sum_{n=1}^{n=\infty} \left\{ \sin((2n-1)(EO+1)\pi/2) \cdot \sin((2n-1)(w_s t + \pi/2R - (B+A)/2)) \right. \\ \left. \cdot 4/(\pi(2n-1)\sin((2n-1)\pi/2R)) \right\} + R(EO).$$

This example shows the opposite trend to that desired since although the even harmonics are cancelled the energy of each of the remaining odd harmonics is increased above that for an equivalent minimum energy wave by the factor $1/(\sin((2n-1)\pi/2R))^2$.

Other non minimum waveforms may be generated by the quantizer system when an input perturbation of two or more units peak to peak amplitude is used. These



Output Component

N = number of waveform levels - 1

E_1 = a waveform level - $N/2$

E_2 = E_1 + one waveform interval

ENERGY COMPONENTS OF MULTILEVEL WAVEFORMS

D4.1.1.2c

waveforms are similar in form to the example when symmetrical modulation is used but differ greatly when assymetrical modulation is used. The example for a sawtooth perturbation discussed in the previous chapter is described by the expression below.

$$E = EO + \sum_{n=1}^{n=\infty} \frac{1}{n\pi} [\sin(n(kw_p t + 2\pi EO)) - k \cdot \sin(n(w_p t - \pi))].$$

k is the peak to peak perturbation amplitude. The interval between levels is one unit. The interesting feature of this example is the shift of modulated energy from the lower harmonics to the harmonics which are multiples of k. This shift is balanced by the increase in energy of the lower harmonics over the peak of that for minimum energy by a factor of k/2. (In making this comparison remember the distance between steps of the previous examples is two units). This form of switching wave would result in a ripple, after filtering, with only a small variation in amplitude as the output component is changed over a wide range. This contrasts strongly with the behaviour of minimum energy waveforms.

These non minimum energy waveforms have one feature in common. That is the energy in the harmonics relative to the total waveform energy. The form of the energy distribution for this type of waveform is derived in appendix A 4.1.1.2b and displayed in diagram D 4.1.1.2c. The main feature of interest is the extra energy of the harmonics which is independent of the modulation. The modulated component of the harmonic energy is the same function of output level as for the non minimum case.

These three non minimum energy waveforms do not seem capable of satisfying the aim of the investigation.

They are a very small group of the possible non minimum waveforms and may not be representative of what is possible since they are very similar in form.

4.1.2 a.c. Waveform Levels

The most common a.c. waveform level used in switching amplifiers is a sinewave. The switching wave has the same period as the sinewave or a harmonic of the sinewave. The switch control signals have the same period as the sinewave. For this case the general expressions for the output component and harmonics of the switching wave are subject to the conditions below.

$$a(h,i) = \begin{cases} 1 & \text{for } h=1 \\ 0 & \text{for } h \neq 1 \end{cases} \quad \phi(h,i) = \phi - \pi/2$$

The output component is described by

$$EO = (\sin(B + \phi - \pi/2) - \sin(A + \phi - \pi/2)) / (2\pi).$$

The r^{th} of the harmonics is described by

$$ER = \sum_{s=\pm 1} \frac{1}{2\pi(s-r)} \left\{ \begin{array}{l} \sin(r(w_s t) - B(r-s) + s(\phi - \pi/2)) \\ -\sin(r(w_s t) - A(r-s) + s(\phi - \pi/2)) \end{array} \right\}.$$

A and B are defined by the equations

$$A = S_A^{-1}(e) \text{ and } B = S_B^{-1}(e).$$

The output component is now a nonlinear function of two variables which contrasts with the case for d.c. waveform levels where the output component is a linear function of B-A. The harmonics are also described by more complex expressions. Each harmonic is the sum of four phase modulated sinewaves each of which has a different amount of phase

modulation. These terms cannot be grouped so that their total amplitude may be expressed as a simple function of the output component as is possible for d.c. levelled switching waves. The expression below, derived in appendix A.4.1.2 is the nearest approach to a similar form.

$$ER = \frac{1}{\pi} \left\{ \begin{aligned} &\sin(r(w_s t - (B+A)/2)) \cdot \sin((A+B)/2 + \phi - \pi/2) \\ &\cdot \sum_{s=\pm 1} \frac{s \cdot \sin((r-s)(B-A)/2)}{(r-s)} \\ &+ \cos(r(w_s t - (B+A)/2)) \cdot \cos((A+B)/2 + \phi - \pi/2) \\ &\cdot \sum_{s=\pm 1} \frac{\sin((r-s)(B-A)/2)}{r-s} \end{aligned} \right\}$$

Notice in this expression and the last that the case $r=s=\pm 1$ must be evaluated by taking the limit as s tends to unity.

The two common methods of modulation are single edged modulation and phase modulation. For single edged modulation one edge, usually B , is held fixed while the other is controlled to produce the desired output. For pulse phase modulation the sampling waves for A and B are identical, apart from a shift in time, so that B follows A by a fixed interval if a constant input is applied to both samplers.

For a single edged modulation and other width modulations the amplitudes of all harmonics are zero for zero output since both the terms above, within the summations, are zero for $A = B$. Normally a modulator only permits a single sign for $B-A$ so that width modulators have zero output at one end of the output range.

As the output increases so does each harmonic energy increase. The phase relationship is very complex.

For pulse phase modulation the terms within the summation are constant. The cosine component has an amplitude linearly dependent on the output component. The sine component has an amplitude elliptically related to the output component. The phases of both components are nonlinearly related to the output component by an arcCos function.

4.1.2.1 Harmonic Cancellation

By using I waveform levels with the same waveshape but with uniformly spaced phases and by using sampling waves with the same restrictions it is possible to cancel all the harmonics of the switching wave not integral multiples of I .

The conditions may be stated mathematically by

$$a(h,i) = a(h,o) \text{ for all } i,$$

$$\phi(h,i) = \phi(h,o) + 2\pi hi/I,$$

$$S_{Bi}^{-1}(e) = S_{Bo}^{-1}(e) - 2\pi i/I, \text{ and}$$

$$S_{Ai}^{-1}(e) = S_{Ao}^{-1}(e) - 2\pi i/I.$$

Under these conditions of symmetry the r^{th} harmonic is described by

$$E = \sum_{h=0}^{h=H} \sum_{s=\pm 1} a(h,o)/(2\pi(sh-r)) \left[\sum_{i=1}^{i=I} \sin(r(w_s t - \theta) + 2\pi ir/I + s(h\theta + \phi(h,o))) \right] \begin{matrix} e=S_{Bo}^{-1}(e) \\ e=S_{Ao}^{-1}(e) \end{matrix}$$

$$E = \sum_{h=0}^{h=H} \sum_{s=\pm 1} \bar{I} \cdot a(h,o)/(2\pi(sh-r)) \cdot$$

$$\left\{ \begin{array}{l} \left[\sin(r(w_s t - \theta) + s(h\theta + \phi(h,o))) \right] \text{ for } r=1,2I\dots \\ \theta = S_{Ao}^{-1}(e) \\ 0 \text{ for } r=1,2I\dots \end{array} \right\}$$

These conditions of symmetry are widely used as a means of increasing the effective supply frequency. It is possible to cancel particular harmonics by other choices of sampling waveform phasing when asymmetry of the waveform levels is present but the situation is not easily described for a general case.

Notice that there is no restriction on the form of the supply voltage waveshape. It may have any waveform from a d.c. level to a square wave with a d.c. component, however, the conditions of symmetry require each waveform level to have the same d.c. component so that levels with no a.c. component form trivial switching waves.

Each of the I waveform levels may form part of the switching wave for a maximum of one I^{th} of a period. This places an upper bound on the difference between, $S_B^{-1}(e)$ and $S_A^{-1}(e)$ of $2\pi/I$ radians. For differences less than this the switching wave has an interval of zero level between leaving one level and taking up the next level.

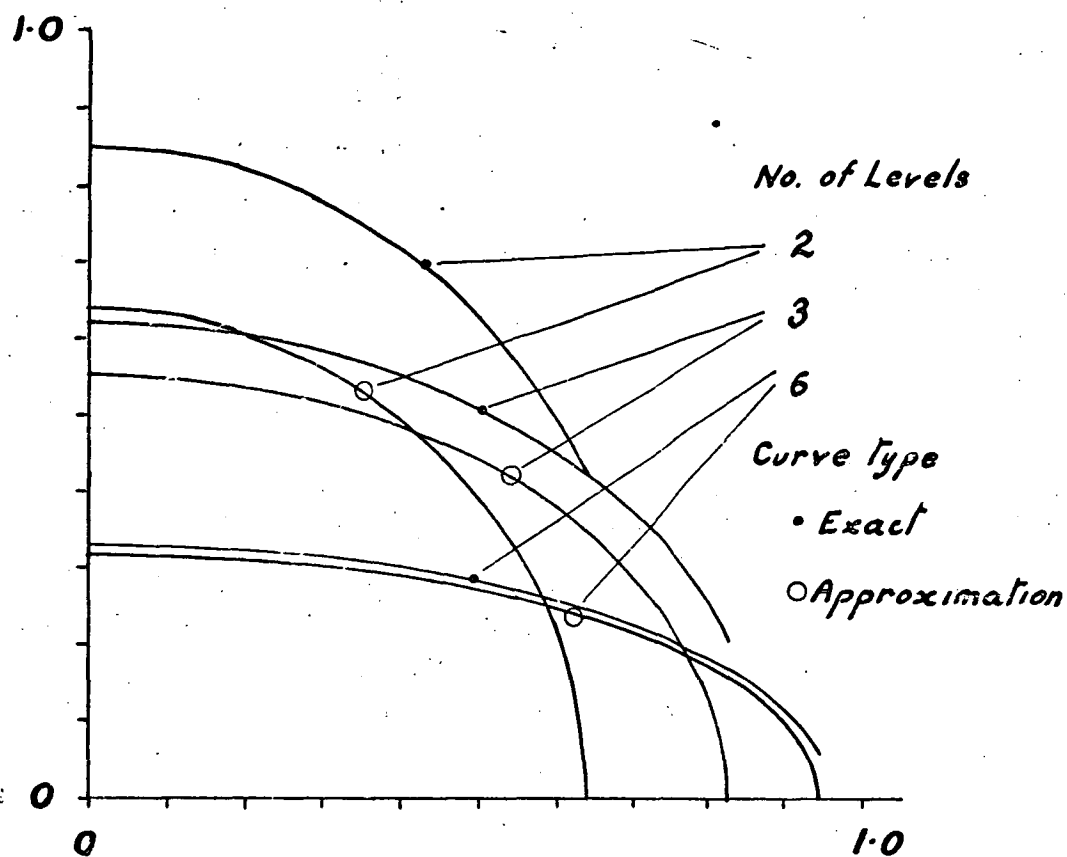
It is usually desired that the switching wave average have the largest possible range. To obtain maximum output component the switching wave must follow the envelope of the supply waveform. When this is done the switching wave follows each supply for the maximum

possible proportion of a period. Furthermore the phases for taking up and relinquishing a given level are determined for this output level. Provided some law relating the modulation of the switching instants is used these phases will define the proportions of the modulation. Thus for example pulse phase modulation, which has a nominally constant pulse width, has its pulse width defined by this criterion. Similarly single edged pulse width modulation has the phase of the fixed edge set by the same criterion.

4.1.2.2 Some Thyristor Generated Switching Waves

As examples of a.c. levelled waveforms encountered in practice consider the thyristor based waveforms of diagram 1. These are forms of pulse phase modulation and a mixed modulation with elements of pulse width and pulse phase modulations depending on the output level. The production of these waveforms is described in chapter 1 where they are referred to as continuous current waveforms without and with diode clamping respectively, these names being related to the method of generation. For small output components requiring pulse widths of less than the maximum allowed, the diode clamped waveform exhibits pulse width modulation with the trailing edge fixed at the zero crossing of the waveform level. For larger output components the trailing edge of one waveform level coincides with the leading edge of the succeeding level so that pulse phase modulation occurs. Pulse phase modulation will not occur unless more than two waveform levels are used.

The algebraic expressions describing an a.c. waveform are not very enlightening in that it is hard to visualise how the harmonic energy varies with output level. One method assisting in this regard is to consider



Phase Modulation

Amplitudes of Fundamental components

D4.1.2.2a

approximations to the waveforms. Thus for phase modulation the switching wave is approximated by a triangular wave. The step of the approximate wave corresponds in magnitude and phase to the step of the switching wave but linear variation between steps is assumed rather than segments of sinewave. Obviously there will be large percentage errors at the extremes of output range or when the number of waveform levels is small but the approximation is surprisingly accurate away from these extremes. If the average phase of the two pulse edges of a level is denoted by ϕ then the approximate switching wave is described by

$$E = (I/\pi) \sin(\pi/I) \sin\phi - 2 \sin(\pi/I) \cos\phi \sum_{n=1}^{\infty} \frac{1}{n\pi} \sin(nI(\omega_s t - \phi)).$$

The accuracy of the approximation may be gauged by comparing harmonic amplitudes and phases with the exact values for a range of values of the output component (which is written above as a function of ϕ). This is not feasible as a hand calculation and use was made of a digital computer. An Algol program was used to generate tables of harmonic components for 2, 3, 6 and 12 waveform level cases. The tables form appendix A 4.1.2.2a. Comparison of the tables with the above expression show that for zero output component the error with six waveform levels is less than 3% while for twelve levels the error is less than 1% of the true harmonic amplitude.

Diagram D 4.1.2.2 shows the amplitudes of the fundamental harmonics of the actual and approximate waveforms, for two, three and six level cases, as functions of output component. Remembering that the fundamental of a six level waveform has the same percentage error as

the third harmonic of a two level waveform, it is apparent that the third and subsequent harmonics of a two level waveform are close to the approximate curves. Examination of tables shows that the amplitude of a harmonic at maximum output is close to one third the value at zero output and that the phase change is less than that of the approximate waveform with the greatest departures near maximum output.

Three features of the approximate waveform have equivalents or parallels with d.c. levelled switching waves with many levels. These are, first, harmonic amplitude is inversely proportional to harmonic number, second, the ratio of maximum output component to maximum harmonic amplitude is proportional to the number of levels, and third, the phase of the n^{th} harmonic is modulated with an index proportional to the product of n and the number of levels.

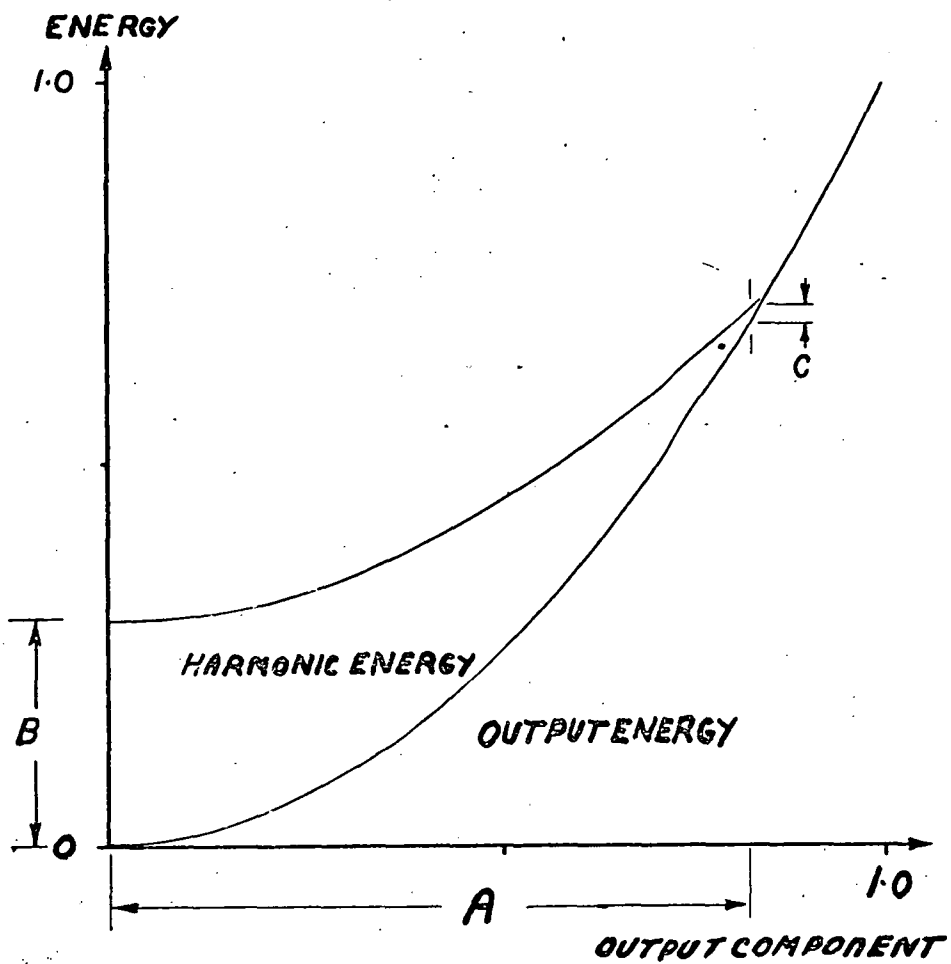
Some of the features which differ are, maximum output is not independent of the number of levels but is a nonlinear function of this number, harmonics are modulated by an elliptic function of output component rather than a cosine function, and phase modulation of the harmonics is not linearly dependent on output level but upon an arcsine function of this variable.

The total energy of the switching wave is given by

$$ET = (I/2\pi) \cdot \int_{\phi-\pi/I}^{\phi+\pi/I} \sin^2 \theta \, d\theta = 1/2 \left[1 - (I/2\pi) \cdot \sin(2\pi/I) \cdot \cos 2\phi \right] .$$

The output component is described by

$$EO = (I/\pi) \sin(\pi/I) \sin \phi .$$



Levels Proportion	2	3	4	6	12
A	.637	.828	.900	.955	.988
B	.500	.294	.182	.086	.022
C	.095	.022	.009	.002	.0001

ENERGY DISTRIBUTION - A.C. LEVELED SWITCHING WAVE
PHASE MODULATION

D 4.1.2.2 b

The harmonic energy may be determined as a function of output level by replacing ϕ in the total energy expression by an expression derived from the last equation then subtracting the energy of the output component. This yields the expression below.

$$EH = \frac{1}{2} \left[1 - (I/2\pi) \sin(2\pi/I) - 2EO^2 \left[1 - \pi/I \cot(\pi/I) \right] \right] .$$

Diagram D 4.1.2.2b, which shows the energy distribution for a switching wave with three levels, may be used in conjunction with the table to visualise the diagram for other numbers of levels. Notice that both the total energy and the output component are parabolic functions of output component. The difference between the two curves is the harmonic energy. The table shows how the number of levels influences the harmonic energy. As the number of levels increases the harmonic energy becomes smaller so that a twelve level waveform has an harmonic energy of about two percent of the maximum output for output components near zero.

The form of convergence of the total energy to the output energy as the number of levels is increased differs markedly from that for the d.c. levelled waveform of the minimum energy variety. Both forms have parabolic curves representing the harmonic energy as a function of output level but whereas the d.c. levelled waveforms have distinct segments of parabola with cusps between corresponding to the levels of the waveform the a.c. levelled waveform is a single curve with a maximum at zero output and a zero point beyond the maximum possible output.

Notice how the maximum output, designated by A in the table and on the diagram, varies with the

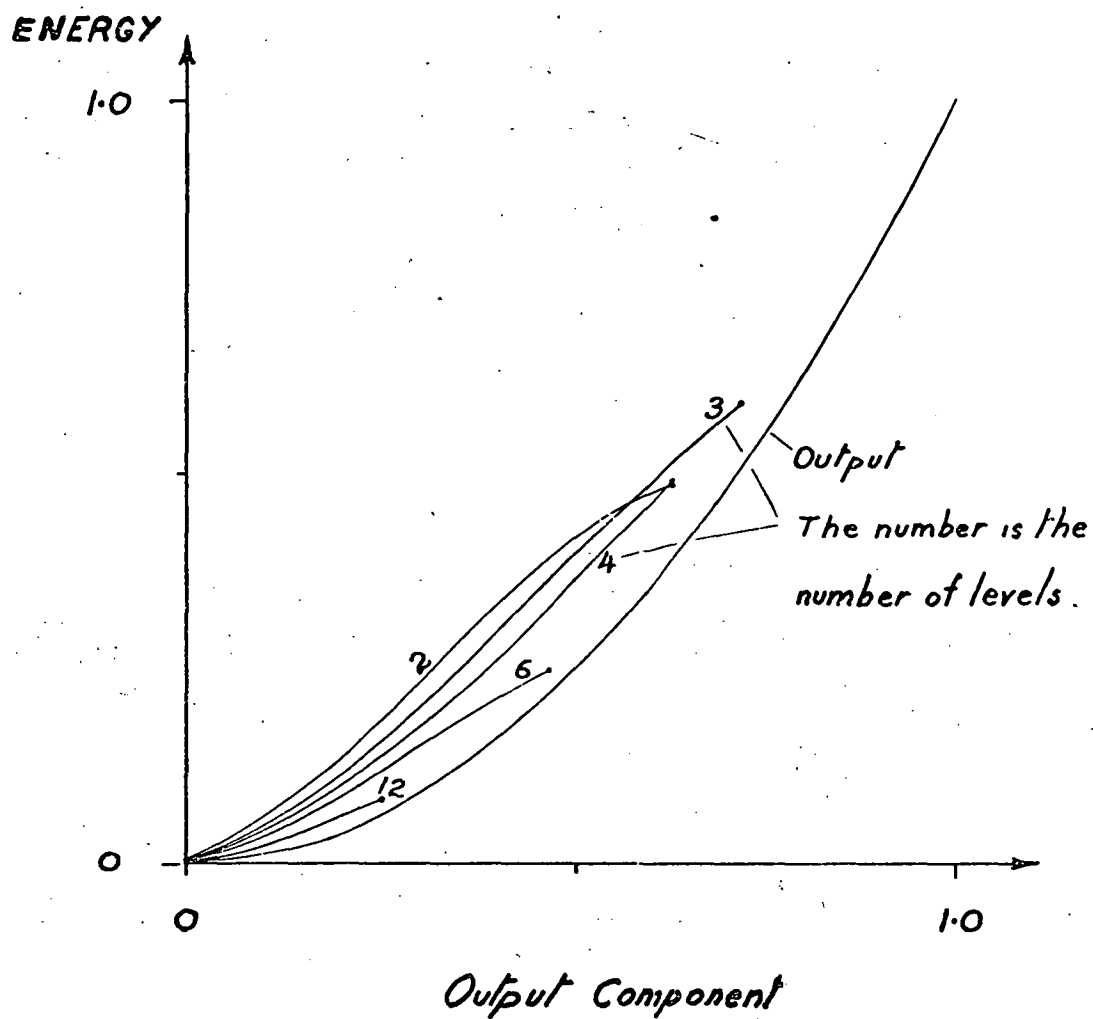
number of levels. Initially the convergence towards the limit of unity is rapid as the number of levels is increased but slows rapidly. The deviation from unity is approximately an inverse square function of the number of levels so that doubling the number of levels quarters the difference between maximum output and unity. The functions describing B and C are approximately inverse square and inverse fourth power functions of the number of levels for numbers of levels greater than six.

The diode clamped waveform differs from the phase modulated waveform when the lowest point of this switching wave equals or is less than the clamping voltage, in this case zero. The step size and width of the diode clamped switching wave vary with output level and are zero for zero output component.

A straight line approximation of the waveform may be used to form an estimate of the harmonic amplitudes but is not as simple as that for phase modulation. The analysis of such an approximation, shown in appendix A 4.1.2.2b, indicates that, for situations where the product of pulse width and harmonic number are much greater than unity, the amplitude of a harmonic is approximately proportional to pulse width divided by harmonic number. Calculated amplitudes, based on the exact expressions, from appendix A 4.1.2.2a and these differ from the estimates by as much as twenty five percent. The phase of a harmonic varies approximately with the product of pulse width and harmonic number.

The energy of the total switching wave is obtained from the expression

$$ET = (I/2\pi) \int_{\pi-B}^{\pi} \sin^2\theta \, d\theta = (I/4\pi) [B - \sin(2B)/2] .$$



Energy Distribution - A.C. Levelled Wave

Pulse Width Modulation

D 4.1.2.2c

The output component is given by

$$EO = (I/2\pi) \int_{\pi-B}^{\pi} \sin\theta \, d\theta = (I/2\pi) [1 - \cos B] .$$

The energy of the total waveform as a function of EO may be found by eliminating B. The energy diagrams for a number of waveform levels are shown in diagram D 4.1.2.2c. Each curve is terminated at the point where phase modulation begins and corresponds to the energy diagram of phase modulation at that particular output level. The curves are all based on the same expression but differ in their scales and their maximum output limits. The curve for twelve levels is the curve for two levels with the axes expanded six times, and thus corresponds to a short segment very close to the origin on the two level curve.

The energy of the harmonics may be zero when the desired output component corresponds to the clamping level. Apart from this zero the curves are not touching the curve for output component but are nearest when the output reaches the level where phase modulation commences. In the case of two level waveforms the harmonic energy is less than the equivalent phase modulated wave for the entire output range. The other cases have lower harmonic energy near zero output but require phase modulation to reach full output and thus have the same energy at the point of change over and thereafter.

The two switching waves considered here are members of the very wide range of possible waveforms having a.c. levels. Their sinewave levels are rather simple compared to the possible shapes but even so the algebraic description of the switching waves is far from simple to visualise. The algebraic manipulation of more

complex waveforms is not really feasible and use of computer programs of the simple type outlined is almost essential. Valuable insight as to the nature of the computed harmonics may be gained by the use of approximate waveform analysis. The aim of approximations should be towards compounds of triangular and sawtooth waveforms to give straight line approximations to the waveform. Some waveforms with complex fourier series have relatively simple piecewise time functions. The calculation of harmonic amplitudes by the computer program may usually be oriented towards the use of these piecewise descriptions in the appropriate integrals rather than the fourier series expressions used in these examples.

For these examples the amplitudes of the harmonics exceed those for switching waves with a comparable number of d.c. levels and similar ranges of output component. Compare the ratios of maximum first harmonic amplitude to output component for the minimum energy, d.c. levelled, waveform and the phase modulated waveform where both have R levels. For the former this ratio is $2:\pi R$, for the latter $1:R$ so that the d.c. levelled waveform has maximum fundamental component of approximately 64% that for the a.c. levelled waveform.

A second comparison may be made using the ratio of square root of the mean, over the output range, of the total harmonic energy, to the output range. These ratios are $1:R\sqrt{6}$ and approximately $\pi:2R\sqrt{2}$ for d.c. and a.c. waveform levels respectively. The relative values are approximately 0.56:1 respectively.

From these two comparisons it appear that a.c. levelled waveforms have a relatively poor ratio of output range to ripple. This is obviously true for

examples given but is not necessarily true in general since it is easy to think of schemes where by the average ripple is halved at the fundamental harmonic. One such scheme would be to add to the waveform levels a fixed component which balances the fundamental at a particular output level. This has no effect on the mean of the switching wave or the output range but does cancel the harmonic over portion of the output range and thus reduces the ratios described. The disadvantage of this course is the added complexity due to the provision of the desired waveform which will be a harmonic of the waveform levels. The principle may also be applied to d.c. levelled waveforms with similar effects.

4.1.3 The Asymptotic Waveform

All switching waves have steps. For some waveforms with a.c. levels these steps may have zero amplitude for particular values of output component but usually step amplitudes are non zero. Provided the steps of a wave are non zero there is a frequency above which the harmonic amplitudes may be estimated, to within some degree of accuracy, by the phase and amplitude of the steps of the wave. The interval between steps is neglected. The frequency depends on the waveform of levels used; it is zero for d.c. levelled waveforms and some a.c. levelled waveforms. For those waveshapes where the frequency is non zero it is usually a function of output component as well.

The amplitudes and phases of harmonics above this frequency converge as the harmonic number increases, to those for a switching wave with the same step size but with uniform slope between steps. If the switching wave to be estimated has N steps the n^{th} of which has amplitude $a(\text{EO}, n)$ and phase $\phi(\text{EO}, n)$ then the asymptotic

expression for the wave is

$$E = EO + \sum_{r=1}^{r=\infty} \sum_{n=1}^{n=N} a(EO,n)/(r\pi) \cdot \sin(r(w_s t - \phi(EO,n)));$$

where EO denotes the output component. The r^{th} harmonic is a sum of N terms which when re-expressed as a single term is a function of EO and r yielding the equivalent expression

$$E = EO + \sum_{r=1}^{r=\infty} a_1(EO,r)/r\pi \sin(r(w_s t - \phi(EO,n))).$$

Limits may be found for both the amplitude and phase functions. For the amplitude function

$$|a_1(EO,r)| \leq \sum_{n=1}^{n=N} |a(EO,n)|.$$

This is only an upper limit to the value and corresponds to a situation where every step of the wave contributes the maximum possible to the expression. Most d.c. levelled waveforms reach this limit at one or more values of output component depending on the harmonic number. a.c. levelled waveforms with width modulation have similar properties but those with phase modulation follow the limit as output component is varied.

The range of the phase function is set by the range of the steps of the wave and is less than the range of the step with greatest range. In many cases step phases occur in pairs of opposite sign and the phase of the harmonics produced is zero or constant.

The lower harmonics of many a.c. levelled waveforms exceed those of the asymptotic expression. A good example of this is the phase modulation example with sinewave levels discussed previously. The approximate

waveform used there corresponds exactly with the asymptotic waveform.

4.1.4 Harmonic Cancellation

For switching waves with any form of level, a group of R waveforms differing only in their phasing relative to one another may be phased so that their addition results in cancellation of all harmonics not integer multiples of R . The most convenient form of addition is parallel connection of the filtered outputs of the individual switching wave generators. The effective switching wave corresponds to the mean of the individual waveforms. The harmonics of this mean not cancelled by the averaging have their original amplitudes but the lowest frequency harmonic remaining is R times the frequency of the original. The output component range and range of step phases are not altered by the averaging process.

The asymptotic expressions for the new and old waveforms have similar relationships to one another but the frequency at which the harmonics of the new waveform fall within a specified tolerance of those of the new asymptotic waveform is unaltered. Thus in terms of the number of harmonics between this frequency and the lowest frequency of the switching waveform the difference between new and old waveforms is a reduction by the ratio $1:R$. In this sense the summation process results in a waveform nearer the asymptotic expression than the original.

Summary of the Characteristics of the Harmonics of Waves due to Natural Sampling

The amplitude of a harmonic of a d.c. levelled wave varies sinusoidally with output component with a period and magnitude inversely proportional to harmonic number. The total energy, of the d.c. levelled waves examined, is a linear function of output component over each range of output component where the levels used by the switching wave do not change. For the minimum energy waves a new level is introduced and a previous one discarded when the output component passes through a waveform level. This results in a total energy curve which is a series of chords between points on the parabola of output component energy corresponding to waveform levels. The total energy curves of the three non minimum energy waves examined have a similar shape but have an additional energy related to the extra number of wave levels involved. These switching waves have no obvious advantage over minimum energy waves.

Multi phase a.c. supplies with symmetrical phasing may be used to produce switching waves with an effective frequency greater than the supplies by a factor equal to the number of phases. Two sinewave levelled waves of this type which are associated with thyristor controlled waves were examined in detail. Both exhibit a strong convergence of total wave energy to the output component energy as the number of phases is increased but differ from d.c. levelled waves in that these curves do not touch at many points as multi level waves do. The two a.c. levelled waves differ in that one has zero harmonic energies at zero output while the other has a maximum at this output.

All multi phase and multi level waveforms have

spectrums which may be approximated by the spectrum of a wave, with the same size steps but with linear chords between steps. All types of switching waves can be added to others of the same type when suitably phased, to produce cancellation of harmonics so that the effective sampling frequency is increased by the number of component waveforms and the number of levels is increased. d.c. levelled switching waves produced by equivalent hardware to a.c. levelled waves have approximately 0.6 the mean and peak harmonic energies for equivalent output component range.

CHAPTER IV PART B

Some aspects of the high frequency components of switching waves produced by Natural Sampling.

The discussion leads through the properties of the switching wave spectra to the formation of a graph of passband noise to signal ratio as a function of passband width. Curves are shown for waves with d.c. and sinewave levels. The discussion demonstrates the methods used, their limitations, and their application to other types of waveform level. As intermediate results the signal/sideband noise as a function of signal amplitude for the two wave types are derived.

4.2 Spectra of Waves with a.c. Control Signals

The description of switching waves discussed earlier concentrated on the allocation of components to particular harmonics of the switching wave repetition rate. The output component is shown there to modulate the amplitude and phase, often nonlinearly, of each harmonic. Provided the output component has a periodic waveform each modulated harmonic may be represented by the sum of a number of unmodulated sinewave components. The frequency of each sinewave is separated from the harmonic frequency by an integer multiple of the output component frequency. The amplitude and phase of each sideband of the harmonic frequency is determined, for a given type of switching wave, by the waveshape and amplitude of the a.c. part of the output component, and by the d.c. part of the output component. These are the parameters by which sidebands are described.

Earlier the general fourier series of a switching wave was derived. The expression for the r^{th} harmonic is

$$ER = \sum_{i=1}^{i=I} \sum_{h=0}^{h=H} \sum_{s=\pm 1} \bar{a}(h,i) \left[\begin{array}{c} \theta = S_B^{-1}(e) \\ \Delta \sin(r(w_s t - \theta) + s(h\theta + \phi(h,i))) \\ \theta = S_A^{-1}(e) \\ / (2\pi(sh-r)) \end{array} \right] .$$

Each term of this expression is a phase modulated sinewave with a phase related to the control signal by either of the relationships

$$E\theta = (sh-r)S_B^{-1}(e) \quad \text{or} \quad (sh-r)S_A^{-1}(e).$$

For a linear amplifier the control signal, e , and output component are linearly related so that these expressions also define the phase as a function of

output component. Each phase modulated sinewave may be resolved into its separate sidebands by standard techniques giving the transformation below.

$$\sin(rw_s t + s\phi(h, i) + (sh-r)S^{-1}(e)) := \sum_{n=-\infty}^{n=\infty} C(n) \sin((rw_s + nw_m)t + s\phi(h, i) + \psi(n)) .$$

The co-efficient, $C(n)$, and phase, $\psi(n)$, of each sideband are determined by the a.c. and d.c. parts of the output component, by the shape of the sampling wave, S , and by the factor $(sh-r)$.

The amplitude and phase of the n^{th} sideband of the r^{th} switching wave harmonic is given by the expression

$$\text{ERH} = \sum_{i=1}^{i=I} \sum_{h=0}^{h=H} \sum_{s=\pm 1} \bar{a}(h, i) \left[\Delta_{S_a}^{S_b} C[n] \sin((rw_s + nw_m)t + s\phi(h, i) + \psi(n)) \right] .$$

The form of the r^{th} harmonic is re-expressed after the summations indicated giving the form shown by the expression

$$\text{ER} = \sum_{n=-\infty}^{n=\infty} \text{CT}[n] \sin((rw_s + nw_m)t + \psi T(n)) .$$

Usually both CT and ψT are nonlinear functions of the a.c. amplitude and d.c. part of the output component.

The sidebands may have frequencies above or below the harmonic frequencies with which they are associated. The n^{th} sideband of the r^{th} harmonic has a

frequency less than that of the output component when n and r satisfy the inequalities

$$|rw_s + nw_m| < w_m.$$

Since such a sideband cannot be filtered from the output component without materially affecting the latter it is important to know the relative amplitudes of the sideband and the output component. This measure of the quality of the amplifier output provides one point for the comparison of different types of switching wave.

The first step in obtaining this information is the examination of the characteristics of phase modulation, the second is the estimation of the effects of the summation process on the basic properties of the phase modulated wave. Both these are influenced by the type of switching wave used.

4.2.1 The Spectrum of Phase Modulation

A phase modulated sine wave is described by

$$E = \sin(w_s t + f(t) + f_0), \text{ where } f(t) \text{ is the}$$

alternating component of the modulation angle and f_0 the direct component. The alternating component may be a single periodic waveform or a number of periodic waveforms or an aperiodic waveform. The first two cases may be analysed in terms of Fourier series; the last requires the use of continuous spectra based on the use of the Fourier transform. The following analysis is restricted to the use of Fourier series.

4.2.1.1 A Single Periodic Modulation

For a single periodic modulation, with angular frequency w_m , the phase modulated sinewave is shown in appendix A 4.2.1.1 to be described by

$$E = \sum_{r=-\infty}^{r=\infty} a[r] \sin(w_c t + f_o) + b[r] \cos(w_c t + f_o), \text{ where}$$

$$a[r] + jb[r] = \frac{1}{2\pi} \int_0^{2\pi} e^{j(f(\theta) - r\theta)} d\theta.$$

The best know example is that for a cosine modulation angle where

$$f(w_m t) = x \cdot \cos(w_m t).$$

For this case

$$a[r] + jb[r] = J_r(x) [\cos(r\pi/2) + j \sin(r\pi/2)].$$

The coefficients are Bessel functions. Tables of Bessel functions are readily available and may be used to find the coefficients when sinewave modulation is of intrest. Any other form of modulation requires the evaluation of the integral expression since tables do not exist for other waveshapes. It is possible to express the coefficients for other waveshapes in terms of Bessel functions though this is usually difficult.

4.2.1.2 Multiple Periodic Modulations

A modulation angle may be the sum of a number of periodic functions. Suppose such an angle is composed of I functions, $f_i(w_i t)$, so that

$$f(t) = \sum_{i=1}^{i=I} f_i(w_i t).$$

The i^{th} function coefficients may be evaluated separately and re-expressed in the form

$$a[i, r] + jb[i, r] = c[i, r] e^{j\theta[i, r]}.$$

The fourier series representing the complete modulation of the sinewave is derived in appendix A 4.2.1.2. The expression is

$$\begin{aligned} E &= \sin(w_c t + \sum_{i=1}^{i=I} f_i(w_i t) + f_o) \\ &= \sum_{q=-\infty}^{q=\infty} \left\{ \prod_{i=1}^{i=I} c[i, r[i, q]] \right\} \sin(w_c t + f_o + \\ &\quad \sum_{i=1}^{i=I} (r[i, q] w_i t + \theta[i, r[i, q]])), \end{aligned}$$

where each of the possible sequences of the I integers, $r[1, q]$ to $r[I, q]$, corresponds to a single integer q in such a way that

$$\begin{aligned} \sum_{i=1}^{i=I} r[i, q] w_i &\geq \sum_{i=1}^{i=I} r[i, q-1] w_i, \text{ and} \\ \sum_{i=1}^{i=I} r[i, 0] w_i &= 0. \end{aligned}$$

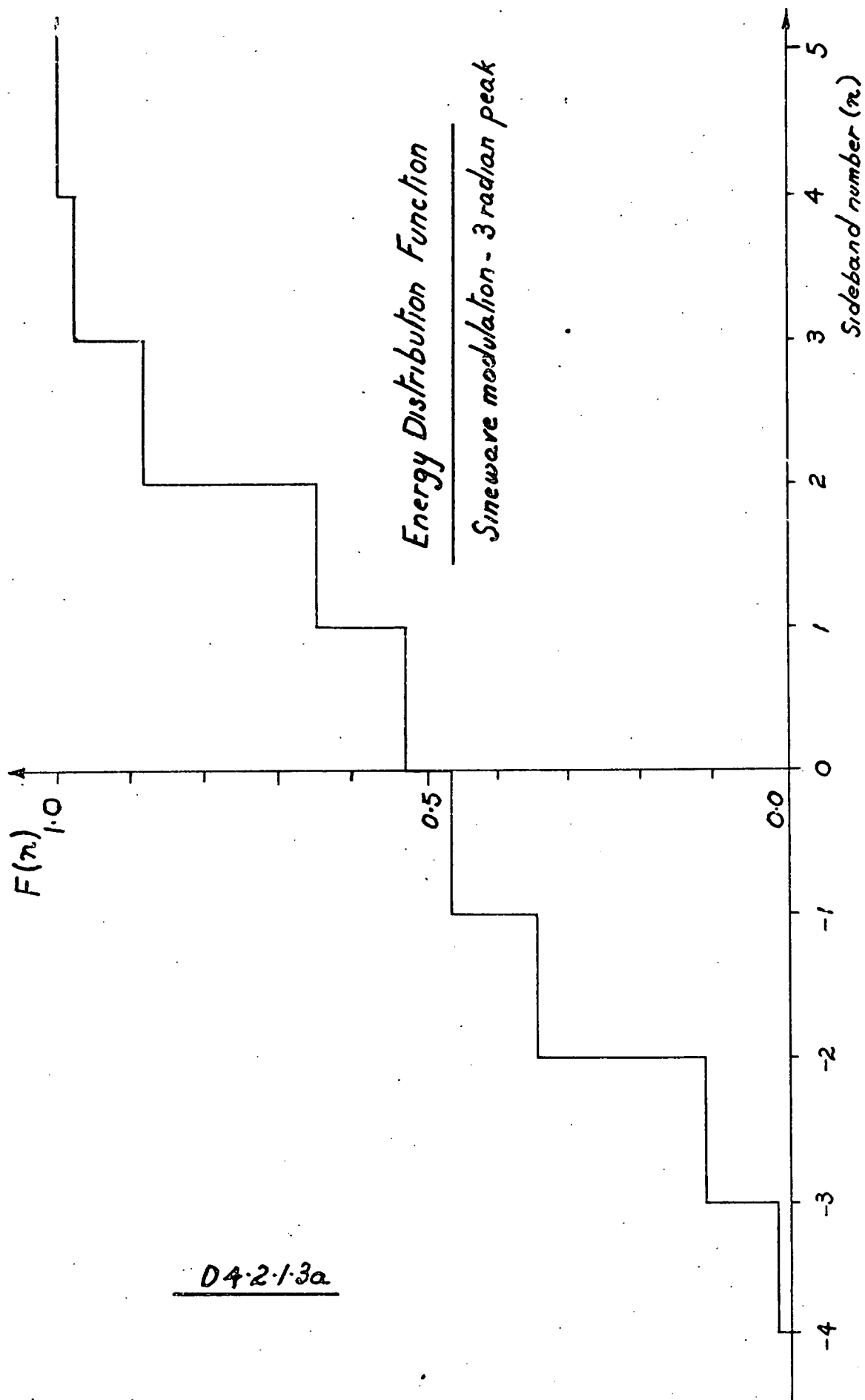
The fourier series contains components with frequencies which correspond to the sums and difference of all the harmonics of each of the I components. The coefficient

of the term corresponding to a frequency $aw_1 + bw_2 + cw_3 + \dots$ is given by

$$E = c[1,a] \cdot c[2,b] \cdot c[3,c] \dots, \text{ while the phase is } E = \theta[1,a] + \theta[2,b] + \theta[3,c] + \dots$$

Provided no two periods of the individual modulations are integer multiples of a common period, none of the components of the series will have the same frequency except in the sense that positive and negative frequencies are the same.

In the section dealing with single periodic modulation it was mentioned that the Fourier series co-efficients may be expressed in terms of Bessel functions. The form of this expression may be gauged by means of the above relationship. Each term of the fourier series representing the periodic modulation is regarded as a separate modulation. Thus each term of the resultant fourier series has co-efficients which are products of Bessel functions. Furthermore, because the modulations have frequencies which are integer multiples of a basic frequency many terms have the same frequency. The end result is that for each harmonic of the basic frequency the co-efficient of the fourier series is an infinite sum of products of Bessel functions. The method is usually considered impracticable for modulation fourier series with more than two terms.



D4.2.1.3a

4.2.1.3 The Energy Distribution Descriptions

A phase modulated sinewave may have a sideband with zero frequency. This occurs when the frequency of a component, or intermodulation product, of the phase modulation function is related by an integer ratio to the sinewave frequency. Provided this is not the case, the energy of any phase modulated signal is independent of the form of phase modulation used. This property is convenient since the modulation form influences only the distribution of the energy amongst the sidebands and not the total energy of these.

One way of describing the energy distribution amongst the harmonics of a phase modulated sinewave is the function

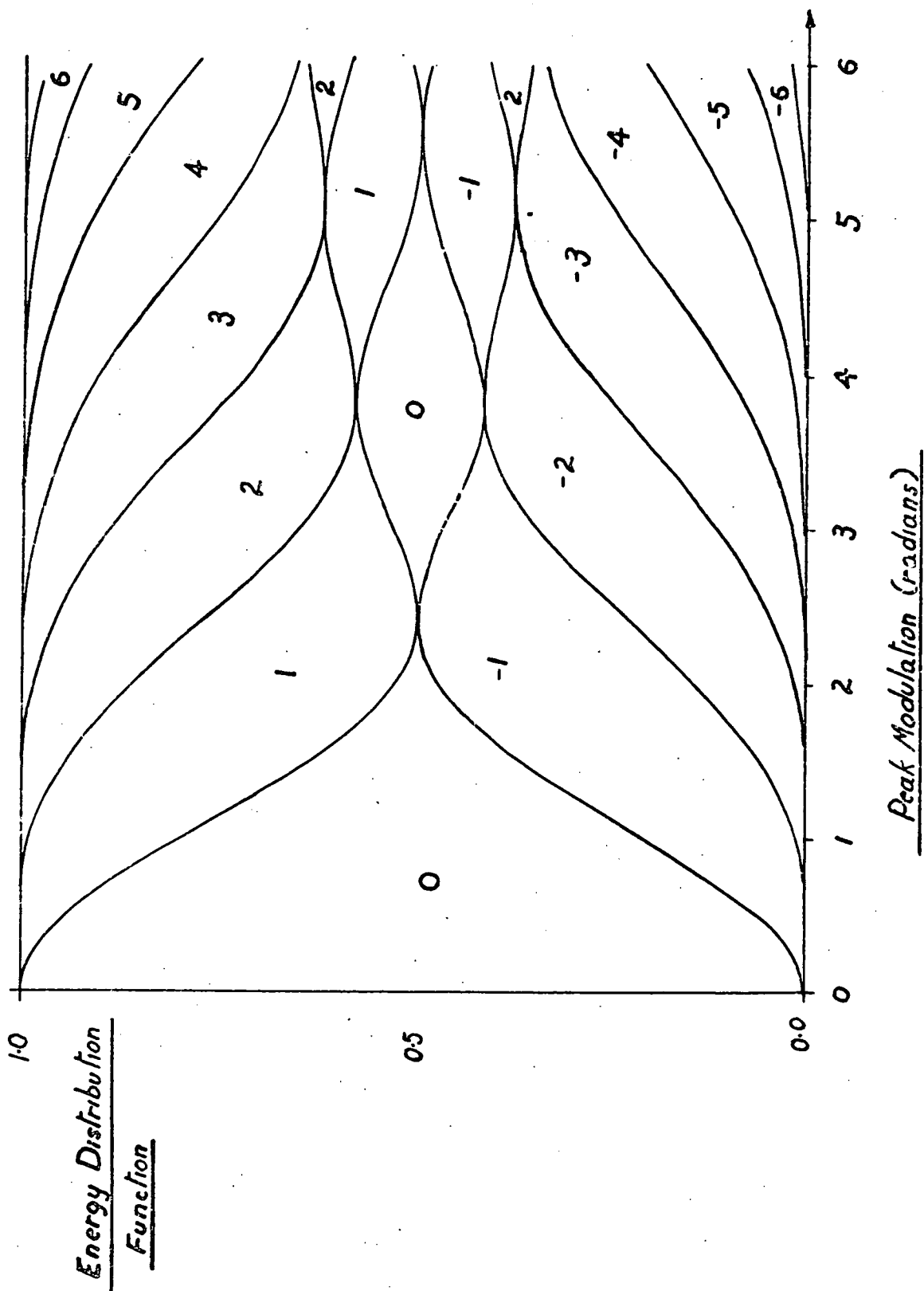
$$F(n) = \left(\sum_{m=-\infty}^{m=n} c[r]^2 \right) / \left(\sum_{m=-\infty}^{m=\infty} c[r]^2 \right), \text{ where } c[r]$$

is the modulus of the r^{th} sideband below the carrier frequency. The function expresses the total energy of the sidebands below the $n-1^{\text{th}}$ harmonic as a function of the total wave energy. Thus the range of values of the function is

$$0 \leq F(n) \leq 1, \text{ while the function has a}$$

positive step through each integer n as n increases. The function is illustrated in diagram D 4.2.1.3a for sinewave phase modulation with a peak phase of three radian.

The energy distribution function can display only one set of sideband energies associated with a single modulation function. It is more often desirable to see how the energy distribution varies as some



D4-2-1-36

parameter of the modulation function is varied. By plotting the energy levels at which the steps of the energy distribution occur as functions of the modulation parameter a more informative display is produced. The example shown in diagram D 4.2.1.3b is that for a sinewave phase variation where the peak amplitude of the modulation is used as the parameter.

The energy distribution function is redefined by

$$F(m,x) = \sum_{n=-\infty}^{n=m} (C[m,x])^2, \text{ where } C \text{ is also redefined}$$

as a function of a modulation parameter x , as well as of m . The curves plotted are versus x with m as a parameter identifying curves.

A convenient way of identifying the energy of the sidebands is to label the spaces between curves since, for a given value of x , the vertical range between adjacent curves corresponds to the energy of a single sideband.

The example has an energy distribution function defined by

$$F(m,x) = \sum_{n=-\infty}^{n=m} (J_n(x))^2. \text{ It should be compared to}$$

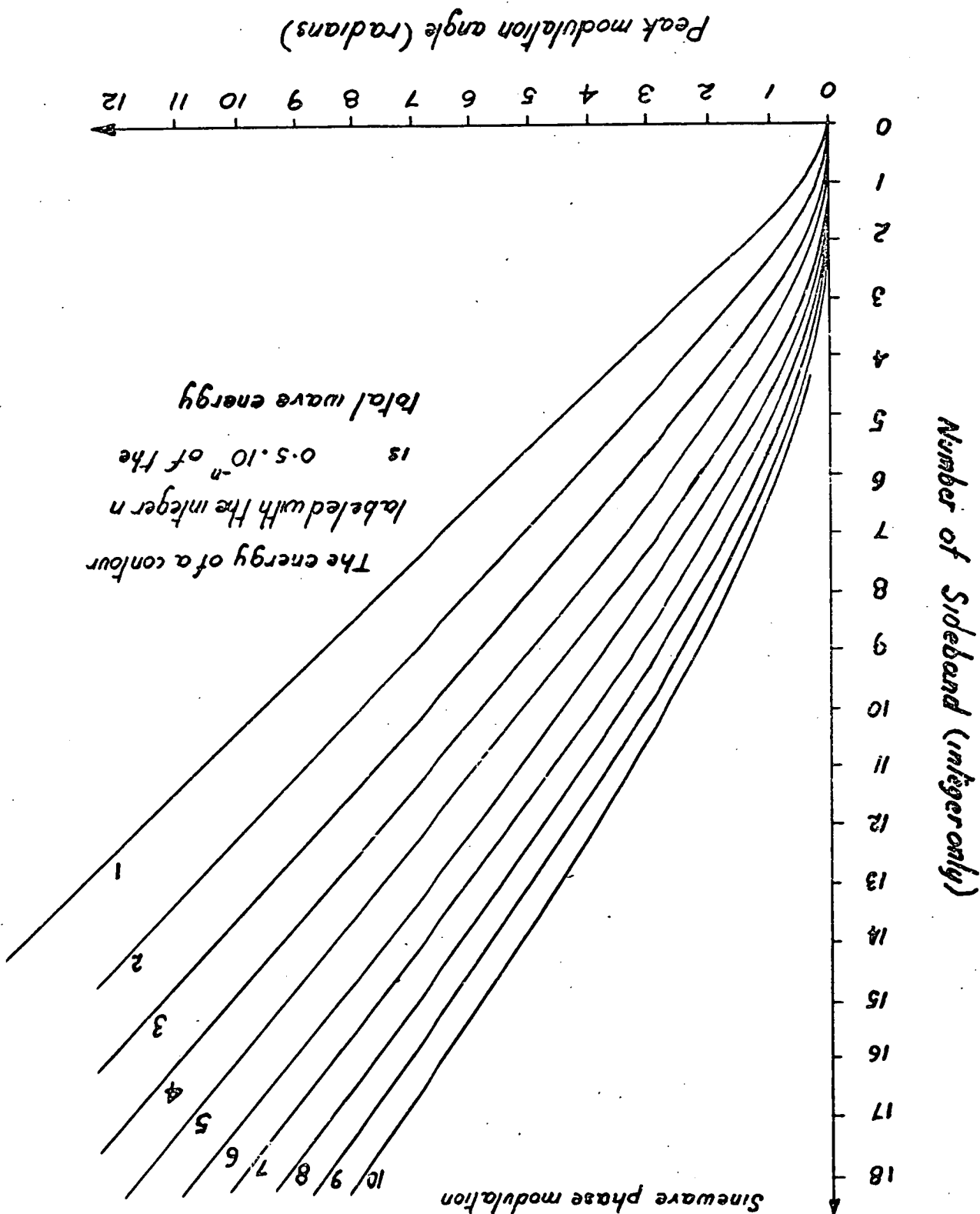
the previous example at the section with $x = 3$.

An alternative display of the energy distribution may be formed by using the energy as a parameter and plotting m versus x . An example is shown in diagram D 4.2.1.3c. The energy contour map has a set of points for each energy value. Each point of a set corresponds to an integer value of m and an associated value of x . For each set of points the relationship,

$$F(-m,x) = \text{Energy of contour, is true.}$$

ENERGY CONTOUR MAP

Sine wave phase modulation



The energy of a contour labeled with the integer n is $0.5 \cdot 10^{-n}$ of the total wave energy

Peak modulation angle (radians)

D 4.2.1.3c

In order to identify the points of a set a line is used to join them. Points on the line not corresponding to integer values have no meaning for discrete spectra.

The energy contour display is best suited to description of only half the sidebands of a modulation. The display contrasts with the other forms of display in that the low energy values of the distribution corresponding to the higher sideband numbers are very prominent features. For this reason it is used to describe the energy below a given sideband when the energy concerned is less than ten percent of the total. The contours for higher energies than this are seldom drawn since the values may be read directly from an energy distribution diagram similar to the previous example.

4.2.1.4 Sideband Amplitudes - Numerical Evaluation

The amplitudes of the sine and cosine components of the m^{th} sideband of a phase modulated sinewave are described by the real and complex parts of the expression

$$EM = \frac{1}{2\pi} \int_0^{2\pi} e^{j(f(\theta) - m\theta)} d\theta, \text{ where } f(\theta) \text{ is the modulation waveform.}$$

The expression may be re-arranged as two integrals of the form below.

$$EM = \frac{1}{2} \left\{ \frac{1}{\pi} \int_0^{2\pi} e^{jm\theta} \cos(f(\theta)) d\theta + \right. \\ \left. j/\pi \int_0^{2\pi} e^{jm\theta} \sin(f(\theta)) d\theta \right.$$

These two integrals may be recognised as the coefficients of the m^{th} harmonics of the Fourier series representing $\cos(f(\theta))$ and $\sin(f(\theta))$ respectively. Algebraic reduction

of these integrals to tabulated functions is feasible for only a few modulation waveforms such as sinewaves and piecewise linear functions of time. For the majority of modulation waveforms evaluation of the coefficients of these Fourier series must be by numerical methods.

In a numerical process integration is replaced by summation. Ideally an infinitely closely spaced set of samples are used to define an approximation to the exact waveform. In practice it is desirable to use the minimum number of samples possible to attain a desired accuracy. Normally equally spaced samples are used. Thus the equivalent of the expression for the m^{th} harmonic of a function, $g(\theta)$, with $2N$ equally spaced samples over the period is the expression

$$\frac{1}{N}(D_m + j E_m) = \frac{1}{N} \sum_{n=1}^{n=2N} (\cos(m\pi n/N) + j \sin(m\pi n/N) g(\pi n/N)).$$

The relationship between the true sine and cosine coefficients of the m^{th} harmonic of the function, $g(\theta)$, A_m and B_m , to the numbers D_m and E_m is examined in appendix A 4.2.1.4 where it is shown that the equation below is true.

$$D_m + j E_m = 2N/E(m) \left\{ \left[A_m + A_{2N-m} + A_{2N+m} + A_{4N-m} + \dots \right] + j \left[B_m - B_{2N-m} + B_{2N+m} - \dots \right] \right\}, \text{ where}$$

$$E(m) = \begin{cases} 1 & \text{for } m = 0 \text{ or } N \\ 2 & \text{for } 0 < m < N \end{cases}.$$

Accurate values for A_m and B_m are obtained by using D_m and E_m when the value of N is such that the terms with indexes other than m are small enough to be neglected. Most modulation waveforms have rapidly convergent phase modulation spectrums so that all sidebands having a coefficient index greater than some

critical number may be neglected. If this number is I then the minimum value of N required to specify the i^{th} harmonic to the degree of accuracy required is specified by the equation

$$2N = I + i + 1.$$

As an example consider the Fourier series for $\sin(x \cos(\theta))$. The m^{th} odd harmonic has an amplitude $J_m(x)$. Suppose it is desired to evaluate the coefficient of the third harmonic, for x at unity, correct to six decimal places. Now the harmonic with amplitude near 10^{-6} is the seventh. The ninth harmonic is an order of magnitude smaller than this. Thus $E_3/2N$ will be within the desired tolerance of B_3 provided

$2N - 3 > 7$, that is the number of samples used is greater than ten.

In practice tables of the modulation form under investigation are not usually available so the information above must be found by trial and error.

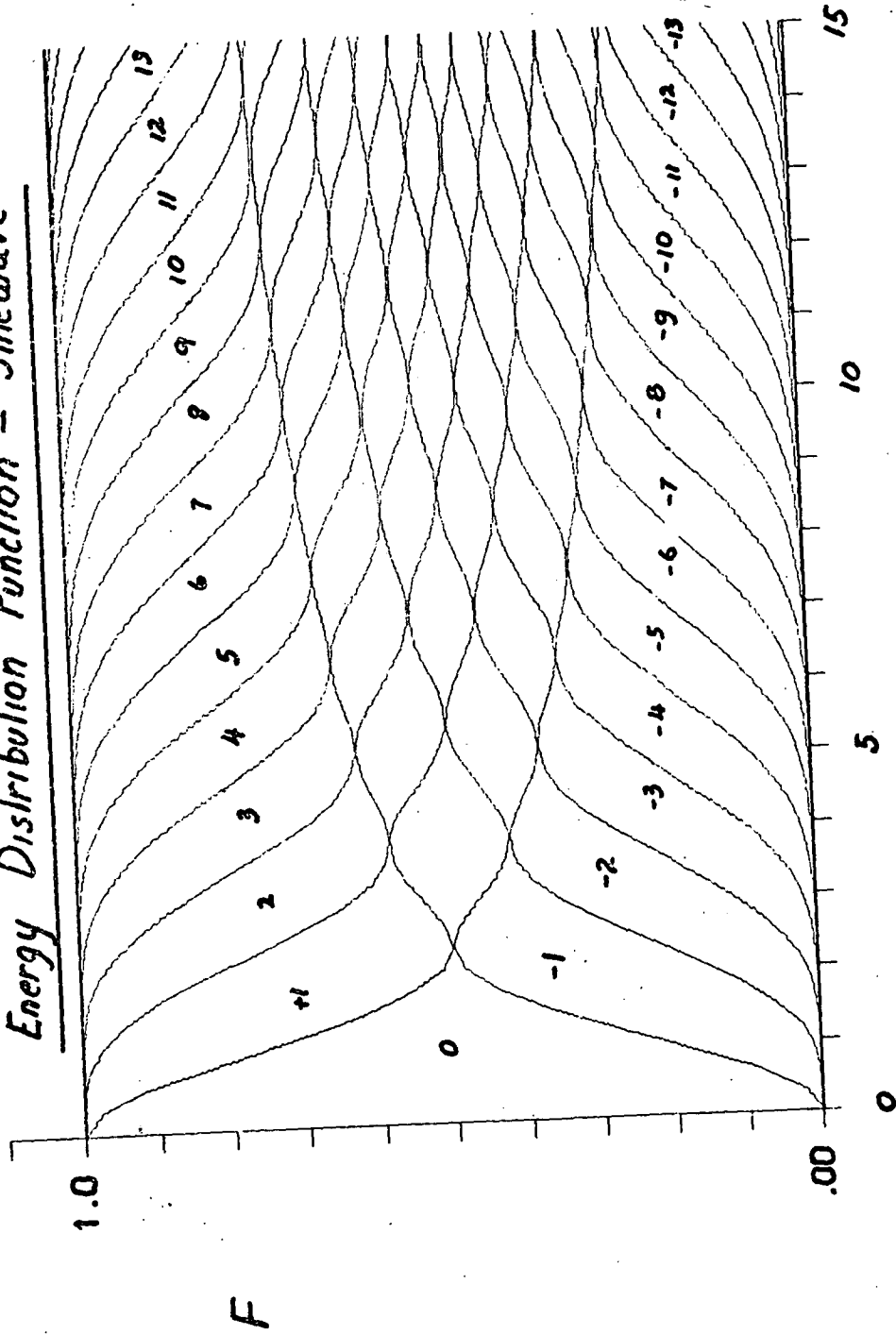
4.2.1.5 Limitations of Numerical Processes

The nature of the information processed by these numerical methods is restricted in several ways. The number of samples of the modulating signal must be finite, so must the decimal places of the answers calculated. These limitations have the following effects.

The input signal must have a finite number of sampling points, say $2N$. This number of samples can describe, without ambiguity, a signal with bandwidth corresponding to N harmonics or less. That is the bandwidth of the modulating signal is limited.

Most phase modulated signals have an infinite number of finite sidebands. The numerical process sets

Energy Distribution Function - Sinewave



Peak Modulation Amplitude (radian)

D4.2.1.5

a limit on the number of sidebands which may be calculated if finite length arithmetic is used since the inevitable round off required causes errors in the calculated amplitude. This error is of similar absolute magnitude for all sidebands so those with smaller amplitudes are submerged in the error noise. There is no point in attempting to evaluate sidebands with such small amplitudes and since these are usually the higher sidebands this sets an upper limit on the number of sidebands which may be estimated. Should a numerical accuracy less than the limit imposed by finite arithmetic be required then a corresponding lesser number of sidebands need be evaluated.

The number of sidebands, with amplitude greater than a value set by a numerical accuracy requirement, is a strong function of both modulation waveform and amplitude. To illustrate this point consider diagram D 4.2.1.5 where the energy diagram of a phase modulated signal with sinewave modulation is presented. As modulation amplitude is increased the outer sidebands increase in energy until they reach a peak value when the modulation amplitude is comparable to the sideband number. Thus the number of significant sidebands increases with increase in modulation amplitude. Now since the number of sidebands evaluated equals the number of samples it may be appreciated that the choice of this latter number is very much influenced by the exact modulation waveform being analysed. This requirement usually controls the number of modulation waveform samples used since it is normally the maximum of the two minimum sample numbers required.

Outline of Computation Sequence

The process for evaluating the sideband amplitudes of a phase modulated wave thus consists of

three steps. First from the specification of the modulating signal and experience or tabulated functions, choose a value for the number of samples required so that both the modulating signal and modulated signal will be specified to the desired accuracy. Second, perform the numerical operations outlined so that sideband estimates are formed. Third, confirm the accuracy of these estimates by checking that the sidebands converge to the permissible error level as the sideband number increases to N . In the event that convergence does not occur to the required degree increase $2N$, the number of samples, and repeat the sequence.

4.2.2 The Sidebands of Switching Waves

The introductory passage to the section describing Periodic Outputs outlined in a general way the properties of the components of the switching wave. The phase modulated nature of these components was emphasised. Methods for the computation of band limited phase modulated waves have been discussed briefly so that the essential information required for a detailed discussion of the sidebands which may effect the switching amplifier output may now proceed. Initially it is intended to describe a relatively simple waveform to show the nature of the sidebands, and their variation with switching wave parameters. The properties of more complex waves will then be described in terms of the features introduced during the discussion of this example.

A Switching Wave with one Modulated Step

Consider the expression below.

$$E = f(w_m t) + \sum_{r=1}^{\infty} \frac{2}{r\pi} \left[\sin(r(w_s t + \pi f(w_m t))) - \sin(r(w_s t - \pi)) \right]$$

The expression describes a switching wave with the following features. First, the d.c. levels of the wave have values corresponding to the odd integers so that each step is of two units in magnitude. Second, the number of wave levels is determined by the range of $f(w_m t)$. If, for instance, $f(w_m t)$ is restricted to the range between plus and minus unity then the switching wave has levels above and below this range, that is plus and minus unity. Third, only the positive going step of the wave is modulated, furthermore the phase modulation is linearly related to the output component.

Each harmonic of the wave is the difference between a modulated and an unmodulated sinewave. The expression for the r^{th} harmonic may be reformed in the manner below.

$$\begin{aligned} ER &= 2/r\pi \left[\sin(r(w_s t + \pi f(w_m t))) - \sin(r(w_s t - \pi)) \right] \\ &= 2/r\pi \left\{ \sum_{m=-\infty}^{\infty} A[m,r] \sin(rw_s t + mw_m t) + B[m,r] \cos(rw_s t + mw_m t) \right. \\ &\quad \left. + (-1)^r \sin(rw_s t) \right\}. \end{aligned}$$

where $A[m,r]$ and $B[m,r]$ are the inphase and quadrature components of the m^{th} sideband of the sinewave modulated in phase by $\pi r f(w_m t)$. Notice the $A[m,r]$ and $B[m,r]$ define the m^{th} sideband of the r^{th} harmonic in such a way that variation of the d.c. component of $f(w_m t)$ varies only the sideband phase, not the sideband amplitude. One consequence of this is that variations of the d.c. component of $f(w_m t)$ do not alter any sideband amplitudes of the switching

wave though the zero order sidebands of each harmonic, which are formed by the vector sum of the phase modulated carrier and the unmodulated sinewave, do vary with the d.c. component of $f(w_m t)$.

4.2.2.1 The Switching Wave Components within the Passband

Suppose that the switching amplifier passband extends from zero to w_p in frequency. The output filter would ideally pass all components of the switching wave with frequencies within this range. Normally all the components of $f(w_m t)$ would fall within this range, that is if $f(w_m t)$ has finite harmonics for harmonic numbers less than N then the relationship

$$w_b > Nw_m \text{ is implied.}$$

The sidebands with frequencies within the passband are lower sidebands of each harmonic with harmonic numbers, n , such that

$$|rw_s + nw_m| < w_p \text{ is valid. (n negative implies lower sideband)}$$

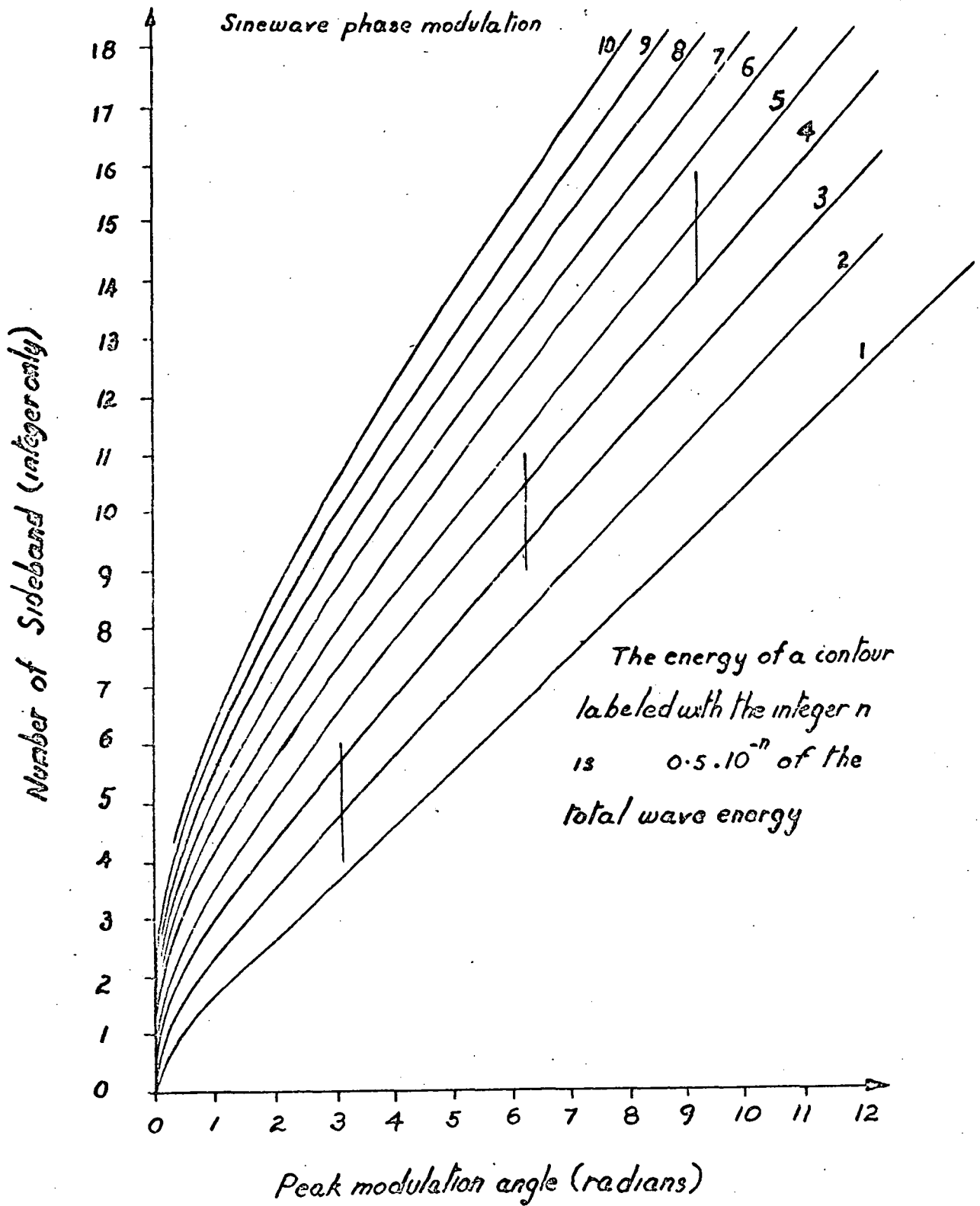
The number of sidebands, of a given harmonic, with frequencies within the passband is the integer below $2w_p/w_m$.

4.2.2.2 Passband Energy Estimation by Contour Map for Sinewave Output

Suppose $f(w_m t) = x \sin w_s t$. The passband energy may be estimated for given values of w_s/w_m and w_p/w_m by the following steps. First, the modulation of the r^{th} harmonic is rx . Second, the sidebands of interest are those nearest in number to rw_s/w_m and within the band w_p/w_m on either side. These two features may be used to

ENERGY CONTOUR MAP

Sinewave phase modulation



D4-2-22

draw short vertical lines on the contour map for a phase modulated sinewave. Each line corresponds to the range of sidebands associated with a given harmonic and modulation index. The position in the X direction on the map is $r\pi x$. The vertical position and length correspond to the range of sidebands within the passband, that is the line extends from

$$n = rw_s/w_m - w_p/w_m \text{ to } n = rw_s/w_m + w_p/w_m.$$

Diagram D 4.2.2.2 shows the situation for $w_p = w_m$ and $w_s = 5w_m$ when x is unity.

Third, for each harmonic estimate the energy within the band of sidebands and use this to form a weighted sum corresponding to the expression

$$E = \sum_{r=1}^{r=\infty} \left(\frac{2}{r\pi} \right)^2 \sum_{\substack{n \leq +w_p/w_m - rw_s/w_m \\ n > -w_p/w_m - rw_s/w_m}} (A[n,r]^2 + B[n,r]^2) / 2.$$

The energy so calculated is valid provided w_s/w_m is not an integer ratio since there is a step at these values due to a phase sensitive vector sum of waveform components with coincident frequencies so that the independence of energies of components is not valid at such points.

For the example shown in diagram D 4.2.2.2 the energy contributed by sidebands of the first harmonic is approximately 3% of the total energy of this harmonic. The corresponding percentages for the sidebands of the second and third harmonics are approximately 0.1 and 0.01 respectively. Thus the energy of the switching wave sidebands with frequencies within the passband is given by

$$E = \frac{1}{2} \left\{ \left(\frac{2}{\pi} \right)^2 \cdot .03 + \left(\frac{1}{\pi} \right)^2 \cdot .001 + \left(\frac{2}{3\pi} \right)^2 \cdot .0001 + \dots \right\}$$

units

$$\approx .006. \text{ units}$$

Thus the noise to these sidebands is about 22 db below the energy of the wave or 19 db below the output signal energy.

This method for forming an estimate of the sideband energy in the passband may also be used in conjunction with energy distribution maps with minor modifications.

The method may be extended to calculate the ripple associated with a filter by placing weighting factors on the terms of the summation. Each weighting factor corresponds to the energy response of the filter at the sideband frequency.

Because this method is based on measurements from graphs the accuracy is not high but the advantages of the method over "blind" numerical calculations are important. It is possible to see which terms are dominant in the summation visually. This allows the trends of passband energy to be appreciated quickly as functions of the switching wave parameters, passband width, modulation frequency, and modulation amplitude. These features will now be examined.

4.2.2.3 Passband Energy Variation with Modulation Amplitude

Consider the previous example, in particular the lines on the diagram. Reducing the modulation has a similar effect to changing the scale in the X direction so that each of the lines specifying the sidebands is moved towards the X origin in proportion to their original values. This will result in a decrease in energy for all harmonics.

Thus for example reducing x from 1.0 to 0.5 results in the following contributions, for each harmonic,

to the passband energy, $4.05 * 10^{-5}$, $5 * 10^{-9}$, and $4.4 * 10^{-14}$. This change illustrates two interesting features. First, although the control signal is reduced by a factor of 2 in amplitude the sideband energy is reduced by three orders of magnitude. This very strong effect on signal to ripple ratio will be referred to again during the discussion of waves with two modulated steps. Second, the relative magnitudes of the contributions of individual harmonics also changed strongly. The second and third harmonic were approximately in the scale $1/30$ and $1/300$ respectively of the first harmonic in the original example, but these ratios changed to approximately 10^{-5} and 10^{-9} for the example above. Thus for small modulation amplitudes the dominant sideband group is that of the first harmonic.

For larger values of x some of the sidebands with frequencies within the passband, may fall within the central band of diagram D 4.2.1.5. In this case passband energy must be calculated from this diagram since the contour map cannot be easily defined or used. The central band or fan has the following features. Each sideband merges with the fan after a monotonic increase to its maximum energy as peak modulation amplitude is increased. The modulation amplitude, a , at which maximum sideband energy occurs for the n^{th} sideband is approximately given by

$$a = 1.1n + 0.9 \text{ radians.}$$

After reaching the peak energy the sideband diminishes to zero energy for a value of modulation of approximately $1.5n$. As modulation amplitude is further increased the sideband energy oscillates between zero and an upper limit which diminishes with increase in modulation amplitude.

Within the fan adjacent sideband pairs have a combined energy which is almost constant, that is their oscillations are almost orthogonal. The fan boundary, defined by the lines joining the first minima of the sidebands, gradually spreads as modulation amplitude is increased.

Consider the example for $x = 3.5$. The peak phase for the r^{th} harmonic is $11r$ radians and the sidebands of interest are $5r^{\text{th}}$ and the $(5r-1)^{\text{th}}$. From diagram D 4.2.1.5 and other sources the passband energies corresponding to the sidebands of the first four harmonics are

$$\begin{aligned} EP &\approx \frac{2}{\pi^2} \left\{ .057 + .029/4 + .019/9 + .015/16 + \dots \right\} \\ &\approx .0136. \end{aligned}$$

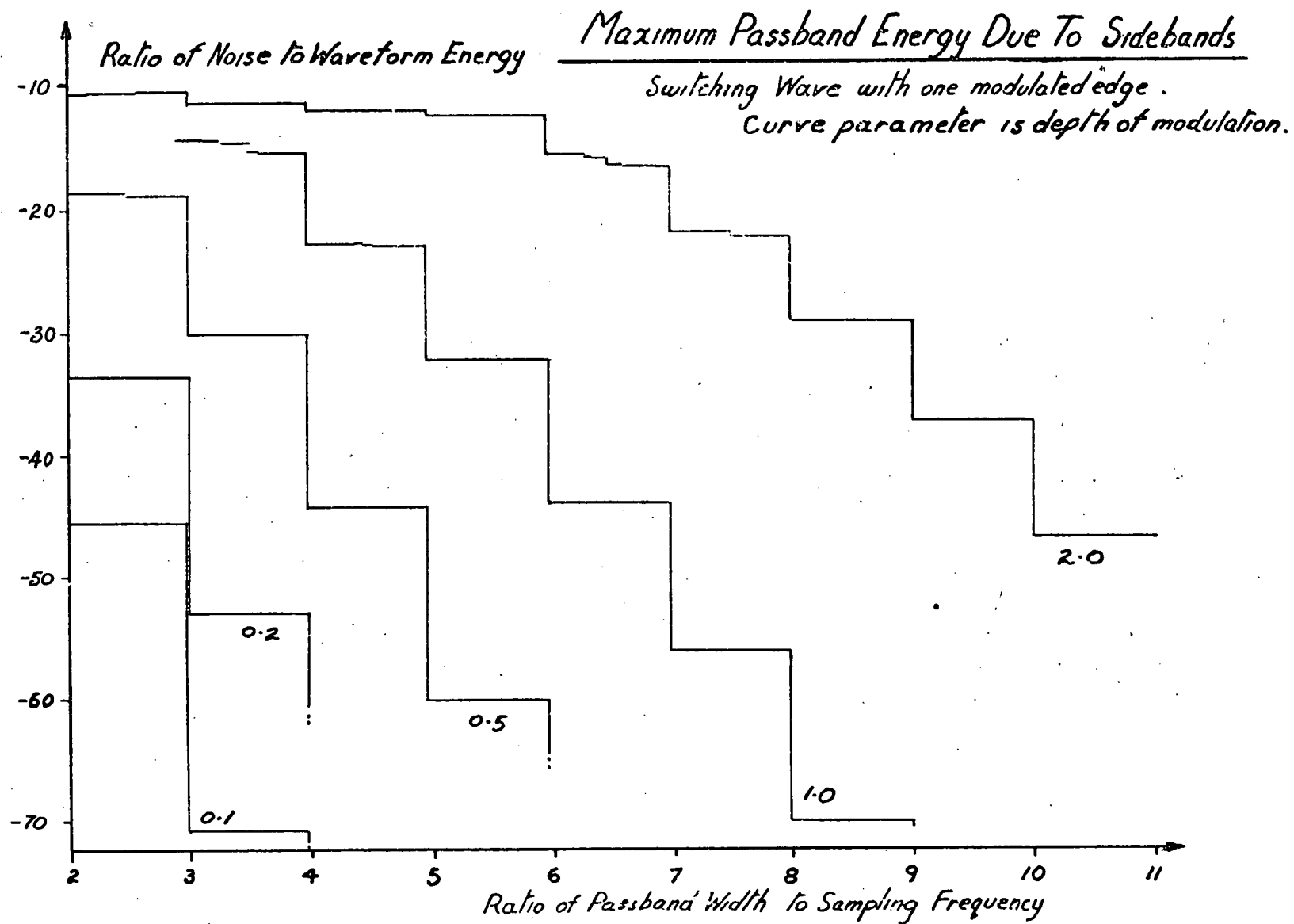
As x is increased this energy diminishes. The proportions of the various harmonic groups remain almost constant. It is shown in appendix A 4.2.2.3 that for x large the energy of the sidebands in the passband is approximately given by

$EP = .0493/x$ and that the proportions due to each harmonic group are approximately inverse cubes of the harmonic number.

4.2.2.4 Passband Energy Variation with Bandwidth and Input Frequency

Note the effect of increasing the bandwidth on the lines used in diagram D 4.2.2.2. An increase in the parameter w_b/w_s causes the lines to extend at both ends by equal amounts. Thus a greater number of sidebands are within the passband and passband energy will increase since the new set include the original sidebands. Thus for other parameters constant an increase

D4.2.2.4a



in bandwidth causes an increase in passband energy.

The effect of a variation in w_m is more complex. Both ends of the lines move upwards if w_m is reduced but the length of the line is increased also. Thus more sidebands fall in the passband but their net energy will not necessarily increase since the original sidebands are not members of the new set. Provided the sidebands are not within the central fan of diagram D 4.2.1.5, the increase in their number will not offset their diminution in energy, that is reduction in w_m causes reduction in the energy of the passband sidebands. Should the sidebands be entirely in the fan then passband energy will increase with diminution in w_m provided no sidebands move outside the high energy region on the borders of the fan.

Maximum Passband Energy

Suppose the output amplitude and the bandwidth are fixed and w_m is chosen to maximise the passband energy. What form will the curves for maximum passband energy take? Diagram D 4.2.2.4a shows the curves for several values of modulation amplitude when these are plotted versus w_s/w_b . The portions of the curves such that

$\pi \times w_b/w_s > 1$, that is those portions for which maximum energy may correspond to more than two sidebands within the passband, are approximations based on hand calculations but are in error by less than 1 db. The modulation amplitudes shown are 0.1, 0.2, 0.5, 1.0 and 2.0.

The rapid diminution of the energy of the sidebands within the passband as w_s/w_b and as modulation depth, x , are reduced is easily seen. Notice that as modulation depth is increased the worst energy nears an upper limit of approximately -10 db., that is about one

tenth the total wave energy falls within the passband as sidebands. The relatively small size of the sidebands the higher harmonics may be seen from the size of steps between integer values of w_s/w_b . The steps at integer values are predominantly due to the first harmonic sidebands entering and leaving the passband.

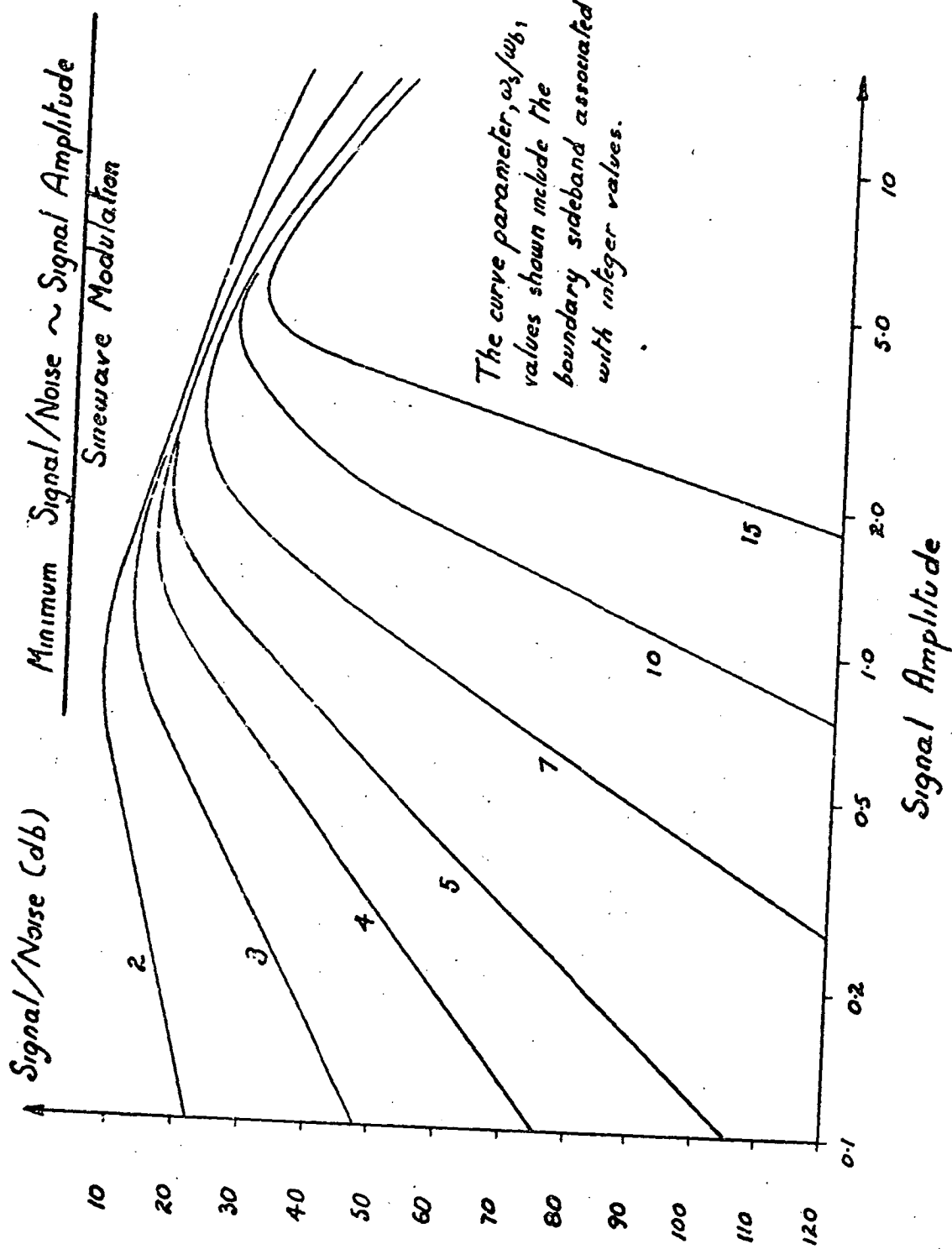
These curves give the passband noise for the best possible filtering of the switching wave. Any real filter will pass more unwanted components of the switching wave to the output of the amplifier. The corresponding curves of output "noise" energy of a switching amplifier would not have sharp steps, as these curves have, but smooth curves lying above those shown. In such a situation the noise would also contain sidebands outside the nominal passband and some sampling frequency components. For small values of modulation amplitude these latter components would exceed the sidebands in energy.

In some circumstance it is necessary to know the ratio of signal energy to "noise" energy rather than the absolute noise energy. The ratio, hereafter referred to by S/N , is a measure of the signal quality. The S/N ratio is a usefull way of comparing the properties of different classes of switching amplifier since the absolute signal and noise values do not require normalisation for comparison purposes.

Consider the S/N as a function of x , that is with w_s/w_b constant. Because sideband energy varies very slowly with x for values of x and w_s/w_b such that

$$\pi x w_b/w_s > 1 \quad \text{the } S/N \text{ ratio is almost}$$

proportional to modulation component energy in this region. Outside this region the sideband energy diminishes, as a function of x , more rapidly than the modulation component



D4-2-2-4b

energy, $x^2/2$ so that S/N increases with separation from the boundary in both regions giving a minimum at the boundary. Diagram D 4.2.2.4b shows S/N as a function of modulation component, x , for several values of w_s/w_b . Notice the almost linear variation of S/N, measured in db, with signal amplitude drawn on a log scale, when signal amplitude is small. The slope of this portion of the curves is approximately given by

$$\Delta(S/N)/\text{decade of signal} \approx 20(w_s/w_b - 1) \text{ db/decade.}$$

The minimum ratio value also increases with w_s/w_b but not linearly.

4.2.2.5 Multi-level Waveforms

By confining the output to the range between two adjacent levels, a two level switching wave capable of producing sinewave outputs, with amplitudes of at most one unit, is defined. Over this output range the S/N is a monotonic function of output level except for w_s/w_b below 2.5. For switching waves with higher numbers of levels the range of output signal is extended. A switching wave producing an output of amplitude ten units must have at least twenty one levels. Thus these curves describe waveforms with up to twenty levels.

Normally, the number of switching wave levels of a given amplifier is fixed. The maximum output possible would produce a switching wave using all the levels. The worst S/N may occur for outputs other than maximum when the number of wave levels is large. By using fewer waveform levels, but the same output range, a lower worst value of S/N may be obtained. On this basis it would appear that a two level switching wave has best performance.

This is not realised in practice due to the

method used to produce multi-level waves. These are produced by summing a number of suitably phased two level waves. The value of w_s chosen for the individual component waves is usually the maximum possible consistent with the switching speed of the components used, since this minimises the output and supply filtering requirements and maximises w_s/w_b . The phased addition process effectively cancels all harmonics, and their sidebands, of w_s below the n^{th} when n waves are added. This means that the practical limit of w_s is n times that of a two level wave. Any comparison of S/N ratio should weigh w_s/w_b according to the number of levels used.

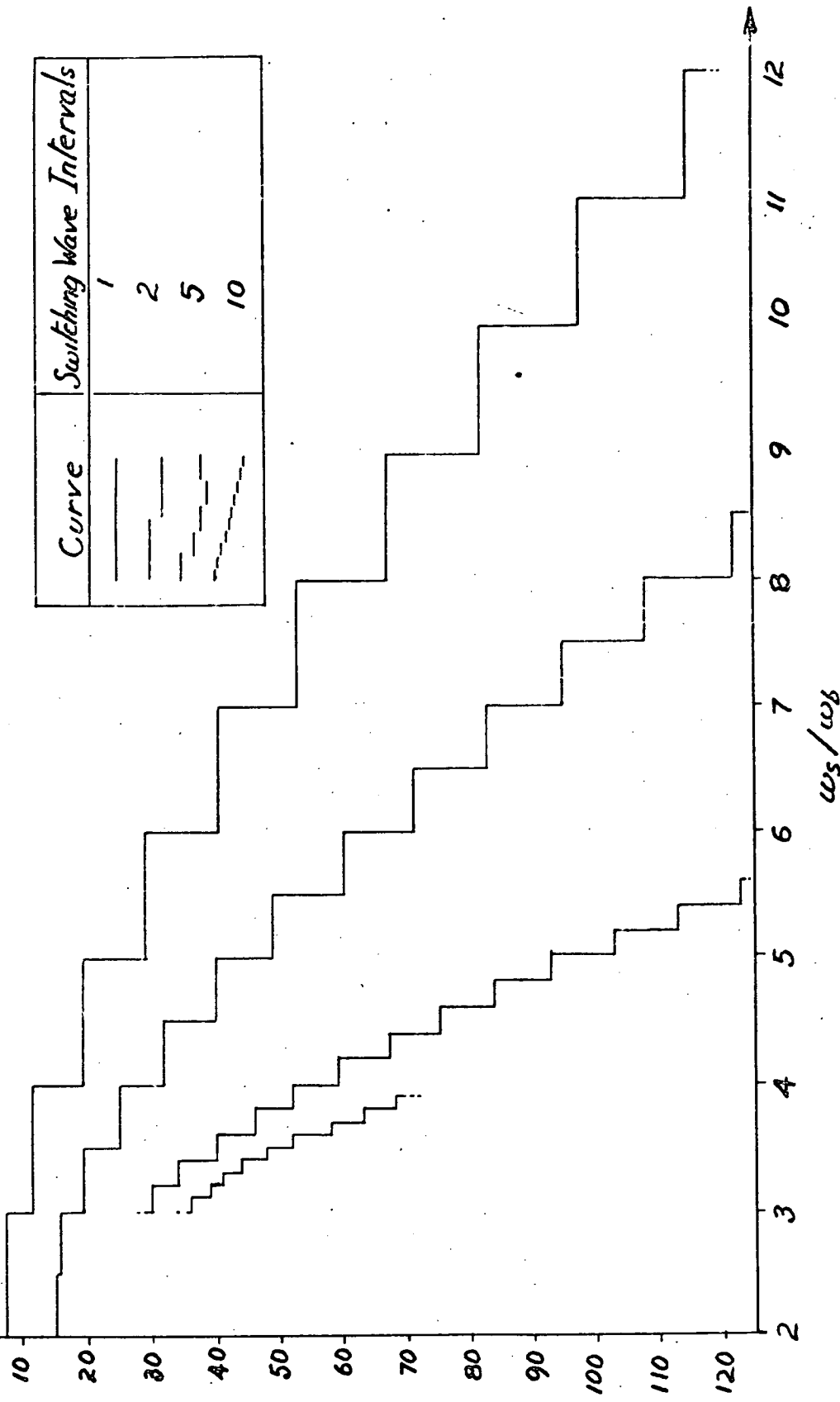
Diagram D 4.2.2.5 shows S/N, at maximum output, as a function of w_s/w_b , for two, three, six, and eleven level waveforms. The value of w_s/w_b used is that of the component two level waveforms. The maximum outputs of these multi-level waves correspond to the minimum S/N ratio over the output range provided w_s/w_b is greater than 2.5. This may be verified by noting that each curve of S/N corresponding to a value of $n w_s/w_b$ in diagram D 4.2.2.4b is below or near its maximum for an n unit sinewave output.

This basis of comparison suggests that best performance is obtained with a larger number of levels. Thus, for instance, a two level wave with 100 db S/N ratio required $w_s/w_b > 11$ compared to 7.5 for a three levelled wave and 5 for a six level wave. If w_s is limited this implies that worthwhile improvements in passband width may be realised by using more than 2 levels.

It should be remembered that the improvement relies on the cancellation of harmonics and sidebands by phased addition of waveforms. Any unbalance of the waveforms or their phasing will reduce the indicated

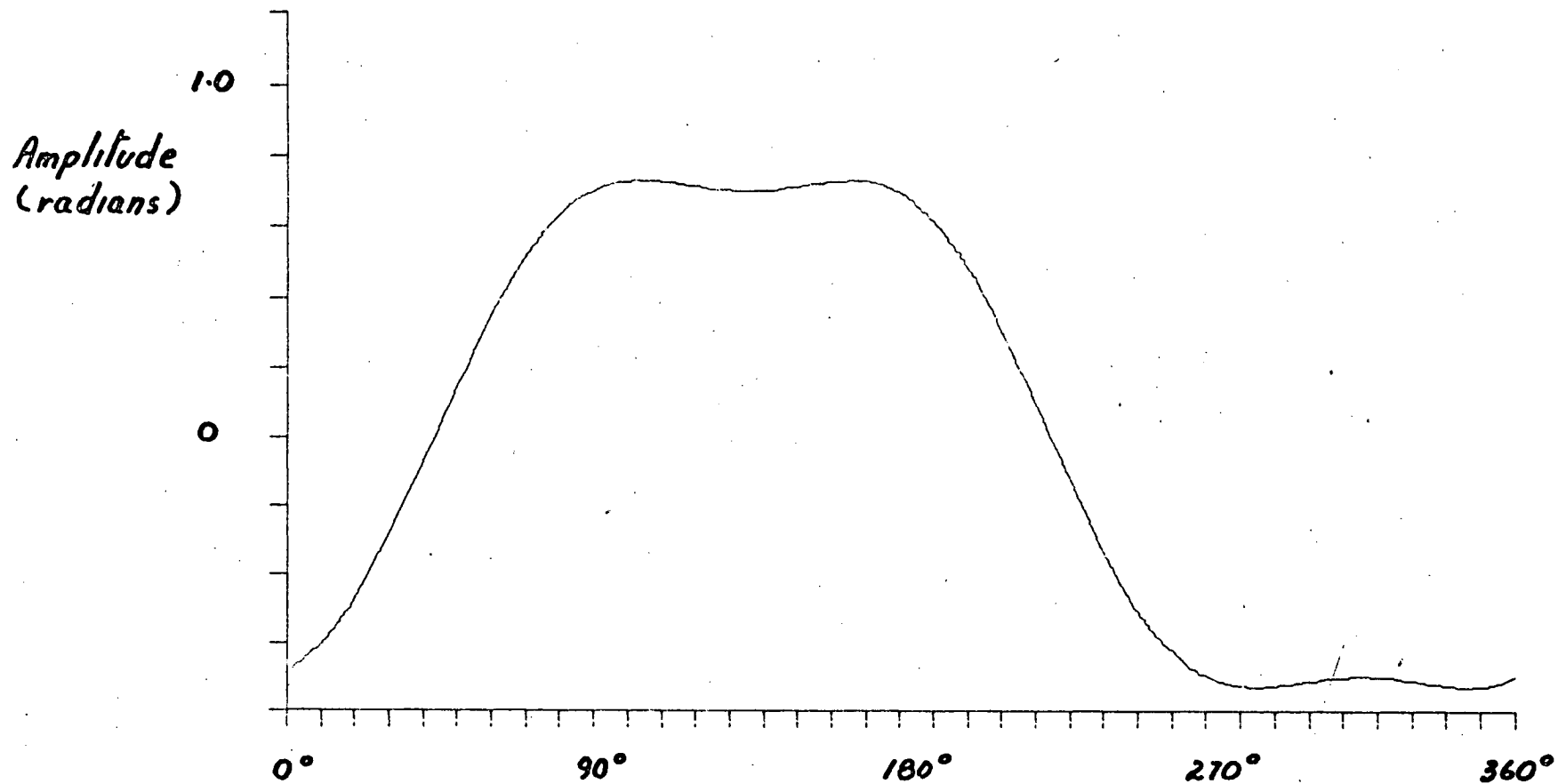
$\Delta S/N(\text{db})$
 $\text{Minimum}\{\text{Signal/Unfilterable Noise}\} \sim \text{Effective}\{\text{Waveform Frequency/Bandwidth}\}$

Curve	Switching Wave Intervals
—	1
—	2
—	5
- - -	10



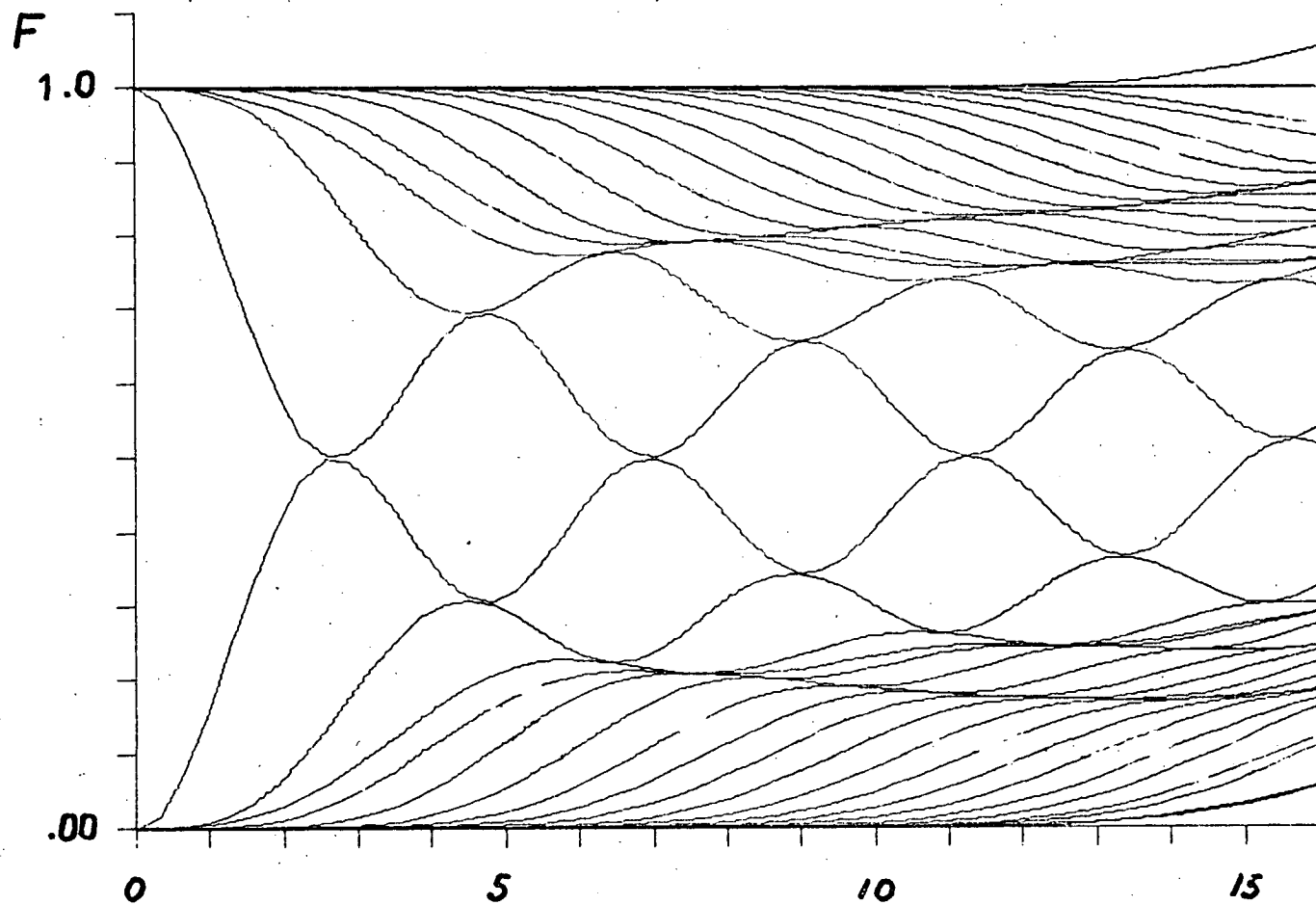
D4-2-25

improvement. The improvement is also gained at the expense of complexity though the additional advantages of more output power and smaller filters also counter balance this disadvantage.



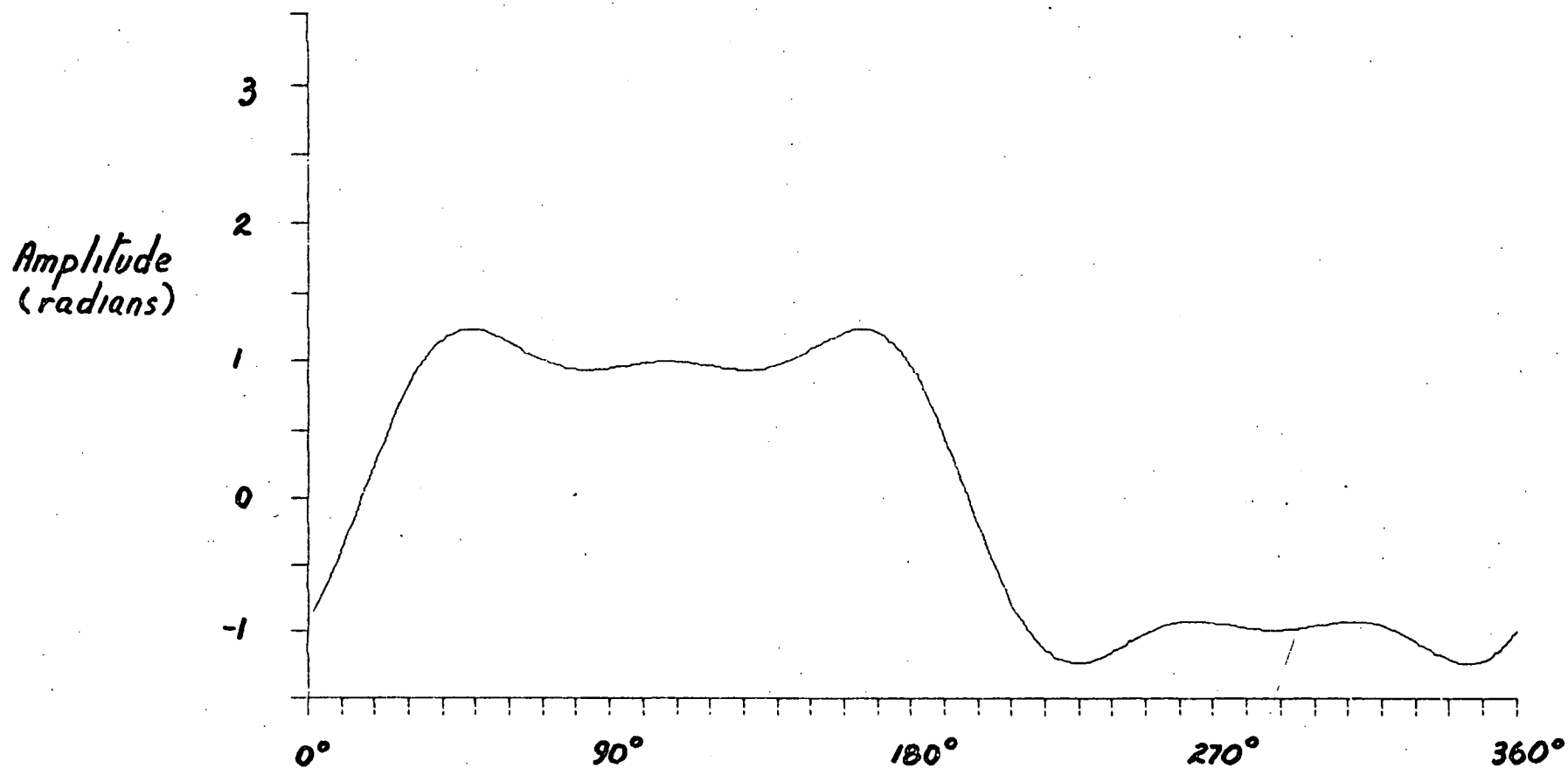
Three Harmonic "Square Wave" Modulation

D4.2.2.6 a



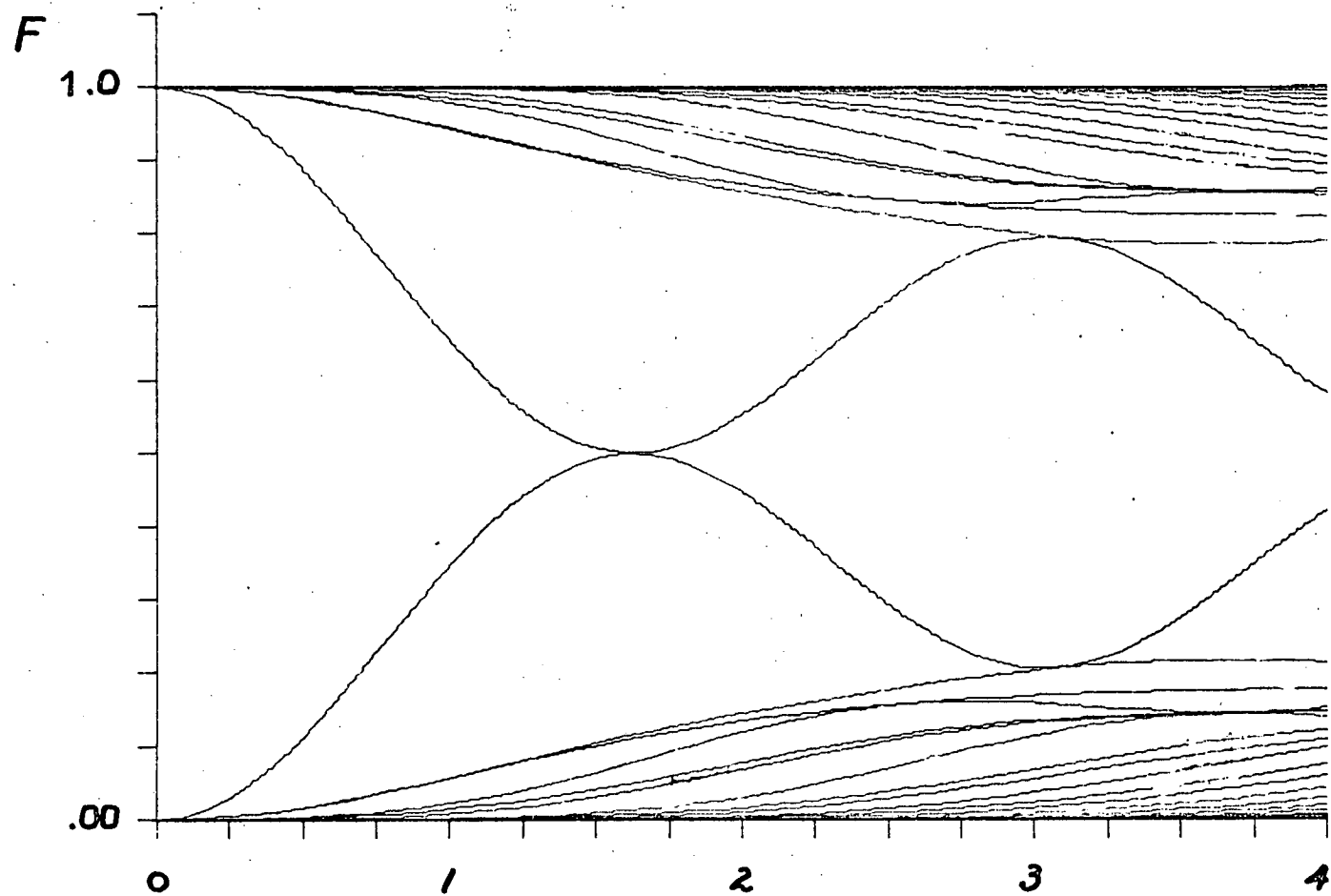
Peak Modulation (radians)

D4.2.2.6 b



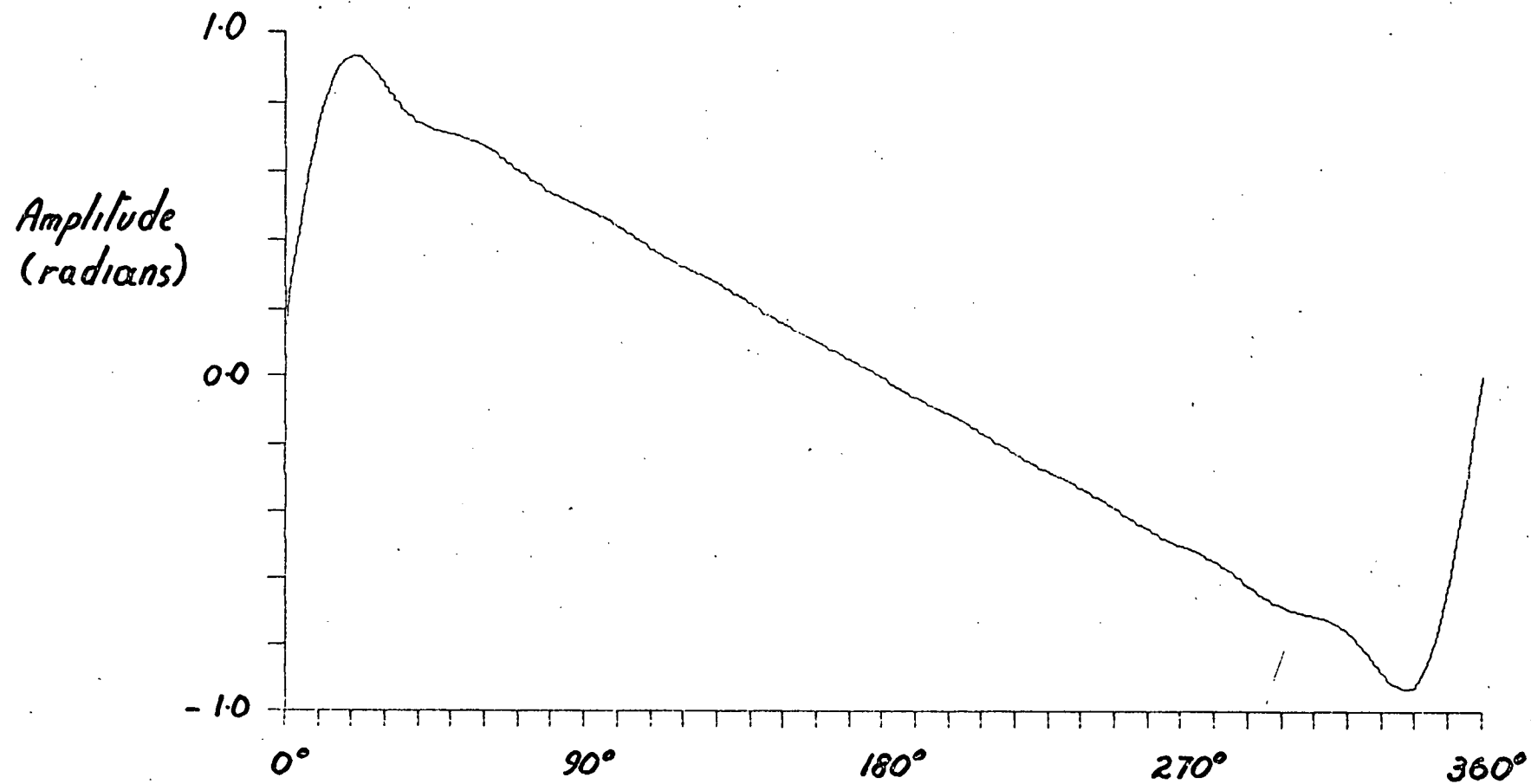
Five Harmonic "Square Wave" Modulation

D 4.2.2.6 c



Peak Modulation (radian)

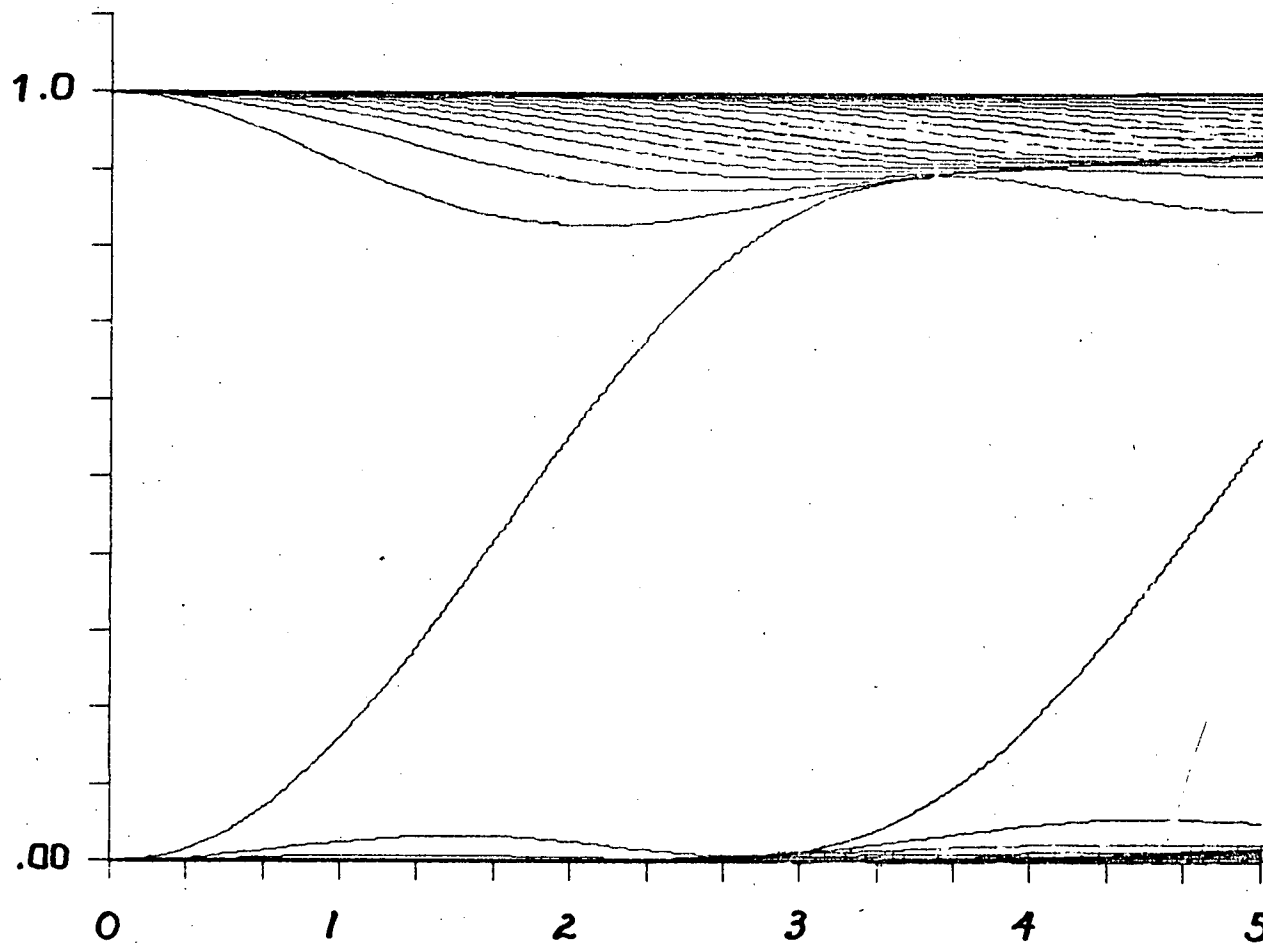
D4.2.2.6 d



Nine Harmonic "Ramp Wave" Modulation

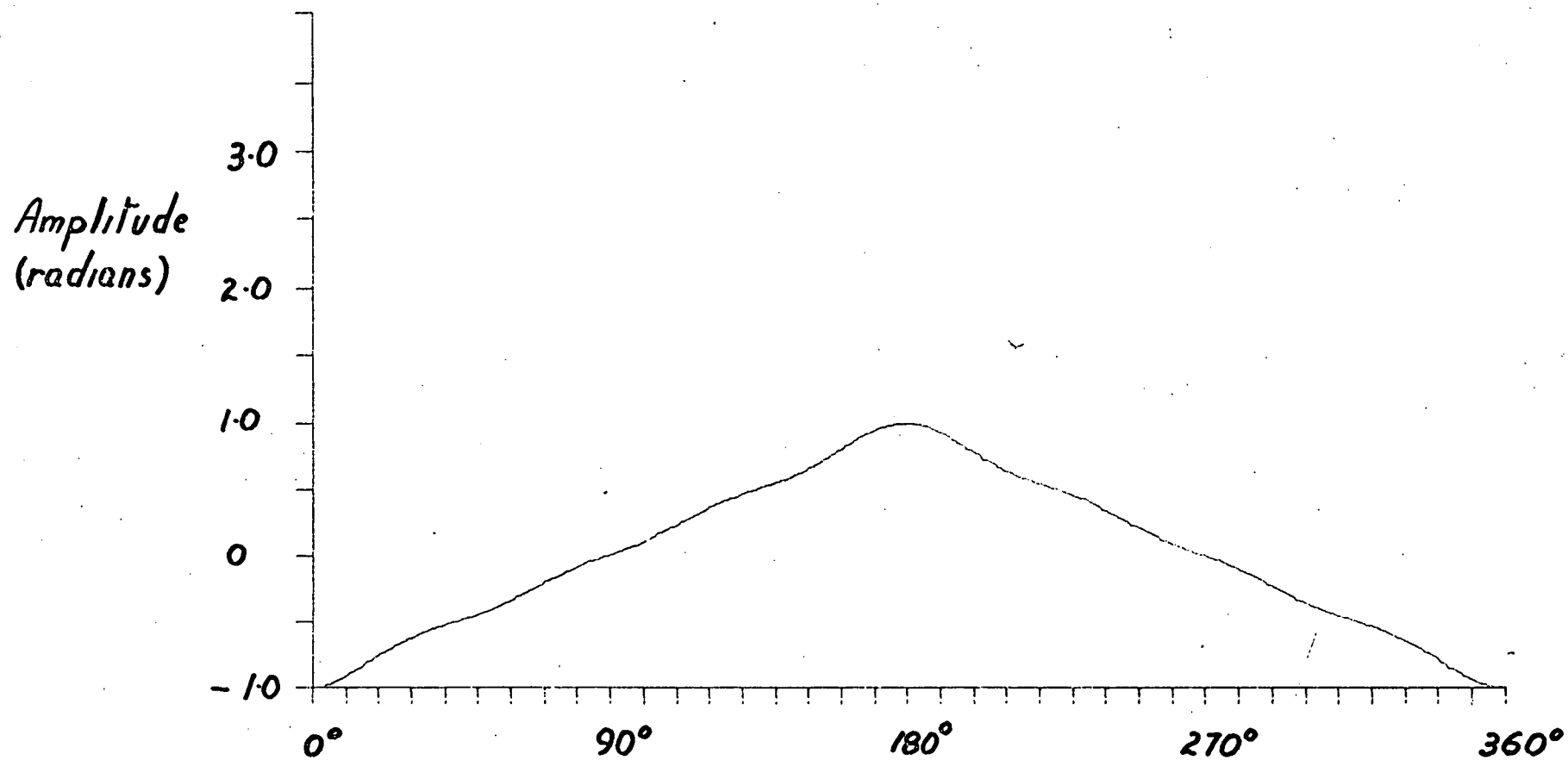
D4.2.2.6 c

F



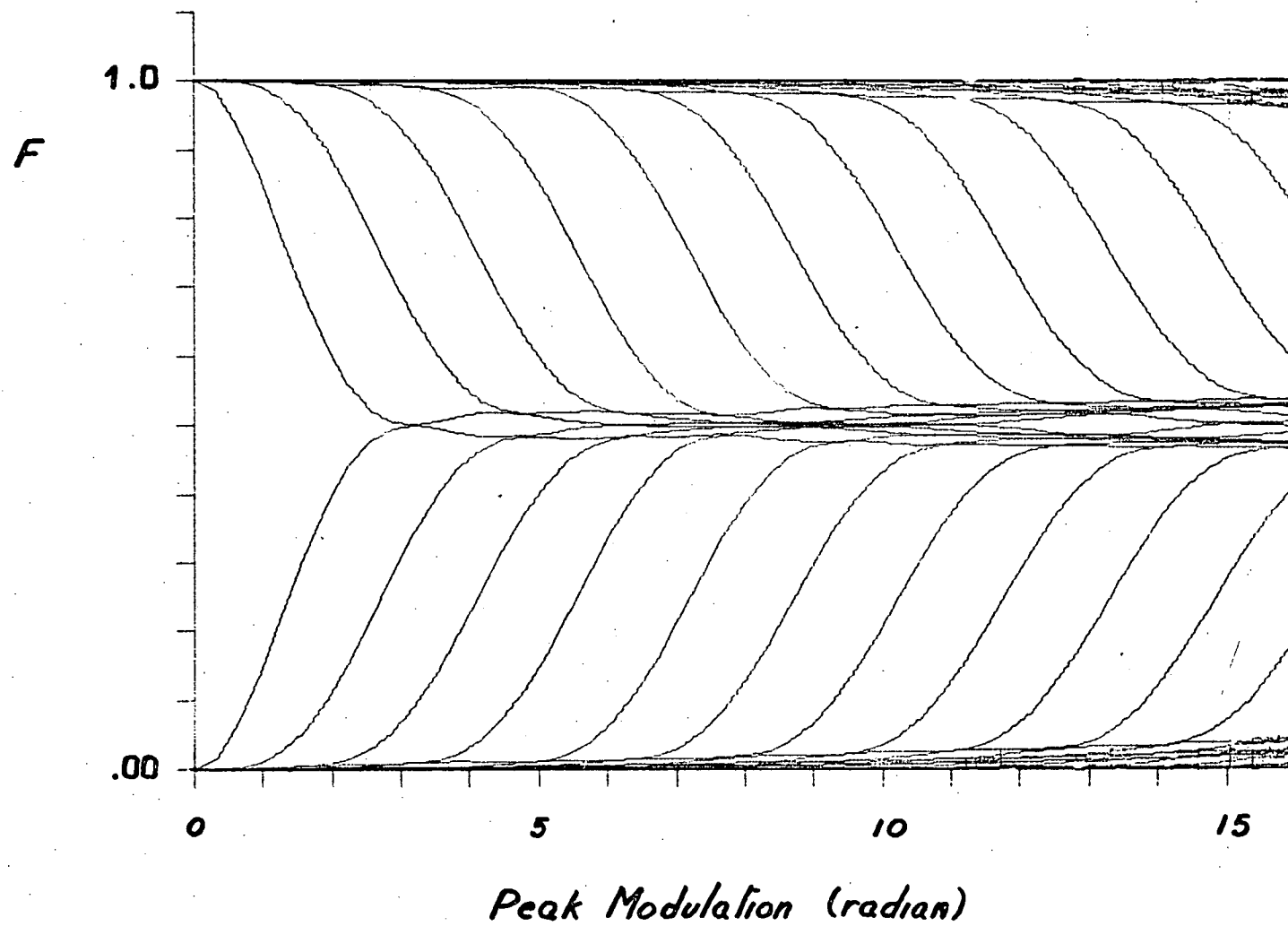
Peak Modulation (radian)

D 4.2.2.6 f

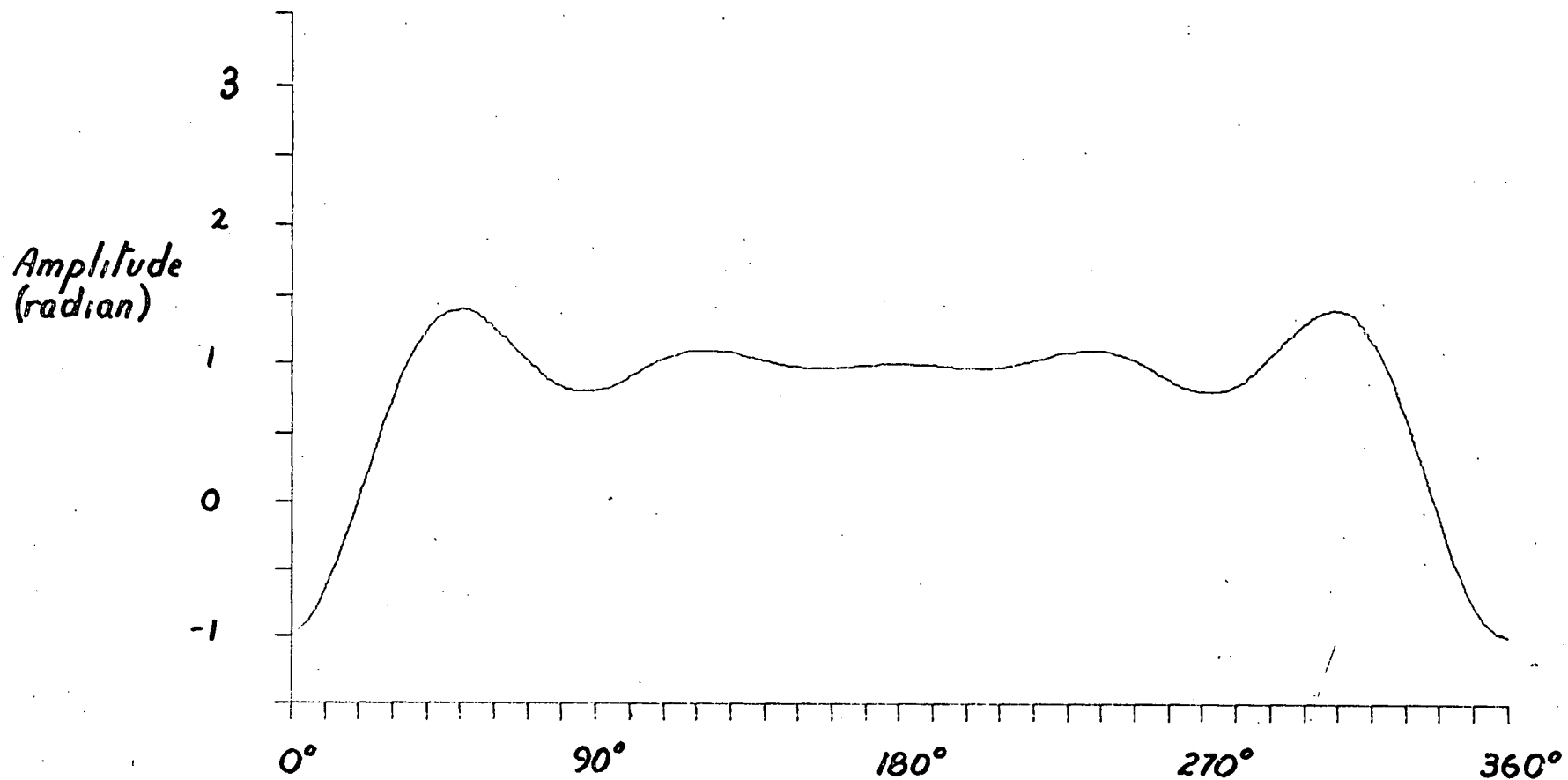


Seven Harmonic Triangular Wave Modulation

D4.2.2.6g

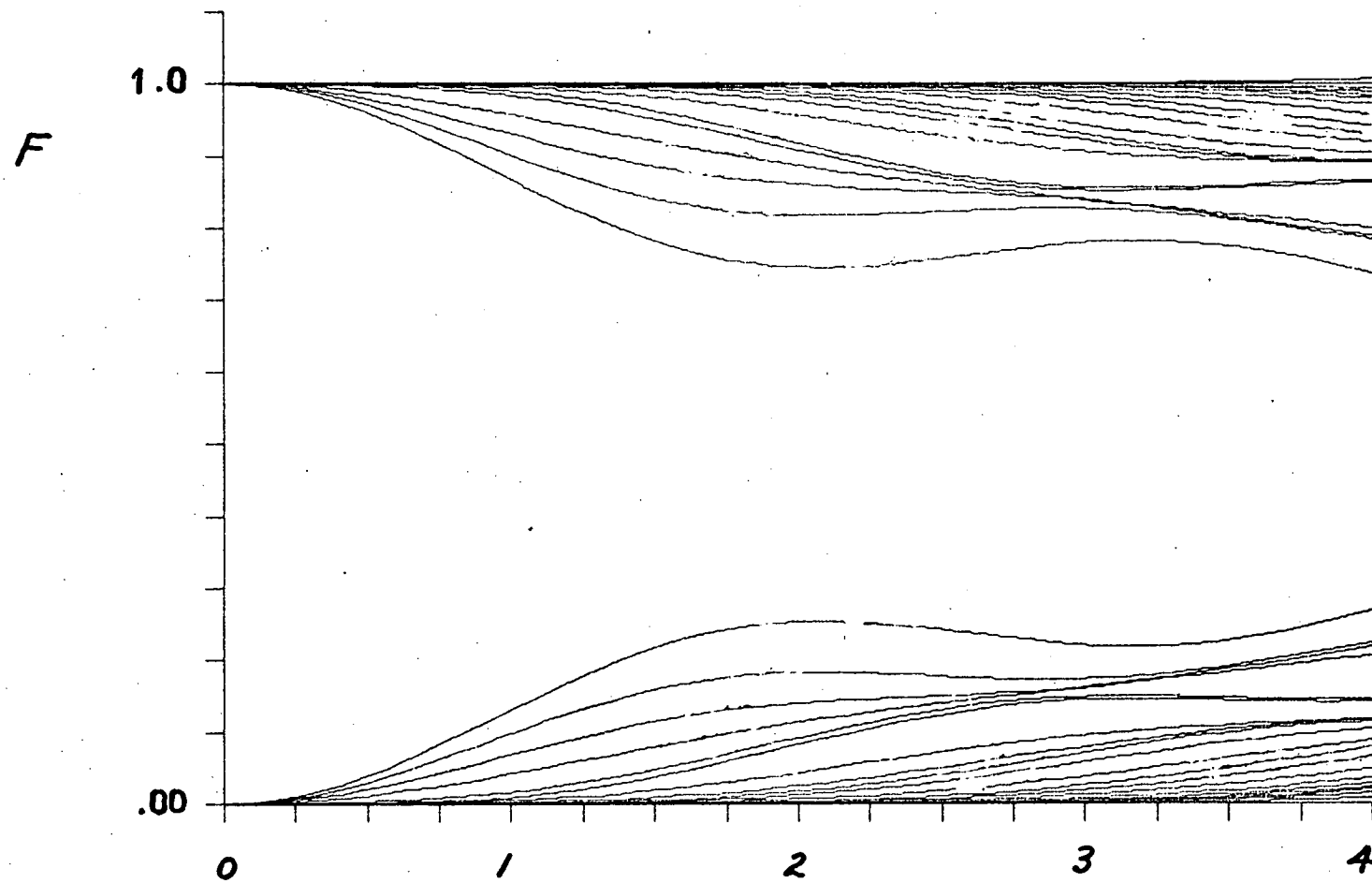


D 4.2.2.6 h



Five Harmonic Impulse Modulation

D4.2.2.6 i



Peak Modulation (radian)

D 4.2.2.6 j

04.2.2.6k

square wave			square			ramp			triangular			unit impulse		
P	S	C	P	S	C	P	S	C	P	S	C	P	S	C
.0	.845	.0	1.0	1.231	-.400	0.1	0.637	.0	-.75	.0	-.821	1.0	.0	-.400
0.7	.0	.0	1.0	.0	.0	0.2	0.308	.0	-.50	.0	.0	1.0	.0	-.400
0.7	.145	.0	1.0	-.200	-.400	1	0.196	.051	1	.0	-.101	1.0	.0	-.400
0.7			1.0	.0	.0	0.9	0.137	.0	1.00	.0	.0	1.0	.0	-.400
0.0			1.0	.0	.200	0.0	0.100	.0	0.75	.0	-.045	1.0	.0	-.200
-.7			-1.0			-.9	0.073	.051	1	.0	.0	1.0		
-.7			-1.0			-.3	0.051	.0	-1.0	.0	-.032	1.0		
-.7			-1.0			1	0.032	.0				1.0		
			-1.0			0.0	0.016	.0				1.0		
			-1.0									-1.0		

Key

P Points on the waveform

S Sine fourier coefficients

C Cosine fourier coefficients

Head of list is first harmonic

tail is highest harmonic

POINTS AND FOURIER SERIES FOR FIVE TEST WAVEFORMS

4.2.2.6 Non Sinusoidal Control Signals

The simple switching wave under discussion has characteristics which limit the usefull bandwidth of the amplifier. The discussion so far has shown how these limits apply to a sinewave control signal. The methods used are also applicable to non sinusoidal waveforms.

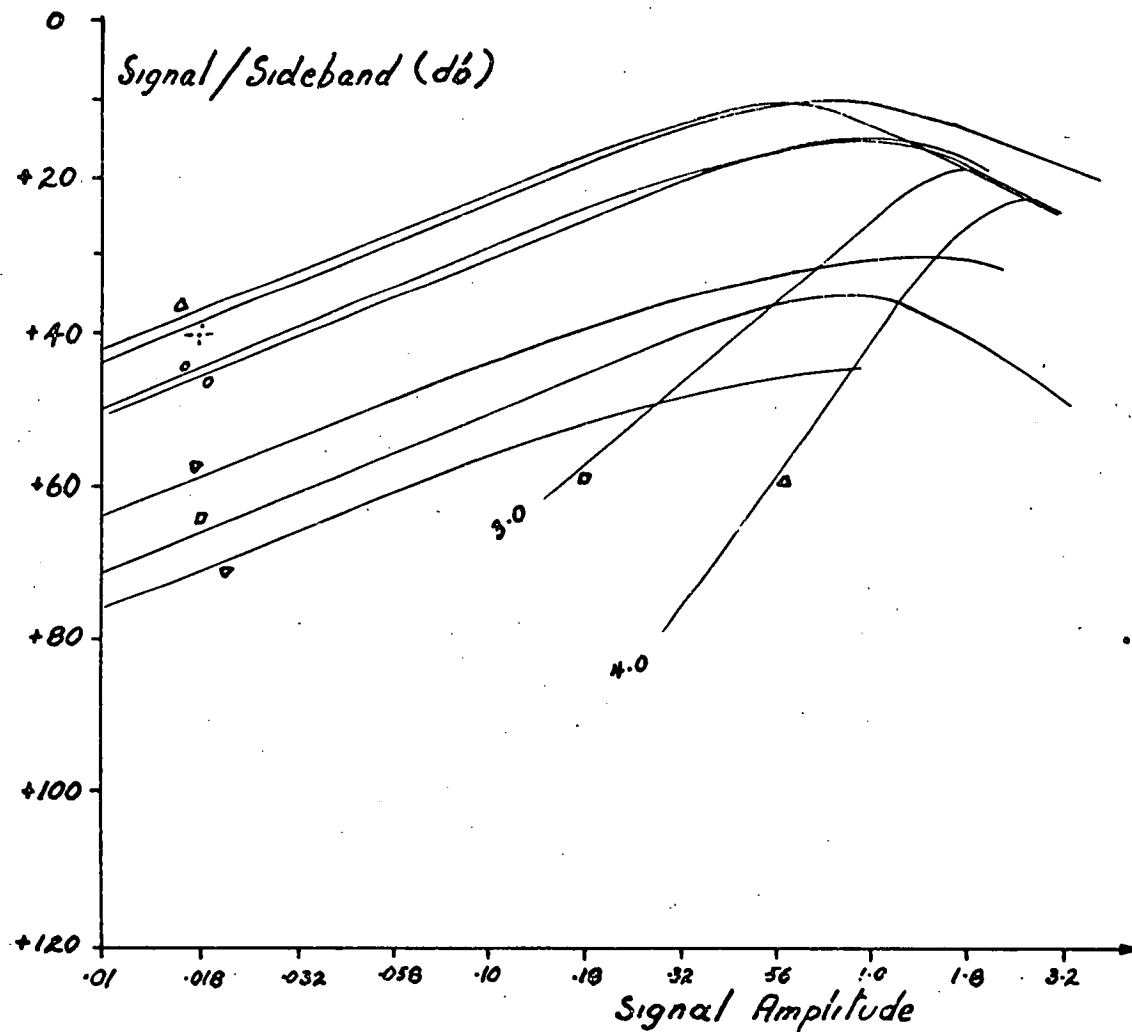
The methods used do not permit non sinusoidal waveform to be analysed but are restricted to band limited signals. In order to illustrate the application of the method, data in the form of energy contour maps and energy distribution diagrams for a number of waveforms are presented and comparisons of the bandwidth and passband noise are made to those aspects of sinewave controlled signals.

The waveforms discussed are controlled by band limited signals generated by fitting Fourier Series through sets of equally spaced points representing the following periodic shapes; rectangular waves, ramp waves, symmetrical triangular waves, and a pulse wave. Diagrams D 4.2.2.6a to D 4.2.2.6j show the waveforms and their energy distributions. The harmonic amplitudes and the number of harmonics of each are described in table D 4.2.2.6k.

In order for comparisons to be made between different output spectrums some features of the modulating, or control, signals must be assumed to be normalised. Two features will be assumed of a unit modulating waveform. First, the peak to peak amplitude is that required to just saturate the amplifier output. Second, the highest control signal harmonic with finite amplitude will always be within the bandwidth of the

D4.2.2.6.1

Signal / Sideband \sim Signal Amplitude



amplifier. For the amplifier of the example the peak to peak control signal amplitude is two units. If the N^{th} harmonic is the highest finite harmonic then the frequency of this harmonic, $w_m \cdot N$ must be less than the amplifier passband, w_p .

This last restriction requires that the n^{th} sideband of the r^{th} harmonic will have a frequency within the passband when n is such that the inequalities below are satisfied.

$$(rw_s/w_m - 1)M < n \leq (rw_s/w_m + 1)M \text{ for } M \geq N$$

This inequality may be used, in a similar way to the corresponding inequality for sinewaves, to specify graphically the energy components due to sidebands of each harmonic of the waveform and so to calculate the total passband energy. The passband energy estimates may be analysed to display their variation with modulation amplitude and amplifier passband width in the same way as for sinewaves.

The curves of figure D 4.2.2.61 are based on this extension of the method for calculating passband noise. These curves are equivalent to the upper curve of diagram D 4.2.2.4b for sinewave modulation and this is shown in addition to the nonsinusoidal cases. The behaviour for input amplitudes larger than unity is not shown as computation is very tedious beyond this amplitude since possible values of w_m less than w_p/m must be considered. When w_m is diminished the number of sidebands to be considered rises, thus increasing the computation greatly.

The examples show a number of interesting features. First, for each value of w_s/w_p the curves have the same asymptotic slope for small x . Second, of the

waveforms examined, none have a larger N/S ratio than the simple sinewave. Third, the absolute S/N ratios for a given value of w_s/w_p differ by less than 10 db. from the sinewave curves.

The reason for the similarity of asymptotic slopes as x diminishes is examined in appendix A 4.2.2.6 where it is shown that for small x the sidebands of importance for each case tend to limits which are power functions of x as x is diminished and that these sidebands have the same power of x for a given value of w_s/w_p . The actual value of the S/N ratio is difficult to estimate by this technique but the variation with x is easily predicted.

The similarity of several curves and the fact that none have N/S ratios greater than those for sinewaves suggest that the sinewave may give a worst S/N ratio. No proof of such a useful result has been found. The idea of an upper limit of the N/S being the property of a particular waveform suggests that by optimising the integral defining the sideband amplitude, (by manipulating the shape of the modulation waveform,) it may be possible to find a worst waveform. This is not so since the bandwidth of the resulted waveform changes with the shape thus nulifying, in an indeterminate way, the effects of the optimisation process.

The possibility of a worst possible waveshape appears to be elusive. The search for such a waveform may be carried out by hand calculation but would best be done by a computer using a suitable search routine.

The value of knowing of a worst possible waveshape would depend entirely on what this turned out to be. The numerical results here suggest that the upper limit of sideband energy is close to if not equal

to that for a sinewave modulation. If the worst possible waveform does not increase the sideband energy appreciably from that of a sinewave then the value of the knowledge is small. I suspect this is the case.

4.2.3 More Complex Switching Waves

The example chosen to introduce the reader to some of the characteristics of switching waves with modulated steps has two simplifying features. First, the waveform discussed has d.c. levels, and second, only one of the two waveform steps is modulated. As a consequence of these two features the sidebands of each harmonic are independent of the d.c. component of the modulating signal. The control signal d.c. component varies the energy of the switching waveform by controlling the harmonic components. This occurs due to the change in phase of the residual harmonics of the modulated step relative to those of the unmodulated step.

The modulated step has an r^{th} harmonic described by

$$E = (2/r\pi) C[r\pi x] \cdot \sin(r(w_s t + \pi DC) + \phi[r\pi x])$$

where x is the modulation amplitude, DC is the d.c. component of modulation, and $C[r\pi x]$, $\phi[r\pi x]$ are functions defined by the waveshape of modulation.

The unmodulated step is described by

$$E = -(2/r\pi) \sin(r(w_s t - \pi)).$$

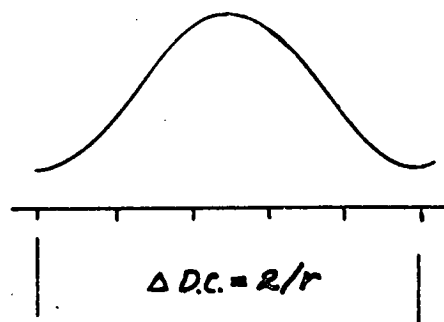
The total r^{th} harmonic is due to both these and is described by

$$E = (2/r\pi) (C[r\pi x] \sin(r(w_s t + \pi DC) + \phi[r\pi x]) - \sin(r(w_s t - \pi))).$$

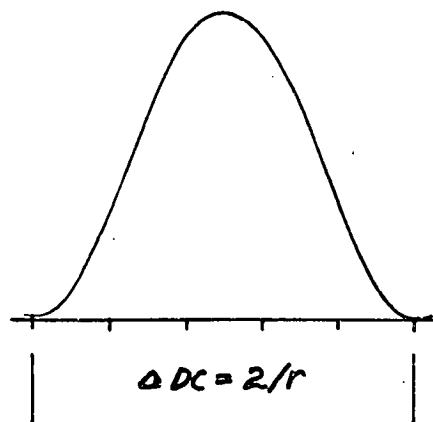
D4.2.36

HARMONIC ENERGY \sim d.c.

profile for a.c. = .46

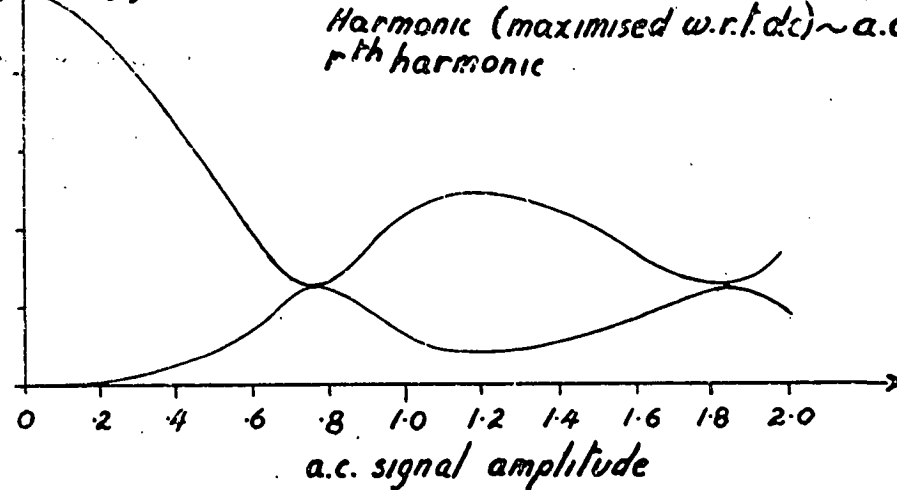


profile for a.c. = .40



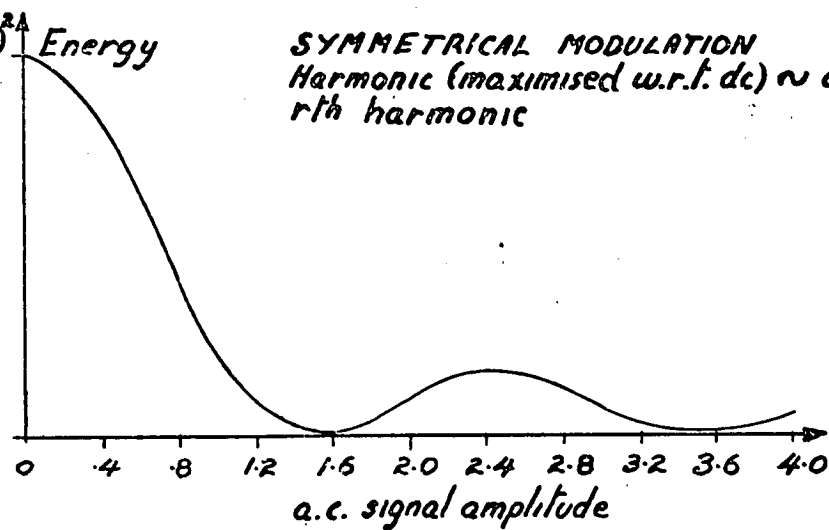
$8/(\pi r)^2$ Energy

SINGLE EDGE MODULATION
Harmonic (maximised w.r.t. d.c.) \sim a.c.
rth harmonic



$8/(\pi r)^2$ Energy

SYMMETRICAL MODULATION
Harmonic (maximised w.r.t. d.c.) \sim a.c.
rth harmonic



The average energy of this component is

$$ERa = (2/(r\pi)^2) (C[r\pi x]^2 + 1 - 2C[r\pi x] \cos(r\pi DC + \phi[r\pi x] + r\pi))$$

Thus the r^{th} harmonic energy is modulated by a sinusoidal function of the d.c. component of the control signal.

The equivalent expression describing a wave with symmetrical modulation of step positions is

$$ERa = 2/(r\pi)^2 \left\{ C[\pi rx/2] + C[-\pi rx/2] - 2C[\pi rx/2] * C[-\pi rx/2] \cdot \cos(r\pi(1+DC) + \phi[\pi rx/2] - \phi[-\pi rx/2]) \right\}$$

Diagrams D 4.2.3a and D 4.2.3b show these two expressions as functions of the d.c. component of modulation, DC, for several values of modulation depth, x. The major difference, shown by these curves, is that minima in the symmetrical modulation case are always zero while those of single step modulation are non zero for x non zero. Notice that, for rx near 0.8, $C[\pi rx] = J_0(\pi rx)$ is zero and the harmonic energy of the simple modulation is constant. The equivalent modulation depth for double modulation requires rx=1.6 but the harmonic energy is then zero. Non sinusoidal waveforms also have zeros in $C[\pi rx]$.

Values of modulation index for which harmonic amplitude does not vary with the d.c. component of modulation may be found from the zeros of the central sidebands of diagrams D 4.2.2.6a to D 4.2.2.6j for the different types of waveforms described there.

The difference between the curves for x=0 and x at some other value in diagrams D 4.2.3a and D 4.2.3b is the energy of the sidebands and the energy distributed to other harmonics due to the presence of

the a.c. component of modulation.

Non symmetrical modulation of the steps of the switching wave gives a harmonic energy of the form

$$ERa = 2/(r\pi)^2 C[\alpha x]^2 \left[1 - 2k \cos(\pi r(DC+1) + \alpha) + k^2 \right] \quad \text{where}$$

$C[\alpha x]$ is the larger of the two sidebands and k is the ratio of the smaller to the larger. The harmonic energy is of similar form to diagram D 4.2.3a but the minimum energy is nearer zero and approaches that of diagram D 4.2.3b as k tends to unity. The value of modulation index, for which variation of harmonic energy with the d.c. value of control signal is zero, is intermediate to those for the extremes given.

4.2.3.1 The Sideband Energy

Expressions describing the energies of the m^{th} sideband of the r^{th} harmonic of the two switching waves, one with a single edge modulated, the other with symmetrical modulation, are

$$ERM1 = 2/(r\pi)^2 C[r\pi x, m]^2, \text{ and}$$

$$ERM2 = 4/(r\pi)^2 C[r\pi x/2, m]^2 (1 - \cos(\pi r(1+DC) + \phi[r\pi x/2, m] - \phi[-r\pi x/2, m])).$$

The energy of the a.c. control signal component is dependent on the control signal waveshape but may be described by

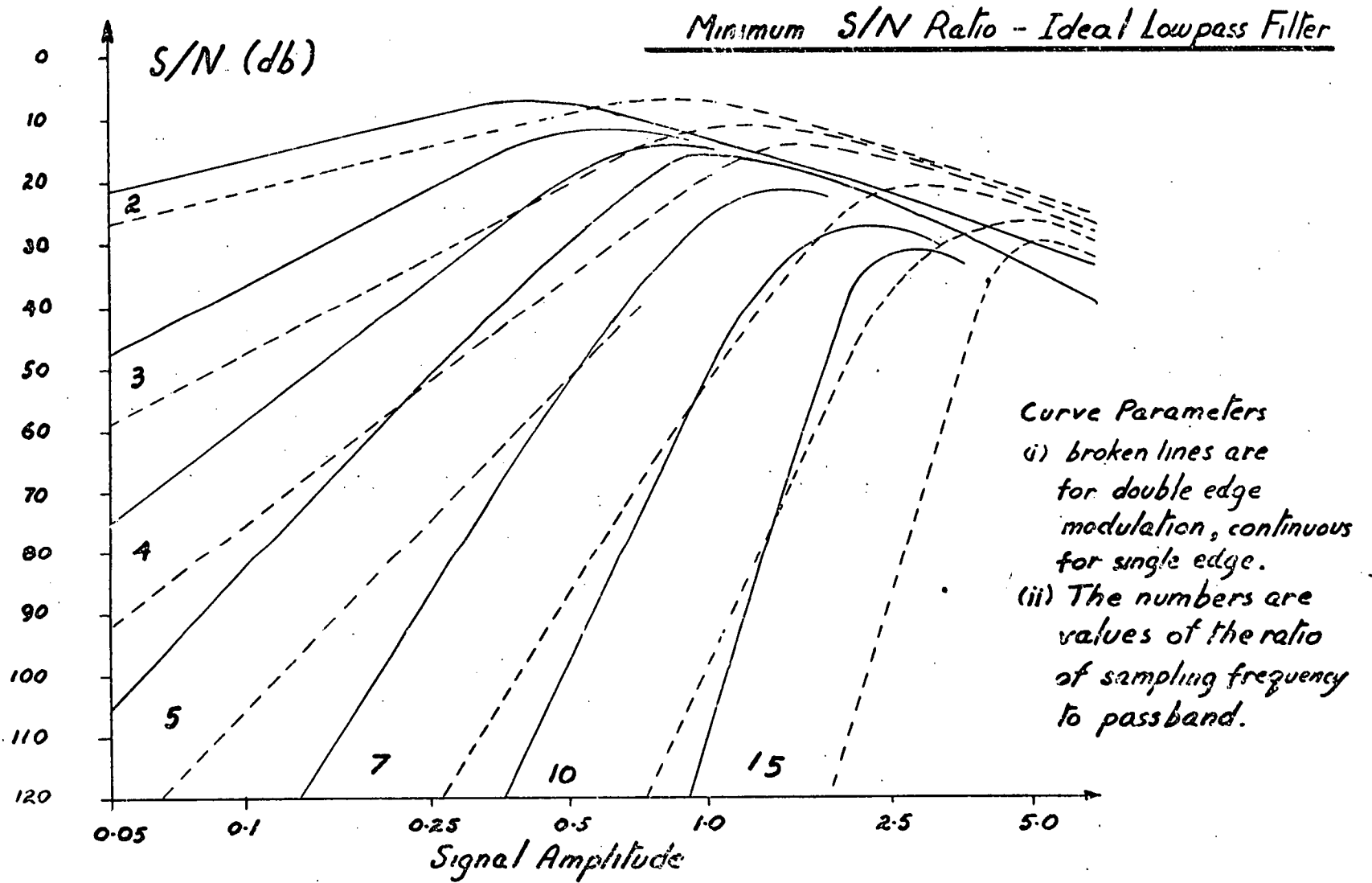
$$ES = x^2 \cdot F \quad \text{where } F \text{ is the mean square of a unit amplitude wave.}$$

The N/S ratios of these sidebands are given by

$$ERM1/ES = 2/(F(r\pi x)^2) C[r\pi x, m]^2, \text{ and}$$

$$ERM2/ES = 2/(F(r\pi x/2)^2) C[r\pi x/2, m]^2 (1/2 - 1/2 \cos(\pi r(1+DC) + \phi[r\pi x/2, m] - \phi[-r\pi x/2, m])).$$

D4.2.3.1



That part of the second expression not a function of DC is the maximum value of the expression; the remainder is of similar form to that for the harmonic energy. The other major difference in the expressions is the effective halving of the modulation index in the latter.

This has a very usefull effect upon the S/N ratio. The passband signal to noise ratio is described by

$$N/S = \sum_{r=1}^{r=\infty} \sum_{m=-\infty}^{m=\infty} G(rw_s - mw_m)^2 E_{rm}/E_S, \text{ where } G(w) \text{ is the}$$

magnitude of the output filter response at frequency w . Since this is a weighted sum of the individual contributions of the various sidebands it follows that both waveforms produce minimum S/N ratios which are of similar form. The only difference is the value of modulation index which produces a given S/N ratio ; twice the modulation index of single step modulation is required for symmetrical modulation to have the same S/N ratio.

Diagram D 4.2.3.1 shows curves of S/N ratio as functions of modulation depth, x . Each curve assumes sinewave modulation and an ideal lowpass filter. The ratio of filter cut off frequency to the sampling frequency is used to identify the curves. Dashed curves are for a single edge modulation.

For small modulation amplitudes the benefit of symmetrical modulation is a function of the sampling frequency to bandwidth ratio . The function is

$$S/N_2 = S/N_1 + 6(w_s/w_p - 1) \text{ db.}$$

Thus, for example, an amplifier with w_s/w_p at 4 has a worst possible S/N ratio which is 18 db higher if symmetrical modulation is used in preference to single step modulation.

For large signal amplitudes double edge modulation has the inferior S/N ratio if w_s/w_p is low. This is not very important for two level waves but a four level wave would require a filter cut off at $1/10$ the sampling frequency for symmetrical modulation to be better than single edged modulation at all values of output. Under these circumstances the low amplitude difference in S/N ratio would be 50 db though the difference at maximum output would be negligible.

The above comparison of symmetrical and simple modulation of switching waves are based on an upper bound of the sidebands of the symmetrical case. This upper bound assumes that all the sidebands of the wave have maximum values for the same value of the parameter d.c. This is not necessarily true so that the improvements described above are possible values. A more exact estimate of the upper bound would require a more complex analysis.

Because the diagram is limited in dimensions the influence of the d.c. component of the control signal cannot be shown but for sinewave modulation the energy of the sidebands is shared between alternate sidebands. Thus, for example, for one value of d.c. component all the even sidebands may be small while for another value all the odd sidebands are small. This effect is due to the phase relationships between the two sideband components produced by the two steps of the wave. Effects of this nature tend to reduce the upper bounds described above but are strongly dependent on the modulating waveform.

4.2.3.2 Multi-phase Waves with Unclamped Sinewave Levels

A switching wave with m symmetrically phased levels, each with waveshape $F(w_s t)$ is described by

$$E = 1/2 a[0, \phi] + \sum_{r=1}^{r=\infty} a[r, \phi] \cos(mrw_s t) + b[r, \phi] \sin(mrw_s t),$$

where the mean phase of the two edges of a switching wave segment is ϕ , and where a and b are defined by the equation

$$a[r, \phi] + jb[r, \phi] = m/\pi \int_{\theta=\phi-\pi/m}^{\theta=\phi+\pi/m} F(\theta) \text{Cis}(m\theta) d\theta.$$

For a sinewave supply of unit amplitude the expression for the switching wave reduces to

$$E = \frac{m}{\pi} \sin(\pi/m) \left[\sin\phi + \sum_{i=\pm 1} \sum_{r=1}^{r=\infty} \left\{ \frac{(-1)^{r+1}}{(mr-i)} \sin(mw_s t - (mr-i)\phi) \right\} \right]$$

The maximum output is not unity but $m/\pi \sin(\pi/m)$. This factor may be omitted if the expression is normalised on output range rather than supply waveform peak value. The peak supply will then be $\pi/m \sin(\pi/m)$ rather than unity.

For linear amplification ϕ and the control signal, $f(w_m t)$ are related by the equation

$$\sin(\phi) = f(w_m t) \text{ for } -1 < f(w_m t) < 1$$

The expression for the waveform now becomes

$$EN = f(w_m t) + \sum_{i=\pm 1} \sum_{r=1}^{r=\infty} \frac{(-1)^{r+1}}{(mr-i)} \sin(mrw_s t - (mr-i) \arcsin(f(w_m t))).$$

Compare the r^{th} harmonic of this waveform with that for an m interval d.c. levelled wave with the

same output range. The two expressions are respectively

$$\text{ENR} = \sum_{i=\pm 1} \frac{(-1)^{r+1}}{(mr-i)} \text{Sin}(mrw_s t - (mr-i)\text{arcSin}(f(w_m t))), \text{ and}$$

$$\text{ENR} = \frac{2}{(r\pi m)} \left[\text{Sin}(mrw_s t + mr\pi f(w_m t)) - \text{Sin}(rm(w_s t - \pi)) \right]$$

Notice the similarities in form; both have two terms; both have amplitudes which decrease with both m and r ; both have modulated components with amplitudes proportional to a function of mr ; and in both cases the modulated components produce phase modulation.

Notice the differences in details; the asymptotes for harmonic amplitude when mr is large differ by a factor of $2/\pi$; the a.c. levelled wave harmonic is a sum of phase modulated vectors the other a difference; and the modulation of the first equation is a nonlinear function of input signal while the latter equation has a linear function. Other differences, in these particular examples, such as the asymmetry of the two terms for the second equation, the opposite signs of modulation amplitudes, and the factor of $(-1)^{r+1}$ are not so important for comparison purposes since some are dependent on phase origins and scales, while others are very example dependent. One important difference not obvious here is a consequence of the type of step phasing. The a.c. levelled wave has pure phase modulation of the steps while the relative phases of steps in the d.c. wave must vary with output component. Thus a symmetrically modulated wave with d.c. levels has opposite signs of modulation function while those for the a.c. levelled wave have the same sign.

Many of the similarities and differences may be related to the physical characteristics of the waveforms

in a simple way. This is especially true for the high harmonics of the a.c. levelled wave. For mr large the expression may be re-phrased to yield an approximation given below.

$$ENR \approx \frac{2(-1)^{r+1}}{mr} \cos(\arcsin f(w_m t)) \sin(mr(w_s t - \arcsin(fw_m t))).$$

This expression describes the approximate waveform which has the same size steps as the actual wave but has a chord, not a sinusoid, joining the steps. Both step amplitude and step phase are nonlinear functions of the output component and these determine the respective amplitude and phase of the r^{th} harmonic of the triangular approximation.

The superficial similarity of form, that of the number of terms, is dispelled by the approximation. The more basic features, those pertaining to the harmonic amplitude and the phase modulation of the harmonic by the control signal are emphasised. The similarity to the first term of the expression for a d.c. levelled wave with single edged modulation is to be expected since this term is also a phase modulated triangular wave. (The other term of this expression describes the other step of the waveform).

The features described above help to form a picture of the waveform so that numerical results have some meaning. This is important when numerical results are obtained from complex (mathematically) formulae. Unless the searcher for limiting cases has some physical basis for the search it is easy to become confused about the meaning of numerical results.

4.2.3.3 Sidebands of Sinewave Levelled Waves

The numerical methods used to calculate sideband amplitudes for d.c. levelled waves may be used in conjunction with the expressions for a.c. levelled waves to calculate these sidebands. Two modifications are necessary. The simpler modification necessary allows for the more complex co-efficients of the phase modulated components of a harmonic. The other modification is required because the bandwidth of the phase modulation is not identical to the bandwidth of the control signal due to the nonlinearity of the arcSine function relating these. This nonlinearity is now described.

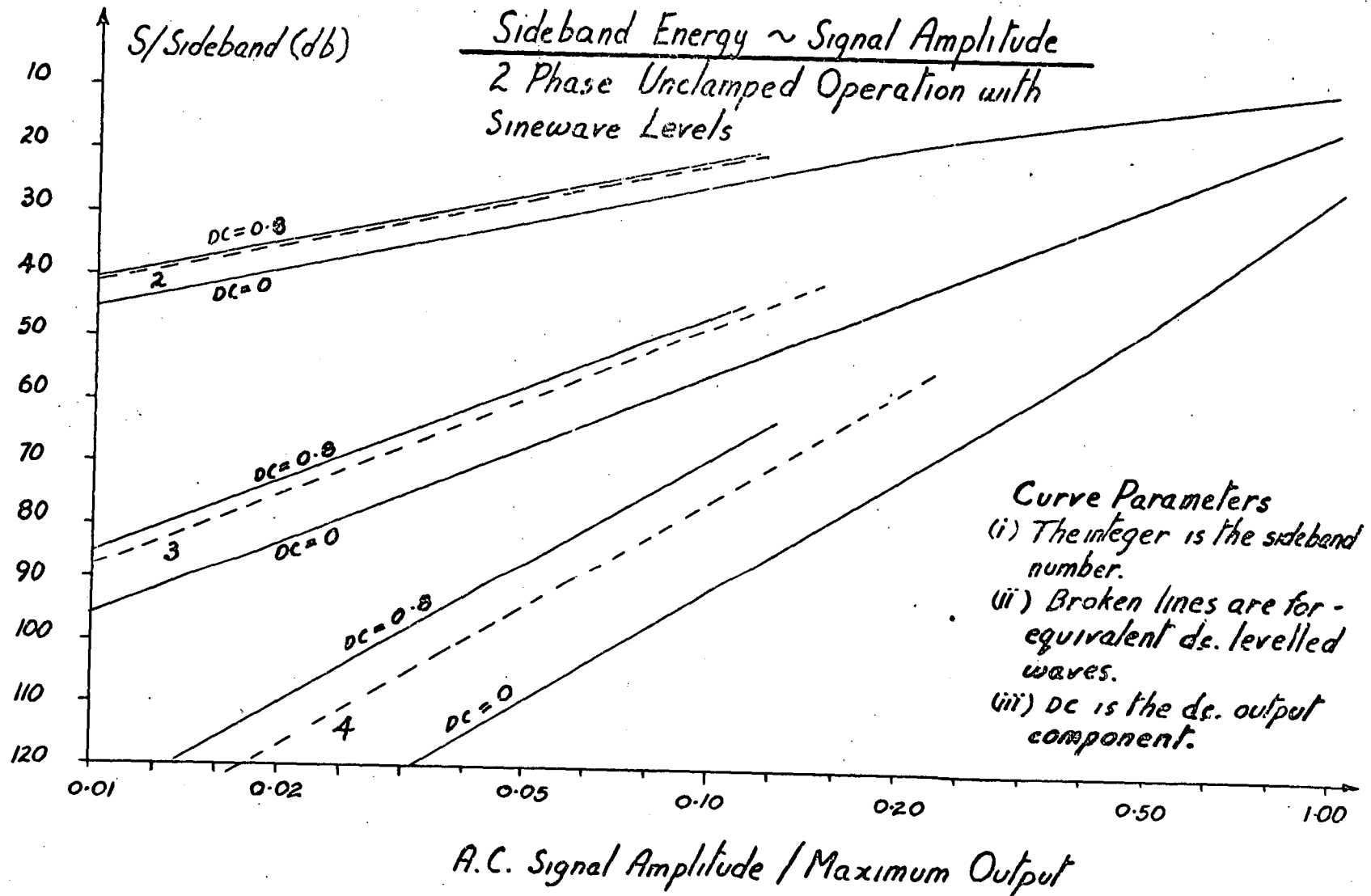
Consider a sinewave control signal for the two limiting cases, first, with very small amplitude, and second, with maximum possible amplitude. For small control signals there is no distortion of waveshape since the arcSine function is smooth but consider the influence of a d.c. component of the control signal. For zero d.c. component the modulation index is as though the arcSine function was a simple multiplier of value unity. As the d.c. component is increased the value of the multiplier increases. For a d.c. component, DC, the multiplier value, M, is

$$M = (1-(DC)^2)^{-1/2} \quad \text{for } -1 < DC < 1.$$

As DC approaches unity the slope of the arcSine function approaches infinity. Near this limit the amplitude of control signal for negligible distortion of waveshape is very small.

For a large control signal the phase signal is a triangular wave. The d.c. component of modulation is zero since the peak modulation of phase in each direction is attained. The peak of the arcSine function

D4.2.3.3



is $\pi/2$ when this unit control signal is used.

The numerical methods require the phase modulating signal to be represented by a band limited fourier series. This is achieved by specifying the modulating signal by a number of uniformly spaced samples of the signal. The difficulty lies in knowing what is really being represented. A sinewave control signal will produce a phase modulating signal which may be assymmetric and may also have sharp spikes if values near maximum output are used. This signal will not be band limited though most energy may be concentrated in the lower harmonics. The samples of this signal can only represent a band limited approximation of the true signal. The question then becomes: how different will the sidebands calculated using these samples be from sidebands of the real signal? The only real way to find an answer may be to see how the spectrum varies as the number of samples is increased. When the change with sample number is small it is assumed the spectrum is near the actual spectrum. This approach was used to obtain the numerical results now discussed.

Diagram D 4.2.3.3 shows the ratio of sideband energy to a.c. signal energy as a function of a.c. signal amplitude for the first harmonic of a two phase wave. Curves are shown for two values of d.c. signal component. The broken curves show the same ratio for a d.c. levelled wave with two levels and one modulated step.

All these curves approach assymptotes as signal amplitude is diminished. For a given sideband the slope of these assymptotes is fixed. This is a feature of all phase modulated waves since the modulation process will produce on n^{th} sideband of a small signal of amplitude x with amplitude proportional to x^n and with

phase independent of x .

The increase in sideband amplitude due to the d.c. signal component is apparent. The effect may be estimated from the zero offset curves since the effective modulation is increased by the factor m referred to earlier. The factor for $DC=0.8$ is 1.67 that is about 0.22 decades. This is approximately correct though the separation is larger for the fourth sideband.

The relationship between curves for 2 phase a.c. levelled waves and single interval d.c. levelled waves may also be estimated. The respective approximate expressions for the $DC=0$ case are

$$ENRAC = \sin(2w_s t - 2f(w_m t))/r \text{ and}$$

$$ENRDC = 2\sin(w_s t - \pi f(w_m t))/\pi r.$$

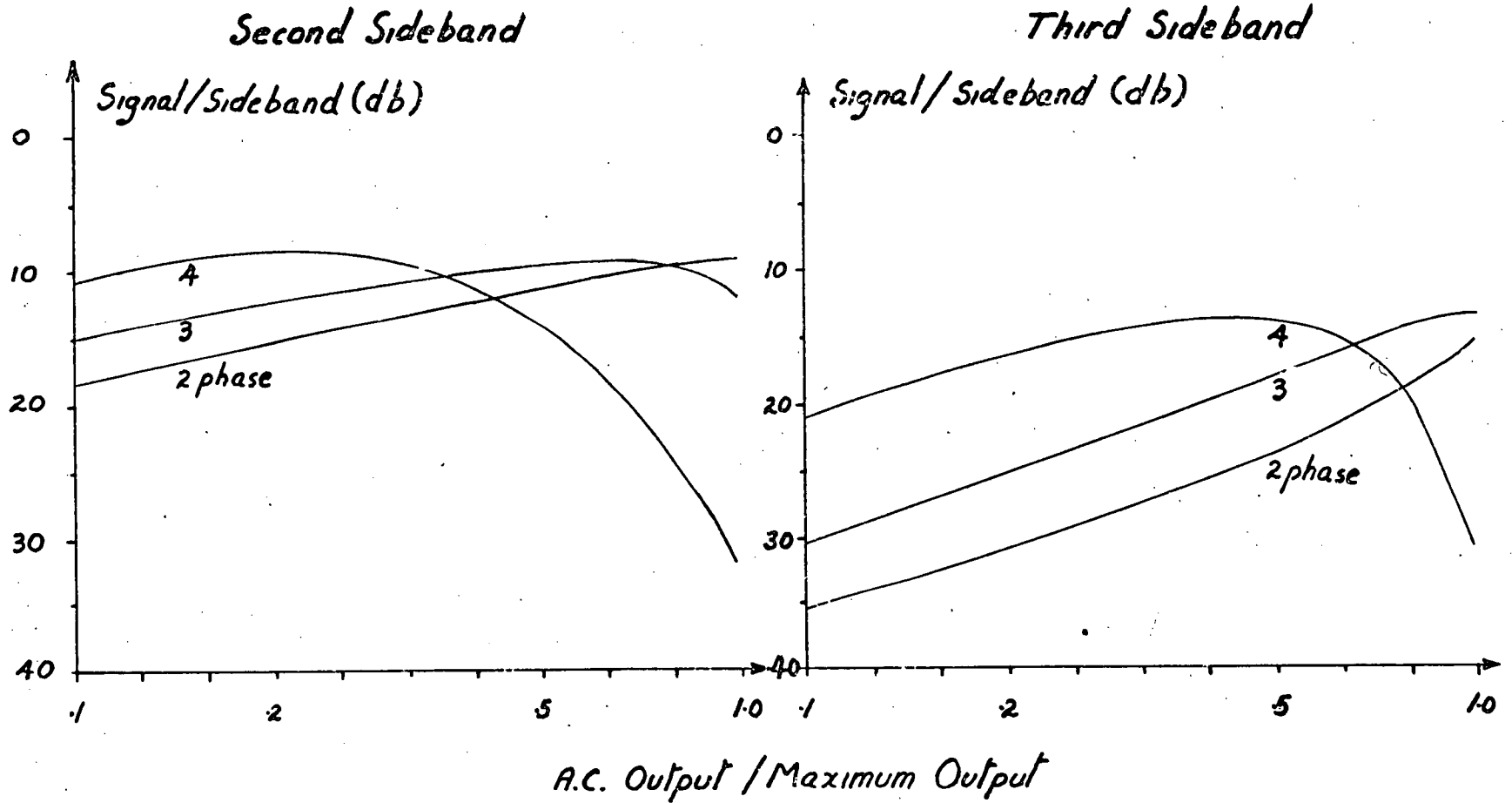
The effective modulation indexes differ by a factor of $\pi/2$ in favour of the d.c. levelled waves while their amplitudes differ by the same factor in favour of the a.c. levelled wave. On this basis a shift of the a.c. levelled curves 0.2 decades to the left and 4 db in level would be expected to yield curves corresponding to those for d.c. levelled waves. This is an overestimate by about 4 db for the two lowest sidebands. Sidebands of higher harmonics and of waves with more phases are estimated more accurately.

FIRST HARMONIC SIDEBAND ENERGY

Peak Sideband	Sideband / d.c. Wave Levels	a.c. signal energy } versus Sideband Number			
		a.c. Wave Sinewave levels			
Number	1 Interval	2	2 Phase	3 Phase	6 Phase
2	10.2	16.9	9.4	9.3	9.4
3	13.5	17.6	15.6	13.2	13.8
4	20.3	18.0	26.3	18.1	16.4
5	29.6	18.5	46.5	27.8	18.2
6	40.7	21.1	45.1	47.3	19.5
7	53.2	26.0	58.4	45.2	22.9
8	67.1	32.5	55.1	57.6	31.2
9	82.2	41.65	64.7	52.3	48.1
10	98	48.6	58.8	61.3	41.9

D 4.2.3.4b

D4.2.3.4a



Minimum Signal / Sideband \sim A.C. Output
Sine Levelled Wave.

4.2.3.4 Worst Sideband Conditions

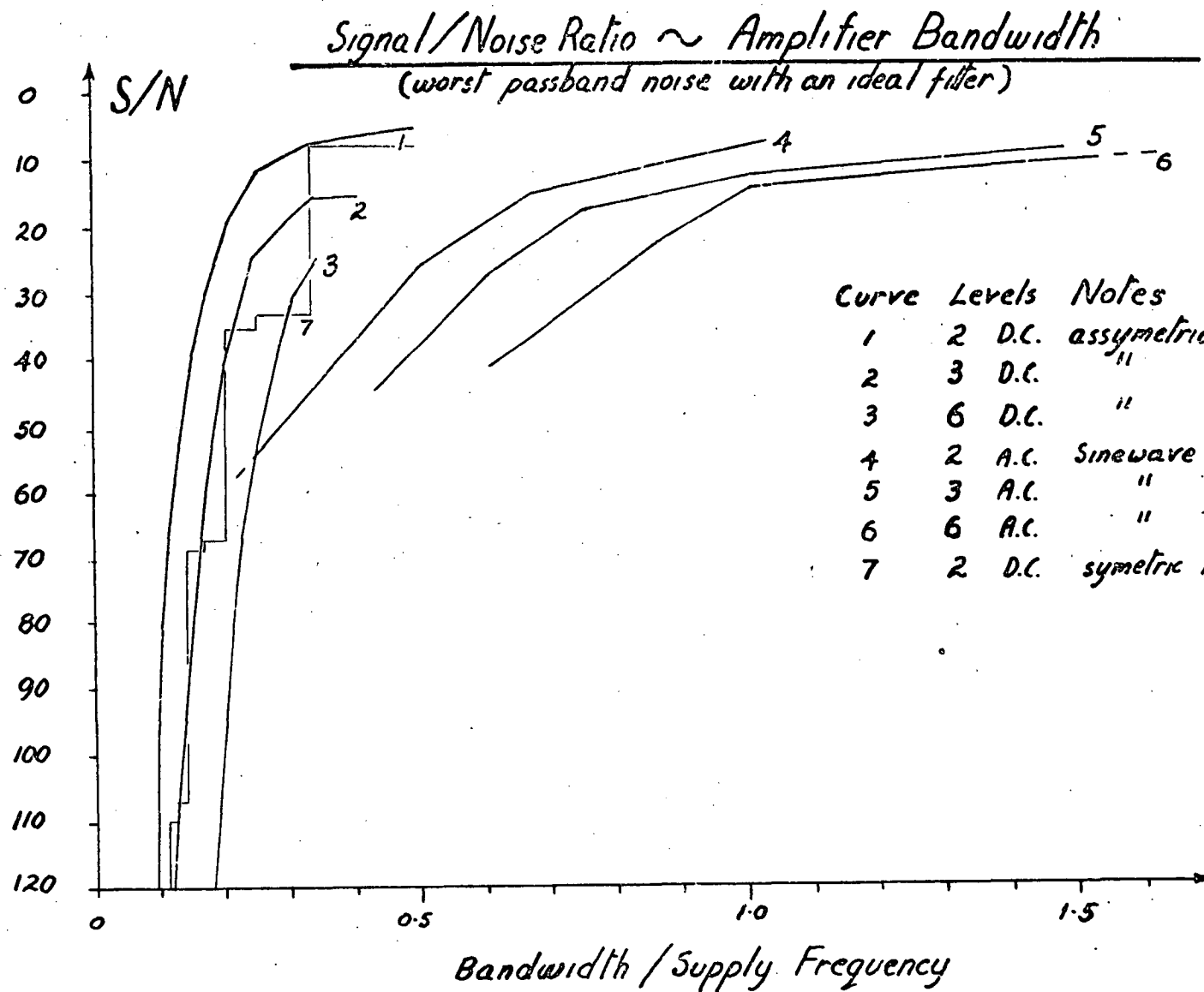
Provided the modulation amplitude is smaller than some critical value the maximum sideband energy is achieved with the maximum d.c. offset possible for that modulation level. By choosing a.c. and d.c. signals so that phase saturation is just attained a maximum for the sideband energy results. Diagram D 4.2.3.4a shows curves of sideband energy to signal ratio as a function of signal amplitude for several sidebands of two, three and six phase waves.

As for the previous curves those for a given sideband have similar slopes for small signals. Notice that the slopes are much lower. The n^{th} sideband with d.c. component constant had a slope of $20(n-1)$ db per decade but these curves have asymptotes of slope near $5n$ db per decade of signal amplitude.

A more important feature is the maximum sideband to signal ratio over the range of signal amplitude. This is the source of passband noise for a switching amplifier. Notice that the a.c. signal amplitude for maximum passband noise does not correspond to maximum signal for waves with many phases. This feature was also present for d.c. levelled waves and is a general feature of phase modulated waves. Each sideband has a peak amplitude which is dependent on the modulation index. Since modulation index is approximately proportional to phase number and proportional to harmonic number as well as signal amplitude, the peak occurs for smaller signal amplitudes as the first two parameters increase.

Table D 4.2.3.4b shows peak sideband energy to signal energy as a function of sideband number and

D4.2.3.5



type of switching wave for several phases of a.c. levelled waves and for two and three levelled waves with d.c. levels and single edge modulation. Notice the higher sidebands of a.c. levelled waves do not increase uniformly with sideband number but split into odd and even sideband groups each a smooth function of sideband number.

4.2.3.5 Maximum Passband Noise

The evaluation curves showing the maxima for sideband noise/signal for each switching wave harmonic allows the calculation of curves for maximum passband noise/signal ratio as a function of amplifier passband/supply frequency ratio. The method used is identical to that for d.c. levelled waves.

Diagram D 4.2.3.5 shows these results. Also shown are equivalent curves for d.c. levelled waves. Only one curve is represented in the proper manner with abrupt steps in level. The other curves are drawn as chords between the tops of the steps. This has been done to prevent the confusion of curves apparent in diagram D 4.2.2.61.

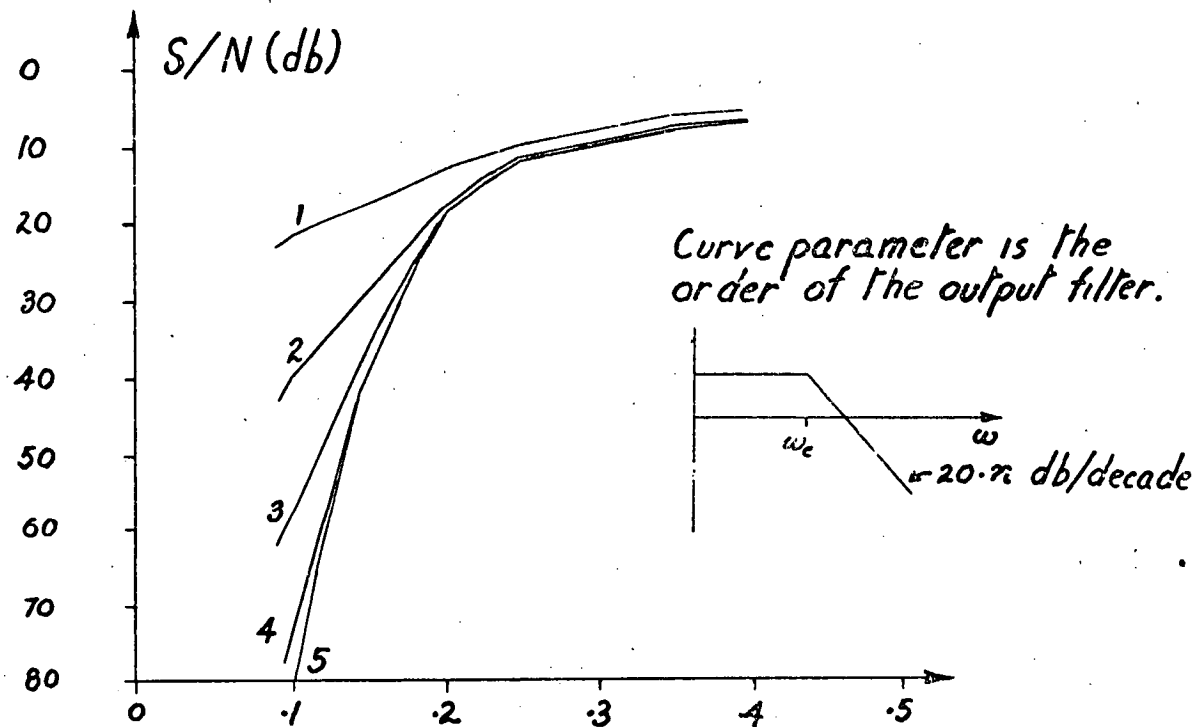
4.2.3.6 Comparing a.c. and d.c. Levelled Waves

a.c. levelled waves allow wider bandwidth amplifiers if S/N is small. The reasons for this are not obvious. One factor is the low modulation index of the dominant component of each harmonic. Another is the triangular modulation waveform associated with maximum sideband energy. The largest sidebands produced by such modulation are closer to the harmonic than are those for sinewave modulation of equivalent index.

The bandwidths of the a.c. levelled waves are as much as twice those for d.c. levelled waves for S/N ratios near 25 db. This is for d.c. levelled waves with

Signal/Noise Ratio \sim Filter Bandwidth

A d.c. levelled wave with one modulated step.



FILTER BANDWIDTH/SAMPLING FREQUENCY

single edge modulation. Double edged modulation reduces this advantage slightly.

4.2.4 The Ideal Filter Assumption

In order to compare different switching amplifiers a limiting case was assumed for the output filter. The ideal bandpass characteristic assumed enabled the estimation of passband energy due to switching wave components other than the desired output. The obvious question arising from this assumption is "How close must the real filter characteristic be to the ideal characteristic before comparable S/N ratios are obtained?" As usual the answer depends to some extent on the circumstances however the ideal and actual S/N ratios are indicated by the following example.

4.2.4.1 Filtering of a Two Level Wave with a Modulated Step

A d.c. levelled wave with one modulated step is filtered by a filter with flat response in the passband and falloff of 20n db per decade in the stopband. The S/N ratio as a function of the filter parameter n is shown by diagram D 4.2.4.1.

For the range of signal to noise ratio shown the fifth order filter is very close to the ideal bandpass characteristic. The fourth order filter begins to deviate at a signal to noise ratio of about 45 db. The third order filter is less accurate and deviates from the ideal for a signal to noise ratio near 25 db.

The order of filter required to approximate the ideal filter depends on the passband noise permitted. If a S/N ratio of 40 db is required the bandwidth of the system with a second filter is 0.1 of the sampling

frequency. With a third order filter the bandwidth increases to about 0.15 but higher order filters will increase this bandwidth by an insignificant amount. This example illustrates the design requirement for output filters.

4.2.5 Summary

As a first step to simplifying the analysis of passband noise it is convenient to assume that identical ideal bandpass filters are used to filter the control signal prior to amplification and the resultant switching wave which contains the output signal. The input signal is thus restricted in bandwidth to the same range as the amplifier output. The output contains only those sidebands which cannot be rejected by the filter. Under the restrictions so imposed a number of periodic control signals were used to find a worst noise producing input signal. Of the range of waveforms and conditions considered the sinewave input signal had the greatest passband noise for a given peak to peak signal amplitude. The results indicate, but do not prove, that aperiodic signals and other periodic signals produce less passband noise than sinewaves.

The examination of passband noise characteristics for all the control signals and switching waves considered shows a number of common features. First, the passband signal to noise ratio for small signal levels is dominated by the contributions to the noise by the sidebands of the first harmonic of the switching wave. Under these conditions maximum passband noise is attained when the frequency of the control signal is the maximum consistent with the band limited input. The signal to noise ratio is then proportional to signal amplitude raised to a power determined the ratio of the amplifier passband width and the sampling frequency.

Second, as the control signal amplitude increases the actual signal to noise ratio exceeds that of the small signal relationship by an increasing

margin until the ratio reaches a minimum value. After this signal level is attained the signal to noise ratio diminishes slowly as amplitude is increased and the frequency of input for maximum noise is reduced from the maximum allowable by the input filter. In some circumstances the amplifier output range may be exceeded before the signal to noise ratio reaches the minimum value described.

Third, graphs of minimum signal to noise ratio obtained in the manner above as functions of amplifier passband show that the practice of phased addition of switching waves and use of multi-phased a.c. levelled waves does increase the allowable amplifier output for a given minimum signal to noise ratio. The increase in bandwidth is less than a factor equal to the number of component waveforms so that the improvement in bandwidth does not match the increase in hardware.

Since practical amplifiers cannot use ideal output filters a brief examination of the amplifier output noise of a simple waveform with several filters of different order was made. The results indicate that the output noise is strongly dependent on the order of filter used. For the example considered the signal to noise ratio was determined more by the noise from components with frequencies outside the passband than those within this band unless the bandwidth corresponded to a passband signal to noise of about 10 db, when a first order filter was used. Higher order filters improved the value.

A fourth order filter gave signal to noise figures near the ideal until values near 60 db were reached.

The different forms of waveform level and modulation examined appear to indicate that a.c. levelled waves using phase modulation are superior to d.c. levelled waves produced by hardware of comparable complexity, at least for signal to noise ratios less than 60 db.

CHAPTER IV

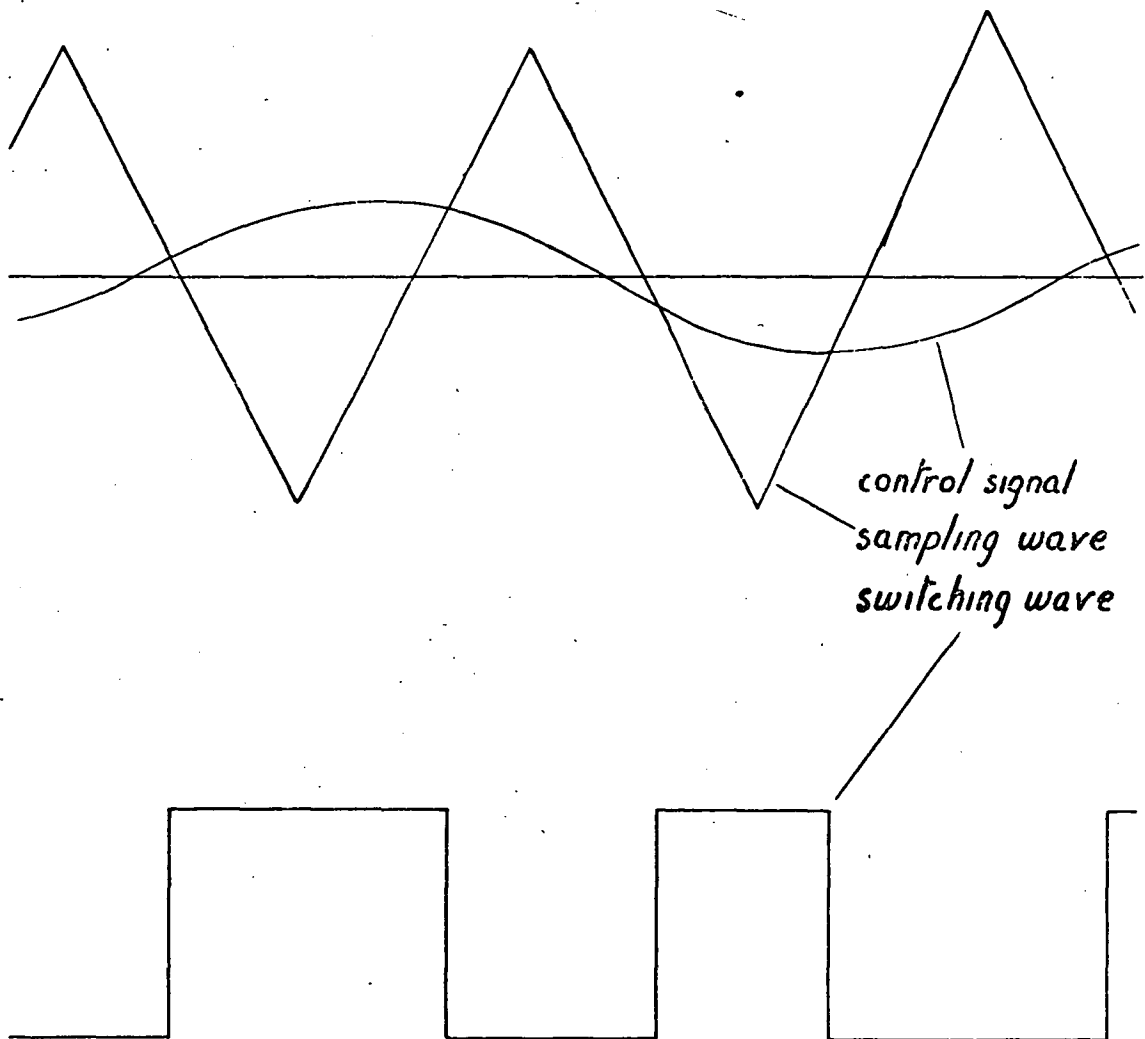
PART C

4.3 Subharmonic Gain

Although switching amplifiers may be designed with linear input output characteristics, using the techniques outlined in chapter III, they have sidebands of the switching wave harmonics with frequencies within the passband. These sidebands were the subject of the previous section. The aim there was to obtain a measure of the energy of those sidebands within the passband so that S/N ratios could be estimated. This general view overlooks a situation where a distortion, similar to harmonic distortion in some respects, occurs.

If the sampling rate and the frequency of the control signal are both multiples of a common frequency, then some sidebands of the switching wave will have frequencies corresponding to the control signal frequency and its harmonics. When this occurs the output appears to have harmonic distortion though the distortion differs from the normal harmonic distortion in several ways. First, the magnitude and phase of the distortion component relative to the control signal vary with the relative phase of the control signal and the sampling waveform. Second, the distortion may give components with frequencies which are fractions of the control frequency. Third, the distortion occurs only at the discrete control signal frequencies mentioned above. Between these frequencies the sidebands do not reinforce control signal harmonics.

There are two approaches to the estimation and description of the distortion arising from this source. The sidebands which cause the distortion may be evaluated and summed to calculate the distortion component, or the dimensions of the switching wave may be used directly to calculate the component. The latter



The Second Subharmonic Situation

D4.3.1

approach is convenient for accurate numerical estimates formed with the aid of a digital computer while the former is convenient for creating a mental picture of what occurs from which the sensitivity of the component to modulation parameters may easily be perceived.

4.3.1 The Subharmonic Case

The discussion from this point is concerned solely with the situation where the control signal frequency is $1/N^{\text{th}}$ the sampling frequency. This frequency is described here as the N^{th} subharmonic of the switching wave. The restriction implies that the distortion components have frequencies which are all harmonics of the control signal. Diagram D 4.3.1 shows a switching wave with a second subharmonic control signal. Notice how the restriction on relative frequencies implies that the sampling and control signals are stationary with respect to one another, though their relative phase is not defined. The switching wave is thus a true periodic wave with a period of N sampling periods when the control signal is the N^{th} subharmonic of the sampling frequency.

Having defined the situation it is proposed to broaden the meaning of the phrase " N^{th} subharmonic" to convey this situation rather than writing phrases such as "when the control signal frequency is the N^{th} subharmonic of the sampling frequency."

4.3.1.1 Computation of Distortion

Because the switching wave is stationary it is possible to compute all waveform dimensions over one period, that is N sample cycles. Provided the waveform levels are analytic functions an accurate calculation of the harmonics of the wave may be made for any

modulation method and control signal and relative phase of these. For a given situation of amplifier and control signal the distortion may be calculated as a function of phase by repeating the process for the desired number of phase values. Notice that the switching wave proportions are a periodic function of the relative phase with a period of $1/N^{\text{th}}$ that of the control signal so that control signal phase values need only change by $1/N^{\text{th}}$ of a period for the full variation of distortion component to occur.

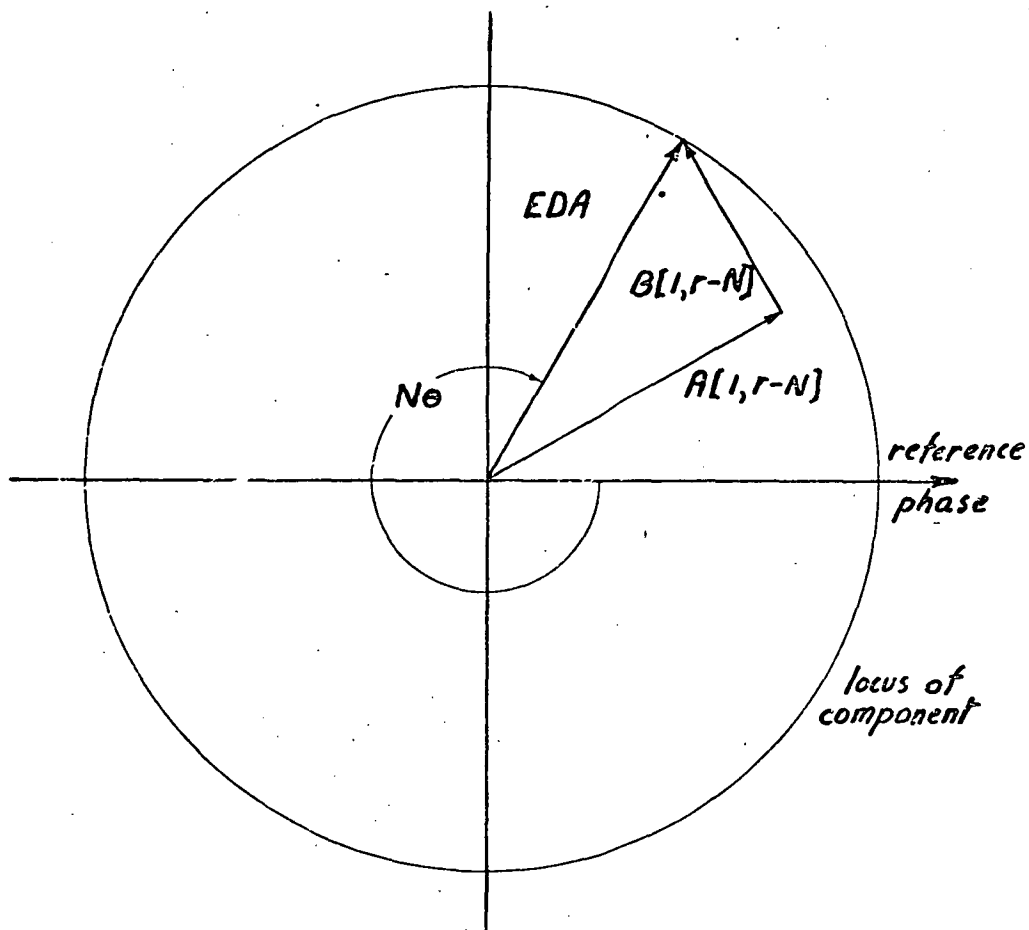
The alternative calculation also yields the harmonic components of the distortion. The first step is the computation of the fourier co-efficients $A[m,s]$ and $B[m,s]$ by which the switching wave is defined by the expression

$$EW = O(w_m t + \theta) + \sum_{m=1}^{m=\infty} \sum_{s=-\infty}^{s=\infty} A[m,s] \cos(mw_s t + s(w_m t + \theta)) + B[m,s] \sin(mw_s t + s(w_m t + \theta)), \text{ where}$$

$O(w_m t)$ is the output component under normal circumstances. The r^{th} distortion harmonic is then found by the summation of those sidebands with frequency $rw_m t$. The expression is

$$ED[R] = \sum_{m=1}^{m=\infty} \sum_{j=\pm r} A[m,j-Nm] \cos(j(w_m t + \theta) - Nm\theta) + B[m,j-Nm] \sin(j(w_m t + \theta) - Nm\theta)$$

The difficulty with this method is the efficient calculation of $A[m,j-Nm]$ and $B[m,j-Nm]$ so that only the important or non infinitesimal values are calculated. In general A and B are results of fourier analysis and if the summation is taken over many terms the computation of EDR is very slow compared to the previous method which requires a single fourier analysis.



Subharmonic Gain Component

D 4.3.1.2

It has the advantage over the previous method that the function of θ is obtained as a set of co-efficients of a fourier series. The periodicity of the error component with the relative phase, θ , is indicated by the expression.

4.3.1.2 Visualisation

The expression for the r^{th} harmonic may be used to form a picture of the harmonic as a function of θ . Consider the component as a vector with a reference vector in phase with the control signal. The expression may be rephrased easily to describe a fourier series in θ but consider only one term of the expression initially. The term is the $(N-r)^{\text{th}}$ lower sideband of the first harmonic.

This is described by the expression

$$EDA = A[1, r-N] \cos(r(w_m t + \theta) - N\theta) + B[1, r-N] \sin(r(w_m t + \theta) - N\theta).$$

As θ is varied the phase of the vector relative to the reference phase of $(w_m t + \theta)$ changes. The magnitude does not. Diagram D 4.3.1.2 illustrates the situation. The locus of the vector path is a circle.

Now consider the terms in the complete expression with positive frequency, those with $j=+r$. The value of m will cause their vectors to rotate m times while the first component rotates once. These vectors are added to the original. Provided they are smaller than the component described above they represent a perturbation of the circular locus described above. The resultant curve is still a closed loop but may be of any shape. The average radius will still be described by the expression above.

The terms of the expression with negative

frequency, those with $j=-r$, have a similar vector representation but the sense of rotation is reversed relative to the control signal vector. The sum of the vectors is a vector with the same period of rotation but with different shape. In practice this second vector is usually much smaller than the first and the perturbation of the circle by the higher harmonic sidebands is usually small so that the curves are nearly circular.

4.3.1.3 Subharmonic Gain

The effective gain of a switching wave may vary considerably when the control frequency is a subharmonic of the sampling frequency. When the switching amplifier is within a feedback loop allowance for this gain variation must be made so that subharmonic oscillations are not set up. To make this allowance requires a knowledge of the gain of the wave.

The effective gain may be defined as a vector with phase and magnitude proportional to phase difference and magnitude ratio respectively of the fundamental component of the switching wave output and a normalised sinewave input. The normalisation of input is such that the effective gain for very low frequency signals is unity.

The effective gain is usefull in the same way as describing functions for dead space and hysteresis, that is, as an approximate way of describing a complex situation. The subject is developed more fully in the next chapter the aim here being to demonstrate the type of curve describing the locus of the vector for several common amplifier types.

The first harmonic of the distortion vector must be normalised by dividing by the control sinewave amplitude before it may be used to describe the deviation from unity of the subharmonic gain.

4.3.2 Natural Sampling

A d.c. levelled switching wave employing natural sampling to produce a sinewave output of amplitude x and with offset, DC, is discussed here. For d.c. levelled waves of this type to produce sinewave outputs the sideband amplitudes are related to Bessel functions. Tables of these functions are readily available and their properties are described in many handbooks. Similar, but untabulated functions describe the sidebands of waves with non d.c. levels. They have similar properties to those described for Bessel functions so that the discussion below is, in most cases, directly applicable to switching waves with other types of waveform levels.

4.3.2.1 Single Edge Modulation

A switching wave with d.c. levels of plus and minus unity with the desired output is described by

$$EW = DC + x \cdot \sin(w_m t + \theta) + \sum_{m=1}^{m=\infty} \frac{2}{m\pi} \left\{ \sin(m(w_s t - \pi(DC + x \sin(w_m t + \theta)))) \right. \\ \left. - \sin(m(w_s t - \pi)) \right\},$$

where θ is the relative phase of the control and sampling signals and the positive going step is modulated. The sidebands of the modulated part of this expression are

$$EWS = \sum_{m=1}^{m=\infty} \frac{2}{m\pi} \sum_{r=-\infty}^{r=\infty} J_r(-m\pi x) \sin(m(w_s t - \pi DC) + r(w_m t + \theta)).$$

The subharmonic restriction for the N^{th} subharmonic is

$$w_s t = N w_m t.$$

The fundamental of the switching wave becomes

$$WF = x \sin(w_m t + \theta) + \sum_{m=1}^{\infty} \sum_{r=-Nm+1}^{\infty} \frac{2J_r(-m\pi x)}{m\pi} \sin((Nm+r)(w_m t + \theta) - Nm\theta - m\pi DC).$$

Substituting r for $r+Nm$ yields the expression

$$WF = x \sin(w_m t + \theta) + \sum_{m=1}^{\infty} \sum_{r=+1}^{\infty} \frac{2}{m\pi} J_{Nm-r}(m\pi x) \cdot r \cdot \sin(w_m t + \theta - mr \cdot (N\theta + \pi DC)).$$

Thus the gain vector is

$$GV = 1 + \sum_{m=1}^{\infty} \sum_{r=+1}^{\infty} \frac{r \cdot J_{Nm-r}(m\pi x)}{(m\pi x/2)} e^{-jmr(N\theta + \pi DC)}$$

For x small compared to $2/\pi\sqrt{N-r}$ the Bessel functions may be approximated to give the expression below

$$GV \approx 1 + \sum_{m=1}^{\infty} \sum_{r=+1}^{\infty} \frac{r}{(Nm-r)!} \left(\frac{m\pi x}{2}\right)^{Nm-r-1} e^{-jmr(N\theta + \pi DC)}$$

For large x the expression may be approximated by

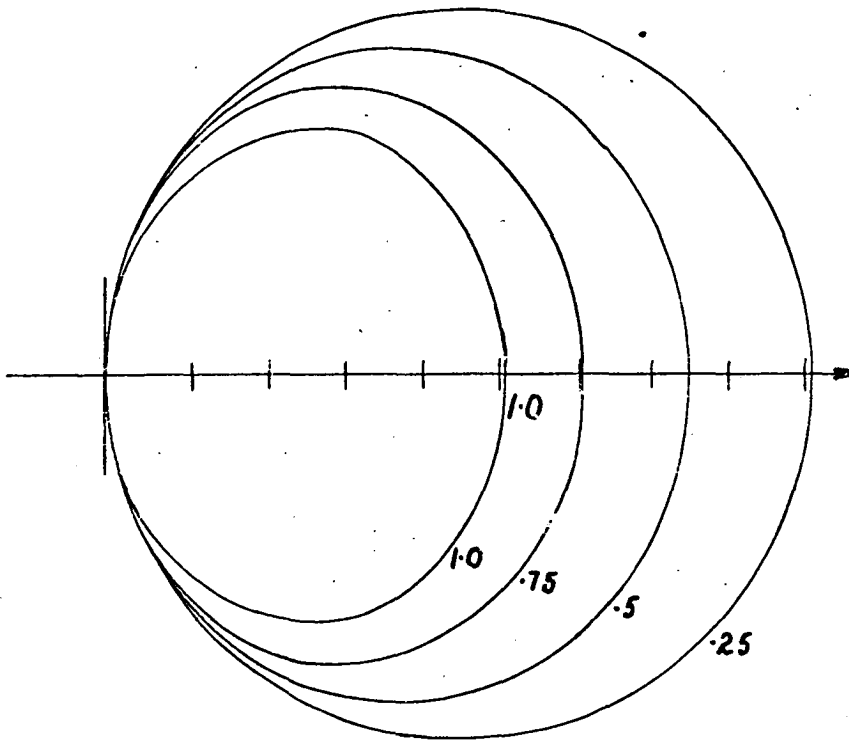
$$GV \approx 1 + \sum_{m=1}^{\infty} \sum_{r=+1}^{\infty} \frac{r}{m} \left(\frac{2}{\pi x}\right)^{\frac{3}{2}} \cos \left[x - \frac{(Nm-r)\pi}{2} - \frac{\pi}{4} \right] e^{-jmr(N\theta + \pi DC)}$$

The Second Subharmonic

For very small control signal amplitude the first sideband of the first harmonic is the sole contributor to the gain vector. This contributor has unit amplitude so the gain vector locus is a circle about unity gain. Where this circle touches the vertical axis at the origin the gain changes, with relative phase,

Second Subharmonic - Sinewave Input

Curve parameter is input amplitude



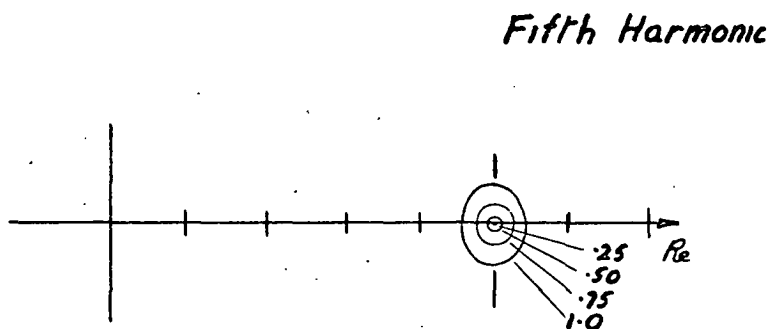
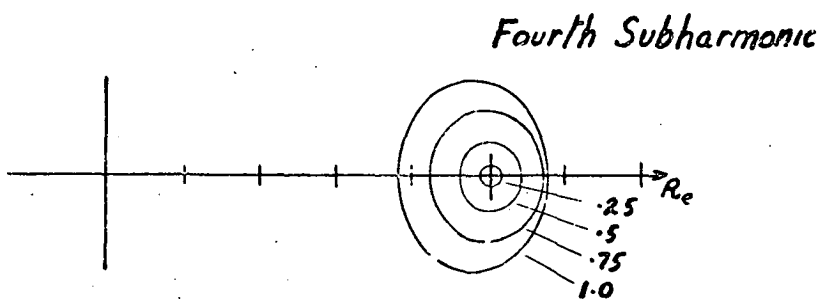
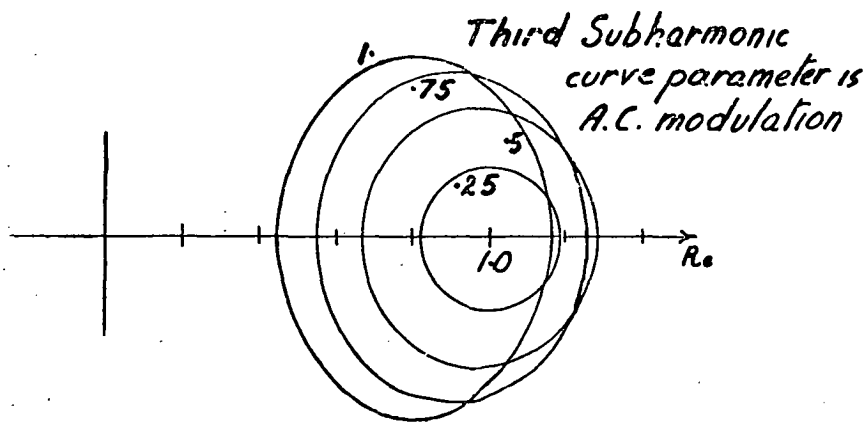
D4.3.2.1a

from quadrature in one direction to quadrature in the other direction as the magnitude passes through zero.

Diagram D 4.3.2.1a shows loci for several non zero signal amplitudes. Notice that all the loci touch the quadrature axis at the origin. A brief consideration of the waveforms of natural sampling suffices to show that for any d.c. component it is possible to choose a relative phase of control signal and sampling signal such that the switching wave has no subharmonic component.

The values of control signal amplitude, x , for the loci shown are too large for the small signal model to be accurate. As x is increased the relative magnitudes of the various components change. The curve shapes reflect this change. For the smallest value of x shown the third sideband of the second harmonic causes the apparent shift in circle centre while the diminution of circle radius is caused by the decrease in magnitude of the first harmonic first sideband component. The elliptical form of the loci for large x is due to the increase in relative magnitude of the third sideband of the first harmonic.

The loci shown applies only to the range of output of a two level switching wave. The expressions apply equally well to multi-level waves. It is interesting to speculate on the possible shapes of the loci for larger values of x but apart from noting that the enclosed areas probably diminish in area due to the $1/m$ term, and the shape may be much more complex due to the higher harmonics, little may be said.



D4.3.2.16

Other Subharmonics

The small signal expression indicates that all subharmonics have circular loci. The circle diameter is given by the expression

$$LD = \left(\frac{m\pi x}{2} \right)^{N-2} \cdot \frac{1}{(N-1)} \cdot$$

For the second subharmonic the diameter is unity but other subharmonics have small signal vectors with magnitudes which are proportional to x raised to an integer power. This means that small signal loci are very close to unity and the loci expand away from unity as x is increased. This contrasts with the $N=2$ case where the loci contract as x increases.

Diagram D 4.3.2.1b shows loci of third, fourth and fifth subharmonics for several values of signal amplitude. Notice the drop in maximum size as N increases. The factor of $1/(N-1)$ has much greater influence than the other terms for N large. The influence of the third sidebands of the first and second harmonics are less for these loci than for the second subharmonic, though their influence is visible as an increase in the eccentricity and in the shift of the loci as x is increased.

For the control signal amplitudes shown these subharmonic loci increase in diameter as x increases. The range of x shown is that corresponding to the two level wave maximum output. For the larger values of x associated with multi-level waves the loci will reach maximum sizes then diminish in size and change shape, as the second subharmonic loci do, as x is increased.

4.3.2.2 Symmetrical Modulation

The waveform expression

$$EW = DC + x \cdot \sin(w_m t + \theta) + \sum_{m=1}^{\infty} \sum_{s=\pm 1} \frac{2s}{m\pi} \sin(m(w_s t - \frac{s\pi}{2})) \cdot (1 + DC + x \sin(w_m t + \theta))$$

has high frequency components described by

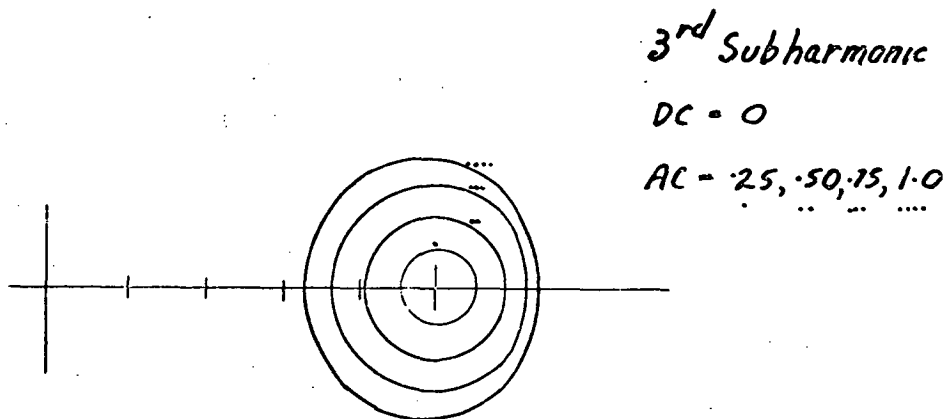
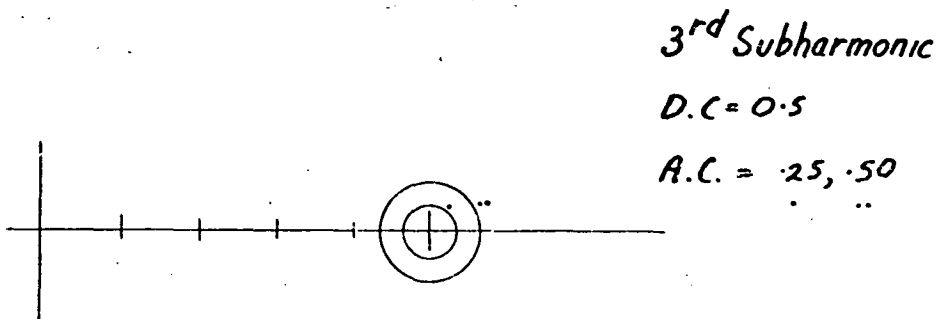
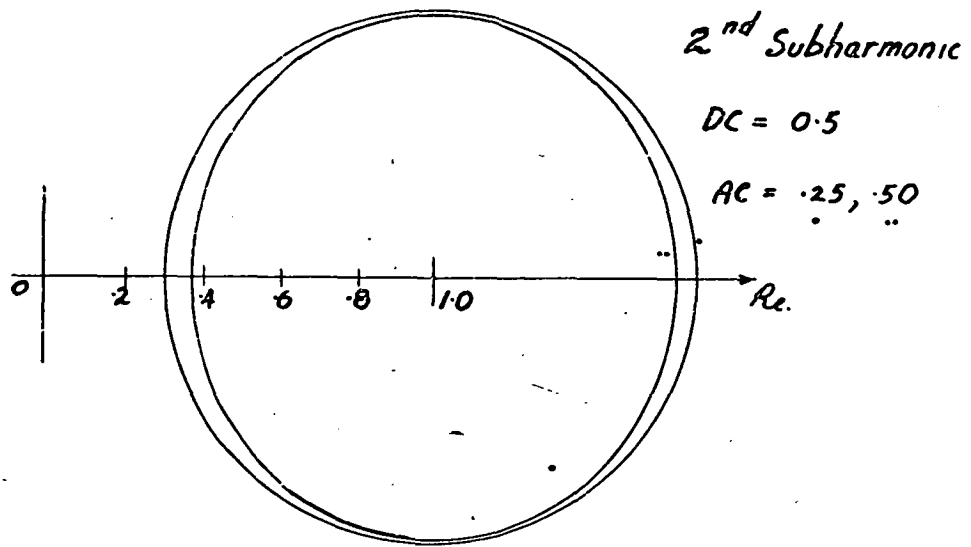
$$EWM = \sum_{m=1}^{\infty} \sum_{s=\pm 1} \frac{2}{m\pi} \sum_{r=-\infty}^{\infty} s \cdot J_r(-s\pi x/2) \sin(m(w_s t - \frac{s\pi}{2}(1+DC))) + r(w_m t + \theta)$$

which may be simplified to give

$$EWM = \sum_{m=1}^{\infty} \sum_{r=-\infty}^{\infty} \frac{4}{m\pi} J_r(m\pi x/2) \cos(mw_s t + r(w_m t + \theta) + \frac{r\pi}{2}) \cdot \sin(\frac{r\pi}{2} - \frac{m\pi}{2}(1+DC)).$$

The contributors to the gain vector are

$$\begin{aligned} FC &= x \cdot \sin(w_m t + \theta) + \sum_{m=1}^{\infty} \sum_{r=-Nm+1}^{\infty} \frac{4J_r(m\pi x/2)}{m\pi} \sin(\pi/2(r-m(1+DC))) \cdot \\ &\quad \cos(r + Nm)(w_m t + \theta + \pi/2 - Nm(\theta + \pi/2)) \\ &= x \cdot \sin(w_m t + \theta) + \sum_{m=1}^{\infty} \sum_{r=\pm 1} \frac{4}{m\pi} J_{-Nm+r}(m\pi x/2) \sin(\pi/2(r-m \\ &\quad (N+1+DC))) * \cos(w_m t + \theta + \pi/2 - rNm(\theta + \pi/2)). \\ &= x \cdot \sin(w_m t + \theta) + \sum_{m=1}^{\infty} \sum_{r=\pm 1} \frac{4}{m\pi} J_{Nm-r}(m\pi x/2) \sin(\pi/2(r+m \\ &\quad (N+1+DC))) * \sin(w_m t + \theta - rNm(\theta + \pi/2)). \end{aligned}$$



Subharmonic Gain Loci For Symmetrical Modulation

D4.3.2.2

Thus the gain vector is described by the complex fourier series

$$\text{GVS} = 1 + \sum_{m=1}^{\infty} \bar{Z} \cdot \frac{-r \cdot J_{Nm-r}(\frac{m\pi x}{2})}{(\frac{m\pi x}{4})} \sin(\frac{\pi m}{2}(N+DC)) \cdot e^{-jmNr(\theta+\pi/2)}$$

This subharmonic gain vector differs in two important respects from that for single edge modulation. The index of the Bessel function is reduced by a factor of two. For subharmonics other than the second this means a reduction in the size of the loci. The other feature is the factor $-\sin(\pi m/2(N+DC))$. This factor influences the shape of the loci by weighting the various harmonics by factors between plus and minus unity depending on the value of the d.c. output component, DC. Thus for instance the odd harmonics of the second subharmonic are zero if DC is zero while the even harmonics of this subharmonic expression are zero if DC is unity.

The absence of the odd harmonics results in a basic loci of much smaller magnitude for a given signal level. The second harmonic sidebands require only half the phase change to be periodic. These two factors result in very complicated loci for small d.c. signal components when the lower harmonic is comparable with the second harmonic. The larger d.c. components have similar curves to those for single edge modulation. The fourth and fifth subharmonics have very small deviations from unity.

Several examples of second and third subharmonics are shown in diagram D 4.3.2.2.

4.3.3 Conclusion

Viewed without consideration of their possible use in the analysis of feedback systems the subharmonic loci have limited usefulness. They are an approximate way of describing the apparent gain of an amplifier when some sidebands have the same frequency as the control signal. The loci described here provides information over a different range of amplifier parameters than the graphs of signal to noise ratio. The former are intended to provide information for the analysis of wideband control loops, the latter for narrow band signal to noise ratios. The two descriptions overlap at their extremes but do not provide the same aspects of a common source of information. The signal to noise ratio curves describes the possible magnitudes of a passband noise energy due to many sidebands while the loci describes the magnitude and phase of particular sidebands, those synchronous with the input signal.

For use in feedback analysis the gain loci are transformed, either numerically or graphically, to give describing functions. These may be used in the normal way to indicate system stability, stability of oscillations and the growth of oscillations as input signal parameters are varied. These aspects of their use have been described previously by others (3).

References

- E. C. Bell, T. Sargent "Distortion and Power Output of P.D. Modulated Amp."
Electronic Engineering Vol. 37 August 1965 PP 540-542
- Bennett "New Results in the Calculation of Modulation Products"
Bell System Tech. Journal Vol. 12 April 1933 PP 228-243
- H. S. Black "Modulation Theory"
N. J.: Van Nostrand 1953 PP 263-231
- F. Fallside, A. R. Farmer "Ripple Instability in Closed Loop Control Systems"
Proc IEE Vol. 114 March 1967 PP 139-152
- E. Fitch "The Spectrum of Modulated Pulses"
J. IEE Vol. 94 PT 3A 1947 PP 556-564
- S. G. Furmage "Subharmonic Instability in Closed Loop Control Systems with Pulse Width Modulation"
Honours Thesis in Electrical Engineering, Uni. Tas.
March 1969
- E. R. Kretzmer "Distortion in Pulse Duration Modulation"
Proc. IRE Vol. 35 November 1947 PP 1230-1235
- C. H. Miller "High Efficiency Amplification Using Width Modulated Pulses"
Proc IREE (Australia) Vol. May 1964 PP 314-323

CHAPTER V

FEEDBACK WITH NATURAL SAMPLING

CHAPTER V : FEEDBACK WITH NATURAL SAMPLING

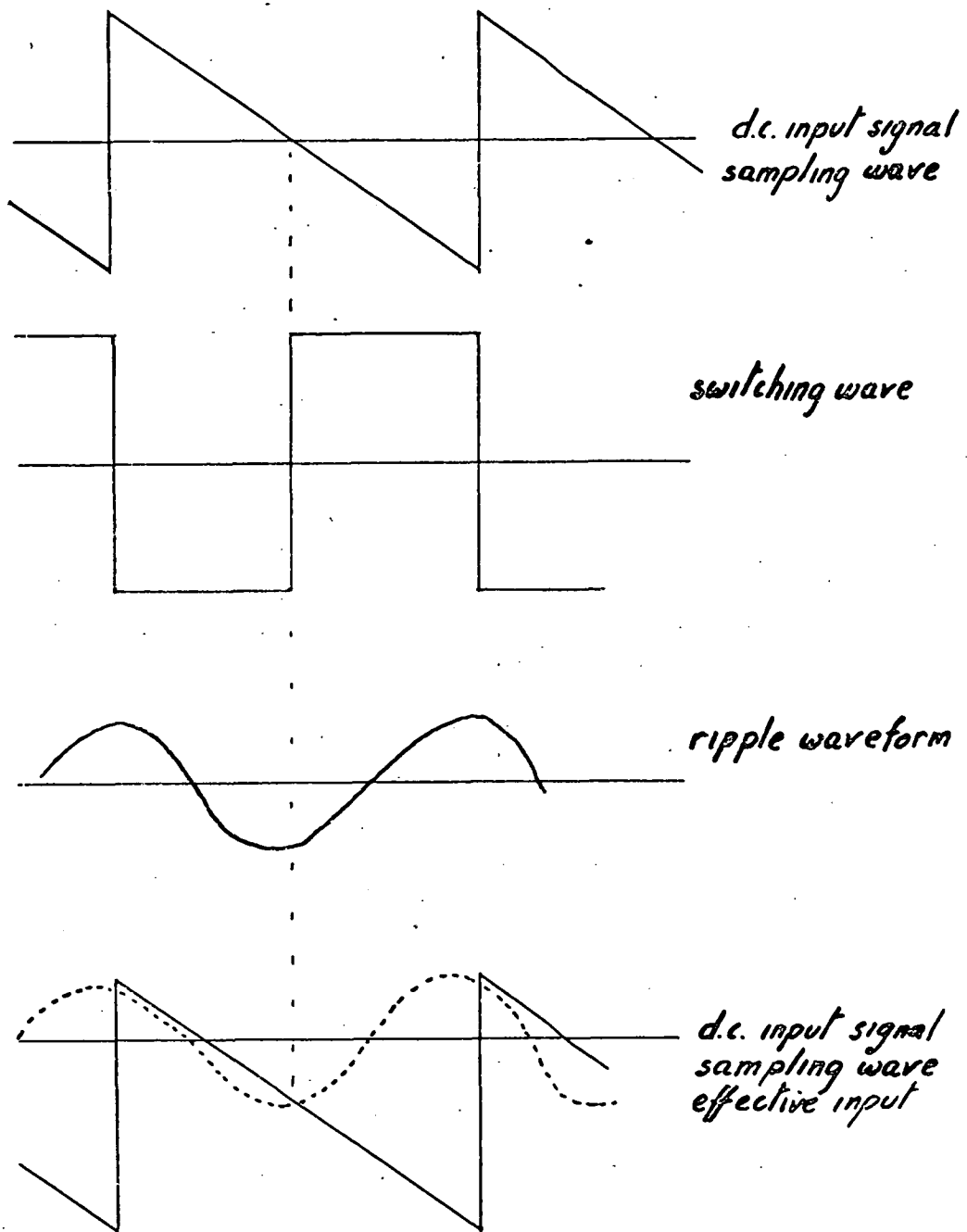
- 5.1 The low frequency characteristics
 - 5.1.1 A method for computing the d.c. input output characteristic
 - 5.1.1.1 Average output and the switching instants
 - 5.1.1.2 Total output waveform and the switching instants
 - 5.1.1.3 The ripple waveform
 - 5.1.1.4 Amplifier input state at switching instants
 - 5.1.2 The amplifier characteristic
 - 5.1.2.1 An example
 - 5.1.2.2 Methods for equation solution
 - 5.1.2.3 Linearity
 - 5.1.3 Limits of computational model
 - 5.1.4 Double sampling, multiple sampling
- 5.2 A.c. control signal performance
 - 5.2.1 Aspects of a.c. models
 - Narrowband feedback
- 5.3 Summary

5. Feedback with Natural Sampling

The classical theory of linear feedback systems assumes the elements of the feedback loop have no variation of gain with signal amplitude. This is not true for switching amplifiers except in special circumstances since the presence of the feedback path causes the sampling process to be modified.

There are two forms of modification which may occur separately or, more usually, simultaneously. First, the ripple produced by the filtering of a switching amplifier output modifies the effective shape of the sampling wave. The ripple is present for both d.c. and a.c. control signal inputs and may cause a gross change in both characteristics from the open characteristic of the amplifier. Second, the gain at subharmonic frequencies is not linear nor even fixed due to the presence of sidebands. These sidebands of the sampling frequency harmonics inter-mingle with the control signal and are themselves amplified by the switching amplifier at all control signal frequencies. The sidebands of these sidebands although small compared to the signal in most circumstances may cause noticeable distortion similar to harmonic distortion and intermodulation distortion.

An exact model for the d.c. characteristic of a switching amplifier when included in a feedback loop is described. Apart from a narrow band model of the subharmonic a.c. control signal no other situation may be modelled exactly. Despite this, switching amplifier performance may be estimated for other conditions by considering the changes in important parameters as conditions are changed from situations where exact analysis may be used.



Sampling with and without Ripple

D 5.1

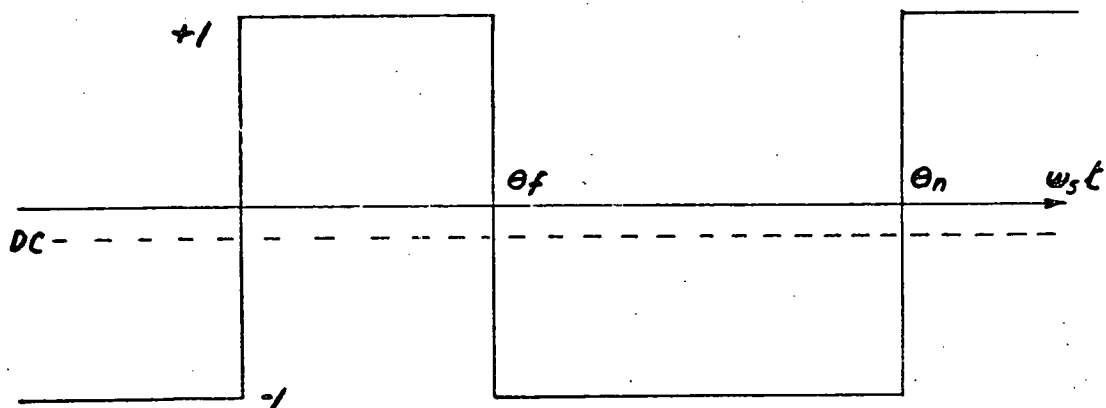
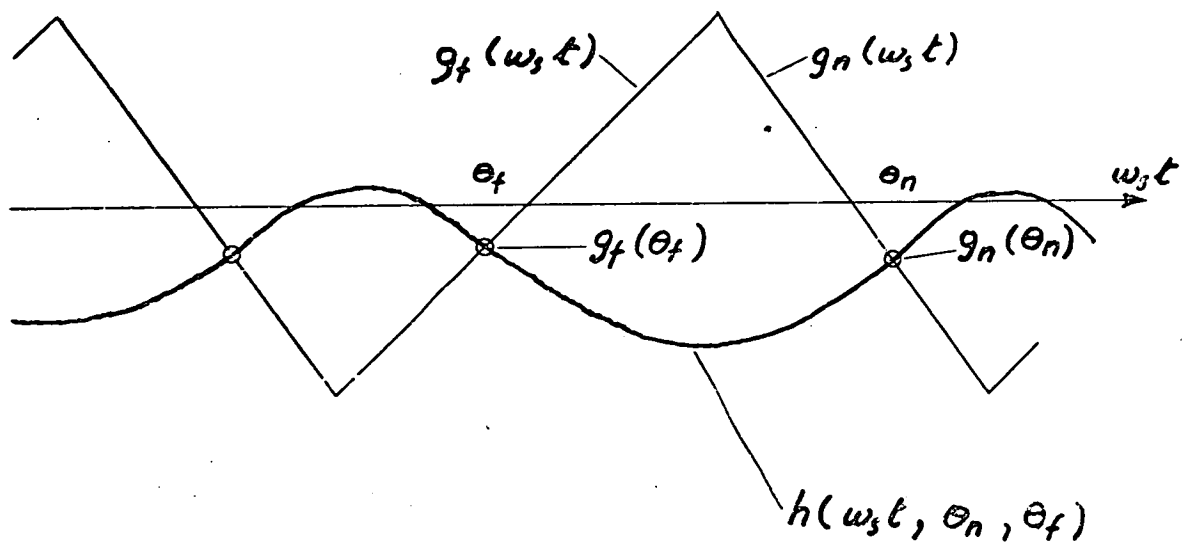
5.1 The Low Frequency Characteristics of Switching Amplifiers in Feedback Loops

A change in the low frequency input to output transfer function occurs when a switching amplifier is placed within a feedback loop. The cause of the change is the injection, into the amplifier input, of ripple from the output. Since this ripple has the same fundamental frequency as the sampling waveforms it changes their effective shapes and thus modifies the transfer characteristic.

To appreciate some of the effects of such a ripple consider diagram D 5.1 where a sequence of waveforms is presented. The upper waveform is the sampling waveform of a d.c. supplied switching amplifier with a d.c. input signal super-imposed. The second waveform is the amplifier output associated with the conditions indicated by the sampling wave and input signal. The third waveform is a ripple wave, at the amplifier input, when the amplifier has a feedback from output to input. The fourth waveform shows the arrangement of input signal, and ripple signal relative to the sampling wave, necessary to produce the same output waveform as the conditions of the first diagram.

The presence of the ripple changes the input signal required to produce the same output signal. Since the ripple waveform changes, in magnitude, shape, and phase relative to the sampling wave, as the output waveform and hence output component change, the difference between the amplifier input signals with and without signals is a function of the output voltage.

To analyse the situation and predict the shape of the d.c. transfer characteristic of a switching amplifier within a feedback loop, a knowledge of



An Illustration of Waveform Names

D 5.1.1

the spectrum of the amplifier output, the frequency characteristics of the feedback path, and the shape of the sampling waveform is necessary. In the following analysis these three subjects are related to the signals at the amplifier input, output, and switch control functions in a general manner. The relationships given are general enough to include most switching amplifiers employing natural sampling. For this reason many of the relationships will appear to be complicated, in the analysis, even though a given amplifier may have a very simple form for these relationships.

5.1.1 The Model

5.1.1.1 Average Output and the Switching Instants

Each switch of a switching amplifier is controlled in such a manner that the average value of the switching wave is maintained constant. Provided the switch control functions associated with each switching wave component are symmetrical, in the case of a.c. supplied amplifiers, or complementary in the case of d.c. supplied amplifiers, then the instants at which the switches turn off, and the instants at which the switches turn on are related to one another by a relationship which does not vary with the input ripple. In the case of a switching wave with m a.c. levels, due to m symmetrical phases, each level is switched on with the same phase relative to the respective supply voltage. Each level is also switched off at the same phase.

A restriction of this form enables the d.c. component of the amplifier to be specified in terms of the phase angles at which a switch turns on and off.

If the phase of switch turn on is θ_n , the

Formula for a.c. Levelled Wave Spectra

DC = d.c. component of switching wave

a_n and b_n are fourier co-efficients of Cos and Sin components describing the n^{th} harmonic

$W(\theta)$ = function describing waveform levels shape
(sinewave levels have $W(\theta) = \text{Sin}(\theta)$.)

m = number of phases forming wave

θ_n = phase of turn on for a waveform level

θ_f = phase of turn off of the same waveform level

$$DC = m/2\pi \int_{\theta_n}^{\theta_f} W(\theta) d\theta$$

$$a_n + j b_n = m/\pi \int_{\theta_n}^{\theta_f} W(\theta) e^{jmn\theta} d\theta$$

For thyristor amplifiers using

(i) phase modulation $\theta_f = \theta_n + 2\pi/m$

(ii) diode clamped operation $\theta_f = \begin{cases} \theta_z & \text{if } \theta_z < \theta_n + 2\pi/m \\ \theta_n + 2\pi/m & \text{otherwise} \end{cases}$

where θ_z is defined by $W(\theta_z) = 0$.

phase of switch turn off is θ_f , and the d.c. output is DC then the relationship is of the form

$$DC = F(\theta_n, \theta_f).$$

Examples are the two level d.c. supplied amplifier where the normalised output ($-1 < DC < 1$) is described by

$$DC = (\theta_f - \theta_n - \pi) / \pi \quad \text{where } 0 < \theta_f - \theta_n < 2\pi;$$

and the a.c. supplied, m phase, amplifier where the normalised output is described by

$$DC = m \int_{\theta_n}^{\theta_f} \sin(\theta/m) d\theta / (2\pi) \quad \text{where } 0 < \theta_f - \theta_n < 2\pi/m.$$

5.1.1.2 Total Output Waveform and the Switching Instants

The complete output waveform is related to the switching instants in a more indirect manner than the d.c. component of the waveform but subject to the same conditions may be written in the form

$$f(\theta, \theta_n, \theta_f) = DC + \sum_{n=1}^{n=\infty} a_n(\theta_n, \theta_f) \cos(n\theta) + b_n(\theta_n, \theta_f) \sin(n\theta),$$

where a_n and b_n are similar expressions to that for DC. θ is the phase of the output waveform relative to some reference instant.

For the previously mentioned d.c. supplied amplifier the terms a_n and b_n are given by

$$a_n(\theta_n, \theta_f) = 2.(\sin(n.\theta_f) - \sin(n.\theta_n)) / n\pi, \text{ and}$$

$$b_n(\theta_n, \theta_f) = 2.(\cos(n.\theta_n) - \cos(n.\theta_f)) / n\pi.$$

The expressions for a.c. supplied amplifiers with symmetrically phased supply voltages and control functions are given in table D 5.1.1.2.

5.1.1.3 The Ripple Waveform

Since the filter is subject only to signals at d.c. and harmonics of the output waveform frequency, a series of magnitude and phase pairs, describing the response at these frequencies, is sufficient to specify the filter. The magnitude of the filter response at the n^{th} harmonic of the output waveform frequency will be described by A_n , and the phase by P_n . The output of the filter when supplied by the amplifier output, that is the feedback signal, is described by

$$h(\theta, \theta_n, \theta_f) = A_o.DC + \sum_{n=1}^{\infty} \left\{ A_n.a_n(\theta_n, \theta_f).Cos(n\theta + P_n) + A_n.b_n(\theta_n, \theta_f).Sin(n\theta + P_n) \right\}.$$

5.1.1.4 Amplifier Input State at Switching Instants

The input signal to the switching amplifier is a d.c. signal with the ripple super-imposed. If the d.c. component is referred to as E_{in} then the amplifier input is given by

$$e_{in} = E_{in} - (h(\theta, \theta_n, \theta_f) - A_o.DC).$$

At the switching instants this signal equals the associated sampling waveform. If the sampling waves associated with the two switching instants, θ_n and θ_f , are $g_n(\theta)$ and $g_f(\theta)$ respectively, then at the switching instants the equations

$$A_o.DC + E_{in} - h(\theta_n, \theta_n, \theta_f) = g_n(\theta_n), \text{ and}$$

$$A_o.DC + E_{in} - h(\theta_f, \theta_n, \theta_f) = g_f(\theta_f) \text{ must be satisfied.}$$

The d.c. component of the input signal, E_{in} , is derived from the control signal, E , and the feedback signal. Their relationship is described by

$E_{in} = E - A_o.DC$. E_{in} is eliminated from the above equations by this means.

5.1.2 The Amplifier Characteristic

The three equations below relate the four variables, DC, Θ_n , Θ_f , and E_{in} . They are

$$DC = F(\Theta_n, \Theta_f),$$

$$g_n(\Theta_n) = E_{in} - \sum_{n=1}^{\infty} \left\{ A_n \cdot a_n(\Theta_n, \Theta_f) \cdot \cos(n\Theta_n + P_n) + B_n \cdot b_n(\Theta_n, \Theta_f) \cdot \sin(n\Theta_n + P_n) \right\},$$

and

$$g_p(\Theta_f) = E_{in} - \sum_{n=1}^{\infty} \left\{ A_n \cdot a_n(\Theta_n, \Theta_f) \cdot \cos(n\Theta_f + P_n) + B_n \cdot b_n(\Theta_n, \Theta_f) \cdot \sin(n\Theta_n + P_n) \right\}.$$

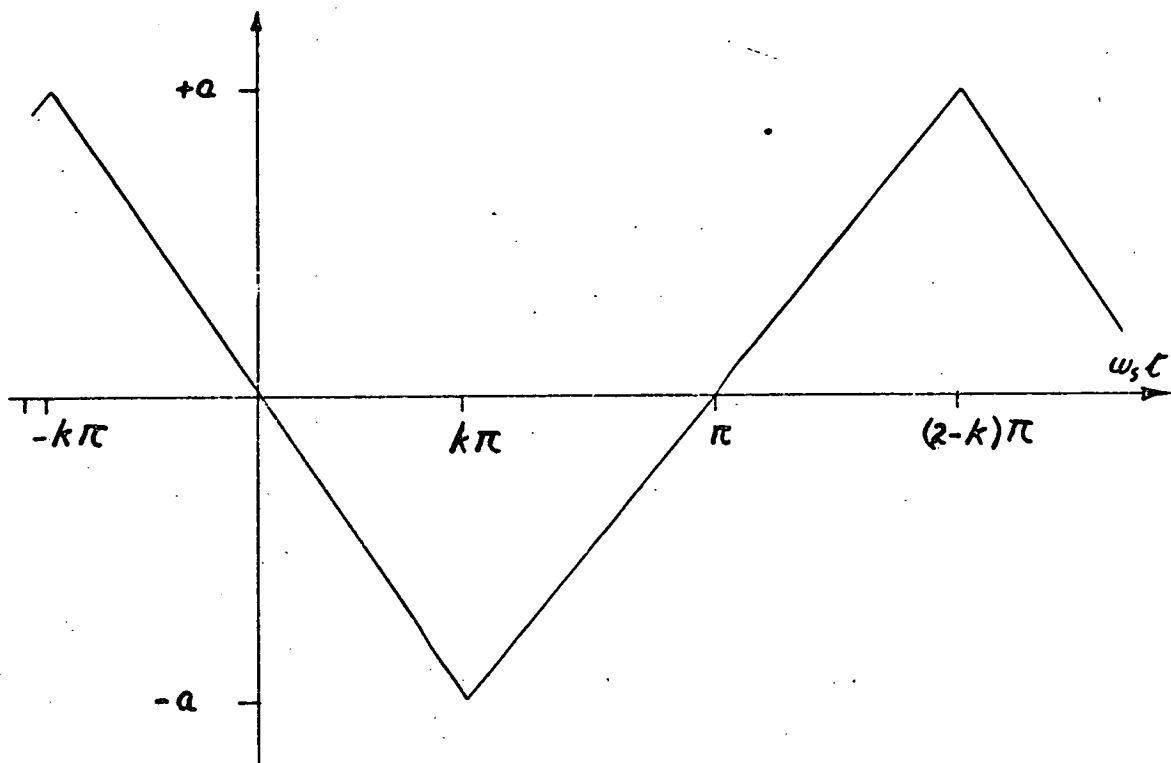
The relationship between DC and E_{in} may be found by the simultaneous solution of the three equations. This relationship describes the effective low frequency transfer function of the switching amplifier. The low frequency characteristic of the entire system outside the feedback loop may be found by substituting the relationship

$E_{in} = E - A_o DC$, in the same manner as a conventional feedback circuit.

It should be noted that the effective characteristic of the switching amplifier depends on the high frequency characteristic of the feedback filter and the shape of the sampling waves. It does not depend on the low frequency filter characteristic.

5.1.2.1 An Example

The feedback path used for a loop containing a d.c. supplied amplifier is equivalent to an integrator with absolute gain at the fundamental frequency of the switching wave of A. The sampling waves are the two slopes of a triangular wave with the proportions indicated in diagram D 5.1.2.1.



Assymmetric Triangular Sampling Wave

D 5.1.2.1

The amplifier output is described by

$$f(w_s t, \theta_n, \theta_f) = DC + \sum_{n=1}^{\infty} \left\{ \sin(nw_s t) \cdot (\cos(n\theta_n) - \cos(n\theta_f)) + \cos(nw_s t) \cdot (\sin(n\theta_f) - \sin(n\theta_n)) \right\} / (n\pi)$$

This may be re-expressed as

$$f(w_s t, \theta_n, \theta_f) = DC + \sum_{n=1}^{\infty} \frac{2}{(n\pi)} \cdot \left\{ \sin(n(w_s t - \theta_n)) - \sin(n(w_s t - \theta_f)) \right\}.$$

The ripple component of the feedback signal is

$$R = - \sum_{n=1}^{\infty} \frac{2A}{(n^2\pi)} \left\{ \cos(n(w_s t - \theta_n)) - \cos(n(w_s t - \theta_f)) \right\}.$$

The sampling waves are described over their respective ranges during one period by

$$g_n(w_s t) = -a \cdot w_s t / (k\pi) \text{ for } -k\pi < w_s t < k\pi, \text{ and}$$

$$g_f(w_s t) = a(w_s t - \pi) / ((1-k)\pi) \text{ for } k\pi < w_s t < (2-k)\pi.$$

The three simultaneous equations are

$$DC = (\theta_f - \theta_n - \pi) / \pi,$$

$$E_{in} = -a \cdot \theta_n / (k\pi) - \sum_{n=1}^{\infty} \frac{2A}{(n^2\pi)} \cdot [1 - \cos(n(\theta_n - \theta_f))],$$

$$\text{and } E_{in} = a(\theta_f - \pi) / ((1-k)\pi) - \sum_{n=1}^{\infty} \frac{2A}{(n^2\pi)} [\cos(n(\theta_f - \theta_n)) - 1].$$

The analytical solution of this set of equations is described in appendix A 5.1.2.2. The three variables are related to the d.c. component of the switching amplifier output by the equations

$$E_{in} = a \cdot DC + A\pi/2 \cdot (1 - DC^2)(1 - 2k),$$

$$\theta_n = -\pi k (DC + \pi \cdot (A/a)(1-k)(1 - DC^2)), \text{ and}$$

$$\theta_f = \pi + \pi(1-k)(DC - \pi(A/a) \cdot k \cdot (1 - DC^2)).$$

5.1.2.2 Methods for Equation Solution

The example above is a particularly simple one in that the equations may be solved analytically. In general this is not so. Some methods for re-expressing the equations as functions of the switching wave d.c. component are now discussed. They apply to particular circumstances but the range of amplifier types to which they apply includes most common amplifiers.

In the example the ripple waveforms were found to be functions of the parameter DC, the d.c. component of the switching wave. This is a common feature. It requires that each output level has only one possible ripple waveform. It is conceivable that some forms of switching wave with a.c. supply levels do not satisfy this condition but the most common amplifiers do. If the ripple waveforms at the sampling instants are functions of the parameter DC then they may be denoted by $G_p(DC)$ and $G_n(DC)$ corresponding to the positive and negative output steps respectively.

The second two equations may now be re-expressed in the form

$$\Theta_i = g_i^{-1}(E_{in} - G_i(DC)) \text{ for } i = n \text{ and } p.$$

These equations may be substituted in the first giving

$$DC = F(g_n^{-1}[E_{in} - G_n(DC)], g_p^{-1}[E_{in} - G_p(DC)]).$$

This equation relates E_{in} and DC. It may be further refined if some restrictions on F , g_i , G_i are considered. For the example F , g_n and g_p were linear functions. In this case the equation may be expressed as

$$E_{in} = a + b \cdot DC + c \cdot G_n(DC) + d \cdot G_p(DC), \text{ where}$$

a , b , c , d are constants. Thus the method is applicable

to d.c. supplied switching amplifiers with linear sampling waves.

When F is a linear function but g_n and g_p are nonlinear, graphical techniques may be used to solve the equation when it is re-expressed in the form

$$DC = a.g_n^{-1} \text{Ein} - G_n(DC) + b.g_p^{-1} \text{Ein} - G_p(DC) .$$

This method may be used when the sampling waves are non-linear.

Symmetrical a.c. supplied amplifiers satisfy the restriction that the ripple waves have equal amplitudes at each step in the switching wave. Since G_n and G_p are identical functions the equation reduces to the form

$$DC = F_1(\text{Ein} - G_1(DC)) \text{ which may be re-expressed as } \text{Ein} = F_1^{-1}(DC) + G_1(DC) .$$

The other two parameters, Θ_n and Θ_f may be expressed as functions of DC by substituting the solution for Ein back into the last two of the original equations then re-expressing these.

It should be appreciated that only in very exceptional circumstances are the ripple waveforms recognisable as simple functions of DC as was the case for the example. In general G_n and G_p are nonlinear functions of DC which may be plotted or evaluated only by summation of the fourier series numerically for a range of values of DC . Thus the calculation of a low frequency transfer characteristic is normally carried out numerically. Fortunately most feedback filters have low pass characteristics and only a few terms of the series are necessary to evaluate the ripple waveform to the required accuracy.

5.1.2.3 Linearity

The relationship between the input signal, E_{in} , and the output, DC , for the example is restated below.

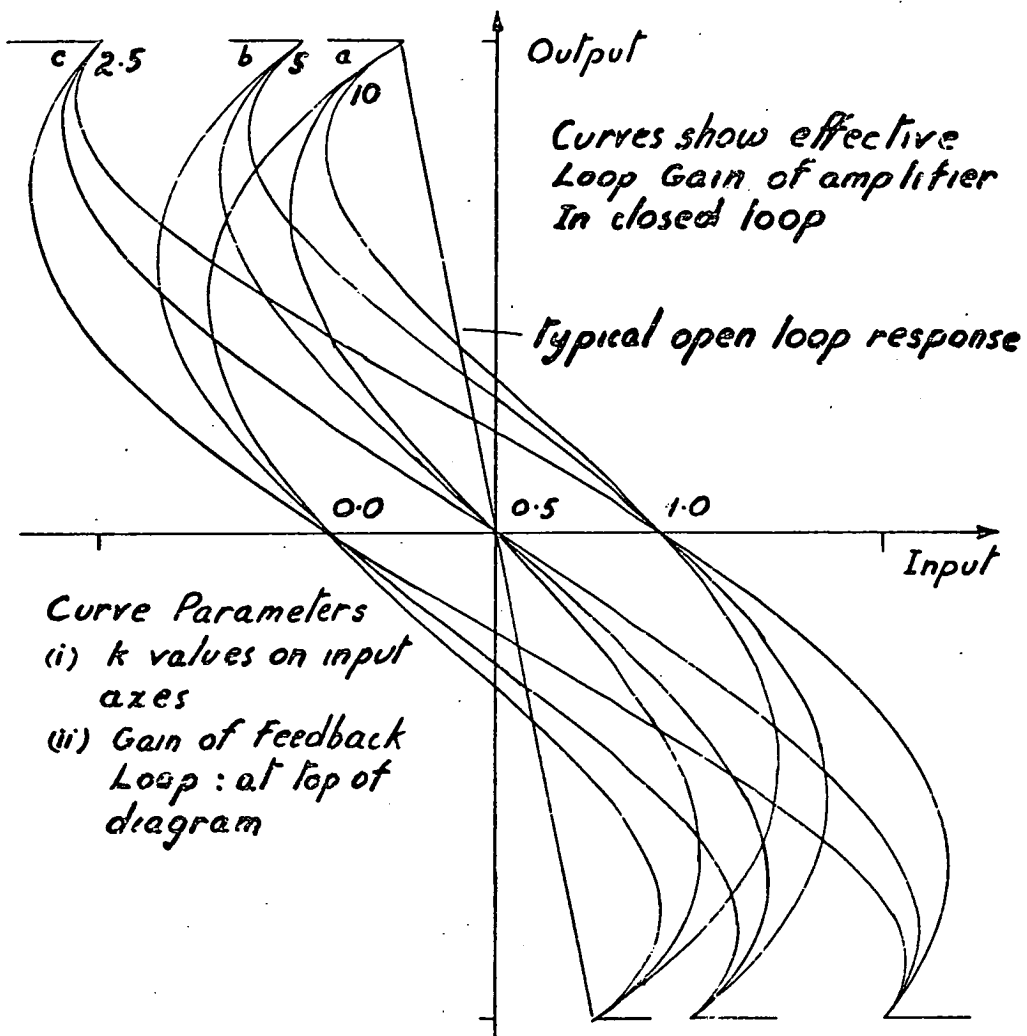
$$E_{in} = a \cdot DC + \pi A(1-2k)(1-DC^2)/2.$$

The nonlinear component is a parabolic shape with zero error at extreme values of DC . It is a function of the sampling waveform proportions and is directly proportional to the filter gain.

This particular example is interesting because the nonlinearity is zero when the sampling wave slopes are equal. This condition is shown, in appendix A 5.1.2.3, to be sufficient, for other filters which have an odd multiple of ninety degrees phase shift at each harmonic of the sampling frequency, to give a linear characteristic. Thus third, fifth, and other odd order filters will give the same linear characteristic if sampling waves of equal slope are used.

The property of, the nonlinear term being zero, at the extreme values of DC , is due to the absence of any switching wave at these values. It is generally true for d.c. supplied amplifiers with switching between the nearest supplies. It also applies to a.c. supplied amplifiers using width modulation, but not to those using phase modulation.

The situation above where the nonlinearity may be zero is not common. Usually the ripple from the feedback loop produces a nonlinearity. In order to demonstrate the form and type of nonlinearity a more general example is considered. The same amplifier form as used in the previous example is coupled to the feedback filter specified by the response $H(s) = 1/((1+1.8s)1.8s)$, where s , the complex



Effective Amplifier Characteristics

D 5.1.2.3

frequency is normalised with respect to the switching wave frequency. Diagrams D 5.1.2.3a to e show the switching amplifier input signal, E_{in} , as a function of the amplifier output, DC. Each diagram describes the switching amplifier characteristic for three values of k and a particular amplifier gain.

The nonlinearity is appreciable, even for low values of loop gain. For values of loop gain greater than two the characteristic has infinite incremental gain near maximum and minimum output. The central portion of each curve has lower incremental gain than the open loop characteristic of the amplifier. Notice that for $k=0.5$, that is for symmetrical modulation of the wave steps, the transfer functions are symmetrical. The transfer functions for k values of 0 and 1 lie to one side or the other of the symmetrical case.

5.1.3 Limits of the Computational Model

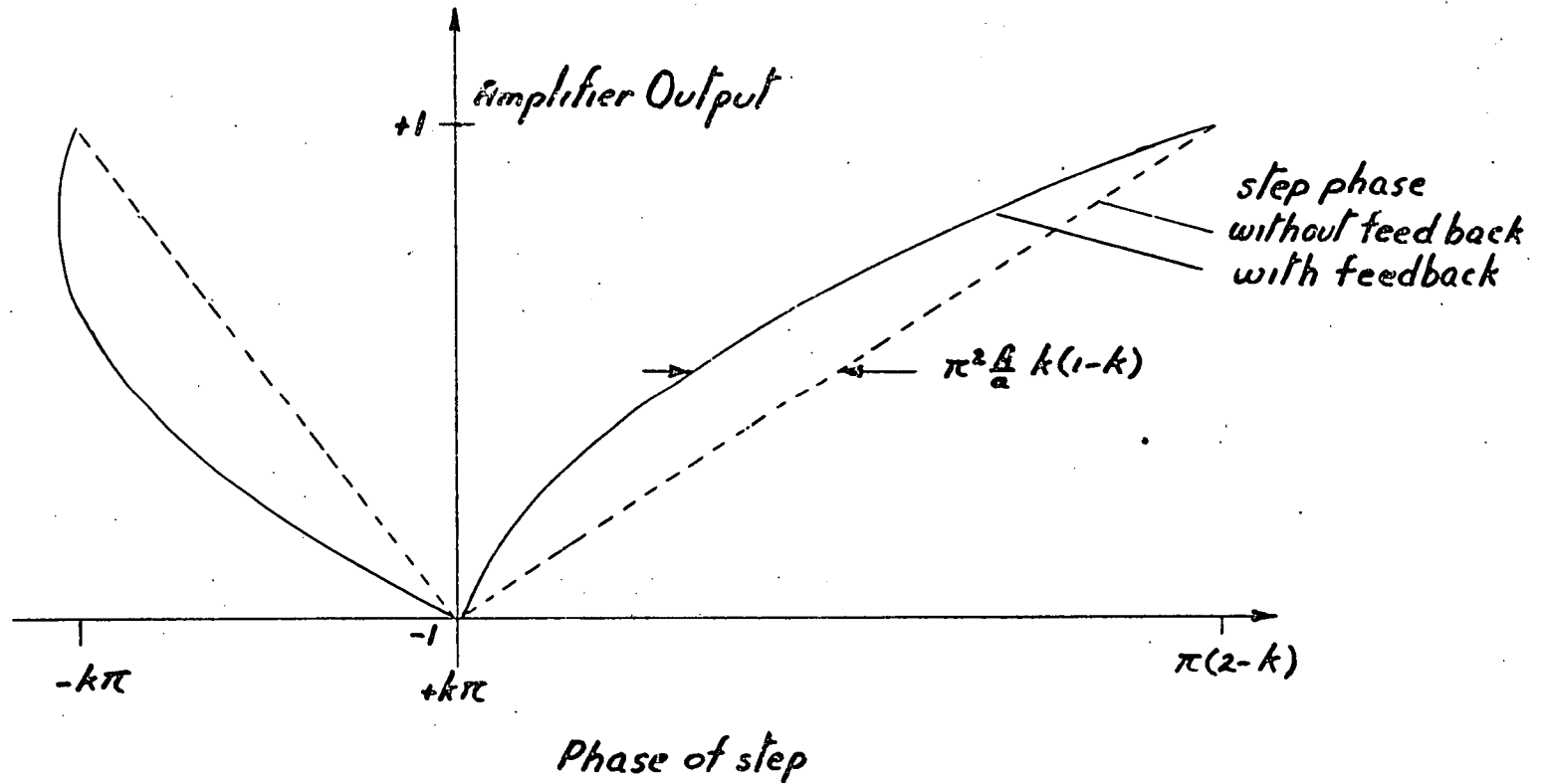
There are two kinds of limit on the amplifier output range, which may be predicted from the model, but beyond which the output may go by a change in the mode of operation of the sampling unit. The computational model cannot describe operation beyond these limits because of the change in operation.

The first limit is indicated by diagram D 5.1.2.3c. The predicted incremental gain of the amplifier becomes infinite then changes sign as the output component nears maximum or minimum values. A real amplifier cannot have such a characteristic. The physical cause of this characteristic is easily appreciated. The loop gain becomes high enough for the ripple waveform to have the same slope as the sampling wave, at the point where these intersect.

Phase of Switching Wave Steps

D.C. levelled wave, integrator feedback

D 5.1.3a



The second limit is based on the limits of the sampling wave amplitude. This limit places a restriction on the possible phases of the switching instants and is referred to as phase saturation hereafter. Figure D 5.1.3a shows the form of the phase at the switching instants according to the algebraic solution for the first example. The phase is expressed as a function of the output component of the switching wave, DC. The expressions describing the solutions are restated below.

$$\Theta_n = -k\pi(DC + \pi(A/a)(1-k)(1-DC^2)).$$

$$\Theta_p = \pi + \pi(1-k)(DC - \pi(A/a)k(1-DC^2))$$

Phase saturation occurs when $\Theta_n = -k\pi$ or $\Theta_p = k\pi$. The range of output for which phase saturation does not occur DC_R , is described by the inequality

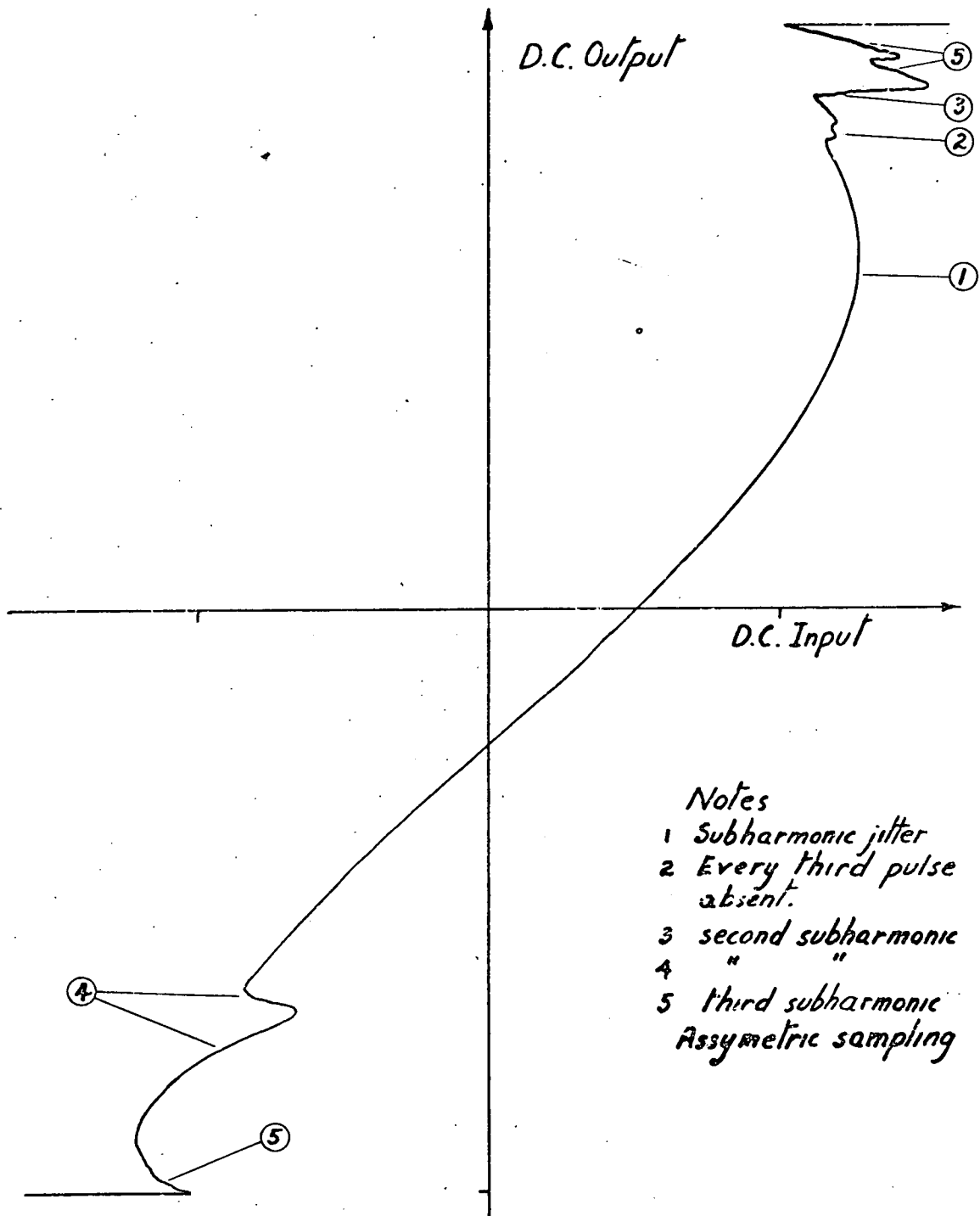
$$1 - \left(\frac{a}{\pi A k}\right) < DC_R < \left(\frac{a}{\pi A (1-k)}\right) - 1$$

For this range to completely enclose the normal output range of plus and minus unity the following restriction must be enforced.

$$a/A \geq 2\pi \cdot \begin{cases} 1-k & \text{if } 1-k > k \\ k & \text{otherwise} \end{cases}$$

Since A/a is the loop gain at the sampling frequency the restriction implies that this loop gain must be less than $1/\pi$ for phase saturation to be absent for all values of k .

The input of a switching amplifier may be of sufficient magnitude for phase saturation to occur without there being a dramatic change in the d.c. characteristics of the amplifier. What happens is as



Input-Output for Amplifier in Feedback Loop

D5-1-3b

follows.

The ripple magnitude is large enough for the d.c. input with ripple wave superimposed to miss one or more peaks of the sampling wave. The resulting switching wave has a frequency which is a subharmonic of the sampling frequency. The ripple waveshape changes and a new stable configuration is achieved. Usually the subharmonic number increases as the input signal nears the limit required to saturate the output. In some instances a jitter between two subharmonic waves or a subharmonic and normal wave may occur. Diagram D 5.1.3b illustrates the form of the d.c. characteristic of a switching amplifier under these circumstances.

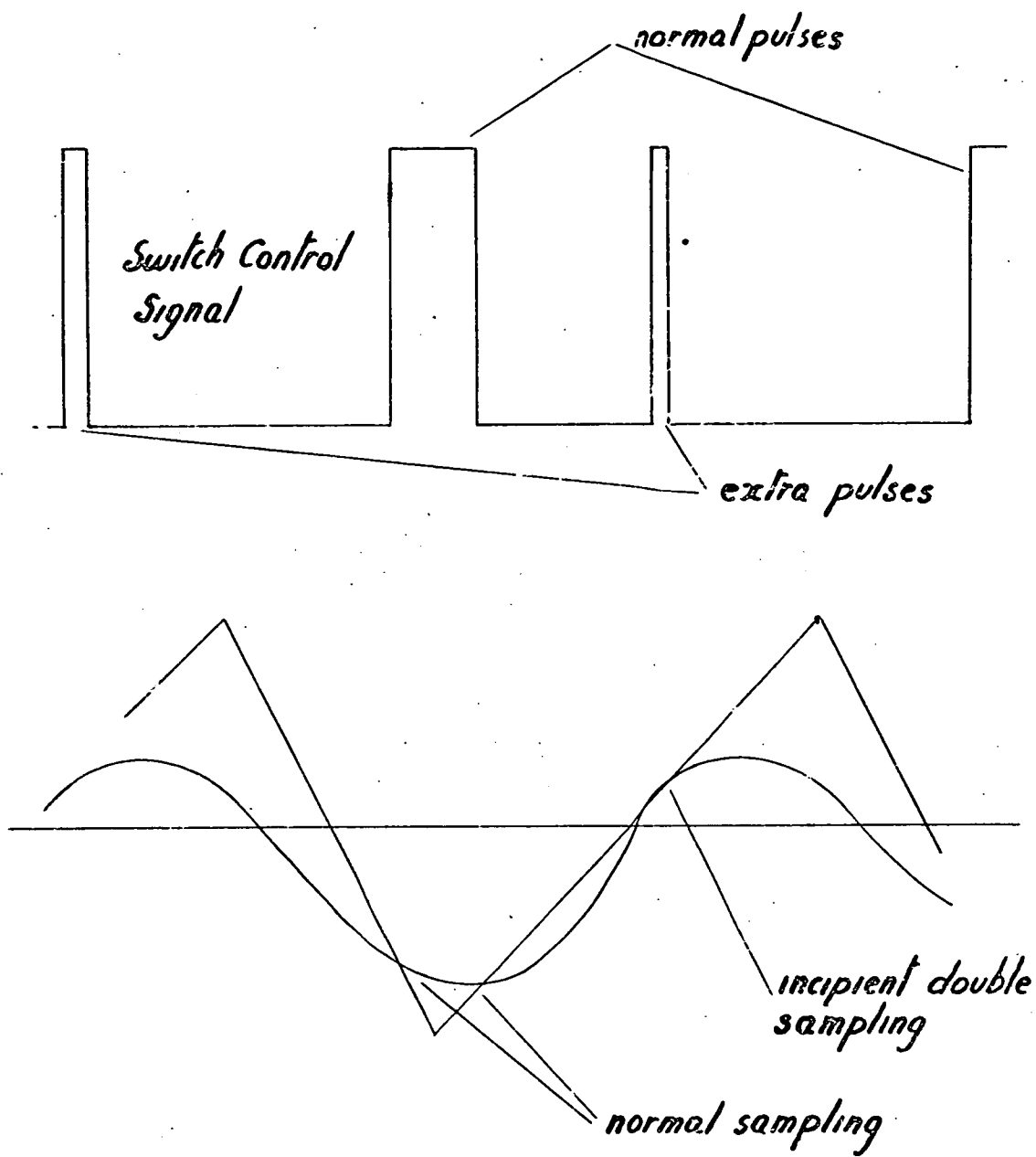
5.1.4 Double Sampling, Multiple Sampling

There is one other limitation to the use of the model for a switching amplifier within a feedback loop. There is a probability of the ripple cutting the sampling wave more than once every sampling interval. No attempt has been made to predict this behaviour. The following observations have been made with respect to d.c. levelled switching waves.

(i) Second and higher order feedback filters were used. The ripple waveshape thus changes slope smoothly and reaches a peak value well after sampling first occurs.

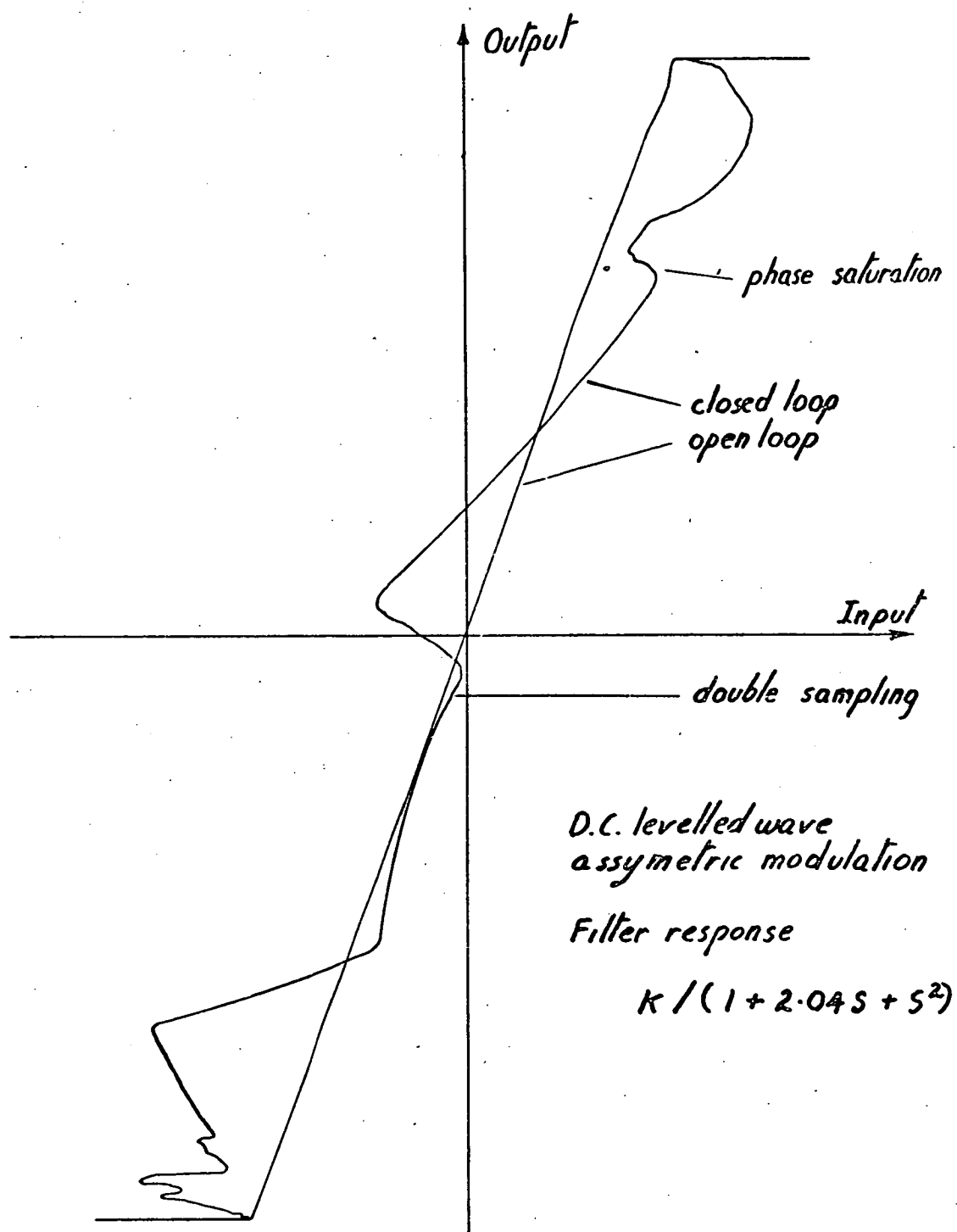
(ii) The loop gains were higher than those required to appreciably limit the output range due to phase saturation but phase saturation did not occur in the range of output over which multiple sampling was observed.

(iii) The number of intersections of the sampling wave with the ripple wave over one sampling interval increased with the increase in loop gain. This causes



Ripple and Sampling Waves of Double Sampling

D5.1.46



A D.C. Input-Output Characteristic

D 5.1.4 a

the effective switching frequency to increase with loop gain.

Diagram D 5.1.4b shows the form of ripple involved in double sampling while diagram D 5.1.4a shows the effect of this on the d.c. characteristic of a switching amplifier. The first diagram indicates a necessary but not sufficient condition for double sampling to occur; the ripple waveform must have greater slope than the sampling wave.

Natural sampling with multiple sampling due to ripple feedback gives an amplifier with d.c. characteristic closer to the open loop characteristic than the normal feedback characteristic with feedback. The nonlinearity is reduced over that range of output where multiple sampling occurs. The effect is not desirable however since switches may be operating at maximum rates consistent with some efficiency or power dissipation rating and the extra dissipation caused by doubling the sampling rate will double the switching loss. For thyristor amplifiers the situation is different. If forced commutation is employed the situation may be very undesirable and extra logic may be necessary to suppress the spurious pulses if it cannot be avoided in other ways.

5.2 a.c. Control Signal Performance

The model just discussed is 'exact' for d.c. control signals, approximate for low frequency signals, and inadequate for high frequency control signals. The presence of a.c. signal components invalidates the assumption that the switching wave consists of components with frequencies at the harmonics of the sampling frequency. An a.c. control signal causes the harmonics

of the d.c. case to divide into carrier and sideband components, the latter with frequencies separated from the harmonic frequencies by multiples of the control signal frequency. The assumption is made when the ripple output from the filter is calculated. The difference in filter response at sideband and harmonic frequencies is the limitation on the accuracy of the model.

This description appears to offer a means to overcome the disability of the model. "Why not calculate the sideband amplitudes and their individual contributions to the ripple waveform in the same way as harmonic components?", the reader may ask. This apparently simple extension of the model to the general a.c. situation is not as simple as it sounds. The object of the ripple calculation is to find the relative phase of the sampling signal and the switching wave steps, thus, the phase of the switching wave is a function of ripple at the sampling instants. Unfortunately the distribution of energy amongst the sidebands is also a function of the phase at the switching instants. This does not prevent a solution but greatly complicates the issue since some form of iterative search technique must be employed to calculate the effective ripple waveform. This has not been attempted.

5.2.1 Aspects of a.c. Models

The a.c. characteristic may be very difficult to calculate but several aspects may be described in outline. First, the feedback ripple will have two parts, the modulated part due to the sidebands and the unmodulated part due to the residual components at harmonic frequencies. The former will influence the a.c. gain the latter the d.c. gain. Second, these two components

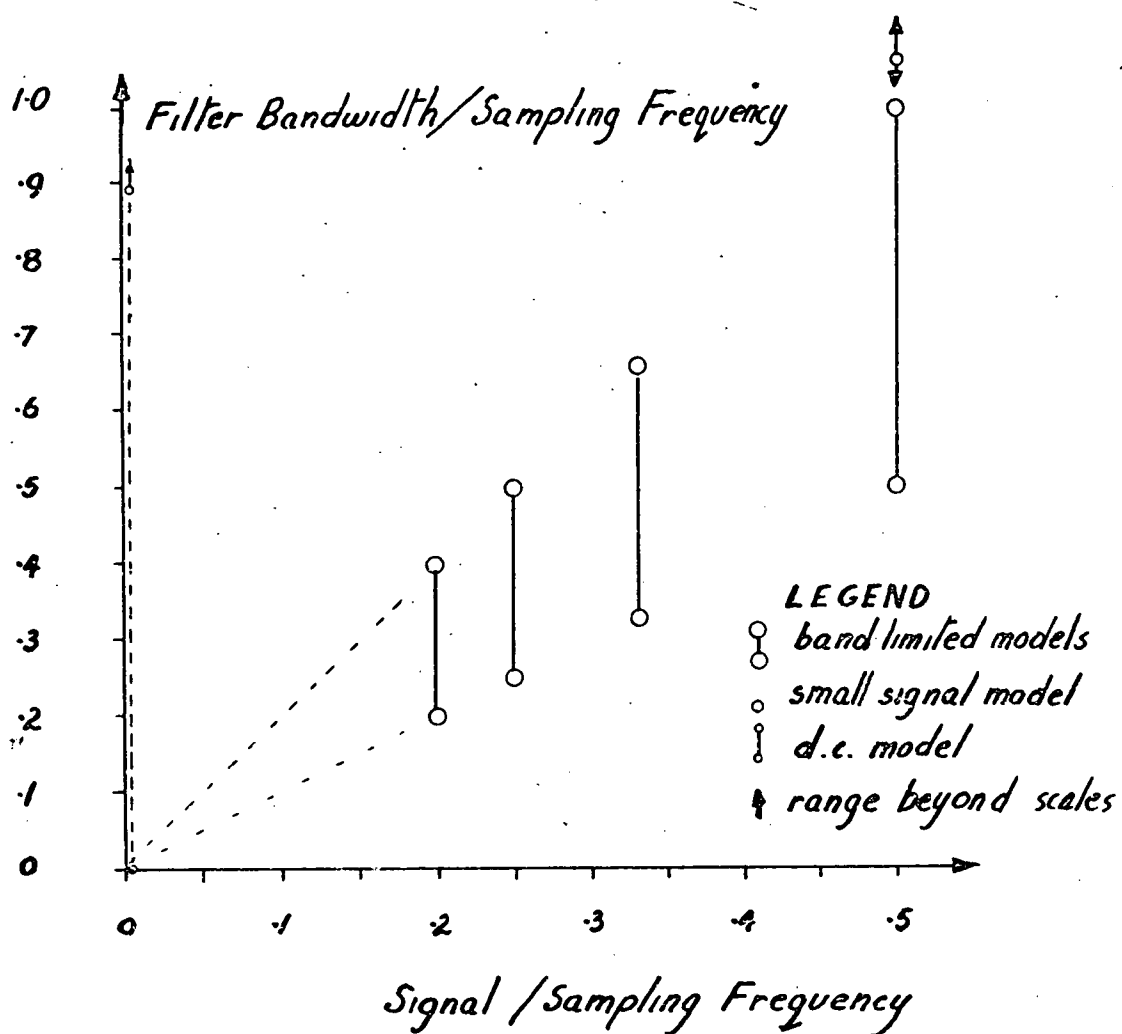
are not independent of one another since changes in either d.c. or a.c. signal components will cause a redistribution of energy amongst the harmonics and sidebands.

5.2.1.1 Narrowband Feedback

An example of the interdependence of and difference between a.c. and d.c. characteristics is provided by the situation where a very sharp cut off filter in the feedback path allows only three sidebands of each harmonic within the passband. If the control signal is a subharmonic of the sampling signal then two of these sidebands have the same frequency as the control signal while the third has zero frequency. The amplifier gain under these circumstances may be evaluated exactly using the techniques outlined in chapter IV. The examples of subharmonic gain loci described there are functions of the relative phase of the sampling and control signals of the switching amplifier. For a given phase value conventional feedback theory may be used to calculate the stability and closed loop response of the system.

The d.c. characteristic with no a.c. signal is linear since harmonic ripple is excluded by the narrow band filter. The open loop amplifier has a nonlinear component due to the zero frequency sideband. Normally this sideband increases with the a.c. signal amplitude. If assymetric sampling is employed then the sideband is also a function of the d.c. component and of the relative phase of the sampling and control signals. The presence of the feedback path makes no difference to these properties of the switching amplifier but does produce a reduction in the system nonlinearity as predicted by conventional feedback theory.

The same rules apply to the situation where control signal is not a subharmonic of the sampling wave. Those sidebands within the passband are reduced at the amplifier output as though they resulted from conventional nonlinearity of the amplifier.



Models of Switching Amplifiers with Feedback

5.3 Summary

Diagram D 5.3 illustrates the parameters associated with the models just discussed. The model for d.c. input-output characteristics is indicated by the dotted vertical line on the left. The bandlimited feedback, subharmonic models are indicated by the fan of solid vertical lines terminated in circles. The small signal second subharmonic model of Fallside and Farmer² is indicated by the small circle with double arrows.

The describing function models, used by Fallside and Farmer and by Furmage³, correspond to the bandlimited feedback, subharmonic models since these are based on the assumption that other feedback signals are negligible. The small signal second subharmonic model of Fallside and Farmer does appear to consider other feedback signals but their effects on the d.c. input-output characteristic are not mentioned.

The diagram has large areas where no exact models are known. At the present time designers assume amplifier behaviour for circumstances near a particular model is near the behaviour of the modelled amplifier. This is particularly true of the subharmonic models based on describing functions where experimental results appear to confirm the assumption. Similar assumptions appear reasonable for the d.c. model.

For small a.c. signal components the energy of the sidebands is small and the ripple is not appreciably changed nor is the d.c. characteristic of the amplifier. For large a.c. signals residual harmonics may be much lower than for small signals and the linearity of the d.c. characteristic correspondingly improved. For small a.c. signal frequencies the a.c. and d.c. characteristics are very similar. For large a.c. signal frequencies the amplifier produces sidebands in the pass-band which may be regarded as spurious inputs rather than

modulation of the ripple. If the feedback loop has a high negative gain then these sidebands are suppressed.

References

R. E. Andeen "Analysis of Pulse Duration Sampled Data Systems with Linear Elements"

I.R.E. Trans on Aut. Control September 1960

F. Fallside, A. R. Farmer "Ripple Instability in Closed Loop Control Systems"

Proc. IEE Vol. 114 March 1967 PP 139-152

S. G. Furmage "Subharmonic Instability in Closed Loop Control Systems with Pulse Width Modulation"

Honours Thesis in Electrical Engineering, Uni. Tasmania
March 1969

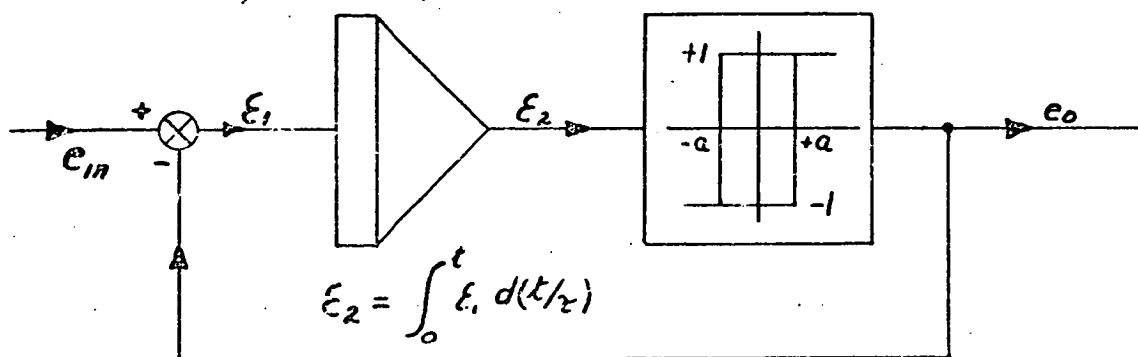
CHAPTER VI : SELF OSCILLATING ENCODERS

- 6.0 System operation
- 6.1 Operation of the constant area sampler
 - 6.1.1 D.c. performance
 - 6.1.2 A.c. performance
 - 6.1.2.1 Oscillation frequency
 - 6.1.2.2 Harmonic distortion
 - 6.1.2.3 Sidebands
 - 6.1.2.4 Subharmonic patterns
 - 6.1.2.5 Phase locking
 - 6.1.2.6 Frequency response
- 6.2 Matching theory and observation
- 6.3 Other self oscillating encoders

CHAPTER VISELF OSCILLATING ENCODERS

The self oscillating encoders discussed in this chapter have the general structure outlined in figure D 6.3. These encoders have been investigated by many independent researchers with the consequence that even the simplest example, one employing an integrator and a schmitt trigger, is known by many names. This encoder is known variously as: a constant area sampler, a rectangular wave modulator, an asynchronous sigma delta modulator, and a pulse ratio modulator.

The first part of this chapter describes the operation of the constant area sampler and indicates those features which can be demonstrated experimentally. The second part indicates those experimentally known characteristics which can be predicted theoretically. The third part of the chapter describes a method for evaluating the d.c. input-output characteristic for all the encoders with the general structure indicated by figure D 6.3. The method itself and the worked examples are described in appendix A 6.3. The limited experimental verification forms appendix E 5.



The Constant Area Sampler

D 6

6.0 Operation of the Constant Area Sampler

This switching amplifier has the block diagram shown in figure D 6. The signal levels described there are normalised with respect to the output voltage levels. The total switching wave energy is independent of the modulation and has a constant value of unity. Note that the device with hysteresis could be normalised also by changing the integrator gain.

The system will oscillate provided the input voltage is less than the maximum and greater than the minimum values of the output voltage. Operation may be visualised over one switching cycle by the following sequence of events. Initially, suppose the output has just switched to plus unity. The integrator output is equal to $+a$. The integrator input is $e_{in} - 1$. The integrator output will move towards $-a$ at a rate dependent on $e_{in} - 1$. When the integrator output reaches $-a$ the output switches to $+1$ and a new error signal is formed. $e_{in} + 1$ is greater than zero and the integrator output slews towards $+a$. The cycle is complete when the integrator output reaches $+a$.

The difference between the integral of input and output after such a cycle is zero. This means the averages of input signal and output signal are equal over any output cycle. It is this property of system which makes it of interest as a switching amplifier.

The name "Constant Area Sampler" is associated with the cycle of oscillation. Each half cycle is complete when the integral of the error signal has the value $\pm 2aT$. Thus each half cycle of error has the same area on a voltage time curve.

6.1 Experimental Measurements

In the absence of a detailed theory of performance or any detailed description of performance of this system the following facets were measured experimentally*. Some of these observations may be matched with theory, others suggest theoretical models.

6.1.1 d.c. Performance

d.c. gain is unity for any signal between maximum and minimum output. Beyond this range the system saturates.

The cycle frequency is a parabolic function of d.c. output component, DC, with maximum at DC=0 and zero's when $|DC|=1$. The cycle frequency w_s is given by the expression

$$w_s/w_o = 1-DC^2, \text{ where } w_o = 2\pi/(4a\tau).$$

6.1.2 a.c. Performance

6.1.2.1 Oscillator Frequency

For small d.c. offsets the mean oscillator frequency for sinewave control signals of amplitude A is described by

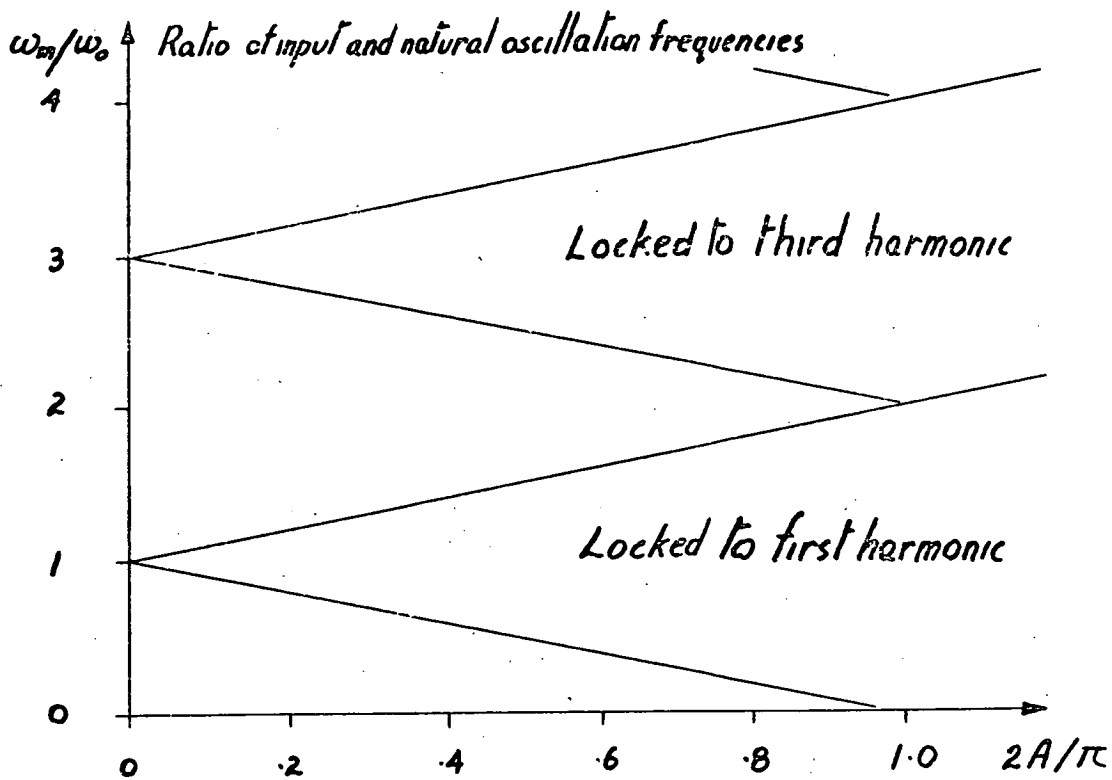
$$w_s/w_s = 1-A^2/2-DC^2, \text{ for } w_{in} \leq w_s/10.$$

The expression appears approximate for large values of A or DC. The error in w_s/w_o is about +2% for A=DC=0.5. The expression is exact for DC=0 or A=0.

6.1.2.2 Harmonic Distortion

Any harmonic distortion is less than -60 db of the signal and intermodulation distortion is less than -80 db of the signal provided the maximum signal amplitude is less than saturation and the highest frequency of the control signal components is less than $w_s/5$. The maximum a.c. signal amplitude for negligible

* See appendix E 5.



$(2/\pi) \cdot (\text{Ratio of peak input signal to maximum output } (+1))$

Conditions For Phase Lock

D 6.1.2.5

distortion falls with frequency above this value.

6.1.2.3 Sidebands

There are sidebands centered on the average cycle frequency and separated from this by multiples of the control frequency. For no d.c. input the sidebands of the first harmonic are even. With d.c. input both even and odd sidebands are present in the passband.

6.1.2.4 Subharmonic Patterns

For large a.c. signals with frequencies of the order of $w_s/4$ or greater stationary switching waves synchronised with the input signal may occur at frequencies which are integer ratio fractions of w_s .

6.1.2.5 Phase Locking

The system will phase lock to the input signal if this has sufficient magnitude. Phase lock to the first harmonic occurs when the input frequency, w_{in} , and sinewave amplitude, A , satisfy the inequality

$$|w_{in}/w_o - 1| < \frac{2A}{\pi}.$$

The phase lock conditions for first and higher harmonics are indicated by the shaded areas of diagram D 6.1.2.5.

6.1.2.6 Frequency Response

For frequencies below $w_s/5$ the gain appears to be unity. No phase shift was detected. Above this frequency low amplitude signals with no d.c. offset appear to have unity gain but high amplitude signals have gains which fluctuate in the vicinity of the subharmonic frequencies. All amplitude signals cause phase lock when their frequency is large enough. Phase capture appears to have little or no effect upon the gain until it occurs though the gain may show some fluctuation since these measurements were not accurate near the phase lock situation.

6.2 Matching Theory and Observation

The frequency of oscillation as a function of a d.c. signal is derived and the extension to a.c. signals discussed in appendix A 6.2a. The only assumption required for the extension to the a.c. formula for oscillation frequency is that the input frequency is low.

The phase locking properties of the system are described in detail in appendix A 6.2b. Although phase lock with sinewaves was investigated experimentally the theory indicates phase lock may occur for a wide variety of signal waveshapes. Stability and phase variation with frequency of the locked signal relative to the input signal are discussed.

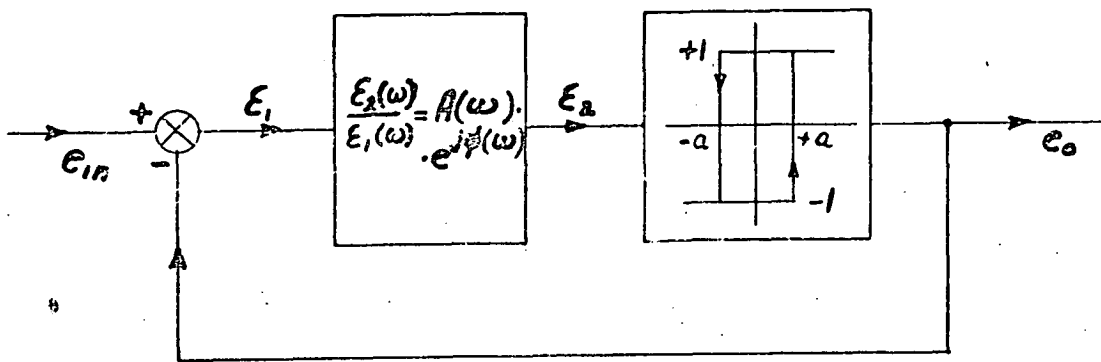
The most important feature of the system as a switching amplifier is the passband noise due to the sidebands. Experimental measurements measured only the first, second, third and fourth sidebands of the first harmonic. Other sidebands are less than -60 db of the maximum output signal.

The experimental results suggest the switching wave has a form given by the expression

$$E = f(t) + \sum_{n=1}^{\infty} \frac{4}{n\pi} \sin\left(\frac{n\pi}{2}(f(t)+1)\right) \sin(n\omega_0(1-f(t)^2)).$$

The observed sidebands were compatible with this expression though only their frequency and presence or absence was noted. No detailed measurement of amplitudes was attempted.

The expression above is similar in many respects to that for the symmetrical modulation of a fixed frequency wave by natural sampling. The sidebands when $f(t)$ is a sinewave of small amplitude would be almost



A More General Self Oscillator - Sampler

D6.3

identical since the $f(t)^2$ component is small. For larger signal amplitudes the sidebands due to this component would extend the energy bandwidth causing larger sidebands within the passband than for natural sampling.

Conclusions

This modulator is relatively simple compared to the natural sampler. It has the obvious disadvantage of a variable period of the switching wave. Since the frequency of the wave falls to zero at maximum output there is a restriction of its use for audio amplifiers where the presence in the passband of large amounts of noise is intolerable. For small output signals its performance is comparable with the best two level wave produced by natural sampling.

6.3 Other Self-Oscillating Switch Controllers

The constant area sampler is one example of a class of self oscillating switch controllers. These controllers use a linear low pass filter rather than an integrater and may use a comparator rather than a device with separation between sensitive levels. Such coders have predictable d.c. input-output relationships but are very difficult to analyse to estimate their a.c. characteristics.

The d.c. input-output characteristic, and the relationship between oscillation frequency and d.c. output level may be obtained using the theory outlined in appendix A 6.3. This theory is exact but may be complicated to use accurately. This is conveniently mechanised by computer program in a similar way to the analysis of the d.c. characteristics of natural samplers in the presence of feedback paths. The theory is very similar.

Two examples of the application of this theory are given in appendix A 6.3b. These examples are integrator feedback and high Q filter feedback. The first is of course a constant area sampler analysis but differs so strongly from the earlier analysis that the result is quite striking. It is probably the only filter for which exact mathematical analysis is possible. The second example is based on the assumption of a filter characteristic which restricts the oscillation frequency to a single value. The resultant input-output characteristic is very nonlinear.

The theory indicates several strong relationships between filter characteristics and the d.c. characteristics. First, the input-output characteristic is exactly linear if the filter response gives an odd multiple of 90° phase shift at the oscillation frequency and each of its harmonics. Second, when the first conditions is not satisfied the linearity may be improved by having a high loop gain at d.c. compared to that at the frequency of oscillation. Third, the output nonlinearity is of the odd symmetric type while the variation of oscillation frequency is of the even symmetric type when both are considered as functions of the output or control signal level.

The strong similarity of these results to those for the natural sampler with feedback is not accidental but a consequence of the similarity in physical structure. The major distinction is simply the lack of a sampling signal.

This model has not been confirmed experimentally beyond the excellent agreement it yields with the simple cases outlined as examples. As such it must be treated as a plausible but unverified model for the d.c. characteristics of this class of self oscillating switch controllers.

References

- A. G. Bose "A Two State Modulation System"
Electrotechnology Vol. 74 No. 2 August 1964 PP 42-47
- J. Das, P. D. Sharma "Rectangular Wave Modulation - A
P.L.M.-FM System"
Electronic Letters Vol. 2 No. 1 January 1966 PP 7-9
- K. C. Johnson "Pulse Modulated Audio Frequency Amplifiers"
Wireless World Vol. 69 No. 3 March 1963 PP 135-136
- G. F. Turnbull, J. M. Townsend "A feedback Pulse Width
Modulated Audio Amp."
Wireless World Vol. 71 No. 4 April 1965 PP 160-168
- Yuan Yu, T. G. Wilson, Et Al "Static DC to Sinusoid AC
Inverter...."
IEEE Trans Mag.3 No. 3 September 1967
PP 250-256

CHAPTER VII : ENERGY FLOW PATH IDEALS STRUCTURES & LIMITS

- 7.1 Nondissipative energy transfer
 - 7.1.1 Filter elements
 - 7.1.2 Current and voltage analogues
 - 7.1.3 Reversible power flow
 - 7.1.4 Supply filtering
 - 7.1.5 The equivalent circuit
 - 7.1.6 Circulation of supply energy
 - Summary of ideals
 - Other features described
- 7.2 Switch array and circuit forms
 - 7.2.1 A classification of switches
 - 7.2.2 Combined elements as switches
 - 7.2.3 Minimum switch requirements of common circuits
 - 7.2.3.1 Natural voltage steps
 - 7.2.3.2 D.c. supplied arrays
 - 7.2.3.3 A.c. supplied arrays
 - Summary
 - 7.2.4 Pairing complementary unidirectional amplifiers
 - 7.2.5 Combinations of switching amplifiers
- 7.3 Switch and filter performance
 - 7.3.1 Filter losses
 - Inductor size transferred power and efficiency
 - 7.3.2 Measures of switch performance
 - 7.3.2.1 Power control capacity
 - 7.3.2.2 Static loss indices
 - 7.3.2.3 Dynamic losses
 - 7.3.2.4 Switch and amplifier ratings for simple arrays
 - 7.3.3 Modifications for the equivalent circuit
- 7.4 Summary

Chapter VII

Energy Flow Path Ideals, Structures, and Limits

Whereas previous chapters have dealt with the information flow through switching amplifiers this chapter examines the ideals associated with the flow of energy from sources to load. In making this examination some of the fundamental aspects of the structures necessary to achieve this task are considered. Ways and means of synthesising these structures from existing circuit elements are discussed. In the course of this discussion the factors defining the boundaries of feasible structures and limits of performance are introduced.

7.1 Non-Dissipative Energy Transfer

Efficient operation of a switching amplifier requires more than the generation of a switching wave. It requires efficient filtering of the switching wave, that is, efficient, effective filters are required. The basic premise of a switching amplifier is that the switching wave may be separated into two components by the output filter and that the undesirable components are not dissipated but rejected while the desired output component is passed freely to the load. There are consequently two aspects to filter performance. First, how well does it separate the desired output from the switching waves? And Second, how great are the losses in the filter? In the following discussion a miscellaneous collection of factors influencing the filter design are introduced and briefly discussed.

7.1.1 Filter Elements

Some switching wave components must be rejected without dissipation by the filter. There are only two ways to achieve this. The impedance of the filter input at the frequencies of these components must appear to be either reactive or else an extreme impedance. For the first case the voltage and current are orthogonal in phase, for the second one or other is infinitesimal so that in both cases no power is dissipated. These restrictions on the filter impedance are achieved only if the filter contains only inductors and capacitors or has such a topology that all resistive components appear as extremes of impedance at the input terminals.

Topology

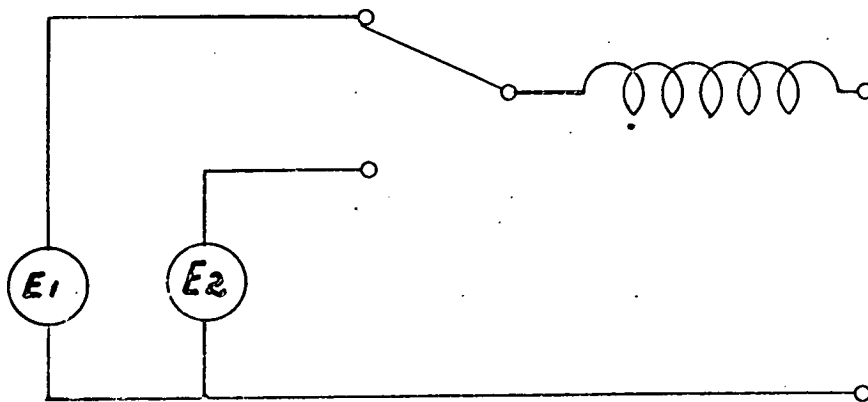
There are two types of storage element for electrical energy. Voltage sources and capacitors are examples of one type, current sources and inductors of the other type. To control by switches an efficient transfer of energy from one storage element to another it is necessary that they be of opposite types. In addition to this obvious requirement the switch array must satisfy several other requirements in order to prevent impulsive dissipation from the energy sources. First, capacitors and voltage sources must not be short circuited and second, inductors and current generators must never be open circuited.

Consider the implications of these restrictions for the switching amplifier shown in diagram D 7.1.1. They tell us that the inductive input element of the output filter is necessary since the switches generate a wave from voltage sources. Similarly the switch structure must appear like a **single pole two position** switch so that voltages are not shorted to one another and so that the inductor always has a current path between its ends.

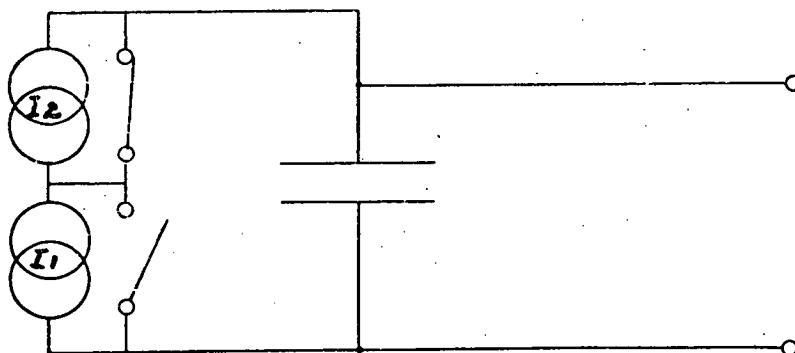
The basic point is simply that a switching wave is formed at a node between storage elements of opposite types.

7.1.2 Current and Voltage Analogues

Switching amplifiers may have energy sources which are voltage or current sources. Voltage supplied amplifiers are discussed in the text as though current supplied amplifiers were non-existent. This is not so. The circuit of the current analogue of any voltage supplied amplifier may be constructed by a simple extension



D 7-1-1



D 7-1-2

of the standard method illustrated by diagram D 7.1.2. The switches of the switch array must be redrawn so that each switch is replaced by a switch and so that open circuits become short circuits and vice versa.

Notice that the filter input element becomes a capacitor and that the new switch array differs considerably from the old.

One interesting point is the number of switches in the arrays of each type of system. Both systems have the same number even though the current sources must be short circuited while not applied to the filter input. The switches are in parallel for the voltage case but in series for the current case. For ideal switches this is not important but real switches have resistance so that a voltage driven system has a lower array resistance than a current driven system if more than two supplies are used. A system with n current sources has $n-1$ switches in the filter current path, a voltage source system has one.*

7.1.3 Reversible Power Flow

The switch array controls the mean voltage (or mean current) supplied to the filter input. The amplifier load determines the mean current at the filter input. The current polarity depends only on the load. The power flow through the filter and array has a direction determined by the current flow. Provided a switch array has bidirectional switches and the energy sources are capable of bidirectional current flow a switching amplifier is a reversible device.

There is a contrast here with conventional amplifiers which dissipate energy when supplying a reactive load. The switching amplifier is able to recover

*For switch leakages a complementary situation applies.

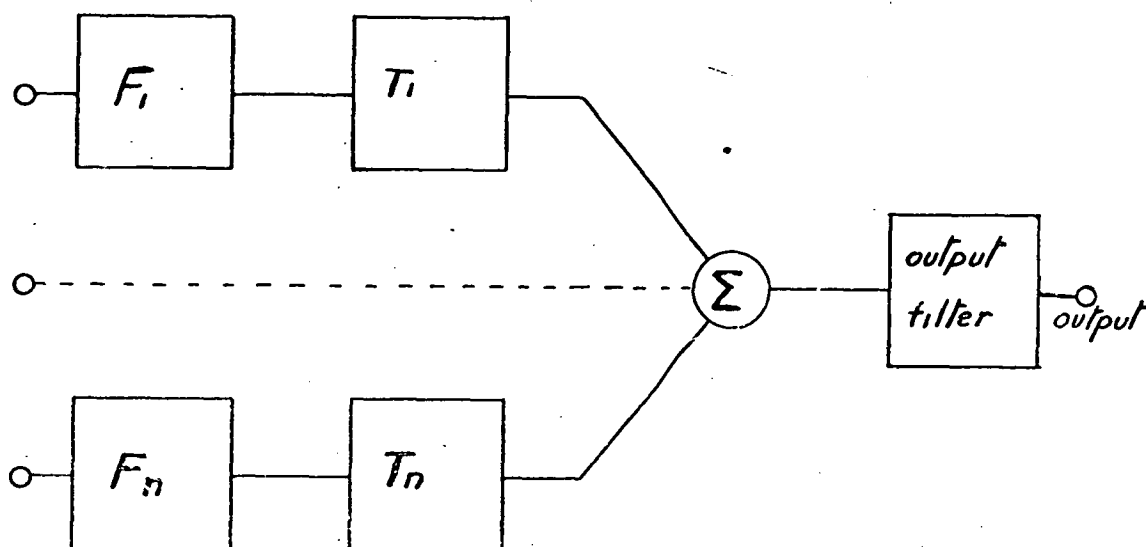
the stored energy of the load so that the net energy transferred over a cycle of output is zero.

It is worth mentioning here that an efficient switching amplifier must have bidirectional switches since the filter is in effect a reactive load to the switch array. The current and voltage of the filter input at a frequency in the stop band will be in quadrature so that energy flows into the filter for half the cycle and is returned to the source during the other half of the cycle.

7.1.4 Supply Filtering

The switch array produces a switching wave with either voltage or current levels. This wave is applied to a filter which reflects the load and causes a current or voltage to appear at the terminals. The switch array allocates this current or voltage to each supply for some interval of time each period. This means that each supply has a load dependent switching wave applied to it by the switch array. In order to provide the necessary current or voltage the supplies must appear to be ideal at high frequencies. This is not normally the case for practical power supplies and extra filtering is required, capacitors are placed across voltage sources and inductors in series with current sources.

Supply filters are often necessary for another reason. The switching amplifier may be situated at a considerable distance from the source of energy with some form of supply line connecting the two. Any switching wave on this supply line can cause radio frequency interference. Supply filtering can eliminate or greatly reduce such undesirable features of switching amplifiers.



Notes

F_i : The filter associated with the i^{th} supply input.

T_i : The transformer associated with the i^{th} supply input. Each of the n transformers has a turns ratio set by the input signal, e_{in} , of the amplifier.

The Low Frequency Equivalent Circuit

D 7.1.5

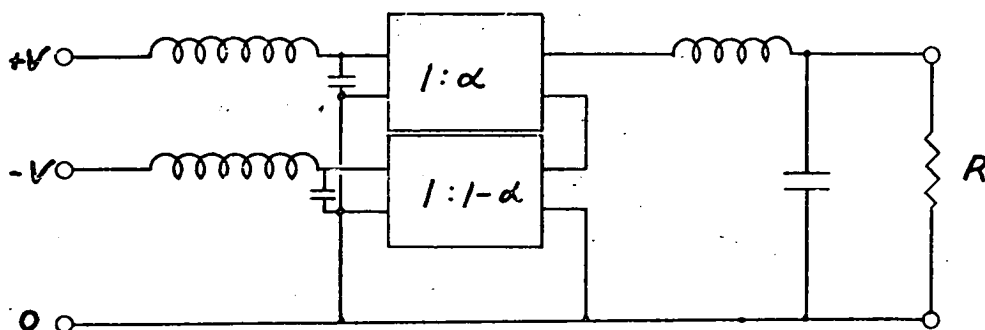
7.1.5 The Equivalent Circuit

Ideally the supply and output filters of a switching amplifier remove all switching wave components other than the supply and load waveforms associated with the control signal. If the residual components of the switching waves are ignored then it is possible to draw an equivalent circuit of a switching amplifier. A general equivalent circuit is described by diagram D 7.1.5.

The supply and output filters are identical to those actually used. The switch array is replaced by an array of ideal transformers in the case of a d.c. supplied amplifier. The a.c. supplied amplifier has the switch array replaced by a frequency converter and an ideal transformer so that supply energy and output energy balance for each supply arm of the circuit. The turns ratios of the ideal transformers are determined by the control signal of the amplifier, that is they vary with the amplifier input signal.

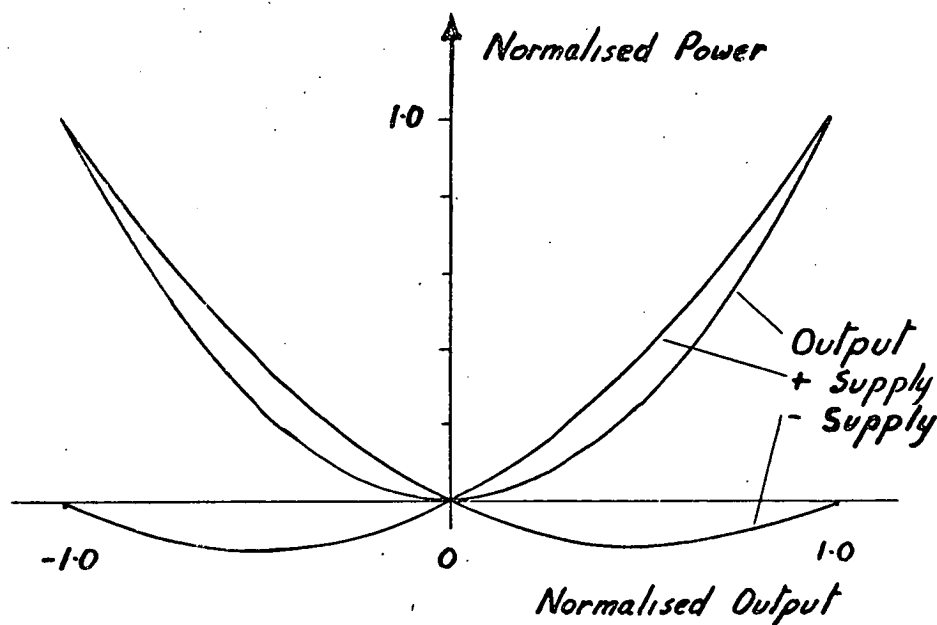
The line diagram does not show all aspects of the equivalent circuit. In particular the summation point is not detailed. For an amplifier applying a voltage wave to the filter the transformer voltages are summed by the placing them in series, the current analogue places the transformer outputs in parallel. The summation thus results in either the current or voltage respectively, at these transformer outputs being common to all the outputs.

One interesting feature of the equivalent circuit is the output impedance. It is easily shown that this is a nonlinear function of the output signal due to the variation of the transformer ratios and hence



Two Level Amplifier with Symmetrical D.C. Supplies

D 7.1.6 a



Output And Supply Power ~ D.C. Output

D 7.1.6 b

the reflected supply impedances with the output signal. This source of amplifier nonlinearity is not obvious without the use of the equivalent circuit.

7.1.6 Circulation of Supply Energy

The equivalent circuit enables one important feature of a switching amplifier to be seen. This is the circulation of energy during a switching cycle. The circulation is not that associated with switching ripple but that associated with the control signal and load conditions. To introduce the discussion consider the simple amplifier with two d.c. supplies for which an equivalent circuit is shown in diagram D 7.1.6a.

The switch array restrictions require that the transformer ratios are as shown. The control signal determines the parameter α . The output voltage V_o is given by

$$V_o = (2\alpha - 1)V.$$

The powers supplied by the positive and negative load, P_+ and P_- respectively, and the power dissipated in the load resistor, P_L , are described by the equations

$$P_+ = \alpha(2\alpha - 1) V^2/R,$$

$$P_- = (2\alpha - 1)(\alpha - 1) V^2/R, \text{ and}$$

$$P_L = (4\alpha^2 - 4\alpha + 1).$$

These powers are displayed in a normalised form in diagram D 7.1.6b, as functions of the output signal.

One feature is of interest. This is the negative power flow through one supply or the other at all output levels except maximum, minimum, and zero. At the other levels energy from one supply passes into the load

filter during part of a switching cycle and is transferred to the other supply during the remainder of the cycle.

This behaviour is due to the common current in the two transformers of the equivalent circuit, this load determined current flows against the voltage of the smaller contributor to the output and thus transfers energy to the associated supply.

Similar behaviour occurs for all switching amplifiers except those using symmetrical switch modulation with a.c. supplies so that all supplies contribute equally to the load at all output levels. For such amplifiers there is a power flow reversal in the supplies for outputs other than maximum or minimum but the reversal is not associated with negative power flow over the whole of a switch closure but with a phase shift between voltage and current waveforms which causes reversal of power flow during each switch closure.

The essential feature is that all switching amplifiers have a movement of energy from source or sources to the output filter during part of the cycle then from the filter to the sources during another part of the cycle. At the same time the output filter may be transferring energy to or from the load.

Summary of Ideals

The important points of the discussion of lossless energy transfer are restated below.

Filter elements are inductors or capacitors so that the filter impedance in the stop band is reactive not resistive.

The switch array and power supplies must be capable of bidirectional power flow since efficient filters imply this phenomena must occur.

Supply sources must appear to have ideal source impedances at high frequencies, so that supply filters are often necessary, since switching waves of a load dependent nature are present on supply lines.

Other Features Described

Any voltage supplied switching amplifier has an analogue with current supplies. This analogue has the same number of switches, supplies, and filter elements.

Switching amplifiers are inherently reversible. The terminals normally regarded as the supply inputs and those regarded as the output terminals may have their roles changed if the control signal generates a switching wave which produces less output than that applied at the load terminals. No net energy is transferred into a reactive load by a cycle of output signal nor is there a net loss from the supplies.

In the case of supplies with a d.c. component which differs between supplies power may be circulated between supplies for some output signal levels.

There is an equivalent circuit for any switching amplifier which satisfies the above ideals.

The equivalent circuit contains inductors, capacitors, ideal transformers and lossless frequency converters. The ideal transformers have turns ratios set by the control signal which by this means controls the amplifier output signal.

Description	Examples of Device Described
CC	short circuit
II	open circuit
CI	diode
AI	transistor in series with diode, valve
AA	transistor, Fet, ideal switch
AC	transistor in parallel with diode
AcI	thyristor, thyatron
AcAc	triac

Table D 7.2.1

Switch Classification of some Devices and Combinations of Devices.

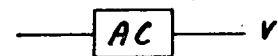
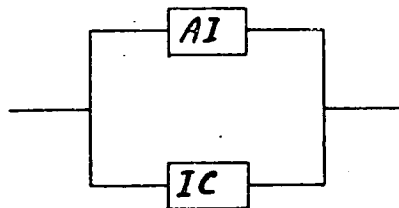
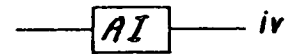
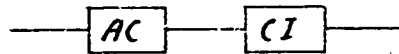
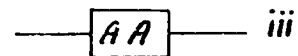
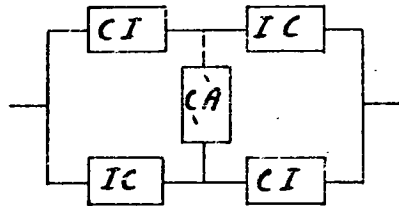
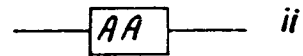
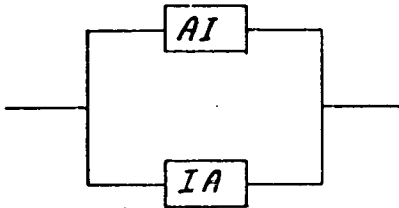
7.2.1 A Classification for Switches

Both the types of switch required by an amplifier and the type of device available may be described by the voltage current relationship of the device. Switches have characteristics which lie in the first and third quadrants of this relationship. An ideal switch has two possible states in each of these quadrants, states corresponding to conduction and insulation. A device may not have or need this ideal characteristic and some means for describing the possible quadrant behaviour is needed. Three symbols are adequate to indicate the gross characteristics, those used here are A, C, and I. An active device which may have either a conducting or an insulating characteristic within a quadrant is described in that quadrant by A, C, and I describe quadrants with conducting and insulating characteristics respectively. The complete specification of a switch is the two symbols describing the two quadrants.

For example a device which conducts in the first quadrant but insulates in the third, the common diode is described by CI. Table D 7.2.1 lists the switch classifications of some common devices and combinations of devices.

Note the use of the suffix, c, to denote an active switch which may be turned on by the control signal but must be commutated to turn off again.

The devices listed in table D 7.2.1 do not have ideal characteristics since all have finite on state voltage drop and finite off state leakage currents. The conduction characteristics of diodes, triacs, and thyristors are non linear, while those of transistors



Compound and Simple switch Equivalents

D7.2.2

and F.E.T.S. are usually linear over the saturation resistance range. The conduction characteristics of valves and vacuum diodes vary widely but high power devices have approximately constant saturation resistance. Thyratrons have a large voltage drop but low dynamic resistance. The off state leakage is not usually important for any of these devices unless germanium semi-conductor devices are used.

Transistors, the devices most commonly used as switches are shown by table D 7.2.1 to be bidirectional. They are not a practical form of bidirectional switch however unless they have symmetrical base-emitter and base-collector junctions. This is seldom the case. Usually the reverse base-emitter breakdown voltage is much smaller than the breakdown voltage of the other junction and the current gains of the device are different. This poses a problem, how may unidirectional active devices such as the transistor be used to provide the switches required of a switch array? One answer would appear to be the combination of the available devices to provide a bidirectional device.

7.2.2 Combined Elements as Switches

The common active and passive devices may be combined with one another to produce other switch types. Diagram D 7.2.2 lists some examples. The convention adopted in these examples to define the quadrant orientation is as follows.

The symbol nearest a terminal of a device describes the behaviour of the quadrant of the voltage current characteristic of the device for which a positive current flows into the terminal. Thus the diode of the fourth example allows current to flow through the diode

from left to right but the current cannot flow in the reverse direction.

Examples (i) and (ii) are ways for combining two unidirectional active devices to achieve a bidirectional switch. The first is suited to transistor type characteristics, the second to valve like characteristics. Example (iii) indicates how a single active device may be used to control both directions of conduction to give a symmetrical switch characteristic. The remaining examples are transformations of one type of unidirectional device to the other type.

Although the combinations outlined are often usefull most suffer from one or both of two basic defects. These are complexity of control circuit and accumulation of parasitics. Consider these aspects of example (iii), a diode bridge about a single active device.

The control signal of most active devices is applied to a terminal of the device and a control terminal. For this example the control voltage must be floating with respect to the terminals of the compounded switch since each end of the active device has either the maximum or minimum of the voltages across the compounded switch. Examples (i) and (ii) have similar control problems.

The off state leakage current of example (iii) is the sum of the leakages of two reverse biased diodes and the active device. The on state voltage drop is the sum of the drops for two forward biased diodes and the active device. The terminal capacitance of the compound switch in the off state is the sum of that for two diodes and the active device.

The increase in parasitics of a switch formed of component devices, by some or all the parasitics of the individual devices used, is encountered with all combinations of devices. The important strategy is to choose those combinations which increase the least important of the parasitics. Thus devices suited to combination by the circuit of example (i) should have low voltage drops while low leakage currents and terminal capacities should be features of devices arranged as in example (ii). The arrangement of elements in circuit (iii) is not good from the point of view of parasitics but is probably one of the easiest combined circuits to control since only one active device is involved.

7.2.3 Minimum Switch Requirements of Common Circuits

Since the synthesis of bidirectional switches from unidirectional elements is not always desirable it is important to produce and use switches with the minimum facilities required by a given circuit or system. It may, for instance, be desirable to produce two unidirectional amplifiers with complementary current characteristics and parallel these to attain a bidirectional amplifier rather than produce a single amplifier with bidirectional switches. In order to make a decision as to the relative advantages and disadvantages of such a choice it is necessary to have a clear idea of the minimum switch requirements of the circuits considered. This section outlines the minimum requirements and other information necessary for such a comparison.

7.2.3.1 Natural Voltage Steps

A natural voltage step is said to occur when the voltage at a switch node is determined by the current into the node due to the connections at the node with all switches in a non-conducting state. The most common example of such a natural step occurs when an active device is switched off while an appreciable current is flowing into an inductive filter. The natural transient so caused results in a voltage across the inductor which causes current reduction in the inductor.

The clamped sinusoidal transient formed in this way does not cause energy dissipation in the switches unless these breakdown due to the high voltage attained as the inductor energy is transferred to the stray node capacitance, or, they have appreciable leakage currents. The transient may be clamped to any voltage along its initial path by a diode which is reverse biased at the instant the active switch is turned off. The initial slope of the transient is proportional to the initial current so that the time interval between switch off of the active device and capture by a clamping diode is inversely proportional to the initial current.

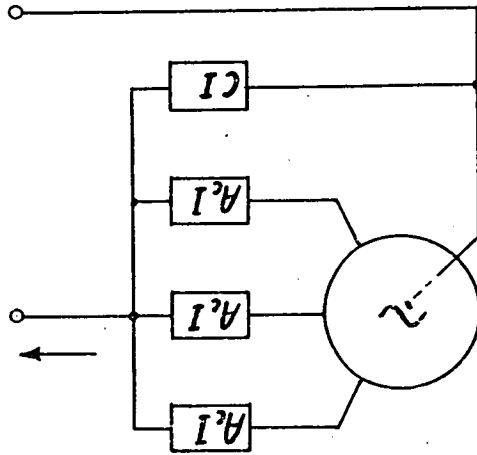
7.2.3.2 d.c. Supplied Arrays

An array with d.c. supplies and unidirectional output current may have natural voltage steps for all steps of one polarity. Forced steps are required for voltage changes of the polarity which increase output current. Forced steps may be applied in the other direction too but since the change in stray capacitance energy is dissipated in the switch this is not particularly desirable. The minimum switch requirements of a unidirectional output current array using natural voltage

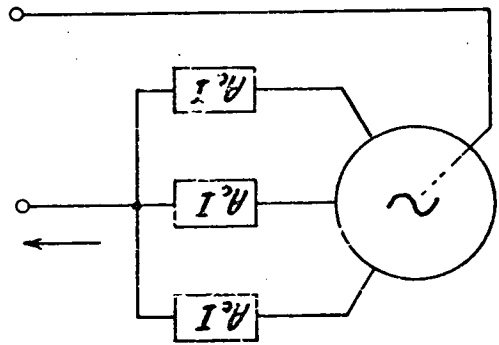
Supply And Switch Arrangements

D 7-2-3

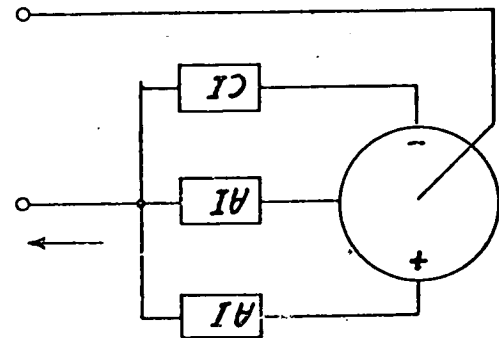
v



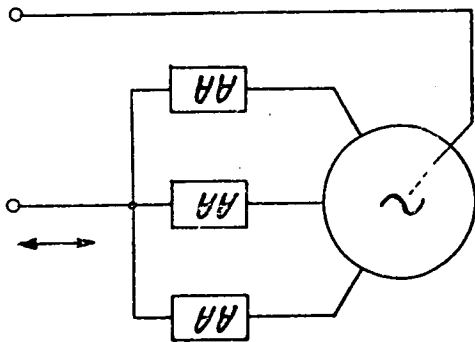
!!!



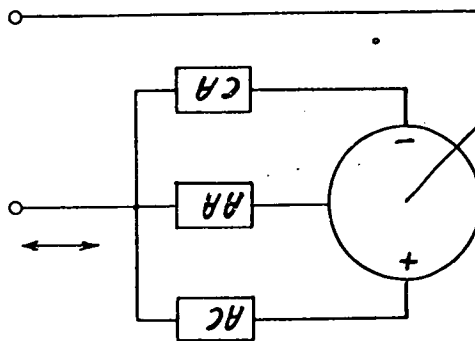
!



iv



!!



steps for one step direction are shown in circuit (i) of diagram D 7.2.3. The insulating part of the highest switch is not required. The middle switch may in fact be many switches connecting many levels or may be absent completely. The lowest switch is a diode.

An array with d.c. supplies and a bidirectional output current has the switch arrangement of circuit (ii). If the output current is of suitable sign and magnitude then natural steps may be used but since it may have either sign and may be very small, forced steps are necessary in some circumstances. Notice that the switch requirements are equivalent to paralleled pairs of the switches of circuit (i) and its current complement.

A two supply array, with unidirectional output current, has a number of simplifying features if natural commutation is employed. These are associated with the need for only one active device. Only one control signal is needed and there is no danger of supply short circuits due to overlap of switch conduction times at switch state transitions. The two level array using forced commutation steps, whether providing unidirectional or bidirectional output current, requires protection against overlap of switch conduction times. This may be attained by modification of control signals for the switches or by inter switch impedances which limit currents during such overlap. In either case circuit complexity is increased.

7.2.3.3 a.c. Supplied Arrays

For unidirectional output current circuits similar to example (iii) of diagram D 7.2.3 may be used. The control signals must be arranged so that the switch turning on forces the output current to flow through it rather than the previously active switch. For the example this means that all node voltage steps are positive, that is are forced. Despite the restriction on voltage step polarity the output voltage range is as great as that for the bidirectional output current circuit shown as example (iv).

The diode clamped circuit shown as example (v) is subject to the positive voltage step restriction also but has only half the output range as the other circuit. This disadvantage is balance to some extent by the noise properties of the modulation form which may be used.

Both these circuits may also use switches which turn on at zero voltage but may be turned off at any current. The associated waveforms are reversed in time order to those discussed above but are otherwise identical. No switch commonly available has this characteristic which is the inverse of that for a thyristor.

The bidirectional array has similar problems to those of the d.c. supplied array with forced voltage steps in that high switch and supply currents during overlap of switch conduction times must be avoided. The problem is more intractable however since natural voltage steps must be avoided due to the lack of suitable voltage sources for use as clamping levels for the node voltage. As a result switch conduction times must be

overlapped and inter-switch currents limited by impedances. This solution is unsatisfactory for most purposes.

Summary

The brief discussion indicates switches of arrays with unidirectional output current are better matched to available device characteristics and are easier to control than their counterparts in arrays with bidirectional output current.

7.2.4 Pairing Complementary Unidirectional Amplifiers

An amplifier with bidirectional output current may be formed by paralleling the outputs of two amplifiers with complementary unidirectional output current capabilities. This technique requires some control circuitry to maintain non zero output currents in each amplifier, duplication of switch control circuitry and some parts of the output filter, and symmetrical designs. This added complexity must be balanced against the difficulty of controlling bidirectional switches in a single array.

Each amplifier of the pair requires a non zero output current for all values of composite amplifier output voltage and current. The simplest, and least satisfactory, way to achieve this is to bias each amplifier to give a circulating current of half the maximum load current at zero output voltage and current for the composite amplifier. As the composite amplifier output current nears maximum the current in the subunit providing the opposite polarity current falls to zero. The disadvantages of this technique are obvious. Even for low outputs the array elements are carrying high currents. These currents waste power on the switch elements and filter and cause a circulation of energy through the amplifier energy sources.

An untried solution to this problem may be to monitor the output currents of the two sub units, select the lowest of these two signals, compare this minimum with a reference level for circulating current, and use the resulting error signal as a differential input to the two sub-amplifiers. Diagram D 7.2.4 illustrates the form of control circuit envisaged. The currents may be monitored by current transformers placed in the individual arrays in series with a switch. These could also be used to monitor maximum current levels and so control overload or protection circuits. Notice that although the two amplifier outputs vary with the output current level, their mean value is constant so the output voltage is constant even while the bias current loop signals are moving towards equilibrium conditions.

7.2.5 Combinations of Switching Amplifiers

An amplifier produced by paralleling two sub-amplifiers is one example of a combination of switching amplifiers. In addition to specific advantages such as achieving bidirection output current capability with unidirectional sub-amplifiers there are a number of advantages associated with the possible forms of the effective switching wave. These are discussed below. The major disadvantage, apart from multiplicity of hardware, is the need to control output current distribution among the individual sub-amplifiers when these are connected in parallel. A fixed bias arrangement is feasible where output impedance is not too low and bidirectional sub-amplifiers are used. For other situations feedback control methods, similar to those outlined for the unidirectional situation, appear suitable.

The phrase, effective switching wave, used

above is intended to describe a switching wave which when filtered produces an output equivalent to that of the combined amplifier. For paralleled sub-amplifiers the effective wave is the average of the individual switching waves. For series connected amplifiers the effective wave is the sum of the individual waves. It follows from this that many complex switching waves with a wide variety of properties may be produced. Several of these will now be discussed.

The waveforms of diagram D 7.2.5a are those for d.c. levelled waves of the type produced by amplifiers with both unidirectional and bidirectional output current capability. The earlier discussions of waveforms of this type were concerned with the passband noise under various modulation conditions. It was shown that multi-level waveforms have appreciably lower passband noise than their component waveforms. For the unidirectional amplifier combination the use of phased switching waves reduces passband noise below that for an equivalent bidirectional amplifier realised with the same number of switches and supplies.

Sub-amplifiers with unidirectional output current and a.c. waveform levels have waveforms of the type shown in diagram D 7.2.5b. Notice that the voltage wave of the negative current sub-amplifier is the reflection of that for the positive current sub-amplifier. The effective switching wave has double edged modulation and a zero level. The resultant wave has many desirable properties including zero output ripple at zero output but does not have harmonic cancellation as the previous example has though harmonic amplitudes are reduced. The difference in sideband energy is similar, for small

outputs, to that between single and double edged modulation of d.c. levelled waves.

Amplifiers employing many sub-amplifiers should combine these with phased addition of waves so that maximum reduction in harmonic amplitudes is achieved. The case for unidirectional a.c. supplied sub-amplifiers referred to above is exceptional in that the direction of steps must be opposite for the two sub-amplifiers due to the method of current transfer between switches of the simplest type available. Switches which may be turned off can be used in such amplifiers to produce waves which may be summed to give harmonic cancellation.

7.3 Switch and Filter Performance

7.3.1 Real Filters - Their Losses

Real filters do not have lossless elements, nor do they reject all switching wave components. As a consequence the ideal model is not achieved. The relationships between filter losses and other parameters are discussed here.

An inductor in the filter of a switching amplifier has three distinct types of loss. First, signal frequencies and d.c. components are attenuated by the winding resistance of the inductors. Second, the filter characteristic is not an ideal low pass one so that the load impedance and winding impedances of the inductors are reflected in the high frequency input admittance. The switching wave will dissipate some energy on this reflected resistance. Third, the material of the magnetic circuit is not ideal and losses associated with the flux density and volume of the magnetic circuit occur for the high frequency components of the switching wave.

The first two losses may be analysed for a given filter and switching wave. For common designs the

first loss is dominant. This may best be illustrated by an example.

A second order filter with damping of 0.6, corner frequency w_c , and having low attenuation for d.c. signals is used to filter the output of a switching wave described by

$$ES = DC + \sum_{n=1}^{\infty} \frac{4}{n\pi} \sin(n\pi/2(DC+1)) \cos nw_s t.$$

The real part of the filter input admittance at the frequency of the n^{th} harmonic may be calculated from the approximate expression derived in appendix A 7.3.1a, and the expression for the total losses for the harmonics formed. The expression is

$$ELA = (1/R)(R_i/R) \cdot (11.5/\pi^2) (w_c/w_s)^2 \sum_{n=1}^{\infty} \sin(n\pi/2(DC+1))/n^4,$$

provided $4w_c < w_s$.

The loss due to the inductor winding resistance, R_i , attenuating the d.c. component is

$$ELS = DC^2 R_i / (R + R_i)^2 \approx (DC^2 / R) \cdot (R_i / R) \text{ for } R_i / R \ll 1.$$

The maximum output signal power is for $DC = 1$ and is $1/R$. The expressions show two things about the relative values of the maxima of these two losses as functions of DC . First, the ratio of the maxima of the two approximate expressions is approximately

$$RL \approx 1.2 (w_c/w_s)^2.$$

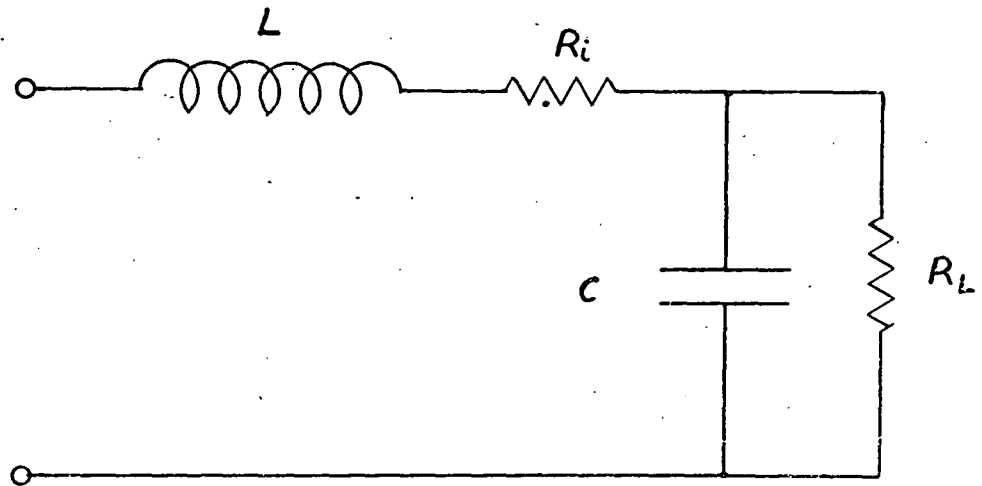
A typical filter may have $w_c/w_s \approx 0.2$. For this value signal loss is nearly twenty times the loss due to the

reflection of inductor loss to the input of the filter. Second, since both losses are proportional to R_i/R , the ratio of inductor to load resistances, a filter efficient for d.c. signals will be efficient at high frequencies also.

The expression for the relative losses maxima ratio is of similar form for higher order filters. The expressions differ slightly since the dominant high frequency loss is incurred in the input inductor while all the inductors contribute to the d.c. signal loss. The third type of loss, that due to magnetic path losses, is not so amenable for comparison since it depends on the core material and the flux density. Usually core materials are chosen so that this loss is small though even this policy is ill defined since the flux has a large signal component with a small superimposed a.c. component. The large signal component may cause the losses due to the a.c. component to fluctuate strongly especially if saturation flux density is approached. Saturation of the inductor material is usually avoided since this not only increases filter losses but may cause nonlinear signal transfer for a.c. signals with frequencies near the corner frequency of the filter.

Real Filters - Inductor Size, Transferred Power, and Efficiency

An efficient inductor stores most of its energy in an air gap and uses the magnetic circuit to provide a flux path from one side of the air gap to the other. The volume of magnetic material required is thus minimised and the flux dependent losses reduced in proportion. Such an inductor has a maximum flux density in the core material **set** by saturation or high frequency



$$R_i = R_L [1 - \eta] / \eta$$

$$L = R_L [1/\sqrt{2} + \sqrt{\eta - 1/2}] / (\eta \cdot \omega_c)$$

$$C = [R_L \omega_c [1/\sqrt{2} + \sqrt{\eta - 1/2}]]^{-1}$$

Normalised Second Order Butterworth Filter

D 7.3.1

loses. For a given set of inductor proportions, defining the shape of the magnetic circuit and the windings, and for a given conductor resistivity there is a relationship between maximum stored energy, E , the inductor time constant, τ , the maximum flux density, B , and a dimension of the inductor, D , such as the length or breadth. The relationship is independent of the length of the air gap provided the geometry of the flux path is not significantly altered. The expression is derived in appendix A 7.3.1.b and restated below.

$$E \cdot \tau = K(B)^2 D^5, \text{ where } K \text{ is dependent on resistivity of the winding and inductor proportions.}$$

For a given filter response the product of E_{\max} and τ may be related to the load power, P , the d.c. filter efficiency, η , and the filter bandwidth, w_c . This may be illustrated by an example.

Diagram D 7.3.1 shows a second order Butterworth filter with each element described in terms of the load impedance R_L , the d.c. efficiency, and the corner frequency w_c .

The inductor energy stored is

$$E = 1/2 \cdot LI^2 = PL(1/\sqrt{2} + \sqrt{\eta - 1/2})/(2\eta w_c), \text{ where}$$

P_L is the output power. The time constant of the inductor is

$$\tau = L/R_i = (1/\sqrt{2} + \sqrt{\eta - 1/2})/(1 - \eta)w_c.$$

The energy, time constant product is thus

$$E\tau = P_L (1/\sqrt{2+\sqrt{\eta-1/2}})^2 / (2w_c^2 \eta(1-\eta))$$

$$\approx P_L / ((1-\eta)w_c^2) \quad \text{for } \eta \approx 1, \text{ that is for high}$$

efficiency filters.

Similar expressions may be derived for any filter configuration with a definite frequency response. The general form of such expressions is

$$E\tau \propto P_L / ((1-\eta)w_c^2) .$$

By combining the two expressions so that $E\tau$ is eliminated the relationship between the inductor dimensions, flux density, and operating frequency and the circuit behaviour as defined by the d.c. efficiency and power transfer through the filter, may be obtained. The relationship is

$$P_L \propto (1-\eta)w_c^2 (\beta)^2 D^5 .$$

The relationship suggests that the power transferred by a given size inductor will diminish as efficiency is increased so that power transferred is proportional to, power lost per unit power transferred.

The power transferred for a given efficiency, frequency, and flux density is proportion to the fifth power of the dimensions of the inductor, that is almost the square of the mass.

If efficiency and size are adjusted while holding the other parameters fixed then a small increase in size reduces the losses appreciably.

The power transfer increases rapidly with frequency and flux density but these parameters have a very significant influence on the high frequency losses which may increase even more rapidly than a square law. The increase in dimensions is also accompanied by an increase in flux dependent losses since these are proportional to volume of magnetic material. This means there exists a trade-off between d.c. and high frequency efficiency when inductor dimensions are considered. Note that for a given flux density, frequency, and d.c. efficiency the high frequency efficiency increases with the dimensions and power level since the volume increases more slowly than the power transferred, D^3 compared to D^5 .

7.3.2 Measures of Switch Performance

Power Control Capacity

A switch can withstand a maximum off-state voltage of V and can carry a maximum on-state current of I . Such a switch when embedded in a circuit can change the flow of energy into any region of the circuit by at most $V \cdot I$. It is convenient to call this volt-amp. product the power rating of the switch.

Static Loss Indices

On state losses are due to the voltage drop across the switch. At maximum forward current the voltage drop on a switch is V_D . The conduction loss factor, F_c , is defined as

$$F_c = V_D / V.$$

This factor is the ratio, when the switch is on, of the power dissipated in the switch and the power rating of the switch.

Off-state losses are due to current leakage through the switch. At maximum applied voltage the leakage current is I_L . The off-state loss factor, F_o , is defined as

$$F_o = I_L / I.$$

This factor is the ratio, when the switch is off, of the power dissipated in the switch and the power rating of the switch.

Both these factors must be small for efficient switching amplifiers since the switches of an array vary their on and off times with the input signal of the amplifier.

Diagram D 7.3.2 shows conduction loss factor and switch power rating for a number of devices operating at maximum output power. These switch elements are selected from data handbooks* available to the author and may not represent the best available devices.

Transistors operating at maximum output power are operating at minimum efficiency since reduction in conduction current increases efficiency at the expense of output power. For a transistor operated at reduced power level the increase in efficiency may be visualised on the diagram by movement on a 45° line from the maximum power point towards the upper left hand corner of the diagram. For thyristors and diodes efficiency is only slightly improved by reduction in current levels since on-state voltage drop is almost independent of current.

The 20 kwatt switch power rating attained by several of the thyristor and diode devices far exceeds that attained by other devices but conduction to off-state voltage ratios of 1:500 limit the maximum conduction efficiency to less than 99.8%.

Several N.P.N. power transistors have switch power ratings of 5 kwatt at efficiencies near 99%. Derating these devices allows comparable efficiencies to those of thyristors at switch power levels near 1 kwatt.

P.N.P. power transistors are not as common nor as high power at comparable efficiencies; the best shown is almost an order of magnitude inferior in either power or efficiency than the best N.P.N. devices while more common devices are of lower quality still. Many N.P.N. devices have comparable efficiencies and power

* Semiconductor Data Handbook 1973, D.A.T.A. Inc.,
New Jersey.

ratings as the better P.N.P. devices.

For transistors and thyristors the power required to hold a device in the on-state is negligible compared to the conduction loss however if low efficiency drive circuits are used their dissipation can exceed that of the transistors or thyristors.

For vacuum tube devices cathode heaters have dissipations equal to or greater than conduction losses. Since this power loss is not included in diagram D 7.3.2 it is easily appreciated that these devices are not competitive with semiconductor devices of comparable ratings however some high voltage high frequency vacuum tubes have no semiconductor equivalents.

Off-state leakage losses of silicon semiconductor are usually lower than on-state losses with typical loss factors less than .002.

Dynamic Losses

Careful commutation of the switches in an array is an essential for high efficiency operation. For most applications requiring low frequency cycling of switch states transition state losses can be neglected when compared with static losses. In the search for higher power and wider bandwidth amplifiers however limits to the rate of switching and the power handling capability of switches are reached. These limits are briefly outlined here.

At the instant a switch changes state it dissipates energy due to a finite rate of change of its voltages and currents. This energy has a maximum value, assuming good commutation, given by the product of three quantities, the off-state voltage across the switch, the

on-state current through the switch, and the time taken for the transition between states. This maximum energy exceeds the dissipation of real switches by a factor of three or more but provides a useful upper bound for comparisons with observed losses.

Most high power thyristors have transition losses such that cyclic operation at full rated power cannot exceed 50Hz. Above this frequency operation at reduced power levels to cycle rates of 400Hz is often permitted. Some devices may be used at kHz rates provided they are suitably derated from their static capability.

Transistors change states at rates dependent on their drive waveforms. For optimum drive waveforms the transition energy is of the order of $0.5 VI/f_T$ where V and I are the voltage and current referred to above and f_T is the gain bandwidth product of the transistor. If the device, while at full rating, is cycled at a rate where the two transitions per cycle cause losses comparable with the conduction losses then the frequency of cycling, f , is related to f_T and the conduction loss factor F_c by the expression

$$f \approx f_T \cdot F_c, \text{ where it is assumed that}$$

the conduction time is the entire cycle length. Lower duty cycles increase this frequency accordingly.

For frequencies near or greater than this the transition losses require the switch rating to be reduced by an appropriate factor.

On this criteria derating of high power transistors, which have $f_T \approx 1\text{MHz}$, must begin at about

20khz while lower power devices with lower conduction losses but $f_T \approx 50\text{Mhz}$, can operate up to about 200khz without derating.

By derating high power transistors efficient medium power switching can be achieved but a second frequency limit is encountered. This occurs when transitions between states begin to overlap. Measurements by Chudabiak and Page indicate this limit occurs at about $0.1 f_T$ for transistors with dissipation less than 10 watt and $0.01 f_T$ for transistors of somewhat higher dissipation.

Switch and Amplifier Ratings for Simple Arrays.

The simple node of switches array imposes relationships between switch power and amplifier output power. During its on time the current through a switch is the sum of output and filter currents, during its off time the voltage across the switch is the difference between that of the source it connects to the node and the node voltage. This voltage has a maximum value which is simply related to the output voltage range of the amplifier. For d.c. arrays and bidirectional many phased a.c. arrays the output voltage range almost equals the maximum off-state voltage of an array switch. Thus the product of the amplifier output voltage range with the maximum output current is of the same order as the switch rating of the highest rated switches of the array.

This very simple relationship is typical of most effective arrays but is a first order approximation only since it makes no allowance for over voltages or currents, the duty cycles of on and off states, or the derating required by dynamic losses associated with commutation. The first two, and last factors can substantially increase the switch ratings required of an array switch, though some reduction is often possible if higher peak currents than the average maximum on current are possible on a pulse basis.

At any instant all the switches of an array, both those on and those off, contribute to the static array losses. For this reason the loss factor of an array is higher than that for any component switch. The effect of provisions for over voltage and current and dynamic losses also change the loss factor though some of these may cancel.

7.3.3 Modifications for the Equivalent Circuit

The voltage drop on conducting switches causes the output voltage of the equivalent circuit to deviate from that predicted by the ideal equivalent described in section 7.1.5. The problem of adapting the circuit described there to include this loss is discussed here.

While a switch is conducting the current flow is made up of two parts, the signal or output current and the filter current. The latter current is ignored for the signal equivalent circuit. The output current flow produces a voltage across the switch. This voltage must also be represented by a voltage across some device in the equivalent circuit. If every switch in the circuit is identical, as in a.c. supplied arrays controlled by phase modulation, then this presents no problem since one conducting switch placed in series with the output filter is exactly equivalent. If however the on characteristic of the switches are different then the equivalent signal impedance is related to the transformer ratios of the circuit but not in a manner suitable for representation as an impedance at the other side of the transformer. In this case the best approximation is an average switch characteristic.

The supply filters of section 7.1.4 have ideally zero high frequency resistance. In practice unfiltered and poorly filtered supplies may be used. The resistance of these supplies at high frequencies results in a voltage drop equivalent to that on the switches and may be transformed in a similar way as a resistance in series with the output of an ideal supply system and array.

7.4 Summary

Chapter 7 describes some aspects of the implementation of switching circuit hardware. The discussion is centered on the energy flow path from the energy source to the load as distinct from the information flow path from the input to the output. The work is concentrated on design philosophy rather than description of individual components. Various structures of switch arrays are briefly examined and their performance discussed.

The discussion starts with various methods of combining elements to form switching arrays and filters to couple the energy source to the load. Attention is drawn to the limitations associated with non-ideal components in the switch array and filter and with the use of non-ideal energy sources. These limitations effect the overall performance of the circuit and are shown to influence the trade-off between efficiency, power capacity, bandwidth, structural complexity, and filter mass.

Chapter VIII

A Perspective

- 8.1 The d.c. input-output characteristic of Natural Sampling
- 8.2 The a.c. input-output characteristic of Natural Sampling
- 8.3 The spectrum of waves controlled by Natural Sampling
- 8.4 Optimisation of sampling wave shape
- 8.5 The asynchronous Natural Sampler
- 8.6 Waves with many levels - Staggered phased addition
- 8.7 Waves with many levels - Quantizer method
- 8.8 Regular Sampling
- 8.9 Natural Sampling with feedback
- 8.10 Self Oscillating Encoders
- 8.11 Equivalent Circuits
- 8.12 Areas for further research

CHAPTER VIII.

The more significant aspects of the material presented in previous chapters are reviewed in this chapter in order to indicate those areas where significant advances have been made to switching amplifier design. In addition some areas are indicated which require further advances before design uncertainties can be removed. The sequence of topics is shown in the chapter subheadings listed on the opposite page.

8.1 The d.c. Input-Output Characteristic of Natural Sampling

The d.c. characteristics of all amplifiers employing natural sampling can be determined by a simple implication chain linking input signal level to the output signal level. The chain involves the phase of the encoder steps, the phase of switching wave steps, and the average of the switching wave passed by the output filter to the load. The chain can be used to numerically evaluate point by point the shape of the input-output characteristic. However it is more usual to regard the input signal as an algebraic variable, and to consider its transformation at each stage of the chain until the output signal is described as a function of the input signal.

This widely used method for determining the d.c. input-output characteristic is an accurate and convenient tool for the switching amplifier designer. By making allowances for non-ideal features such as voltage drops on switches and filters, it provides a precise method for analysing a design. Simple extensions of this method allow the sampling wave and supply waves to be recognised as distinct algebraic functions within the description of input-output characteristic. This extension enables the synthesis of the sampling wave shapes appropriate for a specific I/O characteristic.

Chapter 2 and Chapter 3 used this method to describe switching waves, however the treatment there considered the input signal as an arbitrary function of time. Here we are concerned with d.c. input signals.

In providing the most general possible description of the switching wave, the approach adopted has used a systematic method for subdividing the waveforms within the amplifier. This allows the component associated with each waveform level to be discussed in comparative isolation as its control waveforms are traced from the encoder to the switching wave. After forming descriptions for each component in isolation, these are combined to form the composite waveform description. This may then be examined to determine the potential range of sampling wave shapes which can yield a specified input-output characteristic.

The major distinction between the methods for determining the d.c. input-output characteristic described in this thesis, and those employed by others is the use of a single unified approach using a very general analysis.

8.2 The a.c. Input-Output Characteristic for Natural Sampling

While the analyses of natural sampling due to Bennet¹, Fitch², and Kretzmer³ indicate that the a.c. input-output characteristic of an amplifier employing a linearly controlled binary switching wave with d.c. levels is identical to the d.c. input-output characteristic, no analysis presented in the literatures provides equivalent evidence to show a more general result, namely that the d.c. and a.c. input-output characteristics are identical for any switching amplifier employing natural sampling.

In order to demonstrate this identity, the methods used by the authors above were modified to incorporate the shapes of the sampling waves and the resultant waveform descriptions used to describe switch control functions. This enabled the switching wave to be described using the approach outlined in chapter 2, section 2.4.

The resultant switching wave description, derived in chapter 3, sections 3.1, 3.2, and 3.3, and re-stated in chapter 4, section 4.1, does show the identity between a.c. and d.c. input-output characteristics. The experimental measurements outlined in appendix E1.1 and E1.2 provide confirmation of the analysis for several common amplifiers.

The identity is a very valuable tool to the designer of switching amplifiers, since it assures him that regardless of the manner in which he chooses his sampling and supply waveforms to achieve a specific d.c. input-output characteristic, and provided he uses natural sampling, then the input-output characteristic for a.c. control signals will also be defined and identical to the d.c. characteristic.

8.3 The Spectrum of Waves controlled by Natural Sampling

The description of a linearly controlled binary switching wave with d.c. levels was established by the works of Bennet¹, Fitch², and Kretzmer³, however the spectrum of this wave has been investigated for only one form of input signal, namely a sinewave or a pair of sinewaves. Although natural samplers are used with non-linear encoders, and encoders controlling a.c. levelled

waves, equivalent descriptions of these waves have not been formed and thus no spectral analyses exist apart from specific experimental measurements. Since such spectral analyses are necessary for a systematic appraisal of output filter requirements it is clear that their omission from the literature severely handicaps the designer.

As a first step to rectifying this situation experimental confirmation of the results of Bennet¹, Fitch², and Kretzmer³, was necessary. This work is part of that described in Appendix E, section E1.2. Success in this confirmation encouraged the development of waveform descriptions by the approach described in chapters 2 and 3 and also the development of spectral analyses of switching waves with steps position modulated by functions other than sinusoids.

The developments are used in chapter 4 to analyse the spectrum of many common switching waves. The objective of these analyses is to establish profiles for worst case passband noise contributed by sidebands as functions of amplifier bandwidth normalised with respect to the sampling rate. These functions enable a designer to conveniently establish the inter-relationship existing between the three design variables of output signal quality, amplifier bandwidth, and amplifier sampling rate for any of the common forms of switching wave.

8.4 Optimisation of Sampling Wave Shape

The published descriptions of the input-output characteristic design of amplifiers employing natural

sampling usually assume that the switching wave levels are invariant with time, that is they are either steady d.c. levels or periodic waveforms of fixed amplitude and shape. This is seldom so. Accordingly, one important aspect of encoder design is the realisation of sampling waves which are continuously modified in shape and amplitude to compensate for supply variations.

This aspect of sampling wave design is greatly facilitated by the algebraic definitions of the sampling wave shapes automatically obtained by the approach outlined in chapter 3, sections 3.1.2 and 3.1.3. In theory these algebraic descriptions of the sampling waves may be realised literally as functions of the supply waveforms so that changes in the supply wave-shapes are automatically compensated. In practice the direct realisation may not be realistic because of the complexity of the functions. Even so the ideals embodied within the functional descriptions make it possible to compensate for changes in supply amplitude and, in some cases, supply waveshape changes with very simple circuits.

8.5 The Asynchronous Natural Sampler

A conventional natural sampler assumes at the design stage that the supply waveforms are either invariant periodic functions of time or at least subject to only minor variations of the kind which can easily be compensated by encoder designs of the form just outlined. No natural sampler described in the literature is intended to control an array provided with arbitrary supply voltages.

It is shown in chapter 2, section 2.4 that there is no good reason why an encoder with the desired properties cannot exist provided the supplies can provide sufficient voltage. Furthermore an amplifier employing such an encoder is highly desirable. It would permit a sampling rate much higher in frequency than that employed by encoders using sampling waves synchronous with commercial a.c. supplies. This in turn allows a much wider amplifier bandwidth and a reduction in the size of the output filter. Unfortunately the normal natural sampler cannot be designed for this role since it will produce an output signal modulated by the supply variations unless the sampling rate is synchronous with the supply waveforms.

Section 3.1.4.1 of chapter 3 describes a form of natural sampler which uses three sources of information to control the operation of the encoder. It uses the input signal, the positive supply voltage and the negative supply voltage to continuously control the shape and zero value of the sampling wave, so that the waveform steps of the switching wave are moved to compensate for supply variations as well as to transmit the input signal to the amplifier switching wave.

The analysis of this encoder presented in appendix A3.1.4.1 defines the sampling wave shape as a simple function of the instantaneous supply voltages. The concept and the accuracy of predictions based on the analyses have been subjected to the experimental tests described in Appendix E3. These tests indicate the analysis to be valid for the limited range of conditions tested.

Section 3.1.4.1 of chapter 3 expands the application of the basic concept from a two to multiple supply situation and indicates some of the difficulties in the practical application of this modified form of natural sampler. These proposals have not been tested experimentally, nor have detailed theoretical analyses been made.

In summary then, a new form of natural sampler has been proposed, analysed, and to a limited extent tested. Its practical use has been outlined but not yet implemented. Its application to amplifiers with A.C. supplies appears to have the benefits of wider bandwidth and smaller filter size, benefits which flow from increasing the sampling rate from the supply frequency to a much higher value. Its application to other amplifiers has the benefit of the ability to reject supply waveform fluctuations from the output signal. Its principle disadvantage is the extra complexity required.

8.6 Waves with Many d.c. Levels - Staggered Phased Addition Method.

Mokryzki⁴, Pitman⁵ et al, and Heuman⁶ have described the staggered phase technique as a means of increasing the apparent switching wave frequency by summing together many two levelled switching waves. These authors did not however describe the spectrum of the resultant waves and so were unable to indicate how the amplifier bandwidth varies with the number of phases added together.

The analysis procedures and facilities introduced in chapter 4 are used there to examine the spectrum of such switching waves. In section 4.2.2.5 the interactions between bandwidth, passband noise, and signal level for such switching waves are described. The analysis indicates that although the bandwidth does increase with the number of phases added it does so more nearly as the square root of the total number than linearly as might at first be expected.

This result reduces the uncertainty of a designer as to whether this approach should be adopted or not, since it gives definite answers to questions concerning the relative magnitudes of signal to noise ratios of different forms of switching amplifier.

8.7 Waves with many Levels - Quantizer Method

In their approach to the linearising of the input-output characteristic of a quantizer Chen⁷, McVey⁸, and Parrish et al⁹ have used an input signal perturbation and thus synthesised a new form of natural sampling. They do not appear to have recognised the quantiser output as a form of switching wave nor have they described it in detail, consequently they have embarked upon the development of a theory in parallel with that for conventional d.c. levelled switching waves. A series of papers considered the input-output characteristics resulting from perturbations ranging from a sinusoid to a triangular wave. This is the conventional conclusion regarding the shape of sampling wave required for a linear input-output characteristic.

The use of quantisers by these authors is important to the theory of encoders since it expands

the concepts underlying the use of a single comparator to control a wave with two d.c. levels, to the use of an array of comparators to control a wave with many equally spaced levels. This concept is considered further in chapter 3, section 3.1.5.

The results presented in section 3.1.5 are from an analysis (given in appendix A3.1.5) of the restrictions on the shape of sampling wave required for a given input-output characteristic with particular reference to a linear characteristic. These results do not depend strictly on the use of a periodic sampling wave but are based upon the amplitude distribution of the signal used as the sampling wave. Consequently the analysis is not confined to the conventional natural sampler but is more general in application.

This new approach to switching wave control has not been used in any practical application, apart from obtaining high resolution from A/D converters. It has mainly been tested by comparing the theoretical results with those for natural sampling. It may be useful in areas where non-minimum energy switching waves may be desirable for reasons not now apparent. It is included here in an endeavour to make its existence known.

8.8 Regular Sampling

The presentation by Black¹⁰ of a description attributed to Bennet of a binary, d.c. levelled switching wave controlled by linear regular sampling of a sinusoidal control signal constitutes the sole theoretical contribution to the theory of this form of switching wave control. Black¹⁰ has indicated the drawbacks of

this form of control, in particular the nonlinearity of the input-output characteristic for control signals other than d.c. The accuracy of the description presented by Black¹⁰ was confirmed by measurements which form part of those outlined in Appendix E6.

The summary of Bennet's work given by Black¹⁰ does not indicate the method of derivation of the waveform descriptions. This prevents the use of this description as the starting point for a more general analysis intended to provide descriptions for d.c. levelled waves controlled by nonlinear regular sampling, and thus of a.c. levelled waves linearly controlled by regular sampling. At most the above description can provide a check of one particular result provided by a more general analysis.

As regular sampling can be and is used in situations beyond those at present described theoretically, a more general analysis method which can provide descriptions of the resulting switching waves appeared desirable. Such an analysis was undertaken and is presented in Appendix A 3.2.2a of this thesis.

The analysis generates expressions which describe the output of a d.c. levelled, binary switching wave with any periodic input signal or any combination non-commensurate periodic input signals. The description is partitioned to provide individual descriptions of the positive and negative steps of the wave and is couched in terms of the phase functions rather than the input signal. It is then possible to describe waves with the individual steps controlled by nonlinear functions of the input signal. Thus the sinusoidal input of Black's description is generalised to any combination of non-commensurate signals, the linear input-output

characteristic is generalised to any monotonic nonlinear input-output characteristic, and the combined description of the two waveform edges is separated for individual analysis. This provides the flexibility of analysis necessary to synthesise the descriptions of encoder waveforms used to control multilevelled switching waves with a.c. levels.

Although this last step is now possible in principle it is not to be lightly undertaken because of the complexity of the waveform descriptions of the encoder outputs. It is not attempted in this thesis for this reason. Accordingly the only tests of the analysis presently developed are its consistency with the measurements outlined in Appendix E6 and with the expression previously presented by Black.

8.9 Natural Sampling with Feedback

Andeen¹¹, Fallside et al¹², and Furnage¹³ describe theoretical analyses and practical measurements of feedback systems containing a switching amplifier. Andeen¹¹ describes a situation where sampling akin to regular sampling is used, the others describe systems with natural sampling. These analyses concern the stability of the feedback system and are based upon computation of the effective system gain at the sub-harmonic frequencies.

In attempting to experimentally confirm the works of these authors it became apparent that a fundamental change in the operation of natural samplers occurs when they are placed within feedback loops. It is these circumstances which are analysed in chapter 5, section 5.1.

The analysis provides a means whereby the input-output characteristic of the amplifier can be described for d.c. control signals or control signals with frequencies low enough so that the feedback loop response at the frequency of each waveform harmonic is substantially valid for the most significant sidebands of that harmonic. No references for such an analysis have been found in the literature.

The analysis is substantiated by experimental measurements of two amplifiers, one employing d.c. waveform levels, the other employing a.c. waveform levels, and a range of filter configurations based upon single and double pole loop responses. The measurements are outlined in Appendix E4.

The prediction of input-output characteristic and of the positions of steps in the switching wave provided by the analysis enables two sources of system instability to be determined without recourse to high frequency analyses. These instabilities generate subharmonic switching wave patterns of the form analysed by Andeen¹¹, Fallside¹², and Furnage¹³ but they are consequences of the modified d.c. characteristic, not of an inherent instability at a subharmonic frequency.

Although the work presented in section 5.1 is basically an analysis technique it does provide synthesis guidance to designers since it relates the filter response to the form of the input-output characteristic nonlinearity. Its main role, that of providing a designer with an exact input-output characteristic of the amplifier, fills an important gap in the theory of switching amplifiers.

8.10 Self Oscillating Systems

Johnson¹⁴, Bose¹⁵, Turnbull etal¹⁶, Sharma¹⁷, Camenzind¹⁸ and Yu etal¹⁹ describe practice and theory for self oscillating switching amplifiers of the class outlined in chapter 6. The basic practice is described by Johnson¹⁴, Bose¹⁵ and Turnbull etal¹⁶ while models for various aspects of system performance are described by Bose¹⁵, Sharma¹⁷, and Yu etal¹⁹. Camenzind¹⁸ describes techniques for realising a number of the systems proposed by Bose¹⁵.

Diagram D 6.3 shows a general form of the systems proposed. The particular form shown in diagram D 6 is described by Turnbull etal¹⁶ and Yu etal¹⁹ while the form described by Bose¹⁵ includes a delay with the integrator so that more complex filters may be approximated.

The simple integrator feedback model has a linear d.c. input-output characteristic and a parabolic variation of oscillator frequency with output signal. These aspects are easily established. No exact analysis of the a.c. characteristics have been published. The only model published is that of Yu etal¹⁹. The measurements outlined in chapter 6, section 6.1 and Appendix E5 confirmed the accuracy of the descriptions provided by the above authors. At the same time they indicated that the phenomenon of phase locking of the self oscillation to the input signal was inadequately described. Furthermore, it was apparent that each theoretical analysis for the various self-oscillating encoders was specific to the particular filter used within that encoder. Analyses of these two problems are provided in Appendix A 6.2b and A 6.3 respectively and are outlined in the corresponding sections of chapter 6.

The analysis of phase locking provided in A 6.2b allows the designer to accurately predict the conditions at the onset of phaselocking and thereby to determine a bound to the amplitude and or frequency of an input signal at which serious distortion will occur. As such it has a role as a design limit for the constant area sampler.

A general approach is adopted by the analysis of oscillation frequency and input-output characteristics given in appendix A 6.3 so that it applies to encoders with any form of feedback filter provided the input signal is of low frequency compared to the self oscillation frequency. The analysis is verified for two particular filter configurations by the measurements described in E5.

Chapter 6 thus provides two new tools for the use of designers of self oscillating encoders, namely a means for determining upper bounds for input signal amplitude and or frequency, and a means of analysing the operations of self-oscillating encoders employing feedback filters other than integrators and single section RC filters.

8.11 Equivalent Circuits

Although equivalent circuits are widely used in electrical engineering equivalent circuits for switching amplifiers are uncommon. Amato²⁰ has described an equivalent circuit for the cyclo converter and also commented on the losses associated with unfiltered source currents. While some aspects of the more general equivalent circuit proposed in chapter VII match those of Amato's circuit, the circuit described is an attempt to meld all the important features associated with switching amplifiers into a single unit. This aim is not totally achieved since off-state switch losses and dynamic losses are not included, since these depend on the form of switching wave and the type of switches; features which are not represented in the circuit.

Two important concepts are included. The first of these is the notion that as far as energy flow is concerned, any switch of an array may be regarded as a variable transformer. The second is that the combined effect of all the switches of such an array is equivalent to the summation of transformer outputs in the manner outlined. These two concepts would be almost valueless without the strict definitions of transformer ratios by the switch control functions introduced in chapter II and illustrated in chapter III.

The inner block defined by these two concepts is embedded between the supply and output filters as though it completely replaces the switch array. The process of placing switch conduction losses and high frequency supply losses at appropriate points within the ideal equivalent circuit is a simple extension which incorporates the losses described by Amato.²⁰

8.12 Areas for Further Research

The method of supply ripple rejection outlined in section 3.1.4.1 was not investigated fully in either a practical or theoretical sense. Those aspects examined indicate an approach which can minimise both hardware of the high powered kind, and switching wave energy. To make the approach viable, suitable switches are needed and it is desirable to have a more detailed knowledge of the bandwidth restrictions imposed by the modulation of sidebands by the supply ripple.

The concept of worst input signals introduced in section 4.2 is not fully developed. It may be possible to define such signals on a theoretical basis rather than the empirical basis adopted in this thesis. As an area for further research it may be more an academic exercise than a practical one since it appears unlikely to significantly modify the empirical results.

Medium and high frequency input signal responses of feedback systems are not adequately dealt with in this thesis nor in the available literature. Attempts to predict such behaviour must be based on approximations but the choice of approximations available is not clear. An empirical approach presents a rather fearsome measurement problem but may well be necessary to find the most significant parameters of the situation. Exact numerical modeling by digital computer appears impossible for the problem presently envisaged.

Similar difficulties beset any analysis of the mid-frequency performance of self oscillating systems. A solution of one of these two problems will greatly assist in the solution of the other.

There is one major practical problem associated with all switching amplifiers intended for speech or music reproduction. The output impedance variation with current level causes intermodulation of all filter input currents. For low impedance switches the effect is negligible but most switch arrays use diodes in the reverse current path and the step in voltage from conduction in the forward direction to conduction in the reverse direction causes the intermodulation. This problem is discussed by several authors¹⁸ but no solutions have been proposed.

CHAPTER VIII REFERENCES

<u>Number</u>	<u>Surname</u>	<u>Source of Publication Details</u> <u>(Appendix R Location)</u>
1	Bennet "New Results in the Calculation of Modulation Products" Bell System Tech. Journal Vol. 12 April 1933 PP 228-243	2.1
2	E. Fitch "The Spectrum of Modulated Pulses" J. IEE Vol. 94 PT 3A 1947 PP 556-564	2.2
3	E.R. Kretzmer "Distortion in Pulse Duration Modulation" Proc. IRE Vol. 35 November 1947 PP 1230-1235	2.3
4	B. Mokrytzki "Pulse Width Modulated Inverters for a.c. Motor Drives." IEEE Internat.Con. Rec. IGA-8 March 1966 PP 8-23	2.17

<u>Number</u>	<u>Surname</u>	<u>Source of Publication Details</u> <u>(Appendix R Location)</u>
5	P.F. Pitman, R.J. Ravas, R.W. Briggs "Staggered Phase Technique" Electrotechnology Vol. 83 No. 6 June 1968 PP 55-58	2.28
6	K. Heumann "Development of Inverters with Forced Commutation for Motor Speed Control up to the Megawatt Range" IEEE Trans IGA-5 No. 1 February 1969 PP 61-67	2.36
7	E.S. McVey, P.F. Chen "Improvements of Position and Velocity Detecting Accuracy by Signal Perturbation" IEEE Trans Vol. IECI-16 July 1969 PP 94-98	2.39
8	P.F. Chen "Optimal Signal Perturbation Waveform for Sensing Arrays" IEEE Trans Vol. IM-19 May 1970 PP 135-139	2.42

<u>Number</u>	<u>Surname</u>	<u>Source of Publication Details</u> <u>(Appendix R Location)</u>
9	E.A. Parrish, J.W. Stoughton "Achieving Improved Position Detection Using a Modified Triangular Perturbation Signal" IEEE Trans IM-21 No. 1 February 1972	2.47
10	H.S. Black "Modulation Theory" N.J.: Van Nostrand 1953 PP 263-281	1.2.1
11	Andeen "Analysis of Pulse Duration Sampled Data Systems with Linear Elements" IRE Trans on Aut.Control September 1960	2.7
12	F. Fallside, A.R. Farmer "Ripple Instability in Closed Loop Control Systems" Proc. IEE Vol. 114 March 1967 PP 139-152	2.23
	F. Fallside "Ripple Instability in Closed-loop Pulse Modulation Systems including Inverter Drives" Proc. IEEE. Vol. 115 1968 P 218	2.27

<u>Number</u>	<u>Surname</u>	<u>Source of Publication Details</u> <u>(Appendix R Location)</u>
13	S.G. Furmage "Subharmonic Instability in Closed Loop Control Systems with Pulse Width Modulation." Honours Thesis in Electrical Engineering, Uni. Tas. March 1969	1.3.1
14	K.C. Johnson "Pulse Modulated Audio Frequency Amplifiers" Wireless World Vol. 69 No. 3. March 1963 PP 135-136	2.10
15	A.G. Bose "A Two State Modulation System" Electrotechnology Vol. 74 No. 2 August 1964 PP 42-47	2.12
16	G.F. Turnbull, J.M. Townsend "A Feedback Pulse Width Modulated Audio Amp." Wireless World Vol. 71 No. 4 April 1965 PP 160-168	2.13

<u>Number</u>	<u>Surname</u>	<u>Source of Publication Details</u> <u>(Appendix R. Location)</u>
16	G.F. Turnbull, J.M. Townsend "Efficiency Considerations in a Class D Amp." Wireless World Vol. 73 No. 4,5 April, May 1967 P 154, P 214	2.24
17	J. Das, P.D. Sharma "Rectangular Wave Modulation - A P.L.M.-FM System" Electronic Letters Vol. 2 No. 1 January 1966 PP 7-9	2.15
18	H.R. Camenzind "Modulated Pulse Audio Power Amplifiers for I.C.S." IEEE Trans Vol. AU-14 No. 3 September 1966 PP 136-140	2.21
19	Uyan Yu, T.G. Wilson, Et Al "Static d.c. to Sinusoid a.c. Inverter" IEEE Trans Mag-3 No. 3 September 1967 PP 250-256	2.25

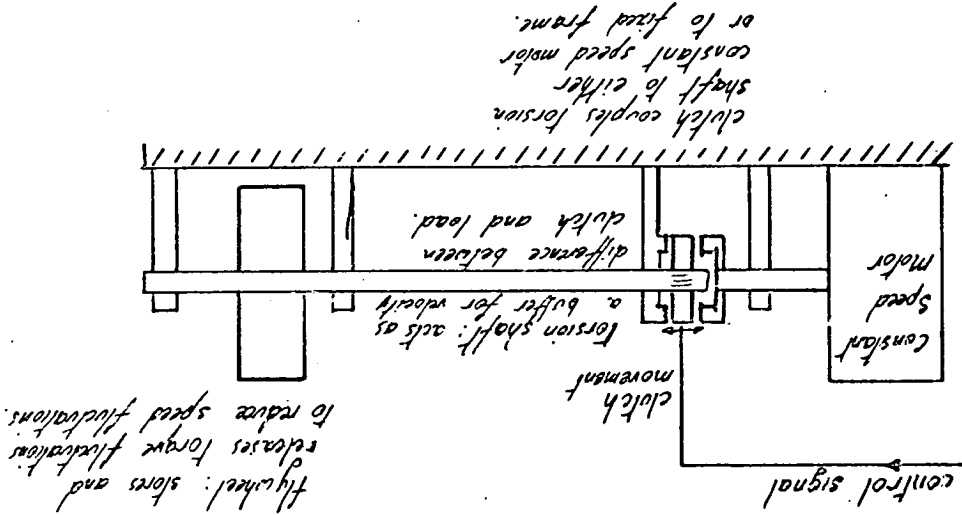
<u>Number</u>	<u>Surname</u>	<u>Source of Publication Details</u> <u>(Appendix R Location)</u>
20	C.J. Amato "An Equivalent Circuit for a Cycloconverter" IEEE Trans IGA-2 No. 5 September 1966 PP 68-73	2.20
	C.J. Amato "Latent Losses in 'lectric Lissies" IEEE Trans IGA-5 No. 5 September 1969 PP 558-565	2.40

Appendix A

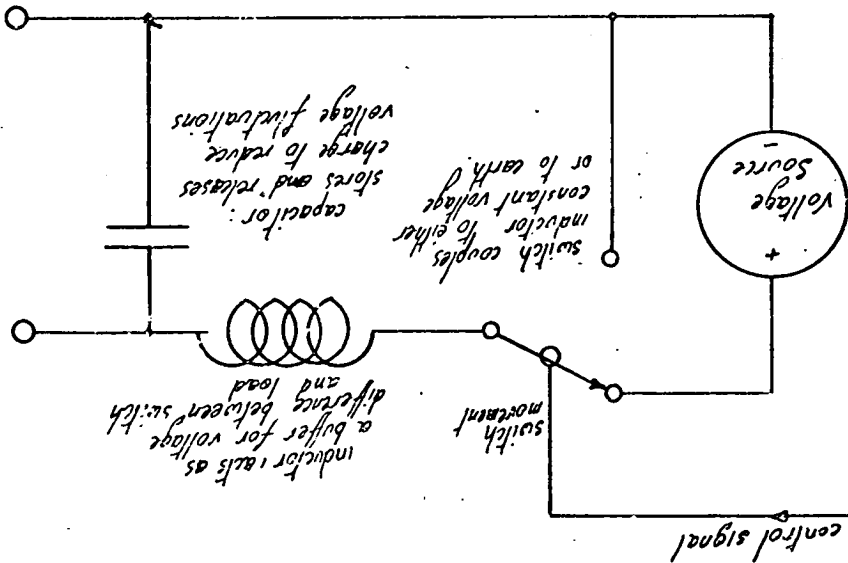
Algebraic & Arithmetical Segments

Note: The numbers of the pages of this section match those of the text from which references to this section are made. To follow such a reference turn to the appropriate part of this appendix. Upon completion of your examination use the section number on the page to return to your starting point.

Energy Flowpath - Mechanical Analogue



Energy Flowpath - Electrical

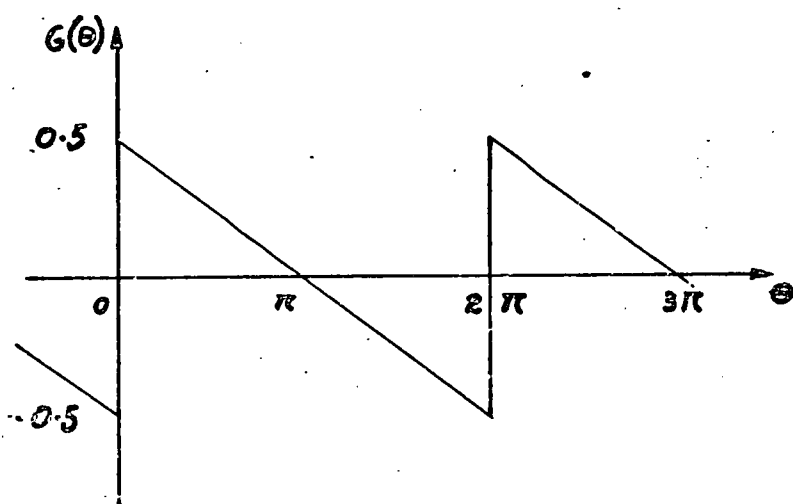


Mechanical Analogue of the Switching
Amplifier

The process whereby information is transferred from a control source to a load by a controlled switching action of devices within the energy flow path is not unique to electrical circuits. Mechanical equivalents are readily envisaged. Consider for example the equivalent electrical and mechanical energy flow paths shown in figure F 1.1.2.

In the analogues shown the energy sources are respectively a constant d.c. voltage and a constant speed drive shaft. These sources are coupled to their respective load filters by an electrical switch and a clutch respectively. The filters consist of series inductor and shunt capacitor for the electrical system while the mechanical system uses a torsion shaft and a flywheel. The electrical system has an equivalent circuit centred upon an infinitely variable voltage transformer; the mechanical system has an infinitely variable gear box in its ideal equivalent.

Parasitics such as switch capacitance and stray inductor capacitance have equivalents of clutch inertia and torsion shaft inertia respectively in the mechanical system. The time required to operate the electrical switches is paralleled by the time required to move the clutch from engagement in one position to engagement in the other position.



THE PERIODIC STEP FUNCTION

F 2.3

Consider the function, $G(\theta)$, defined by

$$G(\theta) = \frac{1}{2} - \frac{\phi_n}{2\pi} \text{ for all } \phi_n = \theta - 2\pi N \text{ such that } 0 < \phi_n < 2\pi$$

where N is an integer. The fourier series expression is

$$G(\theta) = \frac{1}{\pi} \sum_{n=1}^{\infty} \frac{1}{n} \sin n \theta.$$

$G(\theta)$ is sketched in diagram F 2.3 to show the form of variation with θ .

The first equation describes $G(\theta)$ in terms of N and ϕ_n which are the integral number of radians and remainder of θ . This equation may be re-expressed as

$$G(\theta) = \frac{1}{2} - \frac{\theta}{2\pi} + N.$$

Now a function of two variables θ_1 and θ_2 may be formed in the manner of the function below:

$$G(\theta_1) - G(\theta_2) = \frac{\theta_2 - \theta_1}{2\pi} + N_1 - N_2$$

that is

$$N_1 - N_2 = G(\theta_1) - G(\theta_2) + \frac{\theta_1 - \theta_2}{2\pi}$$

Now $N_1 - N_2$ is a function, taking integer values, which changes values when $\frac{\theta_1}{2\pi}$ or $\frac{\theta_2}{2\pi}$ pass through an integer value. The function required to indicate switch state, $g(t)$, is one such that $g(t)$ is either zero or unity. Thus if θ_1 and θ_2 are functions of time, $\theta_1(t)$ and $\theta_2(t)$, we may describe $g(t)$ by

$$g(t) = \frac{\theta_1(t) - \theta_2(t)}{2\pi} + \frac{1}{\pi} \sum_{n=1}^{\infty} \frac{1}{n} \left[\sin n \theta_1(t) - \sin n \theta_2(t) \right]$$

where $0 \leq N_1(t) - N_2(t) \leq 1$. A less general restriction which is sufficient is

$$0 < \frac{\theta_1(t) - \theta_2(t)}{2\pi} < 1$$

This may be proven by re-expressing in terms of N and ϕ_n as

$$0 < N_1(t) - N_2(t) + \frac{\phi_1(t) - \phi_2(t)}{2\pi} < 1$$

which may be relaxed by using the inequality

$$-1 < \frac{\phi_2(t) - \phi_1(t)}{2\pi} < 1, \text{ to give}$$

$$-1 < N_1(t) - N_2(t) < 2 \text{ and remembering that since}$$

N_1 and N_2 are integers this is equivalent to

$$0 \leq N_1(t) - N_2(t) \leq 1.$$

$$\text{Thus } g(t) = \frac{\theta_1(t) - \theta_2(t)}{2\pi} + \frac{1}{\pi} \sum_{n=1}^{\infty} \frac{1}{n} [\sin n\theta_1(t) - \sin n\theta_2(t)]$$

is a function which changes from 0 to 1 when $\frac{\theta_1(t)}{2\pi}$

increases through an integer value or $\frac{\theta_2(t)}{2\pi}$ decreases

through an integer value and changes from 1 to 0 when $\frac{\theta_1(t)}{2\pi}$ and $\frac{\theta_2(t)}{2\pi}$ vary in their respective opposite senses

through integer values, subject to the condition that

$$0 \leq N_1 - N_2 \leq 1$$

or

$$0 < \frac{\theta_1(t) - \theta_2(t)}{2\pi} < 1.$$

The two equations below have been derived in the text

$$V_n(t) = \sum_{i=1}^{i=m} g_i(t) \cdot V_i(t) \quad 1$$

$$\sum_{i=1}^{i=m} g_i(t) = 1 \quad 2$$

Now $V_{\max}(t)$ is the maximum supply voltage at time t and $V_{\min}(t)$ is the minimum supply voltage at time t .
Thus $V_{\min}(t) \leq V_i(t) \leq V_{\max}(t)$

$$\therefore V_n(t) = \sum_{i=1}^{i=m} g_i(t) V_i(t) \leq \sum_{i=1}^{i=m} g_i(t) V_{\max}(t)$$

$$\leq \left(\sum_{i=1}^{i=m} g_i(t) \right) V_{\max}(t) \leq V_{\max}(t)$$

Similarly $V_n(t) \geq V_{\min}(t)$

$$\therefore V_{\min}(t) \leq V_n(t) \leq V_{\max}(t)$$

It may be shown that some components of a switching wave must have a frequency corresponding to the fundamental or harmonics of the $V_{\max}(t)$ waveform whenever the d.c. component of the wave exceeds the minimum value of $V_{\max}(t)$.

This can be demonstrated by showing that a non-zero correlation exists between the a.c. part of the switching wave and a function representing the sign of the difference between $V_{\max}(t)$ and the average value of the switching wave even when such a correlation is minimised.

If the switching wave is described by $e(t)$ and the average of the switching wave by e_0 then the a.c. part of the wave is described by $e(t) - e_0$.

For the sign of the difference between $V_{\max}(t)$ and e_0 we will use the function $S(V_{\max}(t) - e_0)$ where S is defined by

$$S(x) = \begin{cases} +1 & \text{if } x > 0 \\ -1 & \text{if } x < 0 \end{cases}$$

The correlation of the a.c. switching wave components and the sign function over an interval T is defined as

$$R = \frac{1}{T} \int_0^T (e(t) - e_0) S(V_{\max} - e_0) dt.$$

Now when $V_{\max}(t) < e_0$, $S(V_{\max} - e_0) = -1$ and the contribution during such intervals will be

$$R_- = \left(\frac{1}{T} \int_0^T \{e_0 - e(t)\} dt \right) \frac{+1}{2} (1 - S(V_{\max} - e_0)).$$

Suppose we seek to minimise this. The minimum contribution is obtained when $e(t) = V_{\max}(t)$ but even this extreme gives a positive contribution since $V_{\max} < e_0$. The minimum contribution is

$$R_-]_{\min} = \frac{1}{T} \int_0^T (e_0 - V_{\max}(t)) dt \left\{ \frac{1}{2} (1 - S(V_{\max} - e_0)) \right\}$$

When $V_{\max}(t) > e_0$ the contribution to the correlation is

$$R_+ = \left(\frac{1}{T} \int_0^T (e(t) - e_0) dt \right) \left\{ \frac{1}{2} (1 + S(V_{\max} - e_0)) \right\}$$

But during these intervals the average value of $e(t) - e_0$ must be maintained at zero so that it is required that

$$\left(\frac{1}{T} \int_0^T (e(t) - e_0) dt \right) \left(\frac{1}{2} (1 + S(V_{\max} - e_0)) \right) =$$

$$\left(\frac{1}{T} \int_0^T (e_0 - V_{\max}(t)) dt \right) \left(\frac{1}{2} (1 - S(V_{\max} - e_0)) \right)$$

Therefore the two correlation contributions must be equal and thus the minimum correlation will be

$$R]_{\min} = (1 - S(V_{\max} - e_0)) \left(\frac{1}{T} \int_0^T (e_0 - V_{\max}(t)) dt \right)$$

This shows that the minimum absolute correlation possible will be zero only when V_{\max} is greater than the average value of e_0 for the entire measured interval, hence this condition must be satisfied in order that the spectrum of the switching wave, $e(t)$ is not constrained to contain components matching, in frequency, those of the maximum supply voltage waveform, $V_{\max}(t)$.

Over a length of time, τ , three voltages V_i , V_j , and V_r form the levels of the switching wave. Each has a total time of presentation at the output of T_i , T_j , and T_r respectively. The voltages V_i and V_j will be defined as the nearest voltages above and below the desired average of the switching wave. The average voltage, a , is defined by

$$T_i.V_i + T_j.V_j + T_r.V_r = a.\tau$$

By combining this equation with the equation

$T_i + T_j + T_r = \tau$ it is possible to express T_i and T_j in terms of T_r and the other variables by the equations below

$$T_i = (a.\tau - V_j.\tau - T_r(V_r - V_j)) / (V_i - V_j)$$

$$T_j = (a.\tau - V_i.\tau - T_r(V_r - V_j)) / (V_j - V_i)$$

The mean square error between the switching wave and the desired average is given by the equation;

$$M.S. = (T_i(V_i - a)^2 + T_j(V_j - a)^2 + T_r(V_r - a)^2) / \tau$$

By substituting the expressions for T_i and T_j for these variables the error may be expressed as a function of T_r .

$$\begin{aligned} M.S. &= ((a.\tau - V_j.\tau - T_r(V_r - V_j))(V_i - a)^2 - (a.\tau - V_i.\tau - T_r(V_r - V_i)) \cdot \\ &\quad (V_j - a)^2 + (V_i - V_j)(V_r - a)^2 T_r) / ((V_i - V_j).\tau). \\ &= T_r(V_r - V_i)(V_r - V_j) / \tau + ((a.\tau - V_j.\tau)(V_i - a)^2 - (a.\tau - V_i.\tau)(V_j - a)^2) / \\ &\quad (V_i - V_j) / \tau \end{aligned}$$

The mean square error has a component with a positive co-efficient of T_r provided V_r lies outside the range between V_i and V_j . Since the definitions of V_i and V_j ensure that V_r does not lie within the above range it

follows that the mean square error is minimum when T_r is minimum, that is zero.

Thus the minimum mean square error is attained for the switching wave when only the nearest voltages above and below the desired voltage form the levels of the waveform.

The above analysis is valid only for d.c. supply voltages but may be extended to a.c. supply voltages. By considering the above analysis to be true for very short values of τ , then it follows that it is true for longer intervals.

Under the optimum conditions the mean square error is

$$M.S. = (V_i - a)(a - V_j).$$

Let two periodic sampling waves be described by $S_1(ft)$ and $S_2(ft)$ where the repetition frequency is f . Define $(-1)^{k+1} \alpha_k S_k(ft)$, where $\alpha_1 = \alpha_2 = 1$ for pulse width modulation and $\alpha_1 = -\alpha_2 = 1$ for pulse phase modulation, to be monotonically decreasing during the time interval $\beta_{ka} + N < ft < \beta_{kb}$, where k is the integer part of ft and $0 < \beta_{ka} + \beta_{kb} < 2$.

With the restrictions above the function

$$S_k(ft) = x$$

may be used to define the inverse function by

$$S_k^{-1}(x) = ft - N$$

provided both restrictions below apply to x

$$(-1)^{k+1} \alpha_k S_k(\beta_{ka}) > x > (-1)^{k+1} \alpha_k S_k(\beta_{kb}) \quad k = 1, 2.$$

Consider the variable, $\theta_k(t)$, defined by the equation

$$\theta_k(t) = 2\pi(ft - S_k^{-1}(e_{in}(t))).$$

When $e_k(t)$ is an integer $S_k(ft) = e_{in}(t)$, that is

$$\frac{e_k(t)}{2\pi} E_k(t) = e_{in}(t) - S_k(ft) = 0.$$

$$\text{Also } \text{sign} \left(\alpha_k \frac{dE_k(t)}{dt} \right) \Big|_{E_k(t)=0} = \text{sign} \left((-1)^{k+1} \frac{d\theta_k(t)}{dt} \right) \Big|_{\theta_k(t) = \text{integer}}.$$

Thus $\Theta_k(t)$, $k = 1, 2$, are variables of the form required to generate a two state function. Hence the state function defined by natural sampling is

$$g(t) = S_2^{-1}(e_{in}(t)) - S_1^{-1}(e_{in}(t)) + \sum_{n=1}^{\infty} \frac{1}{n\pi} \cdot (\sin n(2\pi ft - S_1^{-1}(e_{in}(t))) - \sin n(2\pi ft - S_2^{-1}(e_{in}(t))))$$

The restrictions on $e_{in}(t)$.

Provided

$(-1)^{k+1} \alpha_k \cdot S_k(\beta_{ka}) > e_{in}(t) > (-1)^{k+1} \alpha_k \cdot S_k(\beta_{kb})$ for $k=1$ and 2 the inverse functions are defined. This restricts $e_{in}(t)$ to values between maxima and minima of the sampling waveforms.

The restrictions on Θ_k , $k=1$ and 2

The restriction on variables, Θ_k , defining the switch function $g(t)$ is

$0 < \Theta_1(t) - \Theta_2(t) < 2\pi$ which may be re-expressed as

$$0 < S_2^{-1}(e_{in}(t)) - S_1^{-1}(e_{in}(t)) < 1$$

The sampling waveforms are composed of alternating segments of $S_1(ft-N)$ and $S_2(ft-N)$. The requirement of the first part of the inequality is that $S_1(ft-N)$ does not intersect $S_2(ft-N)$ while the second requires $S_2(ft-N)$ does not intersect $S_1(ft-N+1)$. That is the two sampling waves must not intersect one another.

Example of Pulse Width Modulation

The example used to illustrate the process of natural sampling with a triangular sampling wave is given a mathematical analysis to show how the expression for coder output may be derived.

For this case a sampling wave with two monotonic sections is used to provide the two sampling waves required. Under the definitions given $S_1(ft)$ is the negative slope and $S_2(ft)$ the positive slope. The allowable input range to the coder lies between the extremes of the sampling wave. For the waveform shown in diagram D 3.1.2a (iv) $g(t)$ is derived as follows;

$$S_2(ft) = 4(ft - N)$$

$$S_1(ft) = -4(ft - N) + 2$$

$$\frac{e_2(t)}{2\pi} = ft - \frac{e_{in}(t)}{4}$$

$$\frac{e_1(t)}{2\pi} = ft + \frac{e_{in}(t) - 2}{4}$$

$$\text{hence } g(t) = \frac{e_{in}(t) - 1}{2} + \frac{1}{\pi} \sum_{n=1}^{\infty} \frac{1}{n} (\sin 2\pi n(ft + \frac{e_{in} - 2}{4}) - \sin 2\pi n(ft - \frac{e_{in}}{4}))$$

The range of input values for $e_{in}(t)$ is

$$-1 < e_{in}(t) < 1.$$

A state function produced by natural sampling described by

$$g_i(t) = S_2^{-1}(e(t)) - S_1^{-1}(e(t)) + \sum_{n=1}^{\infty} \frac{1}{n\pi} (\sin 2\pi n(ft - S_1^{-1}(e(t))) - \sin 2\pi n(ft - S_1^{-1}(e(t))))$$

is used to modulate a supply voltage with the time function description

$$V_i(t) = b_0 + \sum_{n=1}^{\infty} b_n \sin(2\pi nft + \phi_n)$$

The modulated supply voltage contains terms not dependent on f which are described below as $g(t)_i \times V_i(t)]_0$.

$$\begin{aligned} g_i(t) \times V_i(t)]_0 &= b_0 (S_2^{-1}(e(t)) - S_1^{-1}(e(t))) + \sum_{n=1}^{\infty} \frac{b_n}{2\pi n} \\ &\quad \left\{ \cos(2\pi n S_1^{-1}(e(t)) + \phi_n) - \cos(2\pi n S_2^{-1}(e(t)) + \phi_n) \right\} \\ &= \int_{x=S_1^{-1}(e(t))}^{x=S_2^{-1}(e(t))} \left\{ b_0 + \sum_{n=1}^{\infty} b_n \sin(2\pi nx + \phi_n) \right\} dx \end{aligned}$$

$$\text{with } S_1[x] = A_1 \int_0^x \left\{ b_0 + \sum_{n=1}^{\infty} b_n \sin(2\pi nx + \phi_n) \right\} dx + B_1$$

$$\text{and } S_2[x] = A_2 \int_0^x \left\{ b_0 + \sum_{n=1}^{\infty} b_n \sin(2\pi nx + \phi_n) \right\} dx + B_2$$

$$g_i(t) \times V_i(t)]_0 = e(t) \left[\frac{1}{A_2} - \frac{1}{A_1} \right] + \left[\frac{B_1}{A_1} - \frac{B_2}{A_2} \right]$$

Thus the component of the modulated signal not dependant on frequency of sampling will obey the linearity relationship

$$g_i(t) \times V_i(t)]_0 = K_i e(t) + C_i$$

when

$$K_i = \frac{1}{A_2} - \frac{1}{A_1}$$

and

$$C_i = \frac{B_1}{A_1} - \frac{B_2}{A_2}$$

This restriction on sampling waveform may be used for both pulse width and pulse phase state functions.

An alternative method of selecting sampling waveforms exists for pulse phase modulation when the two sampling waves are identical in waveform apart from a shift in time of a fraction, α , of the period. The method is restricted to a.c. supply voltages, $V_i(t)$, of the form

$$V_i(t) = a_0 + \sum_{n=1}^{n=\infty} a_n \sin [2\pi n f t + \phi_n]$$

When modulated by the usual state function, $g_i(t)$, for a natural sampler output the component of the modulation not containing terms dependant on f , $V_{ni}]_0$ is given by

$$\begin{aligned} V_{ni}]_0 &= \alpha a_0 + \sum_{n=1}^{n=\infty} \frac{a_n}{2\pi n} \left\{ \cos 2\pi n (-S_1^{-1}(e(t)) + \phi_n - \right. \\ &\quad \left. \cos (\phi_n - 2\pi n S_2^{-1}(e(t))) \right\} \\ &= \alpha a_0 \sum_{n=1}^{n=\infty} \frac{a_n}{2\pi n} \left\{ +2 \sin(\phi_n + \alpha \pi n + 2\pi n S_1^{-1}(e(t))) \right. \\ &\quad \left. \times \sin(\alpha \pi n) \right\} \end{aligned}$$

where the relationship $\alpha = S_2^{-1}(e_n(t)) - S_1^{-1}(e_n(t))$ has been used.

Thus $V_{ni}]_0 = \text{Function}(S_1^{-1}(e(t))) + \alpha a_0$ where the supply voltage waveshape and α are parameters of the function, Function. In order for linear amplification to result the relationship

$$V_{ni}]_0 = K_i e(t) = F(S_1^{-1}(e(t))) + \alpha a_0 \text{ must be satisfied.}$$

Thus

$$S_1(ft) = \frac{1}{K_i} F(ft) + \frac{\alpha a_o}{K_i}$$

$$= \frac{1}{K_i} \sum_{n=1}^{\infty} \frac{a_n}{n\pi} \left\{ \frac{\sin(2\pi n(ft + \frac{\alpha}{2}) + \phi_n)}{\sin(n\pi\alpha) + \frac{(\alpha a_o)}{K_i}} \right\}.$$

and

$$S_2(ft) = \frac{1}{K_i} \sum_{n=1}^{\infty} \frac{a_n}{n\pi} \left\{ \frac{\sin(2\pi n(ft - \frac{\alpha}{2}) + \phi_n)}{\sin(n\pi\alpha) + \frac{(\alpha a_o)}{K_i}} \right\}.$$

The more general linearity equation with constant C_i may be satisfied giving

$$S_1(ft) = \frac{1}{K_i} \sum_{n=1}^{\infty} \frac{a_n}{n\pi} \left\{ \frac{\sin(2\pi n(ft + \frac{\alpha}{2}) + \phi_n)}{\sin(n\pi\alpha) - \frac{((C_i - \alpha a_o))}{K_i}} \right\}.$$

and

$$S_2(ft) = \frac{1}{K_i} \sum_{n=1}^{\infty} \frac{a_n}{n\pi} \left\{ \frac{\sin(2\pi n(ft - \frac{\alpha}{2}) + \phi_n)}{\sin(n\pi\alpha) - \frac{((C_i - \alpha a_o).)}{K_i}} \right\}.$$

A Sinewave Voltage with Natural Phase
Modulation Switch Control

A supply voltage, $V_i(t)$, described by

$$V_i(t) = \sin(\omega_s t + \phi)$$

is modulated by a state function, $g_i(t)$ arranged to give linear variation of V_{ni} with input voltage, $e(t)$. For this case the switch control function is described by

$$\begin{aligned} g_i(t) &= \alpha + \sum_{n=1}^{\infty} \frac{1}{n\pi} \left\{ \sin n(\omega_s t + \phi + \pi\alpha - \arcsin \left[\frac{\pi(Kie(t) + C_i)}{\sin \pi\alpha} \right]) \right\} \\ &\quad - \left\{ \sin n(\omega_s t + \phi - \pi\alpha - \arcsin \left[\frac{Kie(t) + C_i}{\sin \pi\alpha/\pi} \right]) \right\} \\ &= \alpha + \sum_{n=1}^{\infty} \frac{2}{n\pi} (\sin n\pi\alpha) \cos n(\omega_s t + \phi - \arcsin \left[\frac{(Kie(t) + C_i)\pi}{\sin \pi\alpha} \right]) \end{aligned}$$

Thus the node voltage component V_{ni} is described by

$$V_{ni} = \sin(\omega_s t + \phi) \left\{ \alpha + \sum_{n=1}^{\infty} \frac{2\sin n\pi\alpha}{n\pi} \cos n(\omega_s t + \phi - \arcsin \left[\frac{(Kie(t) + C_i)\pi}{\sin \pi\alpha} \right]) \right\}$$

The expansion of this expression yields terms centred on ω_s , $2\omega_s$, $3\omega_s$ and so on. These are collected and yield the expression for V_{ni} given on the next page.

$$\begin{aligned}
 V_{ni} &= e(t)K_i + C_i + \alpha \sin(w_s t + \phi) - \frac{\sin 2\pi\alpha}{2\pi} \\
 &\quad \sin(w_s t + \phi + 2\alpha \arcsin \left[\frac{K_i e(t) + C_i}{\sin \alpha \pi} \right]) + \sum_{m=2,3,\dots}^{\infty} \frac{1}{m} \\
 &\quad \left\{ \frac{\sin(m-1)\alpha\pi}{(m-1)\pi} \sin(m(w_s t + \phi) - (m-1)\alpha \arcsin \left[\frac{\pi(K_i e(t) + C_i)}{\sin \alpha \pi} \right]) \right. \\
 &\quad \left. - \frac{\sin(m+1)\alpha\pi}{(m+1)\pi} \sin(m(w_s t + \phi) + (m+1)\alpha \arcsin \left[\frac{\pi(K_i e(t) + C_i)}{\sin \alpha \pi} \right]) \right\}
 \end{aligned}$$

For a symmetrical R phase system the expression for the total node voltage is given by V_n for $K_1 = K_2 = K_3 \dots = K_i \dots = K_R$.

$$\begin{aligned}
 V_n &= e(t)RK_i + \sum_{r=1}^R \frac{1}{R} \left\{ \sin(w_s t + \frac{r2\pi}{R}) - \frac{\sin 2\pi\alpha}{2\pi\alpha} \right. \\
 &\quad \left. \sin(w_s t + \frac{r2\pi}{R} + 2\alpha \arcsin \left[\frac{\pi(K_i e(t) + C_i)}{\sin \pi\alpha} \right]) \right\} + \sum_{m=2,3,\dots}^{\infty} \frac{1}{m} \\
 &\quad \left\{ \frac{\sin(m-1)\pi\alpha}{(m-1)\pi} \sin(m(w_s t + \frac{r2\pi}{R}) - (m-1)\alpha \arcsin \left[\frac{(e(t)K_i + C_i)\pi}{\sin \pi\alpha} \right]) \right. \\
 &\quad \left. - \frac{\sin(m+1)\pi\alpha}{(m+1)\pi} \sin(m(w_s t + \frac{r2\pi}{R}) + (m+1)\alpha \arcsin \left[\frac{(e(t)K_i + C_i)\pi}{\sin \pi\alpha} \right]) \right\}
 \end{aligned}$$

With α at the maximum value of $\frac{1}{R}$ the node voltage may be simplified giving

$$\begin{aligned}
 V_n &= e(t)RK_i + \sum_{m=R,2R,\dots}^{\infty} \frac{(\sin(m-1)\pi/R)}{(m-1)\pi} \\
 &\quad \sin \left\{ m(w_s t) - (m-1)\alpha \arcsin \left[\frac{(K_i e(t) + C_i)\pi}{\sin \pi/R} \right] \right\} - \frac{\sin(m+1)\pi/R}{(m+1)\pi} \\
 &\quad \sin \left\{ m(w_s t) + (m+1)\alpha \arcsin \left[\frac{(K_i e(t) + C_i)\pi}{\sin \pi/R} \right] \right\}
 \end{aligned}$$

A supply voltage, $V_i(t)$, described by

$$V_i(t) = \sin(w_s t + \phi)$$

is modulated by a state function, $g_i(t)$, so that a control voltage $e(t)$ is linearly reproduced as the component V_{ni} not dependant on $w_s t$.

The switch control function for this case is described by

$$g_i(t) = \frac{1}{2\pi} \left\{ \arccos\left(2\pi \left[\frac{e(t)}{-A_2} - C \right] \right) - \arccos\left(2\pi \left[\frac{e(t)}{-A_1} - C \right] \right) \right\} \\ + \sum_{n=1}^{\infty} \frac{1}{n\pi} \left\{ \sin n(w_s t - \arccos 2\pi \left[\frac{e(t)}{-A_1} - C \right] + \phi) \right. \\ \left. - \sin n(w_s t - \arccos 2\pi \left[\frac{e(t)}{-A_2} - C \right] + \phi) \right\}$$

where $C = \frac{B_1}{A_1} = \frac{B_2}{A_2}$ so there is zero offset in $V_{ni}]_0$. The resultant node voltage component V_{ni} is given by

$$V_{ni} = \sin(w_s t + \phi) \times g_i(t)$$

The complete expansion is shown on the next page.

$$\begin{aligned}
V_{ni} = e(t) & \left[\frac{1}{A_2} - \frac{1}{A_1} \right] + \frac{1}{2\pi} \left[\sin(w_s t + \phi) \right] \left[\arccos 2\pi \left[\frac{e(t)}{-A_2} - C \right] - \right. \\
& \left. \arccos 2\pi \left[\frac{e(t)}{-A_1} - C \right] \right] + \frac{1}{2\pi} \cdot \\
& \sin \left\{ (w_s t + \phi) - \frac{1}{2} \left[\arccos 2\pi \left[\frac{e(t)}{-A_2} - C \right] + \arccos 2\pi \left[\frac{e(t)}{-A_1} - C \right] \right] \right\} \\
& \times \sin \left\{ \arccos 2\pi \left[\frac{e(t)}{-A_2} - C \right] - \arccos 2\pi \left[\frac{e(t)}{-A_1} - C \right] \right\} + \sum_{m=2,3}^{\infty} \frac{1}{m} \\
& \left\{ \frac{1}{(m-1)} \sin \left[m(w_s t + \phi) - \frac{(m-1)}{2} \left[\arccos 2\pi \left[\frac{e(t)}{-A_2} - C \right] \right. \right. \right. \\
& \left. \left. + \arccos 2\pi \left[\frac{e(t)}{-A_1} - C \right] \right] \right] \times \left(\sin \left[\frac{(m-1)}{2} \left(\arccos 2\pi \left[\frac{e(t)}{-A_2} - C \right] \right. \right. \right. \right. \\
& \left. \left. - \arccos 2\pi \left[\frac{e(t)}{-A_1} - C \right] \right) \right] + \frac{1}{(m+1)} \sin \left[m(w_s t + \phi) - \frac{(m+1)}{2} \cdot \right. \\
& \left. \left[\arccos 2\pi \left[\frac{e(t)}{-A_1} - C \right] + \arccos 2\pi \left[\frac{e(t)}{-A_2} - C \right] \right] \right] \\
& \left. \times \left(\sin \frac{(m+1)}{2} \left[\arccos(2\pi \left[\frac{e(t)}{-A_2} - C \right]) - \arccos(2\pi \left[\frac{e(t)}{-A_1} - C \right]) \right] \right) \right\}
\end{aligned}$$

Arbitrary Waveform Levels

A switch control function, defined by the equation

$$g(t) = S_2^{-1}(e_{in}(t)) - S_1^{-1}(e_{in}(t)) + \sum_{n=1}^{n=\infty} \frac{1}{n\pi} \left\{ \begin{aligned} &\sin(n(w_s t - 2\pi S_1^{-1}(e_{in}(t)))) \\ &- \sin(n(w_s t - 2\pi S_2^{-1}(e_{in}(t)))) \end{aligned} \right\},$$

is used to control two supply voltages $V_1(t)$ and $V_2(t)$ to give a switching wave described by the equation

$$e_o = V_1(t)g(t) + V_2(t)(1-g(t)).$$

Provided the supply voltages are not commensurate with the sampling frequency the terms not dependent on the sampling frequency are given by

$$e_o \Big|_0 = \frac{V_1(t) + V_2(t)}{2} + (V_1(t) - V_2(t)) (S_2^{-1}(e_{in}(t)) - S_1^{-1}(e_{in}(t)) - \frac{1}{2})$$

The first requirement of S_1 and S_2 is, that the term involving $e_{in}(t)$ be proportional to this variable. At the sampling instants the equations

$$e_{in}(t_1) = S_1(w_s t_1) \text{ and } e_{in}(t_2) = S_2(w_s t_2) \text{ are}$$

true. Consider the case where

$$S_1(w_s t) = S_p(w_s t) \cdot f(t) \text{ and } S_2(w_s t) = S_n(w_s t) \cdot f(t)$$

Where S_p and S_n are such that with d.c. supplies they give a linear characteristic that is they obey the equation

$$S_p^{-1}(e(t)) - S_n^{-1}(e(t)) - \frac{1}{2} = e(t).$$

Now at the sampling instants the equations may be re-expressed as

$$e_{in}(t_1) = S_p(w_s t_1) \cdot f(t) \text{ and } e_{in}(t_2) = S_n(w_s t_2) \cdot f(t)$$

$$\text{Thus } S_p^{-1}(e_{in}(t_1)/f(t_1)) = w_s t_1 / 2\pi = S_1^{-1}(e_{in}(t_1)) \text{ and}$$

$$S_n^{-1}(e_{in}(t_2)/f(t_2)) = w_s t_2 / 2\pi = S_2^{-1}(e_{in}(t_2)) \text{ so that}$$

$$e_o \Big|_o = (V_1(t) + V_2(t))/2 + e_{in}(t) \cdot (V_1(t) - V_2(t))/f(t).$$

Thus with $f(t) = V_1(t) - V_2(t)$ the amplifier becomes linear.

The conditions for linear amplification are that the normal sampling waves be modulated with the difference in supply voltages and that the mean of the supply voltages be subtracted from the input.

Note that for nonunity amplifier gain the amount subtracted must be suitably scaled.

The output switching wave under these conditions is described by

$$e_o = e_{in}(t) + \sum_{n=1}^{n=\infty} \frac{1}{n\pi} (V_1(t) - V_2(t)) \cdot$$

$$\left\{ \sin(n(w_s t - 2\pi S_p^{-1}(x))) - \sin(n(w_s t - 2\pi S_n^{-1}(x))) \right\}, \text{ where}$$

$$x = (e_{in}(t) - (V_1(t) + V_2(t))/2) / (V_1(t) - V_2(t)).$$

This waveform has sidebands due to the supply waveforms from both phase modulation and amplitude modulation.

HIGH FREQUENCY COMPONENTS OF THE WAVE - An Example.

A symmetrical triangular sampling wave satisfying the condition

$$(w_s t_p - w_s t_n)/2\pi - \frac{1}{2} = e_m(t) \text{ is described by}$$

$$S_p(w_s t) = 2\left(\frac{w_s t}{2\pi}\right) - \frac{1}{2}$$

$$S_n(w_s t) = -\frac{1}{2} - 2\left(\frac{w_s t}{2\pi}\right)$$

This yields the inverse functions below

$$S_p^{-1}(e_m(t)) = (e_m(t) + \frac{1}{2})/2$$

$$S_n^{-1}(e_m(t)) = -(e_m(t) + \frac{1}{2})/2$$

Thus the n^{th} harmonic of the modified modulator is described by

$$H_n = \frac{1}{n\pi}(V_1(t) - V_2(t)) \left\{ \sin \left(n(w_s t + \pi \left(\frac{e_m(t)}{V_1(t) - V_2(t)} - \frac{1}{2} \right)) \right) - \sin \left(n(w_s t - \pi \left(\frac{e_m(t)}{V_1(t) - V_2(t)} - \frac{1}{2} \right)) \right) \right\}$$

When $V_1(t) - V_2(t)$ is of the form $V(1+p(t))$ and $p(t)$ is small then the harmonic description may be approximated by

$$H_n \approx \frac{V}{n\pi}(1+p(t)) \left\{ \sin \left(nw_s t + n\pi \left(\frac{e_m(t)}{V} \right) (1-p(t)) - \frac{n\pi}{2} \right) - \sin \left(nw_s t - n\pi \left(\frac{e_m(t)}{V} \right) (1-p(t)) + \frac{n\pi}{2} \right) \right\}$$

For $e_m(t) = 0$ the harmonic is simply amplitude modulated by the perturbation of the supplies. There is no phase modulation by the supply perturbation. (This is true whether the approximation is true or not).

For $e_m(t) = \frac{V}{2}$, that is, it is near its maximum value, the harmonic description is

$$H_n = \frac{V}{n\pi} (1+p(t)) \left\{ \begin{aligned} &\sin(n\omega_s t + \frac{n\pi}{2} p(t)) \\ &- \sin(n\omega_s t - \frac{n\pi}{2} p(t)) \end{aligned} \right\}$$

$$= \frac{2V}{n\pi} (1+p(t)) \sin\left(\frac{n}{2} p(t)\right) \cos(n\omega_s t)$$

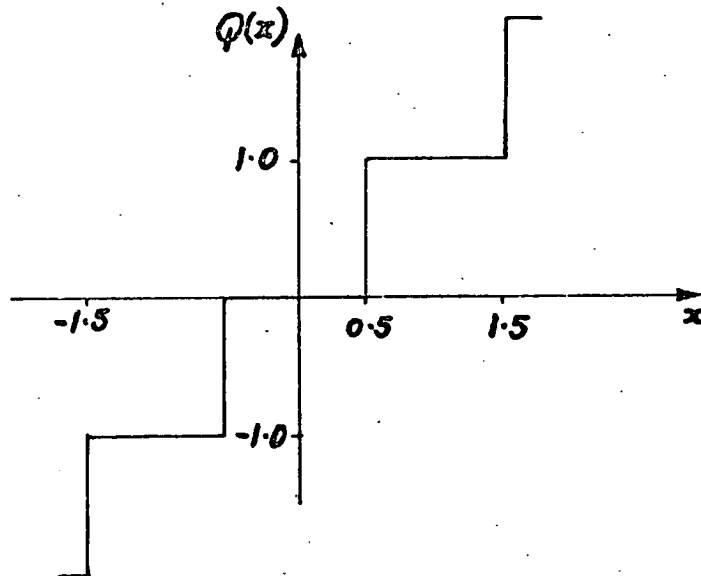
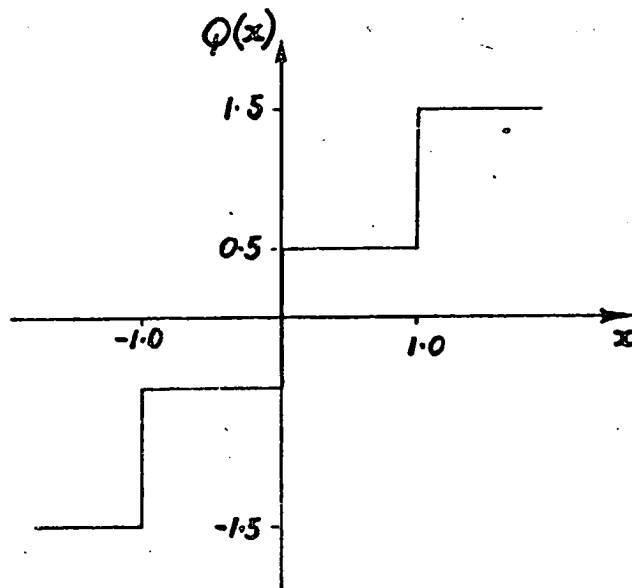
Now for $n = 1$ and $p(t) \ll 1$ the harmonic H_1 is given by

$$H_1 = \frac{2V}{\pi} (1+p(t)) \cdot \frac{\pi p(t)}{2} \cos n\omega_s t$$

$$= V p(t) (1+p(t)) \cos n\omega_s t$$

Thus the modulation is predominantly that of the phase component and it has one term equivalent to amplitude modulation by $p(t)$ alone and a second term equivalent to modulation by $p(t)^2$.

Now suppose $p(t)$ is a sinewave. The two situations examined, zero input signal and maximum input signal, both yield first order sidebands but the latter alone yields small second order sidebands. In the former case the sideband amplitudes are of magnitude corresponding to $\frac{Vp(t)}{n\pi}$, in the latter, $Vp(t)$.



THE TWO QUANTIZER CHARACTERISTICS

F 3.1.5 a(1)

Quantizer Output with Input Perturbation

Two normalised quantizer characteristics are shown in diagram F 3.1.5a. One has zero output for inputs between plus and minus one half unit. The other has outputs of plus and minus one half unit for positive and negative small inputs. The transformation from one to the other is a shift of origin of both input and output axes of one half unit. Each characteristic is described by the two alternative expressions

$$e_o = e_i + \sum_{n=1}^{\infty} \frac{1}{n} \sin(2\pi n(e_i + \frac{1}{2})) / (n\pi)$$

$$= k \text{ where } -\frac{1}{2} < 2\pi n e_i - k < \frac{1}{2} \text{ defines } k,$$

and

$$e_o = e_i + \sum_{n=1}^{\infty} \frac{1}{n} \sin(2\pi n e_i) / (n\pi)$$

$$= \frac{1}{2} + k \text{ where } 0 < e_i - k < 1 \text{ defines integer } k.$$

The latter form of characteristic requires fewer symbols and will be used in the following work. Should the other form of characteristic be of interest then the transformation outlined above may be applied to yield appropriate expressions in lieu of those presented.

The perturbation component of e_i will be referred to as p and the remainder as e where these are understood to represent functions of time $p(t)$ and $e(t)$. The quantizer input is the sum of e and p . The output in terms of these variables is given by

$$e_o = p+e + \sum_{n=1}^{\infty} \frac{1}{n} \sin(2\pi n(p+e)) / (n\pi)$$

$$= p+e + \sum_{n=1}^{\infty} \frac{1}{n} (\sin(2\pi n e) \cos(2\pi n p) + \cos(2\pi n e) \sin(2\pi n p)) / (n\pi)$$

$$\text{Now } e^{j2\pi n p} = \sum_{m=0}^{\infty} (A[n,m] + jB[n,m]) \cos w_m t + (C[n,m] + jD[n,m]) \sin w_m t$$

..., where w_m represents the m^{th} lowest frequency formed by the cosine or sine of $2\pi np(t)$. The co-efficients of these fourier series are specified by the following integrals taken over one period, T , of the perturbation. The integrals are

$$A[n,m] + jB[n,m] = \frac{E(m)}{2} \int_0^{2\pi} \cos w_m t e^{j2\pi np(t)} d(2\pi t/T), \text{ and}$$

$$C[n,m] + jD[n,m] = \frac{E(m)}{2} \int_0^{2\pi} \sin w_m t e^{j2\pi np(t)} d(2\pi t/T), \text{ where}$$

$$E(m) = \begin{cases} 1 & \text{if } m=0 \\ 2 & \text{if } m>0 \end{cases}$$

Using these series the expression for e_o may be regrouped giving

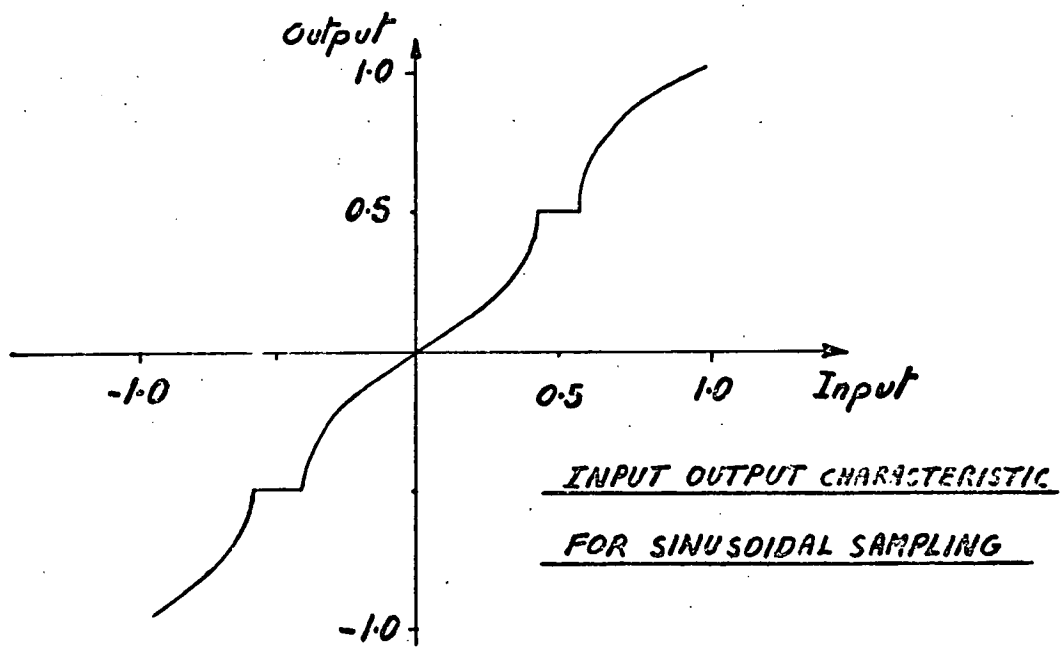
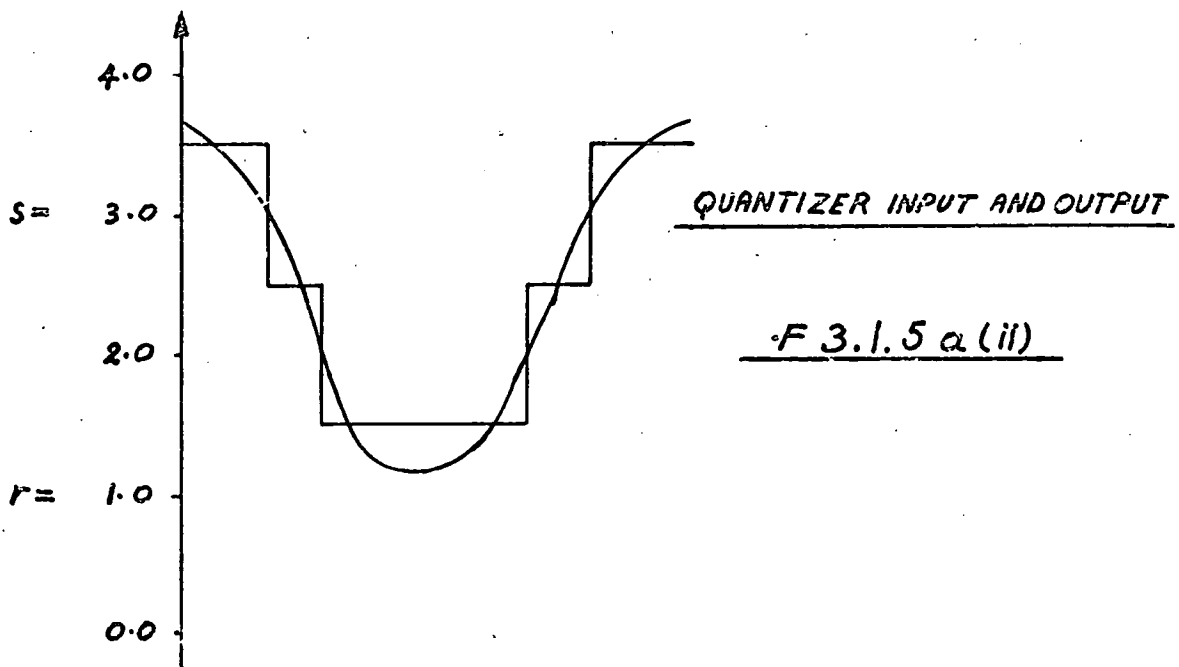
$$\begin{aligned} e_o = & e + \sum_{n=1}^{\infty} \frac{1}{n\pi} ((A[n,0] \sin(2\pi ne) + B[n,0] \cos(2\pi ne)) / (n\pi)) \\ & + p + \sum_{m=1}^{\infty} \left[\sum_{n=1}^{\infty} \frac{1}{n\pi} (A[n,m] \sin(2\pi ne) + B[n,m] \cos(2\pi ne)) / (n\pi) \right] \\ & \cos w_m t + \left[\sum_{n=1}^{\infty} \frac{1}{n\pi} (C[n,m] \sin(2\pi ne) + D[n,m] \cos(2\pi ne)) / (n\pi) \right] \sin w_m t \end{aligned}$$

The output component independent of w_m is re-expressed by the equation

$$\begin{aligned} E = & e + \frac{1}{2\pi} \int_0^{2\pi} p(x) d(2\pi x/T) \\ & + \sum_{n=1}^{\infty} \frac{1}{n\pi} \left(\frac{1}{2\pi} \int_0^{2\pi} \sin(2\pi n(e+p(x))) d(2\pi x/T) \right) / (n\pi), \\ = & e + \left(\frac{1}{2\pi} \right) \int_0^{2\pi} \left(p(x) + \sum_{n=1}^{\infty} \frac{1}{n\pi} \sin(2\pi n(e+p(x))) \right) / (n\pi) d(2\pi x/T), \end{aligned}$$

where for the purposes of integration e may be regarded as a constant.

This expression is in general a nonlinear function of e . The integral represents a periodic



F 3.1.5 a (iii)

function of e and must be zero to obtain a linear characteristic over a range of e exceeding one quantizer step interval.

In order to demonstrate the form of this expression consider the case when $p = a \cos(\theta)$. Now E may be recognised as the average value of the quantizer output over one cycle of p and may be expressed in the equivalent form

$$E = \frac{1}{2\pi} \int_0^{2\pi} \left(\frac{1}{2} + k\right) d\theta \text{ where the integer } k \text{ is defined by}$$

$$0 < e + a \cos \theta - k < 1.$$

An example of the type of waveform over which the integral is taken is shown in diagram F 3.1.5a.ii.

The average value is given by the expression

$$E = (r+s+1)/2 + \sum_{n=r+1}^{n=s} \arcsin((e-n)/a)/\pi \text{ where}$$

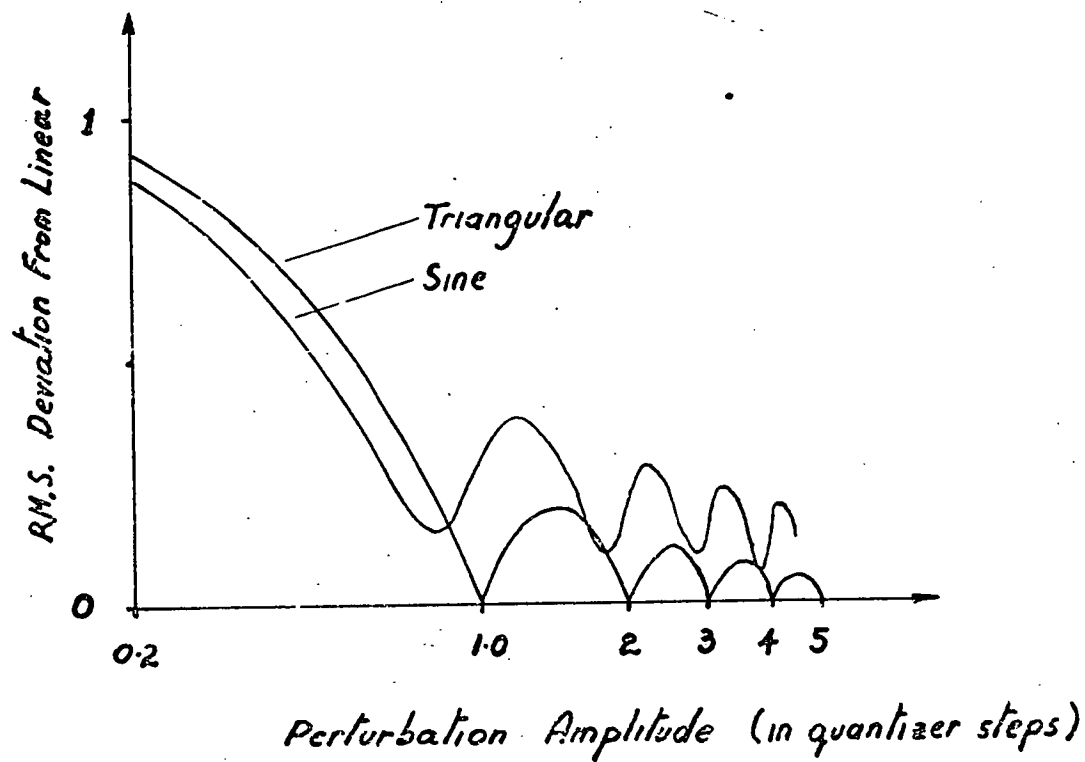
r and s are defined by the inequality pairs

$$0 < r+a-e < 1 \text{ and } 0 < s-a-e < 1.$$

When a is less than half a quantizer step this expression simplifies to

$$E = \begin{cases} k + \frac{1}{2} & \text{if } e-k > a \text{ or} \\ k - \frac{1}{2} & \text{if } e-k < -a \text{ or} \\ k + \arcsin((e-k)/a)/\pi & \text{otherwise, where } |e-k| < \frac{1}{2} \end{cases} \text{ defines } k.$$

This expression is plotted versus e in diagram F 3.1.5a.iii. The periodic nature of the nonlinearity is a prominent feature of the characteristic which is much nearer a linear characteristic than the basic quantizer characteristic. For a sinewave perturbation the r.m.s. error of the characteristic from a linear characteristic



LINEARITY AND PERTURBATION RELATIONSHIPS

F 3.1.5 a (iv)

has minima for peak to peak perturbation values close to integer multiples of a quantizer step. The value of the minima decrease as the sinewave amplitude increase. Diagram F 3.1.5aiv shows the form of variation with perturbation amplitude.

The conditions under which a perturbation gives a linear response are now examined in more detail. For a linear characteristic the integral,

$$E_1 = \frac{1}{2\pi} \int_0^{2\pi} \left(p(x) + \sum_{n=1}^{\infty} \frac{\sin(2\pi n(e+p(x)))}{n\pi} \right) d(2\pi x/T),$$

must be zero for all values of e . This may be re-expressed as

$$\begin{aligned} E_1 &= \frac{1}{2\pi} \int_0^{2\pi} p(x) d(2\pi x/T) \\ &+ \sum_{n=1}^{\infty} \left(\left(\frac{1}{2\pi} \int_0^{2\pi} \sin(2\pi n p(x)) d(2\pi x/T) \right) \cdot \cos(2\pi n e) \right. \\ &\left. + \left(\frac{1}{2\pi} \int_0^{2\pi} \cos(2\pi n p(x)) d(2\pi x/T) \right) \cdot \sin(2\pi n e) \right) / (n\pi). \end{aligned}$$

This expression is a fourier series in e and can be zero only if each of the co-efficients is zero and the d.c. component is zero. Thus p must satisfy the three integral equations

$$\begin{aligned} \int_0^{2\pi} p(x) \cdot d(2\pi x/T) &= 0, \quad \int_0^{2\pi} \cos(2\pi n p(x)) \cdot d(2\pi x/T) = 0. \\ \text{and} \quad \int_0^{2\pi} \sin(2\pi n p(x)) \cdot d(2\pi x/T) &= 0, \end{aligned}$$

The last two equations may be transformed by change of variable giving equations

$$\int_{p_{\min}}^{p_{\max}} \sin(2\pi np) \cdot D(p) \cdot dp = 0,$$

and

$$\int_{p_{\min}}^{p_{\max}} \cos(2\pi np) \cdot D(p) \cdot dp = 0, \text{ where } D(p) \text{ is the}$$

probability density function of p . This function is defined by the expression

$$D(P) = \lim_{dp \rightarrow 0} \left\{ \left(\text{of the probability that the amplitude of } p \text{ lies between the values } P+dp/2 \text{ and } P-dp/2 \right) / dp \right\}.$$

The two integrals are zero for all values of n if $D(p)$ is of constant value between the two limits of integration and if the two limits of integration differ by an integer.

When $D(p)$ has a constant value between the maximum and minimum values of p the average of p , the first of the three integrals, is the average of the maximum and minimum values of p . For this to be zero the maximum and minimum values of p must be equal in magnitude but opposite in sign.

The class of perturbation giving a linear characteristic to a quantizer are those satisfying the following three conditions.

(a) The probability that $p(x)$ exceeds a level P , must be a linear function of P provided P lies between the maximum and minimum values of $p(x)$.

(b) The difference between maximum and minimum values of $p(x)$ must be an integer multiple of one coder step.

(c) The maximum and minimum values of $p(x)$ must be symmetrical about zero.

Linearity and Perturbation Amplitude

A perturbation with linear distribution of amplitude but having a peak to peak amplitude not an integer multiple of a quantizer step will give a nonlinear characteristic. The shape of the nonlinearity is evaluated below for the case when the peak to peak amplitude, k , is not necessarily an integer.

The sampling wave is assumed to have the following properties;

$$D(p) = \begin{cases} 1/k & \text{for } p_{\min} < p < p_{\max} \\ 0 & \text{otherwise} \end{cases}, \text{ and} \\ p_{\max} = -p_{\min} = k/2.$$

The co-efficients for the fourier series are given by

$$A[n,0] = \int_{-k/2}^{k/2} \cos(2n\pi p) \cdot 1/k \cdot dp = \sin(n\pi k)/(n\pi k), \text{ and}$$

$$B[n,0] = \int_{-k/2}^{k/2} \sin(2n\pi p) \cdot 1/k \cdot dp = 0.$$

These co-efficients give the fourier series expression, for the Error, of

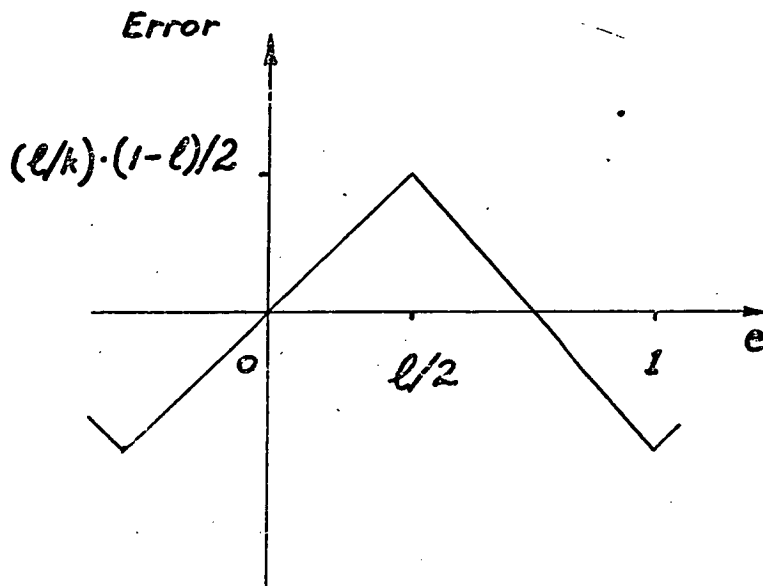
$$\text{Error} = 1/(k) \sum_{n=1}^{\infty} \sin(n\pi k) \cdot \sin(2n\pi e)/(n\pi)^2.$$

The piece-wise description of this error, as a function of e over the period

$-1/2 < e < 1-1/2$, where 1 is defined by

$0 < k-K=1 < 1$ for K an integer, is

$$\text{Error} = 1/(k) \cdot \begin{cases} e(1-1) & \text{for } 1/2 < e < 1/2, \\ 1/2(1-2e) & \text{for } 1/2 < e < 1-1/2 \end{cases}$$



ERROR AS A FUNCTION OF INPUT

F 3.1.5b

The function is sketched in diagram F 3.1.5b.

When k is near zero the error function approaches the error for a quantizer and is described by the second function, of the two, over the major portion of the period.

Perturbation Waveform and Linearity

The section, dealing with quantizer produced waveforms when a perturbation is added to the input, uses transformed integrals, representing the fourier co-efficients, with the probability density function as one term. The analysis below describes the low frequency terms of the quantizer output entirely with respect to the probability distribution function of the amplitude of the perturbation.

The low frequency component is described by

$$E = e + \frac{1}{2\pi} \int_0^{2\pi} p(x) dx + \sum_{n=1}^{\infty} A[n] \cos(2\pi n e) + B[n] \sin(2\pi n e),$$

where the co-efficients $A[n]$ and $B[n]$ are defined by the real and complex parts respectively of

$$E = \frac{1}{2\pi} \int_0^{2\pi} e^{-j\pi(2np(x)-1/2)} \cdot d\left(\frac{2\pi x}{T}\right) / (n\pi).$$

This expression may be transformed then re-arranged in the manner below

$$\begin{aligned} E &= \int_{p_{\min}}^{p_{\max}} e^{-j\pi(2np-1/2)} \cdot D(p) \cdot dp / (n\pi), \\ &= \int_{p_{\max}-k}^{p_{\max}} e^{-j\pi(2np-1/2)} \frac{dP(p)}{dp} \cdot dp / (n\pi), \end{aligned}$$

where the inequality $p_{\min} - 1 < p_{\max} - k < p_{\min}$ defines k .

Integration by parts yields

$$E = P(p) \cdot e^{-j\pi(2np-1/2)} \cdot (1/n\pi) \Bigg|_{p=p_{\max}-k}^{p=p_{\max}}$$

$$-2 \int_{2\pi(p_{\max}-k)}^{2\pi p_{\max}} e^{-j(2\pi p_{\max} n - \pi)} P(2\pi p/2\pi) \cdot d(2\pi p/2\pi)$$

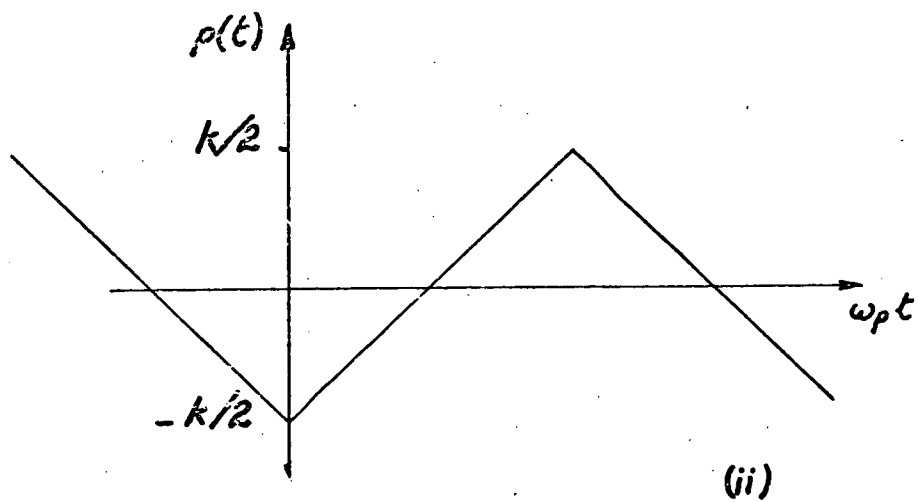
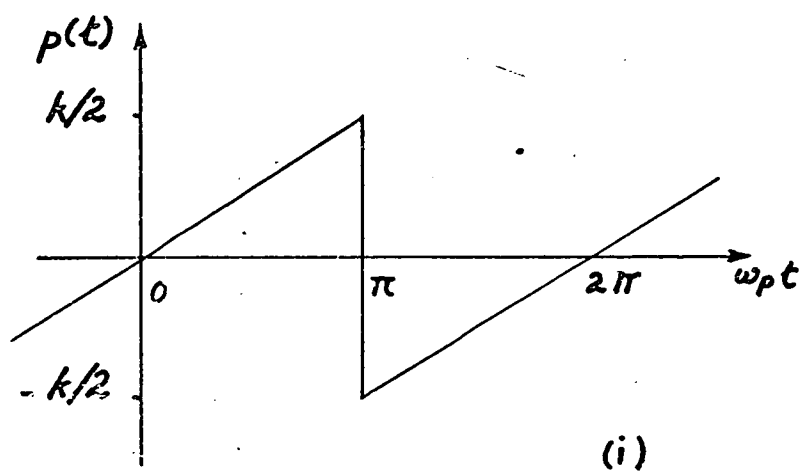
$$E = e^{-j(2\pi p_{\max}-1/2)/n\pi} \cdot \frac{1}{\pi} \int_{-2\pi p_{\max}}^{2\pi(1-p_{\max})} e^{jn\theta} \sum_{m=0}^{m=k-1} P(m-\theta/2\pi) d\theta,$$

where $\theta = -2\pi p$. These co-efficients define two recognisable fourier series. The first describes a ramp with positive unit steps at values of e removed from $-p_{\max}$ by any integer. The second is the a.c. component of the function within the integral. The function representing the low frequency component of the quantizer output is

$$E = e + \left(\frac{1}{2} - 1 - p_{\max}\right) - \sum_{m=0}^{m=k-1} P(m-e) + C \text{ where}$$

$-p_{\max} < e - E = 1 < 1 - p_{\max}$ for E an integer defined 1, and where

$$C = \frac{1}{2\pi} \int_0^{2\pi} p(x) \cdot d\left(\frac{2\pi x}{T}\right) + \frac{1}{2\pi} \int_{-2\pi p_{\max}}^{2\pi(1-p_{\max})} \sum_{m=0}^{m=k-1} P(m-\theta/2\pi) \cdot d\theta.$$



PERTURBATION WAVEFORMS

F 3.1.5 d

Natural Sampling and Multi-level Waveforms

Two examples of waveforms satisfying the linearity conditions are discussed below. The waveforms are a ramp or sawtooth and a symmetrical triangular wave. Both satisfy the requirements outlined previously provided they have no d.c. component and have peak to peak amplitudes of an integer multiple quantizer step.

A sawtooth waveform, shown in diagram F 3.1.5di, is described by the fourier series

$$p(t) = -k \sum_{n=1}^{n=\infty} \frac{\sin(n(w_p t - \pi))}{n\pi}.$$

The corresponding co-efficients for the waveform spectrum are evaluated by

$$\begin{aligned} A[n,m] + j B[n,m] &= \frac{1}{\pi} \int_{-\pi}^{\pi} \cos m\theta \cdot e^{j2\pi n(k\theta/2\pi)} d\theta \\ &= \begin{cases} 0 & \text{if } m \neq nk \\ 1 & \text{if } m = nk \end{cases}, \text{ where } w_m t = m w_p t = m\theta \end{aligned}$$

defines the variable θ used in the integral, and by

$$\begin{aligned} C[n,m] + j D[n,m] &= \frac{1}{\pi} \int_{-\pi}^{\pi} \sin m\theta \cdot e^{j2\pi n(k\theta/2\pi)} d\theta \\ &= \begin{cases} 0 & \text{if } n \neq mk \\ j & \text{if } n = mk \end{cases}. \end{aligned}$$

The expression giving the total waveform is

$$\begin{aligned} e_o &= e + p(t) + \sum_{n=1}^{n=\infty} ((\sin(2\pi n e) \cos(n w_p t k) + \cos(2\pi n e) \sin(n k w_p t)) / (n\pi)) \\ &= e + \sum_{n=1}^{n=\infty} (1/(n\pi) [\sin(n(k w_p t + 2\pi e)) - k \sin(n(w_p t - \pi))]). \end{aligned}$$

A symmetrical triangular wave, shown in diagram F 3.1.5dii, is described by the fourier series

$$p(t) = k \sum_{n=1,3,\dots}^{n=\infty} -4/(n\pi)^2 \cos(n w_p t)$$

The co-efficients of the output waveform fourier series are calculated below in two stages, one stage for each set

$$\begin{aligned}
 A[n,m] + jB[n,m] &= \frac{1}{\pi} \int_0^{\pi} \cos m\theta e^{j2\pi n(k(\theta/\pi - 1/2))} d\theta \\
 &\quad + \frac{1}{\pi} \int_{-\pi}^0 \cos m\theta e^{j2\pi n(k(3/2 - \theta/\pi))} d\theta \\
 &= (-1)^{kn} (2/\pi) \int_0^{\pi} \cos m\theta (\cos 2nk\theta + j\sin 2nk\theta) d\theta \\
 &= (-1)^{kn} \begin{cases} 1 & \text{if } m=2nk \\ \frac{2j}{k\pi} \cdot \frac{n}{n^2 - (m/2k)^2} & \text{if } m \text{ odd} \\ 0 & \text{all other } m \end{cases} \\
 C[n,m] + jD[n,m] &= \frac{1}{\pi} \int_0^{\pi} \sin m\theta e^{j2\pi n(k(\theta/\pi - 1/2))} d\theta \\
 &\quad + \frac{1}{\pi} \int_{-\pi}^0 \sin m\theta e^{j2\pi n(k(3/2 - \theta/\pi))} d\theta \\
 &= 0 \text{ for all } m.
 \end{aligned}$$

Thus the fourier series for the cosine term co-efficient of the waveform is

$$E[m] = \sum_{n=1}^{n=\infty} (-1)^{nk} / (n\pi) \begin{cases} \sin(2\pi ne) & \text{if } m = 2nk \\ \frac{2n}{k\pi} \cdot \frac{\cos(2\pi ne)}{n^2 - (m/2k)^2} & \text{if } m \text{ odd} \end{cases}$$

The series for m odd may be summed thus giving

$$\begin{aligned}
 E_1 &= \frac{2}{k\pi^2} \left\{ \frac{1}{2(m/2k)^2} - \frac{\pi}{2(m/2k)} \cdot \right. \\
 &\quad \left. \frac{\cos(m/2k \cdot 2\pi(e + k/2 + 1/2))}{\sin(\pi m/2k)} \right\}
 \end{aligned}$$

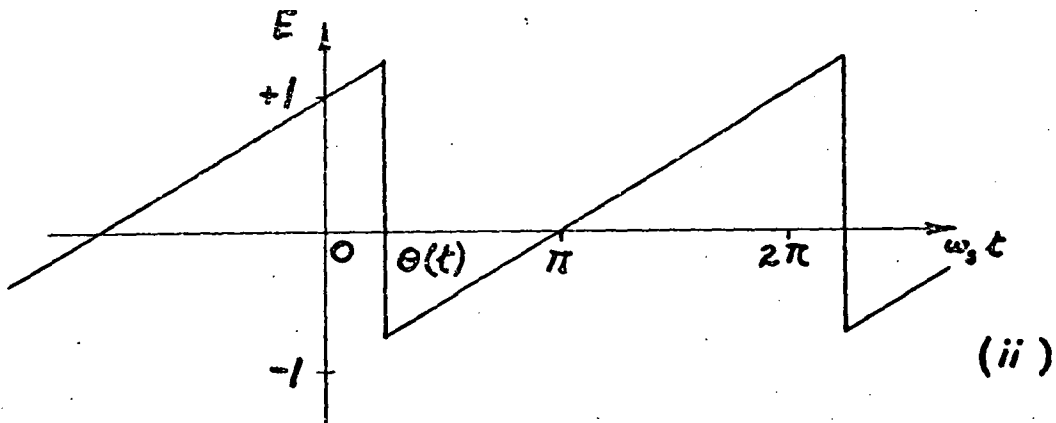
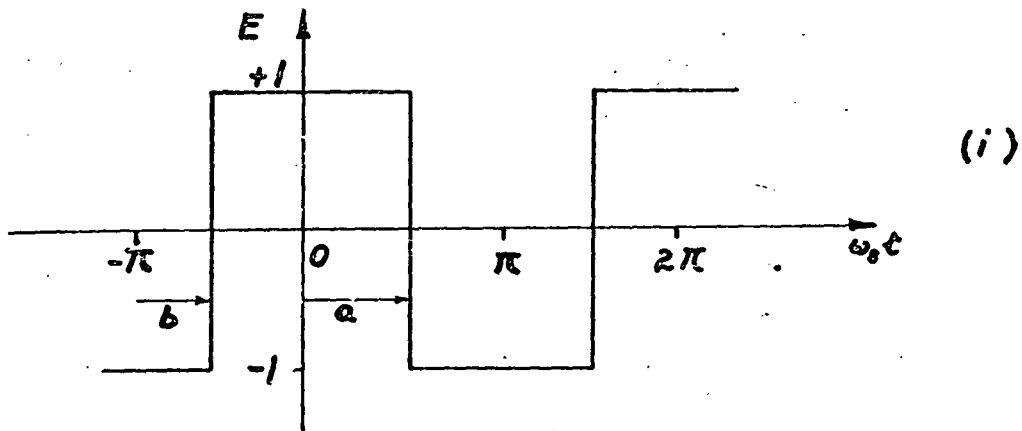
$$\begin{aligned}
 E_1 &= \frac{4k}{(m\pi)^2} - \frac{2}{m\pi} (\cos m\pi/k(e+1/2)) \cdot \\
 &\quad \cos(m\pi/2) - \sin(m\pi/k(e+1/2)) \cdot \\
 &\quad \sin(m\pi/2) / \sin(m\pi/2k) \\
 &= \frac{4k}{(m\pi)^2} + \frac{2}{m\pi} \sin(m\pi/k(e+1/2)) \cdot \\
 &\quad \sin(m\pi/2) / \sin(m\pi/2k).
 \end{aligned}$$

The first term corresponds with the series for $p(t)$ and cancels this. The remaining term forms the co-efficient for m odd. The waveform is described by

$$\begin{aligned}
 e_o &= e + \sum_{m=2,4}^{\infty} \left[\sin(m\pi(e+k/2)) \cdot \cos(mk\omega_p t) \cdot 2/(m\pi) \right] \\
 &+ \sum_{m=1,3}^{\infty} \left[\sin((m\pi/k)(e+\frac{1}{2})) \cdot \sin(m\pi/2) / \sin(m\pi/2k) \cdot \right. \\
 &\quad \left. \cos(m\omega_p t) \cdot 2/(m\pi) \right].
 \end{aligned}$$

For the case of $k = 1$ the expressions simplify to the form

$$e_o = e + \sum_{n=1}^{\infty} \left[(2/n\pi) \cdot \sin(\pi n(e+1/2)) \cdot \cos(n\omega_p t) \right].$$



A SWITCHING WAVE AND THE PERIODIC STEP FUNCTION

F 3.2.2 a

The Spectrum of Regular Sampling

The waveform shown in diagram F 3.2.2ai is described by the equation

$$E = \frac{a}{\pi} + \sum_{m=1}^{m=\infty} \frac{2}{m\pi} \sin(m(w_s t - a)) - \frac{b}{\pi} - \sum_{m=1}^{m=\infty} \frac{2}{m\pi} \sin(m(w_s t - \pi + b))$$

Two component waveforms, of the type shown in diagram F 3.2.2aai, may be combined to produce the above waveform. The following discussion will initially be concerned with the analysis of a single component waveform with a step controlled by regular sampling.

The equation describing the component is

$$E = \frac{w_s t}{\pi} - (1+2k) \text{ for } 2\pi k < w_s t - \theta(t) < 2\pi(k+1)$$

where k is an integer. This may be expressed as the complex fourier series

$$E = \frac{\theta(t)}{\pi} + \sum_{\substack{m=-\infty \\ m \neq 0}}^{m=\infty} j \frac{e^{jm(w_s t - \theta(t))}}{m\pi}$$

For regular sampling $\theta(t)$ is formed by sampling and holding $\phi(t)$, the input signal, at periodic intervals. In order to describe $\theta(t)$ in terms of $\phi(t)$, and $e^{-jm\theta(t)}$ in terms of $e^{-jm\phi(t)}$ use is made of the spectral descriptions of these functions. These are

$$\begin{aligned} \frac{\phi(t)}{\pi} &= \sum_{r=-\infty}^{r=\infty} a[r] e^{jw_r t} \text{ where} \\ a[r] &= \frac{1}{2\pi} \int_0^{2\pi} e^{-jx_r} \frac{\phi(X)}{\pi} dx, \text{ and} \\ e^{-jm\phi(t)} &= \sum_{q=-\infty}^{q=\infty} b[m, q] e^{+jw_q t} \text{ where} \\ b[m, q] &= \frac{1}{2\pi} \int_0^{2\pi} e^{-jx_q} e^{-jm\phi(X)} dx. \end{aligned}$$

There is one feature of the operation of sampling and holding a signal pertaining to the use of nonlinear processing of the signal before or after the operation. The output signal is independent of the order of the sample and hold operator and the nonlinear processor. Thus if the sample and hold operator is referred to as $H(x)$ then the equation below is valid

$$e^{-jmH(\phi(t))} = H(e^{-jm\phi(t)}).$$

The operation of sampling a signal of instants when $(w_s t - \phi) = 2m\pi$, then holding the value between instants results in a transformation of each spectral component of a waveform of the form below.

$$e^{j\omega t} \rightarrow \sum_{n=-\infty}^{n=\infty} e^{j\left[n(w_s t - \phi) + \omega t - \frac{\pi}{w_s}(\omega + n w_s)\right]} \cdot \frac{\text{Sin}\left(\frac{\pi}{w_s}(\omega + n w_s)\right)}{\frac{\pi}{w_s}(\omega + n w_s)}$$

The expression for the waveform when $\phi(t)$ replaces $\Theta(t)$ becomes

$$\begin{aligned} E = & \sum_{r=-\infty}^{r=\infty} \sum_{n=-\infty}^{n=\infty} \frac{a[r] \text{Sin}\left(\frac{w_r}{w_s} + n\right)}{\frac{\pi}{w_s}(\frac{w_r}{w_s} + n)} e^{j\left[n(w_s t - \pi - \phi) + w_r\left(t - \frac{\pi}{w_s}\right)\right]} \\ & + \sum_{\substack{m=-\infty \\ m \neq 0}}^{m=\infty} \sum_{q=-\infty}^{q=\infty} \sum_{n=-\infty}^{n=\infty} \frac{j}{m\pi} e^{j\left[m w_s t + n(w_s t - \pi - \phi) + w_q\left(t - \frac{\pi}{w_s}\right)\right]} \\ & \times b[m, q] \frac{\text{Sin}\left(\pi\left(\frac{w_q}{w_s} + n\right)\right)}{\frac{\pi}{w_s}\left(\frac{w_q}{w_s} + n\right)}. \end{aligned}$$

The term of the series corresponding to $w_q = 0$ is given by

$$E1 = \left[\sum_{\substack{n=-\infty \\ n \neq 0}}^{\infty} \sum_{\substack{m=-\infty \\ m \neq 0}}^{\infty} .0 \right] + \sum_{\substack{m=-\infty \\ m \neq 0}}^{\infty} \frac{j b[m, 0]}{\pi m} e^{j m w_s t}.$$

After substituting N for $m + n$ the term for the remaining values of w_q becomes

$$E2 = \sum_{N=-\infty}^{\infty} \sum_{m=-\infty}^{\infty} \frac{j \sin(\pi \frac{w_q}{w_s}) b[m, q]}{\pi^2 m ((\frac{w_q}{w_s} + N) - m)} e^{j [N(w_s t - \psi) + m\psi + w_q(t - \frac{\pi}{w_s})]}$$

The inner summation over the range of m may be made since $w_q/w_s \neq 0$. This is now carried out.

$$\begin{aligned} E3 &= \sum_{\substack{m=-\infty \\ m \neq 0}}^{\infty} \frac{b[m, q]}{\pi m} e^{j m \psi} \frac{\sin(\pi w_q/w_s)}{(w_q/w_s + N - m)} \\ &= \frac{1}{2\pi} \int_0^{2\pi} e^{-j x q} \frac{\sin(\pi w_q/w_s)}{\pi} \sum_{\substack{m=-\infty \\ m \neq 0}}^{\infty} \left\{ \cos(m(\phi(x) - \psi)) \right. \\ &\quad \left. - j \sin(m(\phi(x) - \psi)) \right\} / (m((w_q/w_s + N) - m)) \cdot dx \\ &= \frac{1}{2\pi} \int_0^{2\pi} e^{-j x q} \frac{\sin(\pi w_q/w_s)}{\pi} \cdot 2 \left[\sum_{m=1}^{\infty} \frac{\cos m(\phi(x) - \psi)}{(w_q/w_s + N)^2 - m^2} \right. \\ &\quad \left. - \frac{j}{(w_q/w_s + N)} \sum_{m=1}^{\infty} \left\{ \frac{\sin(m(\phi(x) - \psi))}{m} + \frac{m \sin(m(\phi(x) - \psi))}{(w_q/w_s + N)^2 - m^2} \right\} \right] \cdot dx \\ &= \frac{1}{2\pi} \int_0^{2\pi} e^{-j x q} \left[\frac{-\sin(\pi w_q/w_s)}{\pi (w_q/w_s + N)^2} + \frac{\cos((w_q/w_s + N)(\phi(x) - \psi - \pi))}{(w_q/w_s + N)(-1)N} \right. \\ &\quad \left. + \frac{j(\phi(x) - \psi + \pi) \sin(w_q/w_s \pi)}{\pi (w_q/w_s + N)} + j \frac{\sin(w_q/w_s \pi)}{(-1)^N (w_q/w_s + N)} \right] \cdot dx \end{aligned}$$

The terms corresponding to $w_q = 0$, those with $x_q = 0$, may be neglected leaving two components one of which corresponds with $a[r]$, the other to a modified form of $b[m,q]$ which will be referred to as $c[q,N]$. Thus

$$E3 = j \cdot a[r] \frac{\sin(\pi w_r/w_s)}{(\pi w_r/w_s + N)} + \frac{c[q,N]}{(\pi w_q/w_s + N)} e^{j[(w_q/w_s + N)(\pi - \phi) + N\pi]} \text{ where}$$

$$c[q,N] = \frac{1}{2\pi} \int_0^{2\pi} e^{-j(x_q)} \cdot e^{-j[(w_q/w_s + N)(\phi(x))]} \cdot dx.$$

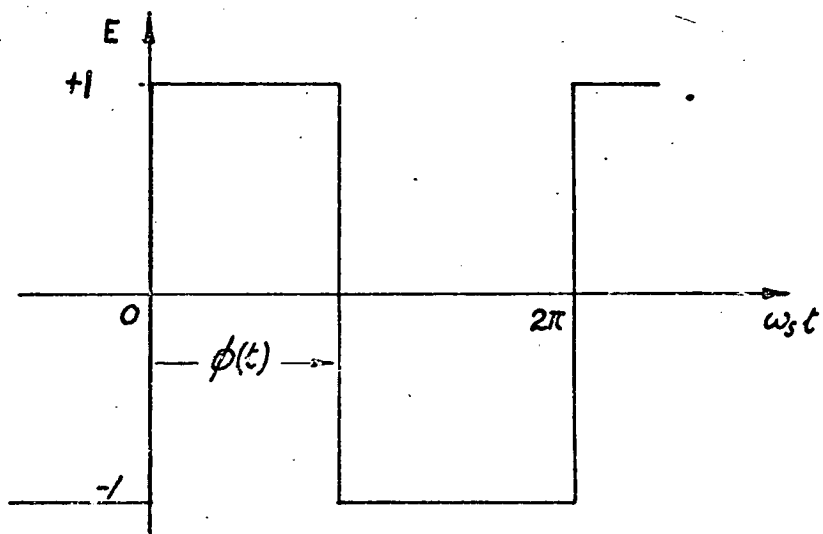
Substituting E3 back into E2 and combining this with E1 yields the waveform component as the expression below

$$E = a[0] + \sum_{\substack{N=-\infty \\ N \neq 0}}^{N=\infty} \frac{j b[N,0]}{\pi N} + \sum_{\substack{N=-\infty \\ N \neq 0}}^{N=\infty} \sum_{\substack{q=-\infty \\ q \neq 0}}^{q=\infty} \frac{j c[q,N]}{\pi (w_q/w_s + N)} e^{j[N w_s t + w_q (t - \phi/w_s)]}$$

Note: In the definitions of $b[m,q]$ and $c[q,m]$ and in the intervening algebra use is made of the symbols w_q and X . These are defined relative to the period, T , of $\phi(t)$ by the expressions

$$X = \frac{T}{2\pi} \cdot x \text{ and}$$

$$w_q = q \cdot 2\pi/T$$



A WAVE WITH ONE MODULATED EDGE

F 32.2 b

Example of Regular Sampling

For the example the waveform of diagram F 3.2.2b is analysed. The only variable phase step is the negative going step. The samples controlling this step are taken at zero phase angle. It is assumed that the delay before the step is linearly related to the input signal which is a sinewave signal. Thus the phase of the step is controlled by the expression

$$\phi(t) = \pi(1 + a \sin w_m t)$$

The calculations of $b[m,0]$, $a[0]$, and $c[q,N]$ are carried out below.

$$\begin{aligned} b[m,0] &= \frac{1}{2\pi} \int_0^{2\pi} e^{-j m \pi} \cdot e^{-j m a \pi \sin(x)} dx \\ &= e^{-j m \pi} J_0(m a \pi) \end{aligned}$$

$$\begin{aligned} c[q,N]_{q \neq 0} &= \frac{1}{2\pi} \int_0^{2\pi} e^{-j q x} \cdot e^{-j \left[\frac{w_m}{w_s} q + N \right] (\pi) (1 + a \sin(x))} dx \\ &= e^{-j \left(N + \frac{w_m}{w_s} q \right) \pi} \cdot \frac{1}{2\pi} \int_0^{2\pi} e^{-j \left[\left[\frac{w_m}{w_s} \right] \cdot q + N \right] \pi a \sin(x) + q \cdot x} dx \\ &= e^{-j \left(N + \frac{w_m}{w_s} q \right) \pi} J_q(\pi a \left[N + q \frac{w_m}{w_s} \right]) \end{aligned}$$

$$a[0] = \pi / \pi = 1$$

The total waveform is then described by the equation

$$\begin{aligned} E &= 1 + \sum_{\substack{N=-\infty \\ N \neq 0}}^{N=\infty} \frac{j e^{j N (w_s t - \pi)}}{\pi^2 N} J_0(N a \pi) \\ &+ \sum_{N=-\infty}^{N=\infty} \sum_{\substack{q=-\infty \\ q \neq 0}}^{q=\infty} \frac{j J_q(\pi a \left[q \frac{w_m}{w_s} + N \right])}{(q \cdot \frac{w_m}{w_s} + N) \pi} e^{j \left[(w_s t - \pi) \cdot N + q \frac{w_m}{w_s} (t - \pi / w_s) \right]} \\ -1 &+ \sum_{N=1}^{N=\infty} \frac{2}{N \pi} \sin N w_s t \end{aligned}$$

$$\begin{aligned}
 E &= \sum_{q=1}^{q=\infty} \frac{2aJq(\pi a(qw_m/w_s)) \sin w_m \cdot q(t-\pi/w_s)}{(\pi a(qw_m/w_s))} \\
 &- \sum_{N=1}^{N=\infty} 2 \cdot \left\{ \frac{\sin N(w_s t - \pi)}{N\pi} \operatorname{Jo}(Na\pi) - \frac{\sin(Nw_s t)}{N\pi} \right\} \\
 &- \sum_{N=1}^{N=\infty} \sum_{\substack{q=-\infty \\ q \neq 0}}^{q=\infty} \frac{2aJq(\pi a(qw_m/w_s + N)) \sin(N(w_s t + \pi) + w_s \cdot q(t - \pi/w_s))}{\pi a(qw_m/w_s + N)}
 \end{aligned}$$

Two Input Components to a Regular Sampler

The same basic waveform as the previous example is generated with a new phase controlling function of the form

$$\phi(t) = \pi(1 + a \sin w_a t + b \sin w_b t).$$

In this example only the passband, or more exactly the non sideband, terms of the output are examined.

$$c[q, 0] = \frac{1}{2\pi} \int_0^{2\pi} e^{-jqx} e^{-j(w_s)(\phi(x))} dx.$$

The above expression defines $c[q, 0]$ but this term may be evaluated more directly as the term of the following expression with complex frequency w_q .

$$\begin{aligned} E &= e^{-j(w_q \pi / w_s)(1 + a \sin w_a t + b \sin w_b t)} \\ &= \sum_{m=-\infty}^{\infty} \sum_{r=-\infty}^{\infty} e^{-j(w_q \pi / w_s + m w_a t + r w_b t)}. \end{aligned}$$

$$J_m(\pi a w_q / w_s) \cdot J_r(\pi b w_q / w_s)$$

$$\text{Thus } c[q, 0] = e^{-j w_q \pi / w_s} J_m(\pi a w_q / w_s) \cdot J_r(\pi b w_q / w_s)$$

$$\text{where } w_q = m w_a + r w_b.$$

The output components of the regular sampler corresponding to the input signal are

$$E = \sum_{m=-\infty}^{\infty} \sum_{r=-\infty}^{\infty} \frac{j J_m(\pi a w_q / w_s) \cdot J_r(\pi b w_q / w_s) \cdot e^{j w_q (t - \pi / w_s)}}{\pi (w_q / w_s)}$$

$$\text{where } w_q = m w_a + r w_b \neq 0.$$

An I levelled switching wave has levels $V_i(w_s t)$ and associated level control functions $g_i(w_s t)$. Immediately prior to a phase of $A_i(e)$ the i th level control function is zero. After this instant and until a phase of $B_i(e)$ is reached the function is unity. The function reverts to zero when the phase passes $B_i(e)$.

The general description of the waveform is

$$E = \sum_{i=1}^{i=I} g_i(w_s t) \cdot V_i(w_s t).$$

The components with frequency $rw_s t$ have amplitudes a_r and b_r defined by

$$a_r + jb_r = \frac{E(r)}{2\pi} \int_0^{2\pi} \sum_{i=1}^{i=I} g_i(w_s t) \cdot V_i(w_s t) \cdot e^{jrw_s t} dw_s t.$$

By moving the summation outside the integral and taking advantage of the zero and unity values of $g_i(w_s t)$ the expression becomes

$$a_r + jb_r = \sum_{i=1}^{i=I} \frac{E(r)}{2\pi} \int_{A_i}^{B_i} V_i(w_s t) \cdot e^{jrw_s t} \cdot dw_s t.$$

$$\text{Thus } E = a_0 + \sum_{r=1}^{r=\infty} a_r \cos(rw_s t) + b_r \sin(rw_s t),$$

$$\text{where } a_0 = \frac{1}{2\pi} \sum_{i=1}^{i=I} \int_{A_i}^{B_i} V_i(w_s t) \cdot dw_s t \quad \text{and}$$

$$a_r + jb_r = \frac{1}{\pi} \sum_{i=1}^{i=I} \int_{A_i}^{B_i} V_i(w_s t) \cdot e^{jrw_s t} \cdot dw_s t.$$

The r^{th} harmonic is described by

$$E = a_r \cos(rw_s t) + b_r \sin(rw_s t).$$

By replacing a_r and b_r by their respective integrals the r^{th} harmonic may be re-expressed as

$$E = \frac{1}{\pi} \sum_{i=1}^{i=I} \int_{A_i}^{B_i} V_{si}(\theta) \cdot \cos(r(w_s t - \theta)) \cdot d\theta.$$

Now the i^{th} waveform level may be described by the Fourier series

$V_{si}(w_s t) = \sum_{h=0}^{h=H} a(h, i) \cdot \cos(hw_s t + \phi(h, i))$, so that the r^{th} harmonic is given by

$$\begin{aligned} E &= \frac{1}{\pi} \sum_{i=1}^{i=I} \int_{A_i}^{B_i} \sum_{h=0}^{h=H} a(h, i) \cos(h\theta + \phi(h, i)) \cdot \cos(r(w_s t - \theta)) \cdot d\theta \\ &= \frac{1}{\pi} \sum_{i=1}^{i=I} \sum_{h=0}^{h=H} \sum_{s=\pm 1} \bar{a}(h, i) / 2 \cdot \int_{A_i}^{B_i} \cos(r(w_s t - \theta) + s(h\theta + \phi(h, i))) \cdot d\theta \\ &= \frac{1}{\pi} \sum_{i=1}^{i=I} \sum_{h=0}^{h=H} \sum_{s=\pm 1} \bar{a}(h, i) / (2(sh - r)) \left[\sin(r(w_s t - \theta) + s(h\theta + \phi(h, i))) \right]_{\theta=A_i}^{\theta=B_i}. \end{aligned}$$

This expression describes the r^{th} harmonic of the switching wave in terms of the inverse sampling functions and the switching waveform levels.

Consider the sum

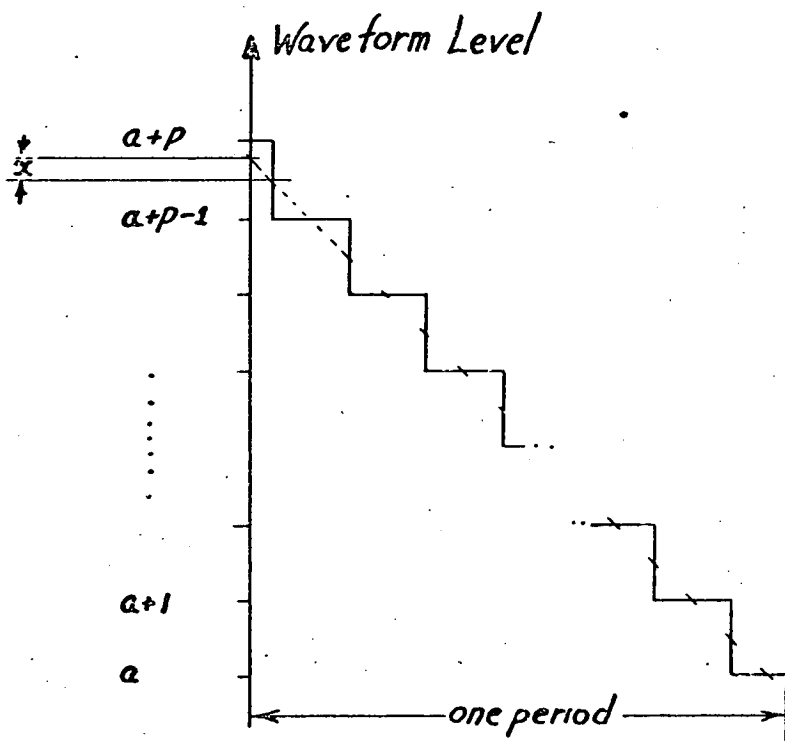
$$\begin{aligned}
 E &= \sum_{r=0}^{r=R-1} e^{jr\pi n/R}, \\
 &= \frac{1-e^{j\pi n}}{1-e^{jn\pi/R}}, \quad (\text{sum of a G.P.})(\text{if } R \neq 1), \\
 &= (1-e^{j\pi n}) \cdot \frac{(1-e^{-jn\pi/R})}{(2-e^{jn\pi/R}-e^{-jn\pi/R})}, \\
 &= (1-(-1)^n) \cdot \frac{2j\sin(n\pi/2R)(\cos n\pi/2R - j\sin n\pi/2R)}{4.(\sin(n\pi/2R))^2}, \\
 &= \begin{cases} (j\cos(n\pi/2R) + \sin(n\pi/2R))/\sin(n\pi/2R) & \text{if } n \text{ odd} \\ 0 & \text{if } n \text{ even} \end{cases}.
 \end{aligned}$$

Thus the sum for $R > 1$ and n even is

$$\begin{aligned}
 E &= \sum_{r=0}^{r=R-1} \cos n(\theta - r\pi/R), \\
 &= \sum_{r=0}^{r=R-1} \cos n\theta \cos(r\pi/R) + \sin n\theta \sin(r\pi/R), \\
 &= (\cos n\theta \sin(n\pi/2R) + \sin n\theta \cos(n\pi/2R))/\sin(n\pi/2R), \\
 &= \sin(n(\theta + n\pi/2R))/\sin(n\pi/2R).
 \end{aligned}$$

Thus

$$\begin{aligned}
 E &= \sum_{r=0}^{r=R-1} \sum_{n=1}^{n=\infty} \frac{(4/\pi n) \sin(n\pi/2(E\theta+1)) \cdot \cos(n(w_s t - (B+A)/2 - r\pi/R))}{(B+A)/2 - r\pi/R)} \\
 &= \sum_{n=1,3,5,\dots}^{n=\infty} \left\{ \frac{(4/\pi n) \sin(n\pi/2(E\theta+1)) \cdot \sin(n(w_s t + \pi/2R - (B+A)/2))/\sin(n\pi/2R)}{(B+A)/2 - r\pi/R)} \right\}
 \end{aligned}$$



F 4.1.1.2

A switching wave is produced by a quantizer when the input signal has a perturbation superimposed. The mean of the switching wave is linearly related to the average input signal provided the perturbation component has maximum and minimum symmetrical about zero, a uniform distribution of amplitude between maximum and minimum values, and peak to peak amplitude of an integer number of quantizer steps. The energy of such a switching wave may be described in terms of the average input or output over a range of one quantizer step.

One quantizer step is taken as a unit of output and input amplitude. The perturbation is p units peak to peak. The peak combined quantizer input exceeds a critical level of the quantizer input by an amount x , a fraction of one unit.

An example of the situation described forms diagram F 4.1.1.2. The description which follows applies to any form of perturbation obeying the restrictions above but is oriented to the situation shown in the diagram.

The average value of the switching wave is $a+(p-1)/2+x$. The energy of the switching wave is given by

$$\begin{aligned}
 E &= 1/p \left\{ a^2(1-x) + (a+1)^2 + \dots + (a+p-1)^2 + (a+p)^2 \cdot x \right\} \\
 &= 1/p \left\{ a^2 + a^2 + a^2 + \dots + a^2 + a^2 \right. \\
 &\quad \left. + 0 + 2a + 4a + \dots + 2(p-2)a + 2(p-1)a \right. \\
 &\quad \left. + 0 + 1^2 + 2^2 + \dots + (p-2)^2 + (p-1)^2 + p(2a+p) \cdot x \right\} \\
 &= (a+(p-1)/2)^2 + x(2(a+(p-1)/2)+1) + (p^2-1)/12
 \end{aligned}$$

The energy of the average is $(a+(p-1)/2+x)^2$.

The energy of the remainder of the switching wave is

$$E_2 = x - x^2 + (p^2 - 1)/12. \text{ Note that } 0 \leq x \leq 1.$$

Alternative Expression for r^{th} Harmonic - a.c.
Levelled Waveforms

$$\begin{aligned}
 ER &= \frac{1}{2\pi} \sum_{s=\pm 1} \frac{1}{(s-r)} \left\{ \sin(rw_s t + (s-r)B + s(\phi - \pi/2)) \right. \\
 &\quad \left. - \sin(rw_s t + (s-r)A + s(\phi - \pi/2)) \right\} , \\
 &= \frac{1}{2\pi} \sin(r(w_s t - (B+A)/2)) \sum_{s=\pm 1} \left\{ \cos(r(A-B)/2 + sB + s(\phi - \pi/2)) \right. \\
 &\quad \left. - \cos(r(B-A)/2 + sA + s(\phi - \pi/2)) \right\} / (s-r) \\
 &+ \frac{1}{2\pi} \cos(r(w_s t - (B+A)/2)) \sum_{s=\pm 1} \left\{ \sin(r(A-B)/2 + sB + s(\phi - \pi/2)) \right. \\
 &\quad \left. - \sin(r(B-A)/2 + sA + s(\phi - \pi/2)) \right\} / (s-r) , \\
 &= \frac{1}{\pi} \left\{ \sin(r(w_s t - (B+A)/2)) \sin((A+B)/2 + \phi - \pi/2) \sum_{s=\pm 1} \frac{s \cdot \sin((r-s)(B-A)/2)}{(r-s)} \right. \\
 &\quad \left. + \cos(r(w_s t - (B+A)/2)) \cos((A+B)/2 + \phi - \pi/2) \sum_{s=\pm 1} \frac{\sin((r-s)(B-A)/2)}{r-s} \right\} .
 \end{aligned}$$

A 4.1.2.2a

Harmonics for Thyristor Amplifier Switching Waves

These tables describe 2,3,6, and 12 phase waveform for both diode clamped and continuous current modes of operation.

Each page is headed by an integer specifying the number of phases and either the character D or the character C to specify diode clamped or continuous operation.

Each page has 10 columns. The contents of these columns, from right to left, are as follows.

The phase of thyristor turn on, relative to the previous zero crossing of the sine wave supply voltage, measured in degrees.

The d.c. component of the waveform relative to the peak supply waveform amplitude.

The remaining columns contain the amplitude descriptions of the first eight harmonics of the switching wave. Each amplitude is specified by two numbers. The upper and lower numbers of the N th such column of the table describing an M phase wave are the cosine and sine components of the $N \times M$ th harmonic of the supply wave frequency.

The range of output states for which diode clamped and continuous waves are identical are omitted from the former tables.

Only the positive output range of continuous current waveforms are described since step phases and harmonic amplitudes for negative outputs may be found by negating the tabulated values for the step phase and cosine amplitudes .

C 2

+90.00	+.00	-.00000	-.00000	-.00000	.00000	.00000	-.00000	-.00000	.00000
		-.84883	.33953	-.21827	.16168	-.12861	.10685	-.09141	.07989
+80.90	+.10	-.19671	.18704	-.17155	.15115	-.12702	.10054	-.07316	.04634
		-.81761	.27863	-.13065	.05157	-.00119	-.03207	.05291	-.06386
+71.60	+.20	-.37368	.30096	-.19878	.09006	.00257	-.06267	.08385	-.07045
		-.72632	.11848	.05965	-.12446	.12214	-.07981	.02249	.02814
+61.80	+.30	-.51117	.29204	-.05457	-.09395	.11247	-.04012	-.04206	.07046
		-.58242	-.07744	.18541	-.10771	-.01598	.08537	-.06885	.00255
+51.00	+.40	-.58945	.15729	.12302	-.10274	-.04186	.08109	.00207	-.06127
		-.39965	-.21880	.11925	.07367	-.09124	-.01911	.07120	-.01088
+38.20	+.50	-.58877	-.03613	.12124	.07171	-.03971	-.06426	.00057	.04822
		-.20131	-.21751	-.06611	.07159	.06974	-.01715	-.05681	-.01165
+19.50	+.60	-.48939	-.12754	-.04926	-.00436	.02302	.03391	.03014	.01653
		-.03170	-.05491	-.06382	-.05714	-.03828	-.01400	.00795	.02150
+1.000	+.64	-.42461	-.08508	-.03658	-.02041	-.01306	-.00910	-.00673	-.00519
		-.00000	-.00001	-.00001	-.00002	-.00002	-.00003	-.00003	-.00004

C 3

+119.9	+.00	.00000	.00000	.00000	.00000	-.00000	.00000	.00000	.00000
		.62025	.28354	.18607	.13880	.11076	.09217	.07894	.06904
+113.0	+.10	.19563	.18286	.16269	.13669	.10682	.07529	.04437	.01612
		.58432	.21404	.08749	.01736	-.02606	-.05199	-.06459	-.06661
+106.0	+.20	.36543	.27240	.14908	.03087	-.05207	-.08463	-.07040	-.02800
		.48080	.04026	-.10197	-.13112	-.09403	-.02894	.03020	.06086
+98.70	+.30	.48555	.21976	-.02701	-.12400	-.06967	.03165	.07336	.03261
		.32240	-.14771	-.17145	-.03702	.07620	.07987	.00564	-.05546
+91.00	+.40	.53639	.05056	-.15887	-.03255	.09214	.02904	-.06311	-.02753
		.13035	-.24403	-.03720	.11717	.03033	-.07531	-.02818	.05381
+82.70	+.50	.50537	-.13378	-.07442	.10990	-.02302	-.05854	.05401	.00862
		-.06565	-.18419	.12879	.01392	-.08528	.04441	.03228	-.05434
+73.40	+.60	.39114	-.19810	.10150	-.02177	-.03390	.05811	-.05226	.02644
		-.22741	-.00309	.07951	-.09338	.06848	-.02571	-.01510	.03953
+62.10	+.70	.21137	-.07304	.04966	-.04129	.03704	-.03433	.03228	-.03053
		-.30826	.13806	-.08750	.06208	-.04632	.03534	-.02711	.02063
+44.60	+.80	.02604	.07335	-.04646	.00880	.01683	-.02374	.01524	-.00041
		-.25303	.04328	.02157	-.03584	.02357	-.00258	-.01345	.01771
+30.80	+.83	.00001	.04746	-.00002	-.01176	.00003	.00532	-.00004	-.00307
		-.20695	.00001	.02087	-.00002	-.00758	.00004	.00395	-.00005

C 6

+150.0	+.00	-.00000	.00000	-.00000	.00000	-.00000	.00000	-.00000	.00000
		-.32740	.16027	-.10643	.07972	-.06373	.05309	-.04550	.03981
+143.9	+.10	-.18707	.15127	-.10075	.04658	.00014	-.03121	.04311	-.03756
		-.26656	.05023	.03247	-.06415	.06338	-.04259	.01374	.01250
+137.9	+.20	-.30196	.09201	.06253	-.07342	-.00248	.05012	-.02393	-.02504
		-.10697	-.12689	.08320	.02620	-.06227	.01354	.03751	-.02980
+131.6	+.30	-.29816	-.09401	.05276	.07421	.00912	-.04424	-.03239	.01386
		.08947	-.11971	-.08619	.01489	.05982	.02416	-.02858	-.03516
+125.2	+.40	-.17448	-.13203	-.09620	-.05800	-.02171	.00774	.02686	.03436
		.24180	.06147	-.00963	-.04334	-.05365	-.04759	-.03140	-.01124
+118.4	+.50	.01758	.03758	.04031	.04023	.03910	.03737	.03521	.03273
		.27984	.13145	.08128	.05475	.03770	.02550	.01622	.00888
+111.0	+.60	.18453	.12163	.03091	-.03316	-.04949	-.02652	.00844	.02861
		.17888	-.02867	-.07690	-.05245	-.00325	.03137	.03438	.01186
+102.8	+.70	.22602	-.03845	-.05932	.04086	.02024	-.03496	-.00082	.02654
		-.01053	-.10247	.04173	.03573	-.03837	-.00912	.03095	-.00541
+93.00	+.80	.10028	-.06177	.05081	-.04266	.03467	-.02653	.01844	-.01073
		-.15490	.06300	-.02864	.00910	.00352	-.01175	.01667	-.01891
+79.50	+.90	-.07388	.05086	-.00026	-.02424	.01668	.00386	-.01479	.00869
		-.09573	-.02101	.03601	-.01150	-.01340	.01738	-.00369	-.01010
+60.80	+.95	-.05477	-.01355	-.00611	-.00352	-.00232	-.00166	-.00127	-.00101
		-.00001	-.00002	-.00003	-.00005	-.00006	-.00007	-.00008	-.00009

+165.0	+.00	-.00000	.00000	.00000	.00000	-.00000	.00000	.00000	.00000
		-.16592	.08253	-.05497	.04121	-.03296	.02747	-.02354	.02060
+159.1	+.10	-.15430	.05377	.02637	-.04054	.00669	.02315	-.01856	-.00608
		-.05867	-.06205	.04790	.00609	-.03210	.01452	.01429	-.01957
+153.3	+.20	-.10646	-.07969	-.04655	-.01380	.01099	.02325	.02272	.01306
		.12279	.01352	-.02704	-.03793	-.03035	-.01353	.00389	.01537
+147.3	+.30	.08018	.07020	.05214	.03113	.01094	-.00528	-.01549	-.01902
		.13632	.03545	-.00497	-.02393	-.02944	-.02563	-.01623	-.00486
+141.1	+.40	.14714	-.03971	-.03332	.03417	.00442	-.02487	.00892	.01424
		-.03747	-.06420	.03764	.01589	-.02982	.00351	.01959	-.01234
+134.6	+.50	-.00446	.00962	-.01051	.01076	-.01081	.01076	-.01066	.01052
		-.14324	.07056	-.04624	.03389	-.02630	.02111	-.01729	.01432
+127.6	+.60	-.13158	.00575	.04345	-.00418	-.02590	.00388	.01832	-.00376
		-.01208	-.06537	.00459	.03249	-.00398	-.02148	.00381	.01593
+119.9	+.70	-.00789	-.00055	.00081	.00128	.00150	.00161	.00168	.00173
		.11731	.05833	.03882	.02908	.02323	.01933	.01654	.01444
+110.9	+.80	.09609	-.02657	-.01968	.02294	.00006	-.01533	.00826	.00694
		-.01987	-.04065	.02564	.00778	-.01937	.00506	.01110	-.00991
+99.40	+.90	-.05806	.02699	.00647	-.01698	.00657	.00704	-.00941	.00118
		-.03875	-.02116	.02185	-.00177	-.01197	.00893	.00255	-.00844
+75.80	+.99	.01403	-.00363	.00171	-.00104	.00071	-.00053	.00041	-.00033
		.00002	-.00004	.00007	-.00009	.00011	-.00012	.00014	-.00015

D 2

+180.0	+.00	-.00000	.00000	.00000	.00000	.00000	.00000	.00000	.00000	.00000
		.00000	.00000	.00000	-.00000	.00000	-.00000	-.00000	.00000	
+133.3	+.10	.08750	-.08596	-.09415	.01045	.03704	-.02085	-.03280	.01230	
		-.16358	-.11924	.02633	.05556	-.01789	-.03538	.01546	.02508	
+111.8	+.20	.00262	-.19912	.06280	-.02097	-.04146	.04441	-.03853	.00542	
		-.33958	.02324	.06125	-.07435	.04840	-.00868	-.02363	.03624	
+93.20	+.30	-.17567	-.07874	.01771	-.04545	.02820	-.03823	.02952	-.03416	
		-.42231	.16557	-.10288	.07256	-.05406	.04127	-.03174	.02425	
+75.10	+.40	-.36841	.09338	-.12360	.05951	-.04012	-.00191	.01686	-.03487	
		-.38318	.09270	-.00610	-.03557	.05225	-.05158	.03933	-.02104	
+55.10	+.50	-.49666	.06694	.01593	-.07661	.00809	.03125	-.03425	-.01066	
		-.23494	-.08973	.08351	.00404	-.05090	.02561	.02125	-.03180	
+27.70	+.60	-.48145	-.10277	-.01438	.02174	.02251	.00331	-.01598	-.02123	
		-.04286	-.06341	-.05317	-.02197	.00957	.02396	.01731	-.00027	
+1.400	+.64	-.42461	-.08508	-.03658	-.02041	-.01306	-.00910	-.00672	-.00519	
		-.00001	-.00001	-.00002	-.00003	-.00003	-.00004	-.00005	-.00005	

D 3

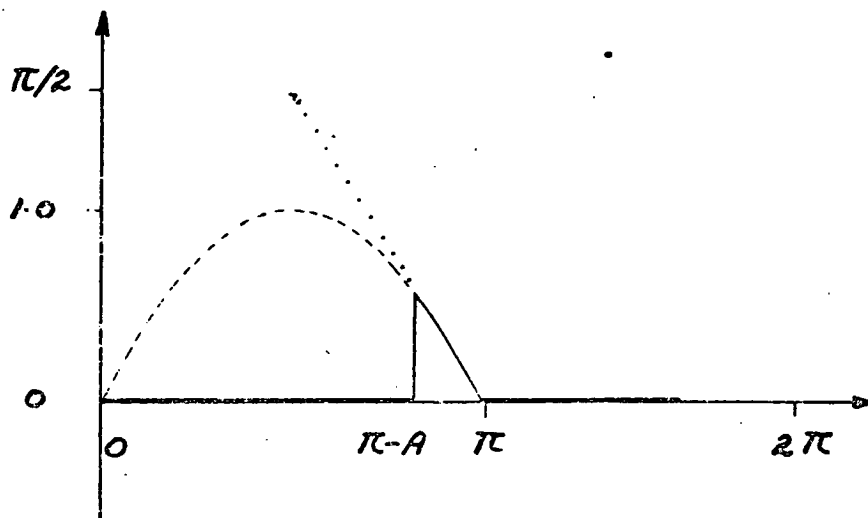
+180.0	+.00	.00000	.00000	.00000	.00000	.00000	.00000	.00000	.00000
		.00000	.00000	.00000	-.00000	.00000	.00000	.00000	.00000
+142.2	+.10	-.04476	-.11492	.02573	.04203	.02471	-.02224	-.02502	-.00564
		.17337	-.05325	-.06501	-.00796	.03357	.02637	-.00652	-.02412
+125.5	+.20	.10265	-.08692	-.05033	-.06486	-.04708	-.04595	-.03169	-.02615
		.29910	.12018	.06177	.02971	.00885	-.00548	-.01520	-.02129
+111.8	+.30	.29781	.09420	.10888	.06661	.05336	.02284	.00741	-.01266
		.28398	.09187	.02386	-.01303	-.03341	-.04215	-.04199	-.03534
+99.30	+.40	.44042	.10419	-.00101	-.08038	-.04367	.00837	.04548	.02551
		.14885	-.09395	-.10523	-.02867	.04104	.05128	.01212	-.02844
+87.20	+.50	.47428	-.07175	-.08606	.03602	.05291	-.04280	-.02284	.03437
		-.04492	-.15736	.04373	.06771	-.04140	-.03519	.03804	.01694
+75.10	+.60	.38727	-.18539	.08164	-.00287	-.04164	.04840	-.02705	-.00417
		-.22126	-.00915	.07702	-.07738	.04140	.00285	-.03296	.03844
+62.20	+.70	.21137	-.07303	.04964	-.04125	.03699	-.03425	.03217	-.03039
		-.30824	.13801	-.08743	.06198	-.04620	.03520	-.02696	.02046
+60.00	+.72	.17925	-.04113	.01810	-.01022	.00659	-.00463	.00346	-.00269
		-.31012	.14177	-.09304	.06940	-.05538	.04609	-.03947	.03452

D 6

+180.0	+.00	.00000	.00000	.00000	.00000	.00000	.00000	.00000	.00000	.00000
		.00000	-.00000	.00000	.00000	.00000	.00000	-.00000	-.00000	
+153.5	+.10	-.04719	-.05281	.03429	-.03845	.02566	-.02102	.01023	-.00460	
		-.15365	.06070	-.02568	.00602	.00616	-.01339	.01685	-.01734	
+142.2	+.20	-.22983	.08406	-.04449	-.01128	.03000	-.03336	.01378	.00512	
		-.10650	-.01593	.05274	-.04824	.02222	.00648	-.02358	.02365	
+133.3	+.30	-.28246	-.06256	.05872	.03628	-.03022	-.03580	.00881	.02791	
		.07898	-.10615	-.04288	.04246	.03694	-.01777	-.03161	.00371	
+125.5	+.40	-.17383	-.12972	-.09190	-.05230	-.01597	.01182	.02780	.03142	
		.24037	.05942	-.01095	-.04258	-.05000	-.04112	-.02317	-.00307	
+120.0	+.48	-.02748	-.00688	-.00316	-.00186	-.00126	-.00094	-.00074	-.00061	
		.28354	.13880	.09217	.06904	.05519	.04598	.03940	.03447	

D 12

+180.0	+.00	.00000	.00000	.00000	.00000	.00000	.00000	.00000	.00000
		-.00000	.00000	.00000	-.00000	-.00000	.00000	.00000	.00000
+161.3	+.10	-.11551	.04453	-.02695	-.00052	.01208	-.01758	.01116	-.00271
		-.05686	-.00358	.02412	-.02545	.01555	-.00200	-.00862	.01250
+153.5	+.20	-.10562	-.07690	-.04204	-.00920	.01345	.02195	.01762	.00592
		.12139	.01203	-.02677	-.03469	-.02439	-.00668	.00900	.01656
+150.0	+.26	-.00378	-.00109	-.00060	-.00042	-.00034	-.00030	-.00027	-.00026
		.16027	.07972	.05309	.03981	.03184	.02653	.02274	.01990



Linear Approximation to the Diode Clamped Wave

F4.1.2.2b

The Harmonic Amplitudes of a Periodic Triangular Pulse

The pulse is a straight line approximation of a wave produced from a sinewave and is illustrated by diagram F 4.1.2.2b.

The quadrature and inphase components of the r^{th} harmonic are specified by the real and complex parts of the expression

$$E = 1/\pi \int_{\pi-A}^{\pi} (\pi-\theta) e^{jr\theta} d\theta$$

$$= (-1)^r/\pi \left[j\theta e^{-jr\theta}/r + e^{-jr\theta}/r^2 \right]_{\theta=A}^{\theta=0}$$

Thus the r^{th} harmonic is described by the expression

$$E = (-1)^r/\pi \left[\begin{aligned} &\cos(r\omega_s t) \cdot (\theta \sin(r\theta)/r + \cos(r\theta)/r^2) \\ &+ \sin(r\omega_s t) \cdot (\theta \cos(r\theta)/r - \sin(r\theta)/r^2) \end{aligned} \right]_{\theta=A}^{\theta=0},$$

$$= (-1)^r/\pi \left[\begin{aligned} &(\theta/r) \sin(r\omega_s t + \theta) + (1/r^2) \cos(r\omega_s t + \theta) \end{aligned} \right]_{\theta=A}^{\theta=0},$$

$$= (-1)^r/\pi \left[\begin{aligned} &(1/r^2) \cos r\omega_s t - (1/r^2) \cos(r\omega_s t + A) - \\ &(A/r) \sin(r\omega_s t + A) \end{aligned} \right],$$

$$= (-1)^{r+1} (A/r\pi) \left[\begin{aligned} &\sin(r\omega_s t + A) - (2/rA) \cdot \sin(r\omega_s t + A/2) \cdot \\ &\sin rA/2 \end{aligned} \right].$$

Notice that this expression is that for the harmonics of the sum of a sawtooth waveform and an asymmetric triangular wave. The waveform above may be visualised in these terms quite readily.

For $rA \gg 2$ the harmonic has magnitude $A/r\pi$ and phase $r(A+\pi) + \pi$.

It should be remembered that the original waveform was approximated with the proviso that A is small so the true restriction on the final approximation is that r is large compared to $2/A$.

If the waveform corresponds to one of the levels of a symmetrically m -level waveform then the r^{th} harmonic of the total waveform is described by the expression

$$E = (-1)^{rm+1} (A/\pi r) \sin rm(\omega_s t + A) \quad .$$

Phase Modulation

A function, $f(w_m t)$, is used to phase modulate a sinusoidal function of time. The following sequence of equivalent expressions enable the co-efficients of a Fourier series representing the phase modulated signal to be described.

$$\begin{aligned} E &= e^{j(w_c t + f(w_m t))} \\ &= e^{jw_c t} (\cos(f(w_m t)) + j \sin(f(w_m t))) \\ &= e^{jw_c t} \left(\sum_{r=-\infty}^{r=\infty} a[r] e^{jr\theta} + j b[r] e^{jr\theta} \right), \end{aligned}$$

$$\text{where } a[r] = \frac{1}{2\pi} \int_0^{2\pi} \cos(f(w_m t)) \cdot e^{-jrw_m t} dw_m t$$

$$\text{and } b[r] = \frac{1}{2\pi} \int_0^{2\pi} \sin(f(w_m t)) \cdot e^{-jrw_m t} dw_m t.$$

$$\text{Thus } e^{j(w_c t + f(w_m t))} = \sum_{r=-\infty}^{r=\infty} (a[r] + j b[r]) e^{j(w_c t + rw_m t)}$$

$$\text{Thus } \sin(w_c t + f(w_m t)) = \sum_{r=-\infty}^{r=\infty} (a[r] \sin(w_c t + rw_m t) + b[r] \cos(w_c t + rw_m t)).$$

$$\text{where } a[r] + j b[r] = \frac{1}{2\pi} \int_0^{2\pi} e^{j(r(x) - rx)} dx.$$

Sinusoidal Phase Modulation Notes

$$e^{jz\sin(\theta)} = \cos(z\sin(\theta)) + j\sin(z\sin(\theta))$$

$$= 2 \sum_{n=0}^{n=\infty} E(n) J_n(z) \begin{cases} \cos(n\theta), & n \text{ even} \\ j\sin(n\theta), & n \text{ odd} \end{cases}$$

$$= \sum_{n=-\infty}^{n=\infty} J_n(z) e^{jn\theta}$$

$$e^{jz\cos(\theta)} = \cos(z\cos(\theta)) + j\sin(z\cos(\theta))$$

$$= 2 \sum_{n=0}^{n=\infty} E(n) J_n(z) \begin{cases} (-1)^{n/2} \cos n\theta, & n \text{ even} \\ j(-1)^{n-1/2} \sin n\theta, & n \text{ odd} \end{cases}$$

$$= \sum_{n=-\infty}^{n=\infty} J_n(z) e^{jn(\theta+\pi/2)}$$

Multiple Signal Phase Modulation

The following passage indicates the form of the spectrum of the signal

$$E = e^{ja_0} \left\{ a_0 + \sum_{m=1}^{m=\infty} \sin(w_m t + p_m) \right\} \quad \text{and is based}$$

on the identity

$$e^{ja_m \sin(w_m t + p_m)} = \sum_{r=-\infty}^{r=\infty} J_r(a_m) e^{jr(w_m t + p_m)}.$$

Substituting the identity into the expression gives

$$E = e^{ja_0} \prod_{m=1}^{m=M} \sum_{r=-\infty}^{r=\infty} J_r(a_m) e^{jr(w_m t + p_m)}$$

This expression is the sum of terms each having the form

$$\left\{ \prod_{m=1}^{m=M} J_{i[m,r]}(a_m) \right\} e^{j(a_0 + \sum_{m=1}^{m=M} i[m,r] (w_m t + p_m))}$$

where $i[m,r]$ may have any integer value. These terms may be grouped according to their complex frequency.

If S_q terms have frequency w_q then the expression becomes

$$E = \sum_{w_q=-\infty}^{w_q=\infty} e^{jw_q t} \sum_{S_q} \left\{ e^{ja_0} \prod_{m=1}^{m=M} J_{i[m,r]}(a_m) \cdot e^{j \sum_{m=1}^{m=M} i[m,r] \cdot p_m} \right\}$$

where

$$w_q = \sum_{m=1}^{m=M} i[m,r] w_m \quad \text{defines } i[m,r] \text{ for each of the}$$

S_q terms.

If each of the M components of the modulating signal are non commensurate with each other then S_q will be unity. Under any other circumstances S_q is infinite.

The fourier series co-efficients may also be evaluated by the integral

$$I[q] = \frac{1}{2\pi} \int_0^{2\pi} e^{-jw_q t} \cdot e^{j(a_0 + \sum_{m=1}^{m=M} \bar{Z} \sin(w_m t + p_m))} d(2\pi t/T),$$

where T is the period of the modulating signal. The two methods are useful in different situations. If the frequencies are not commensurate then the Bessel function series is convenient and easily applied while the integral expression is difficult to apply. If the frequencies are all commensurate then the reverse is true. If the modulation is not entirely of one form or the other then the best approach is to use the integral method for the commensurate part then to use the co-efficients so formed in a similar manner to the Bessel functions of the first method.

Multiple Phase Modulation

A modulation angle is composed of I individual components each of which have known co-efficients when used as a modulation separately. Thus the component $(f_i(w_i t))$ satisfies the equation

$$e^{j(w_c t + f_i(w_i t))} = \sum_{r=-\infty}^{r=\infty} C[i, r] e^{j(w_c t + r w_i t + \theta[i, r])} ,$$

where

$$e^{j\theta[i, r]} \cdot C[i, r] = \frac{1}{2\pi} \int_0^{2\pi} e^{j(f_i(x) - rx)} dx .$$

The total modulation angle is described by

$$f(t) + f_o = f_o + \sum_{i=1}^{i=I} f_i(w_i t) .$$

The spectrum of the phase modulated signal for this angle is given by the expressions

$$\begin{aligned} E &= e^{j(w_c t + f_o + \sum_{i=1}^{i=I} f_i(w_i t))} \\ &= e^{j(w_c t + f_o)} \cdot \prod_{i=1}^{i=I} e^{j f_i(w_i t)} \\ &= e^{j(w_c t + f_o)} \prod_{i=1}^{i=I} \sum_{n=-\infty}^{n=\infty} C[i, n] e^{j(n w_i t + \theta[i, n])} . \end{aligned}$$

The co-efficient of a term with exponent

$$E1 = w_c t + f_o + \sum_{i=1}^{i=I} R[i] w_i t, \text{ is given by}$$

$$E2 = \left(\prod_{i=1}^{i=I} C[i, R[i]] \right) \cdot e^{j\theta[i, R[i]]} , \text{ where } R[i] \text{ is}$$

the i^{th} element of a set of I integers. The integers of

this set may have any value. It is convenient to associate with each set of integers another integer, q , such that the variable w_q , defined by

$$w_q = \sum_{i=1}^{i=I} R[i, q] w_i, \text{ satisfies the condition}$$

$$w_0 = 0, \text{ and } w_q \geq w_{q-1}.$$

The complete series may now be described by

$$\begin{aligned} E &= e^{j(w_c t + f_0 + \sum_{i=1}^{i=I} f_i(w_i, t))} \\ &= \sum_{q=-\infty}^{q=\infty} e^{j(w_c t + f_0 + w_q + \sum_{i=1}^{i=I} \theta[i, R[i, q]])} \cdot \prod_{i=1}^{i=I} C[i, R[i, q]]. \end{aligned}$$

Fourier Series from Periodically Sampled Data

A periodic function, f , is sampled at uniform intervals over one period so that an even number of values $2N$ are known. The function is defined by a Fourier series so that the n^{th} sample, $f(n)$, is described by

$$f(n) = \sum_{i=0}^{i=I} \left\{ A[i] \cos(2\pi n/N) + B[i] \sin(2\pi n/N) \right\} ,$$

where $A[i]$ and $B[i]$ are the Fourier series co-efficients. A new set of co-efficients related to these are defined by the $2N$ samples from the expression

$$D[m] + jE[m] = \sum_{n=1}^{n=2N} (\cos(m\pi n/N) + j\sin(m\pi n/N)) \cdot f(n) .$$

By substituting the actual Fourier series for $f(n)$ into this expression the relationships between these co-efficients and those of the Fourier series may be found.

For $m=0, 2N, 4N, \dots$, the expression becomes

$$D[m] + jE[m] = \sum_{n=1}^{n=2N} \left\{ (1 + 0 \cdot j) \sum_{i=1}^{i=I} (A[i] \cdot \cos(2\pi n/N) + B[i] \cdot \sin(2\pi n/N)) \right\} .$$

$$\therefore D[m] = \sum_{i=0}^{i=I} A[i] \left(\sum_{n=1}^{n=2N} \cos(2\pi ni/N) \right) + B[i] \left(\sum_{n=1}^{n=2N} \sin(2\pi ni/N) \right) .$$

Now

$$\sum_{n=1}^{n=2N} \cos(2\pi ni/N) = \begin{cases} 2N & \text{for } i=0, 2N, \dots, K \cdot 2N \\ 0 & \end{cases} ,$$

where K is an integer defined by $I - 2N < K \cdot 2N \leq I$, while

A

For the expressions, $D[m]$ and $E[m]$, to define the i^{th} harmonic of the Fourier series they must each be functions of only the appropriate co-efficient of the i^{th} harmonic, and not of any other harmonic. This requires that the other harmonics in these expressions be zero. There is often more than one way of choosing the number of samples to satisfy this requirement but the usual method is to choose $2N$ large enough for the terms of these expressions corresponding to r greater than zero to be zero. This is true when

$$2n-m > I \quad \text{when } m=i \text{ is also true.}$$

For these conditions

$D[i] = A[i]$, $E[i] = B[i]$ and the minimum number of samples possible for these results is

$$2N = I + i + 1.$$

If the i^{th} harmonic is estimated from $2N$ samples, where

$$I < 2N < 2I, \text{ by evaluating } D[i] \text{ and } E[i], \text{ then}$$

the actual numbers obtained are related to the Fourier co-efficients by

$$\begin{aligned} D[i] &= A[i] + A[2N-i], \text{ and} \\ E[i] &= B[i] - B[2N-i]. \end{aligned}$$

The last term of these series are not zero if $i > 2N - I$. The differences between $D[i]$ and $A[i]$ and between $E[i]$ and $B[i]$ introduced by the latter terms of these series are referred to as aliasing errors. A special case

$$\sum_{n=1}^{n=2N} \sin(2\pi ni/N) = 0.$$

$$\therefore D[m] = 2N \sum_{r=0}^{r=k} A[r \cdot 2N]$$

and $E[m] = 0$, when m is a multiple of $2N$.

For m not a multiple of $2N$

$$\begin{aligned} D[m] + jE[m] &= \sum_{n=1}^{n=2N} \sum_{i=0}^{i=I} (A[i] \cos(2\pi ni/N) + B[i] \sin(2\pi in/N)) \\ &\quad (\cos(m\pi n/N) + j\sin(m\pi n/N)) , \\ &= \sum_{i=0}^{i=I} \sum_{s=1, -1} \left\{ A[i] \left(\sum_{n=1}^{n=2N} (\cos((m+si)n\pi/N) \right. \right. \\ &\quad \left. \left. + j\sin((m+si)n\pi/N)) \right) \right. \\ &\quad \left. - s \cdot B[i] \left(\sum_{n=1}^{n=2N} (\sin((m+si)n\pi/N) - j\cos((m+si) \right. \right. \\ &\quad \left. \left. n\pi/N)) \right) \right\} / 2 \end{aligned}$$

The sine summations are zero. The cosine summations are zero except when

$m+si=r \cdot 2N$ for $0 \leq r \leq K$, then they are unity.

The complete expressions for $D[m]$ and $E[m]$ for all m are thus

$$D[m] = \begin{cases} 2N \sum_{r=0}^{r=k} A[2N \cdot r] & \text{for } m \text{ any multiple of } 2N, \\ N(A[m] + \sum_{r=1}^{r=k} \sum_s^{+1, -1} A[2N \cdot r + s \cdot m]) & \text{otherwise,} \end{cases}$$

$$\text{and } E[m] = \begin{cases} 0 & \text{for } m \text{ any multiple of } 2N, \\ N(B[m] + \sum_{r=1}^{r=k} \sum_s^{+1, -1} s \cdot B[2N \cdot r + s \cdot m]) & \text{otherwise,} \end{cases}$$

where k is defined by $I - 2N < K \cdot 2N \leq I$.

Numerical Accuracy of Summation

A function is formed from the sum of n numbers. If each number has an error compared to the correct value required for the function then the actual number representing the function will have an error equal to the sum of the errors of the individual numbers. Now the exact errors of an answer derived from a numerical process with a variable control are not known but the statistical nature of the error frequently is. From a statistical description of the error it is possible to estimate the statistical nature of the error of a sum of such answers.

If a group of n numbers with the same statistical properties are summed then the total of the numbers has a distribution which approaches a normal distribution with root mean square deviation $\sigma\sqrt{n}$ as n approaches infinity where σ is the mean square deviation of the numbers summed. Ho.145.

Thus for a number error with a uniform distribution between $+a$ and $-a$ the function error, when a large group of numbers is summed, will approach a normal distribution with a root mean square error of $a\sqrt{n/3}$ when n approaches infinity. The maximum possible error is $a.n$.

As an example consider the situation where 100 numbers are added to form a fourier series and each number has a random error of one unit in the ninth decimal place due to the error in sine and cosine evaluations used in forming each term. For this case the maximum possible error from the addition process is one unit in the seventh decimal place while the root mean square error is less than six units in the ninth decimal place.

where aliasing error may be compensated occurs when the value of $2N = 2I$ and the sine component of the I^{th} harmonic is known to be zero. For this case

$$D[i] = 2 A[i] \quad \text{and} \quad E[i] = 0.$$

The physical situation may be appreciated since the $2I$ samples correspond to the zero positions of the sine component at this harmonic while they correspond to the peaks of the cosine component.

From the numbers above it is clear that numerical error in the summation process is insignificant unless very large numbers are summed to obtain a very small total. For the numbers to be accurate to within one percent the allowable dynamic range is of the order of five decimal places if numbers have nine decimal places.

An Estimate of Passband Energy

The passband energy of a d.c. levelled switching wave using single edged modulation controlled by natural sampling of a sinewave input when two sidebands fall within the amplifier passband.

The energy of the sidebands within the passband is

$$ES = \sum_{r=1}^{r=\infty} 2/(r\pi)^2 \sum_{i=0,1} J_{n-i}^2(r\pi x) \text{ where } n = \text{entier}(rw_m/w_s)$$

Now $J_s(y)$ may be re-expressed as

$$J_s(y) = \sqrt{2/(\pi y)} \cdot \left\{ \cos(y - s\pi/2 - \pi/4) + O(y) \right\},$$

where $O(y)$ has a value of order $1/y$. The energy associated with one harmonic is thus

$$\begin{aligned} ERS &= 2/(r\pi)^2 \cdot 2/(\pi(r\pi x)) \cdot \left\{ \begin{aligned} &\cos^2(r\pi x - n\pi/2 - \pi/4) \\ &+ \cos^2(r\pi x - n\pi/2 - 3\pi/4) \\ &+ E \end{aligned} \right\} \\ &= 4 \left\{ 1+E \right\} / (r^3 \pi^4 x), \end{aligned}$$

where E is of the order of $1/\pi x r$. For x large this last term may be neglected so that the total passband energy is approximately given by

$$EPB = \sum_{r=1}^{r=\infty} \frac{4}{r^3 \pi^4 x} = .049361/x.$$

The Low Amplitude Performance Asymptote

Each harmonic of the modulation waveform contributes individually to the sidebands of a phase modulated wave. Each sideband is the sum of an infinite number of components. These components are contributed by all the harmonics of the sampling wave. The frequency of a component, which matches that of the sideband, is a sum of multiples of each of the harmonic frequencies. The amplitude of a component is a product of Bessel functions whose indicies and numbers correspond to the amplitudes of the harmonics and multiples referred to above, respectively. The phase of the component is related to the individual harmonic phases as the component frequency is to the individual frequencies.

To describe the situation more concisely the following symbols are used to represent the variables introduced above.

The band limited modulating signal is assumed to possess no finite harmonics beyond the N^{th} .

The s^{th} harmonic has amplitude x_s and a phase ψ_s and is associated with the integer multiple m_s .

The component under examination is separated from the carrier frequency by the R^{th} harmonic of the modulating waveform, has amplitude A and phase ϕ . The variables are related to those of the modulating waveform by the equations below.

$$R = \sum_{s=1}^{s=N} m_s \cdot s$$

$$\phi = \sum_{s=1}^{s=N} m_s \cdot \psi_s$$

$$A = \prod_{s=1}^{s=N} J_{m_s}(x_s)$$

For small modulation waveforms x_s is small for all s . This allows an approximation to be made for A since for small x the function $J_{m_s}(x_s)$ is approximated by

$$J_{m_s}(x_s) = (-1)^{m_s} (x/2)^{|m_s|} / m_s!$$

(This is the limit of equation 807.22 DW.)

Substitution of this into the equation for A gives

$$A = \prod_{s=1}^{s=N} (-1)^{m_s} (x_s/2)^{|m_s|} / m_s!$$

For small values of x_s the components with the largest contributions to a sideband are those with the minimum values of m_s since $\bar{Z} A$ is of the form

$$|\bar{Z} A| = (-x/2)^{\sum_{s=1}^{s=N} |m_s|} \left\{ \bar{Z} \prod_{s=1}^{s=N} \left\{ (a_s)^{|m_s|} / m_s! \right\} \angle \psi \cdot m_s \right\},$$

where a_s is the value of x_s for a modulating waveform of unit amplitude and where x is the modulation amplitude.

To find the gradient of curves such as diagram D 4.2.2.4b the lowest power of x_m must be found. Thus the search is for the smallest value of $\sum_{s=1}^{s=N} |m_s|$ for a given value of R .

Call the index of x_m I .

$$I = \sum_{s=1}^{s=N} |m_s| ; R = \sum_{s=1}^{s=N} m_s * s.$$

The object of the search is to find those sets of N integers, m_1, m_2, \dots, m_N , which satisfy the equation for R but give a minimum value for I .

Suppose $I=1$; what values of R are possible? For this value of I all values of m_s are zero except

one which must have unit modulus so that

$$0 < |R| < N$$

Suppose $I=2$. There are two possibilities; there may be two non zero values of m_s , both unity, or one value with modulus 2. The range of R is thus

$$0 \leq |R| \leq 2N$$

For higher values of I there are many more possibilities but the restriction is of the same form as below

$$0 \leq |R| \leq NI.$$

This is the reciprocal of the problem posed. The problem was to find the minimum value of I consistent with a particular value of R . From the equation above the restriction below follows and answers the problem.

$$I \geq R/N = 1 + \text{entier}(R/N)$$

Substituting this into the equation for the sideband amplitude, \bar{Z}_A , yields

$$\bar{Z}_A = (-x/2)^{(1+\text{entier}(R/N))} * \left\{ \bar{Z} \left\{ \prod_{s=1}^{s=N} a_s^{m_s} / m_s! \right\} < \psi \cdot m_s \right\} .$$

Thus the S/N power ratio for passband sidebands with x_m small is of the form

$$S/N = (x/2)^{2 \cdot \text{entier}(R/N)} \cdot K(a_s, m_s, R, \psi_s)$$

where

$$w_s/w_n = R = w_s/w_p.$$

Plotted on log curves the ratio has slopes of
20 entier (R/N) db/decade.

The number of terms contributing to K are too complex to evaluate for more than a small number of modulation harmonics unless there is some simplifying pattern. The complexity is due to the multiplicity of the sets of m numbers which satisfy the minimum index criterion.

A switching wave with m symmetrically phased levels, each with waveshape $F(w_s t)$ is described by

$$E = 2a[0, \phi] + \sum_{r=1}^{r=\infty} a[r, \phi] \cos(mr w_m t) + b[r, \phi] \sin(mr w_m t),$$

where ϕ is the mean phase of the two edges of a segment of the switching wave and where a and b are defined by the equation

$$a[r, \phi] + j b[r, \phi] = m/\pi \cdot \int_{\theta=\phi-\pi/m}^{\theta=\phi+\pi/m} F(\theta) \text{Cis}(mr\theta) d\theta.$$

For a sinewave supply this expression may be evaluated analytically to yield the expression

$$E = m/\pi \cdot \left[\sin(\pi/m) \sin \phi + \sum_{i=\pm 1} \sum_{r=1}^{r=\infty} \left\{ \frac{i \sin((\pi/m)(mr-i))}{(mr-i)} \sin(mr w_s t - (mr-i)\phi) \right\} \right].$$

For linear amplification ϕ and the control signal are related by the equation

$$m/\pi \cdot \sin(\pi/m) \sin(\phi) = f(w_m t) \text{ for } |f(w_m t)| \leq m/\pi \sin(\pi/m).$$

Substituting for ϕ yields the waveform expression

$$\begin{aligned} E &= f(w_m t) + m/\pi \cdot \sum_{i=\pm 1} \sum_{r=1}^{r=\infty} \left\{ \frac{i \sin((\pi/m)(mr-i))}{(mr-i)} \sin(mr w_s t - (mr-i) \arcsin((\pi/m)f(w_m t)/\sin(\pi/m))) \right\} \\ &= f(w_m t) + \sum_{i=\pm 1} \sum_{r=1}^{r=\infty} \frac{(-1)^r}{mr-i} \sin(mr w_s t - (mr-i) \arcsin((\pi/m)f(w_m t)/\sin(\pi/m))) \end{aligned}$$

m phased, sine wave supply. a.c. levelled wave expression reduction

$$E = (a/2) [0, \phi] + \sum_{r=1}^{\infty} \frac{m}{\pi} \int_{\theta=\phi-\pi/m}^{\theta=\phi+\pi/m} \cos(mr w_m t - mr \theta) \sin \theta d\theta$$

r^{th} harmonic is described by

$$\begin{aligned} ER &= m/2\pi \int_{\theta=\phi-\pi/m}^{\theta=\phi+\pi/m} \left\{ \sin(mr(w_s t - \theta) + \theta) - \sin(mr(w_s t - \theta) - \theta) \right\} d\theta \\ &= m/2\pi \left[\frac{\sin(mr w_s t - (mr-1)\theta)}{(mr-1)} - \frac{\sin(mr w_s t - (mr+1)\theta)}{(mr+1)} \right]_{\theta=\phi-\pi/m}^{\theta=\phi+\pi/m} \\ &= m/\pi \left[\frac{\sin((mr-1)\pi/m) \sin(mr w_s t - (mr-1)\phi)}{(mr-1)} \right. \\ &\quad \left. - \frac{\sin((mr+1)\pi/m) \sin(mr w_s t - (mr+1)\phi)}{(mr+1)} \right] \\ (1/2)a[0, \phi] &= m/2\pi \int_{\theta=\phi-\pi/m}^{\theta=\phi+\pi/m} (\sin \theta) * 1 d\theta \\ &= m/2\pi \left\{ \sin(mr\theta + \theta) - \sin(mr\theta - \theta) \right\}_{\theta=\phi+\pi/m} d\theta \\ &= m/2\pi \left[\cos \theta \right]_{\theta=\phi-\pi/m} \\ &= m/\pi \sin \pi/m \sin \phi . \end{aligned}$$

Filters, Triangular Sampling Waves, and Linearity

For triangular sampling waves, the d.c. supplied amplifier of the example and a general feedback filter the solution for the input signal is

$$E_{in} = a.DC - \sum_{n=1}^{n=\infty} \frac{2An}{(n\pi)} \sin(\phi_n) \cdot (2k-1) \\ + (1-2k) \cdot \sin(\phi_n) \cos(n\pi(1+DC)) + \cos(\phi_n) \cdot \sin(n\pi(1+DC))$$

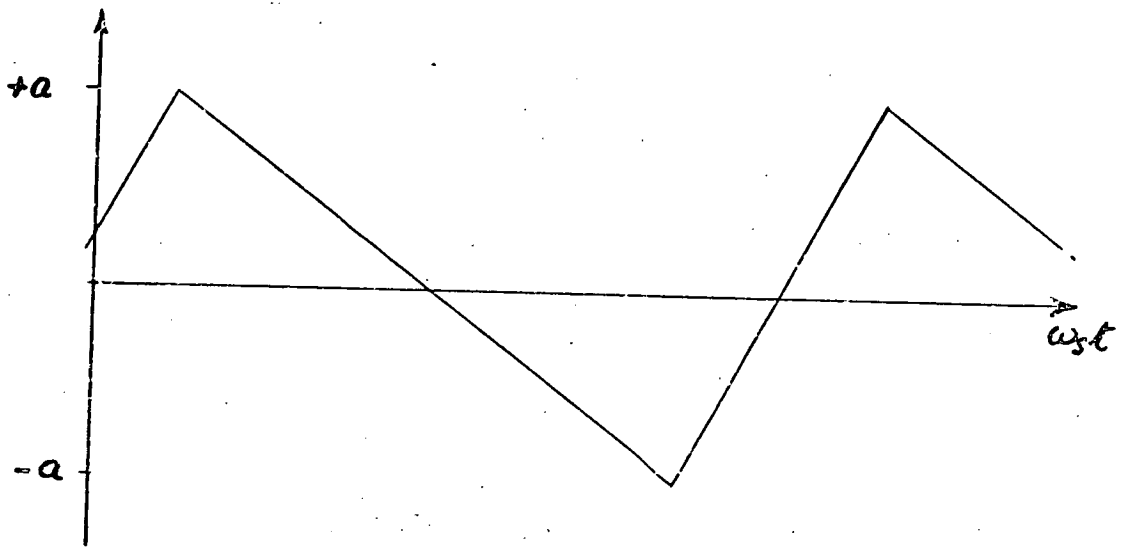
For the two fourier series terms of the variable $\pi(1+DC)$ to be zero, thus giving a linear characteristic, the conditions

$$\cos\phi_n = 0, \text{ and } (1-2k)\sin\phi_n = 0 \text{ must be satisfied.}$$

Thus $\phi_n = (2m-1) \cdot \pi/2$ for m any integer, and

$$k = 1/2, \text{ are sufficient}$$

conditions for a linear characteristic. These conditions require that the sampling waves be of equal slope, and that the filter have an odd number of poles at frequencies much lower than the switching wave frequency.



Integrator Output Ripple for d.c. Control Signal

F 6.2 a

The Cycle Period of the Constant Area Sampler

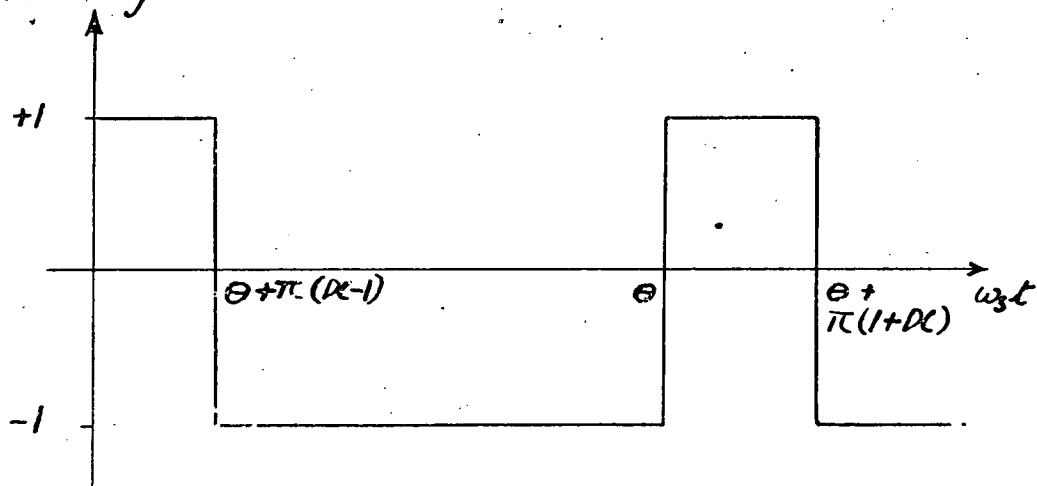
Diagram F 6.2a shows the output of the sampler and of the integrator for a d.c. control signal, DC. The triangular waveform of the latter has amplitude $\pm a$ and slopes of $(DC-1)/\tau$ and $(DC+1)/\tau$. The period is thus the sum of the half cycle times and is given by the expression

$$\begin{aligned} 2\pi/w_s &= \tau \left(\frac{2a}{DC+1} - \frac{2a}{DC-1} \right) \\ &= -4a\tau / (DC^2 - 1) \\ \therefore w_s &= 2\pi(1-DC^2) / (4a\tau) \\ &= w_0(1-DC^2), \text{ where } w_0 = \pi / (2a\tau) \end{aligned}$$

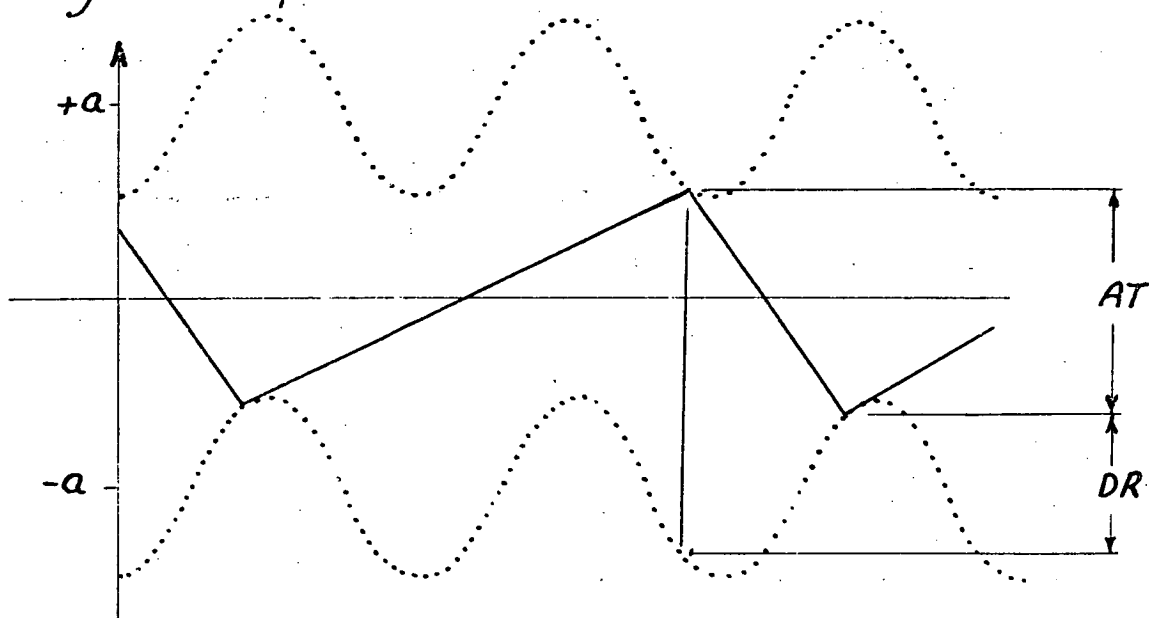
Provided the d.c. component varies slowly the above expression is valid and an average frequency may be calculated. The average period when the input is a sinewave of amplitude A is given by

$$\begin{aligned} w_{sav} &= w_0 \left\{ \text{average of } (1 - (DC + A \sin w_{in} t)^2) \right\} \\ &= w_0 \left\{ 1 - DC^2 - A^2/2 \right\} . \end{aligned}$$

Switching Wave



Integrator Output



Phase Lock Waveforms

F6.2b

Phase Lock of the Constant Area Sampler

There are two aspects of phase locked operation which are important. The first concerns the ability for locking to occur. Conditions for locking may be derived which do not represent stable operating conditions. The second aspect of phase locked behaviour is the stability of operating conditions once established.

Conditions for Locking to Occur

At the instant a positive step of the output occurs the equation

$$+a + \int_0^t e_{in} d(t/\tau) = \int_0^t e_o d(t/\tau) \text{ must be satisfied.}$$

Similarly at the instant a negative step is formed a similar condition with the opposite sign for a must be true. Diagram F 6.2b shows the situation when e_{in} is a harmonic of e_o . For the stable conditions associated with phase lock the equation

$$2a = AT + DR \text{ must be true.}$$

AT , the peak to peak amplitude of the triangle is related to the output frequency w_s and d.c. component DC by the expression

$$AT = \pi(1-DC^2)/(w_s \tau).$$

DR , the change in ripple amplitude during a half cycle of the output waveform is described by the expression

$$DR = 1/(w_s \tau) \int_{w_s t = \Theta}^{w_s t = \Theta + \pi(1+DC)} e_A(w_s t) dw_s t \text{ where } \Theta \text{ is}$$

the phase of the positive step of the output waveform, and e_A is the a.c. component of e_{in} . Substituting these expressions in place of their symbols gives the expression describing the relationship between relative phase, Θ , of

the control and switching waveforms, and the output frequency. The expression is

$$2a = \pi(1-DC^2)/(w_s \tau) + 1/(w_s \tau) \int_{\theta}^{\theta+\pi(1+DC)} e_A(w_s t) dw_s t.$$

Re-arranging this and replacing some terms by w_o yields the expression

$$w_s/w_o = 1-DC^2 + (1/\pi) \int_{\theta}^{\theta+\pi(1+DC)} e_A(w_s t) d(w_s t).$$

where $w_o = \pi/(2a\tau)$.

Sinewave Locking

For a sine wave input with no d.c. component the expression is

$$w_s/w_o = 1 + 2A/(\pi n) \cos n(\theta + \frac{\pi}{2}) \sin(n\pi/2)$$

where A is the sinewave amplitude and n is the harmonic number of the input frequency compared to the cycle frequency.

The limits of the phase lock range occur when the cosine term is maximum or minimum so the boundary of the phase lock range for the n^{th} odd harmonic is given by the expression

$$w_s/w_o = 1 \pm 2A/(n\pi)$$

i.e. $|1 - w_s/w_o| = 2A/(n\pi)$

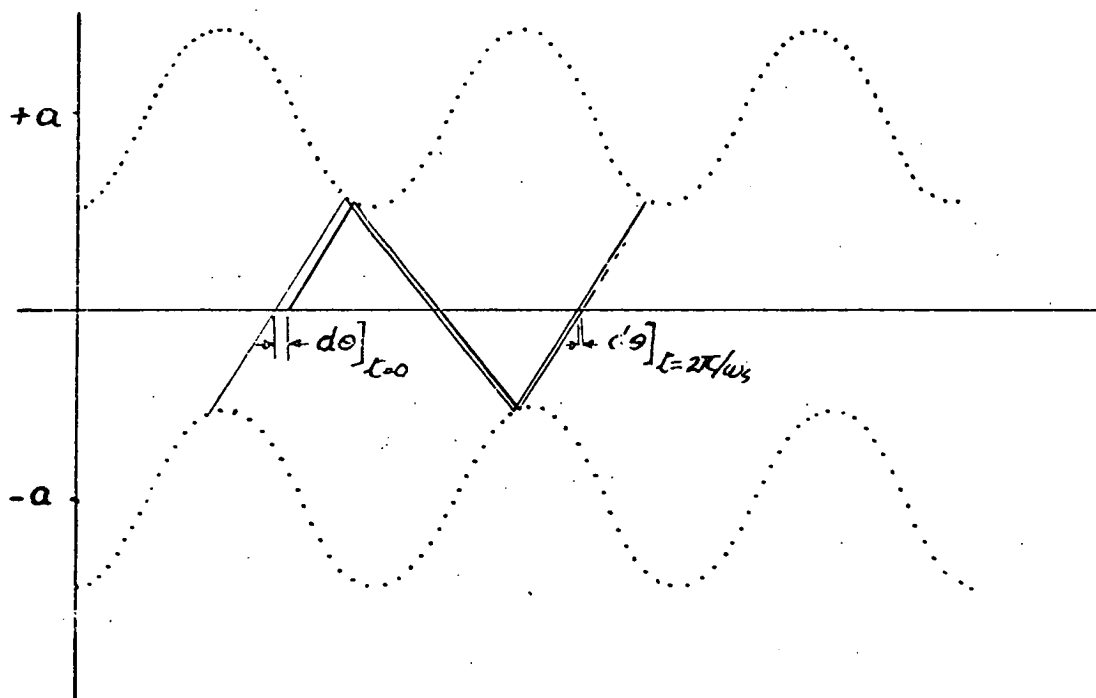
Dynamic Phase Error

The equation

$$w_s/w_o = 1 + 2A/\pi \cos(\theta + \pi/2), \text{ has two solutions for } \theta.$$

These represent one stable and one unstable equilibrium point. For control waves of other shapes than sinewave

Phase Trajectories For Locked Frequencies



F 6.2 c

there may be more than one pair of solutions.

In order to find if a solution of the general equation is stable or unstable the behaviour of the system is examined when the output phase is not θ but $\theta + d\theta$. The small error, $d\theta$, may increase or decrease over one cycle depending whether the system is unstable or stable respectively.

Diagram F 6.2c shows an example of two phase trajectories separated by $d\theta$ at $t = 0$. After the occurrence of the positive output step $d\theta$ changes by a factor k given by the expression

$$k = (1 - DC^2 + 2e_A(\theta + \pi(1 + DC))) / (1 - DC^2)$$

After the negative output step the value of $d\theta$ is changed by a factor l given by the equation

$$l = 1 - 2e_A(\theta) / (1 - DC^2)$$

Thus over one cycle $d\theta$ changes by the factor

$$lk = \left\{ 1 - 2e_A(\theta) / (1 - DC^2) \right\} \left\{ 1 + 2e_A(\theta + \pi(1 + DC)) / (1 - DC^2) \right\}.$$

The system is stable if $|lk| < 1$. The value of $d\theta$ diminishes exponentially if $0 < lk < 1$ or oscillatory decay occurs if $-1 < lk < 0$.

Stability of Sinewave Lock

For a sinewave control signal of amplitude A , with no d.c. component, locked to the first harmonic, the factor lk is described by

$$lk = (1 - 2A \sin(\theta))(1 - 2A \sin \theta)$$

$\therefore lk > 0$ so exponential growth or decay occurs. If $0 < A \sin \theta < 1$ the system is stable. Provided θ calculated

by the static condition satisfies this equation the system is stable. This implies that stable waveforms occur when the positive output step occurs during a negative input region and negative output steps during a positive input region.

d.c. Characteristics of Self Oscillating Amplifiers

A d.c. levelled wave with levels of unit magnitude is described by the expression below. The symbols used have the following meanings

$f(w_s t, \theta_n, \theta_f)$: The switching wave as a function of time, phase of negative step, θ_n , and phase of positive step, θ_f .

DC : The d.c. component of the switching wave

$$f(w_s t, \theta_n, \theta_f) = DC + \sum_{n=1}^{\infty} \frac{2}{n\pi} \left\{ \sin(nw_s t) \cdot (\cos(n\theta_n) - \cos(n\theta_f)) + \cos(nw_s t) \cdot (\sin(n\theta_f) - \sin(n\theta_n)) \right\} / (n\pi)$$

This signal is passed through a filter and produces the ripple waveform below. The symbols describing the filter response have the following meanings

$A(nw_s)$: The amplitude of filter response at frequency nw_s .

$\phi(nw_s)$: The phase of filter response at frequency nw_s .

$R(w_s t, \theta_n, \theta_f)$: The ripple waveform after filtering the switching wave.

$$R(w_s t, \theta_n, \theta_f) = DC \cdot A(0) + \sum_{n=1}^{\infty} \frac{2A(nw_s)}{n\pi} \left\{ \begin{aligned} &\sin(n(w_s t - \theta_n) + \phi(nw_s)) \\ &- \sin(n(w_s t - \theta_f) + \phi(nw_s)) \end{aligned} \right\}$$

This ripple is the ripple at the input of the switch controller.

The ripple values at the instants of positive and negative steps are described by the functions below.

$$R+ = R(\theta_n, \theta_n, \theta_f) \\ = A(o).DC + \sum_{n=1}^{n=\infty} \frac{2A(nw_s)}{n\pi} \left\{ \sin(\phi(nw_s)) - \sin(n(\theta_n - \theta_f)) \right\}$$

and

$$R- = R(\theta_f, \theta_n, \theta_f) \\ = A(o).DC + \sum_{n=1}^{n=\infty} \frac{2A(nw_s)}{n\pi} \left\{ \sin(\phi(nw_s) + n(\theta_f - \theta_n)) - \sin(\phi(nw_s)) \right\}$$

The difference in ripple values and the separation between sensitive levels of the switch controller are equal. When this is so the equation below is satisfied. The symbols used have the following meanings.

a : Half the difference between sensitive levels of the switch controller

$$2a = \sum_{n=1}^{n=\infty} \frac{2A(nw_s)}{n\pi} \left\{ 2\sin(\phi(nw_s)) - 2\cos(n(\theta_f - \theta_n)) \cdot \sin(\phi(nw_s)) \right\}$$

$$\text{i.e. } a = \sum_{n=1}^{n=\infty} \frac{2A(nw_s)}{n\pi} \left\{ \sin(\phi(nw_s)) (1 - \cos(n\pi(DC+1))) \right\}$$

$$\text{since } DC = (\theta_f - \theta_n)/\pi - 1$$

For a given filter and value of output component, DC, this equation must be satisfied for a particular value of sampling frequency, w_s . In some cases no solution exists. This implies that this value of output cannot be attained with the shape of output waveform described. In such cases the output assumed must be attained by more complex waveforms akin to those with subharmonic

components encountered in natural sampling. This has not been closely examined.

In other cases it may appear that several solutions exist. In these circumstances the ripple at the switching instant must be moving, as a function of time, away from the zone between detector sensitive levels. Mathematically this may be stated as follows. "The product of, the output level prior to the switching instant, with, the derivative of the ripple at coder input, must be positive at the instant of switch transition."

In the rare cases where there are still several solutions the true solution is that with the highest value of w_s .

For the value of w_s calculated from the equation the value of the ripple at either of the sampling instants can be calculated. Since the ripple, d.c. input and d.c. feedback component combine to reach the sensitive level of the switch controller at this instant the equation below is true. The symbols used have the following meanings

E_{in} : The d.c. component of the input voltage

$$a = A(o) [DC + E_{in}] + \sum_{n=1}^{n=\infty} \frac{2A(nw_s)}{n\pi} \left\{ \sin(\phi(nw_s)) + \sin(n\pi(DC+1) - \phi(nw_s)) \right\}$$

$$\text{i.e. } E_{in} = -DC + 1/A(o) \left\{ a - \sum_{n=1}^{n=\infty} \frac{2A(nw_s)}{n\pi} \left\{ \sin \phi(nw_s) + \sin(n\pi(DC+1) - \phi(nw_s)) \right\} \right\}$$

This expression may be simplified by noting that the expansion of the second term yields the terms of the identity for the determination of the frequency of oscillation. The final relationships are restated below.

$$a = \sum_{n=1}^{n=\infty} 2A(nw_s) \sin(\phi(nw_s)) (1 - \cos(n\pi(1+DC))) / (n\pi).$$

$$E_{in} = -(DC + \sum_{n=1}^{\infty} 2A(n\omega_s) \cos(\phi(n\omega_s)) \sin(n\pi(1+DC)) / (n\pi A(0))).$$

Notice that the frequency of oscillation is determined by the quadrature component of the filter response while the nonlinearity is related to the direct part of the response.

Two simple examples of the theory for self oscillating systems.

Integrator Feedback

For this example $A(nw_s)\sin(\phi(nw_s)) = 1/(nw_s\tau)$
and $A(nw_s)\cos(\phi(nw_s)) = 0$

The oscillator frequency is given by the equation

$$a = \sum_{n=1}^{n=\infty} 2(1-\cos(n\pi(1+DC)))/(n^2w_s\tau\pi)$$

$$\text{i.e. } w_s = \frac{\pi}{2a\tau} \sum_{n=1}^{n=\infty} 4(1-\cos n\pi(1+DC))/(n\pi)^2$$

$$= \pi(1-DC^2)/2a\tau$$

Although derived in an entirely different way to that in appendix A 6.2a the result is identical. It agrees with experimental measurements.

The characteristic between input and output is linear since the second term, that corresponding to the nonlinearity, is zero.

High Q filter feedback

$$\text{For this example } A(nw_s)\sin(\phi(nw_s)) \approx \begin{cases} 0 & n \neq 1 \\ -A\sin(-\pi+2Q((\frac{w}{w_r})-1)) & n=1 \end{cases}$$

$$A(nw_s)\cos(\phi(nw_s)) \approx \begin{cases} 0 & n \neq 1 \\ -A\cos(-\pi+2Q((\frac{w}{w_r})-1)) & n=1 \end{cases}$$

$$A(0) = -1$$

For a comparator with no backlash the Sin term must be zero so that $w_s = w_r$. The input signal is then described by

$$E_{in} = -DC-2A\sin(\pi(1+DC))/\pi$$

The relationship between the output and the error between output and input, E , is

$$E = DC + E_{in} = 2A \sin(\pi DC) / \pi.$$

This is the average value of the filter output and is applied to the comparator input. Notice that the error is proportional to filter gain at the oscillation frequency, that is near the peak of the high Q point of the filter where phase passes 180° . Notice also that this result predicts a negative gain characteristic for part of the output range if the gain between comparator input and output is considered.

Second Order Filter Impedance at Frequencies
Greater than $4w_c$

The filter analysed has an input inductor of copper resistance R_i and inductance L , a load resistance R , and a load shunting capacitance C . The analysis does not account for high frequency core losses.

The input admittance, Y , of such a filter is given by

$$Y = 1/R(RCS+1)/(LCS^2+S(R_iC+L/R)+1+R_i/R).$$

After substituting jw for s the real part of Y is found to be

$$YR = (1/R)(R_i/R)(R/Lw)(1+(1+R_i/R)/(RCw)^2)/((1+(1+R_i/R)/(LCw)^2)^2+(R_i/Lw+1/RCw)^2).$$

When the filter damping is 0.6 and the d.c. voltage gain is near unity the values of R/Lw_c and $1/RCw_c$ are near 1.2 and R_i/R is small compared to unity. w_c is near $\sqrt{1/(LC)}$. The real part of Y is then approximately described by

$$YRA = (1/R)(1.2w_c/w)^2(R_i/R)(1+(1.2w_c/w)^2)/((1+(w_c/w)^2)^2+(1.2w_c/w)^2).$$

For $w \geq 4w_c$ the error in neglecting the last two terms of the expression is less than 15% so that the real part of the filter admittance at these frequencies is approximately

$$YRA = (1/R)(R_i/R)1.4(w_c/w)^2$$

Inductor Energy and Time Constant due to
Winding Resistance

An inductor has a magnetic circuit with an airgap of area A_c , and length x . The effective length of the remainder of the magnetic circuit is equivalent to an airgap of length z . Let the winding be such that N turns of mean length l_w fill a proportion k_w of the winding area A_w . Let the winding material have resistivity ρ .

The inductance, L , is given by

$$L = \mu_0 N^2 A_m / (x+z)$$

The resistance, R , is given by

$$R = \rho N^2 l_w k_w / A_w$$

The ampere turns, NI , required to achieve a flux density B are given by

$$NI = B(x+z) / \mu_0$$

Now if B is the maximum flux density allowed then the product of time constant and peak inductor energy is given by

$$\begin{aligned} \tau \cdot E &= L/R \cdot LI^2/2 = \mu_0 A_c A_w / (\rho l_w (x+z)) \cdot B^2 A_m (x+z) / (2\mu_0) \\ &= A_c^2 \cdot A_w \cdot B^2 / (2\rho l_w) \end{aligned}$$

This may be re-expressed in terms of D a linear core dimension by the relationship

$$E \cdot \tau = k B^2 D^5 \quad \text{where } k \text{ is defined by the expression}$$

$$k = (A_c/D^2)^2 \cdot (A_w/D^2) / (2\rho(l_w/D))$$

Note that k does not vary between inductors of the same proportions nor does it vary with any parameter of the magnetic circuit apart from the effective area.

Appendix C

The digital computer programs with titles listed in this appendix were developed for two purposes. First, since these programs generate numerical descriptions of those features of switching amplifiers described by the models they enable stringent tests of the models by comparing these descriptions with actual measurements. Second, once the accuracy of a model is known the numerical descriptions generated by the programs may be used as a basis for design, especially where a design requires the equivalent of many experimental measurements.

The programs are written in Algol for Elliot 503 machine of the Hydro-University Computing Centre at the University of Tasmania.

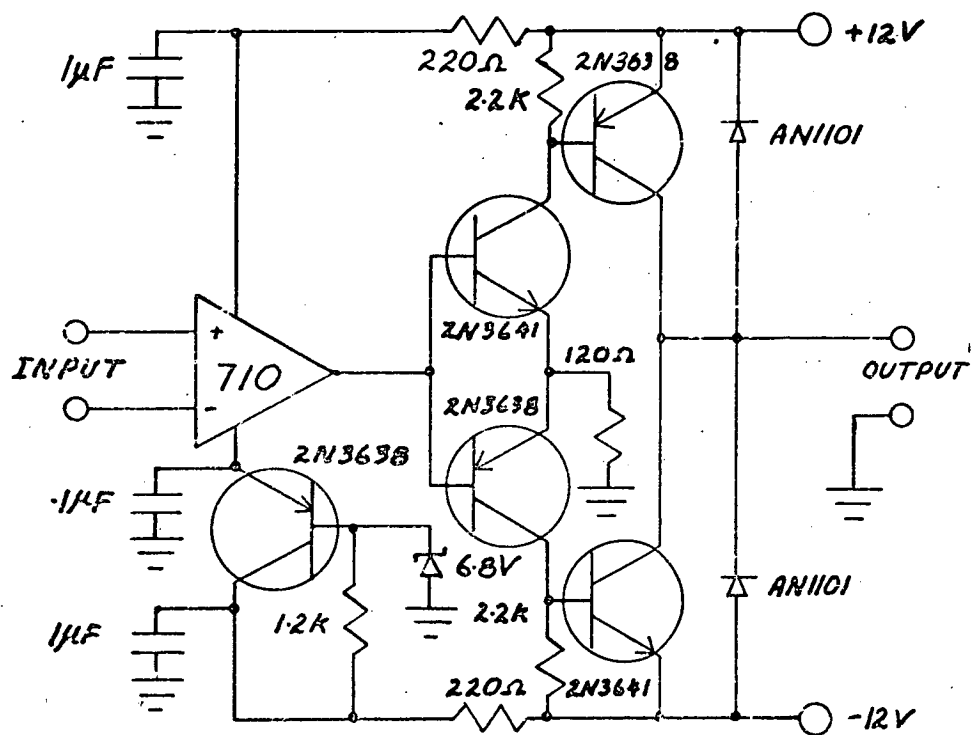
Titles of Programs

- 1 Phase Modulation of Sinusoid Waveforms
- 1.1 Sideband amplitudes, energies, and energy distribution profiles as functions of modulation amplitude and waveform.
- 1.2 Energy distribution contours on the sideband, modulation amplitude plane.
- 2 Harmonic and Sideband Descriptions of Switching Waves
- 2.1 Natural Sampling
- 2.1.1 Amplitude and phase of sidebands of any specified harmonic of a wave with two unit d.c. levels for bandlimited periodic input signals.
- 2.1.2 Sideband energy distributions for each harmonic of a d.c. levelled wave with one step modulated by a control signal.
- 2.1.3 Passband energy as a function of passband to sampling frequency ratio for a d.c. levelled wave with a single modulated step.
- 2.1.4 Harmonic amplitudes of phase modulated, and diode-clamped, sine-levelled waves with d.c. control signals.
- 2.1.5 Sidebands and Harmonics of sine-levelled waves with sinewave signals.
- 2.2 Regular Sampling
- 2.2.1 Sidebands of the first harmonic of a d.c. levelled wave with one step modulated by bandlimited, periodic, control signals.

- 3 Subharmonic Gain and Describing Functions
for d.c. Levelled Waves
- 3.1 Describing functions for natural sampling
 based on phased addition of coincident
 sidebands.
- 3.2 Gains and describing functions for natural
 and regular sampling based on the spectra
 of stationary waveforms.
- 4 Low Frequency Input-Output Characteristics
of Feedback Amplifiers
- 4.1 d.c. levelled waves controlled by natural
 sampling.
- 4.2 Sine-levelled waves with phase modulation
 controlled by natural sampling.

Appendix E

This appendix contains a brief outline of the conditions for measurements and range of measurements associated with the models of switching amplifiers proposed in this thesis. Although grouped under distinct headings which correspond roughly with chapter topics these experiments were conducted over a long period. Most measurements were taken prior to the development of the models proposed in this thesis but many were made after these models were formed in order to test the limits of the predicted behaviour or to explore avenues opened by increases in understanding.



Comparator and Low Power Switch Array

E 1.0

E

E 1.0 Spectra of a Switching Wave with two d.c. Levels Controlled by Natural Sampling

These experimental measurements were made in order to compare the spectra of a wave with two d.c. levels with an algebraic description based upon those of Bennet, Fitch, and Kretzmer. The attributes compared are split into two distinct groups, namely the low and high frequency components of the wave. The comparisons are described in sections E 1.1 and E 1.2 respectively.

The experimental measurements were made at the output of an encoder produced by combining a comparator and switch array of the form shown in figure E 1.0 with a sampling wave generator consisting of one of the function generators listed in appendix E 10. Input signals and power supplies were provided by other items in this list. The encoder output was used to drive a light resistive load.

The expression describing the switching wave is

$$\frac{e_o(t)}{2V_s} = \frac{e_{in}(t)}{e_s} + \sum_{r=1}^{r=\infty} \left\{ \sin(r[w_s t + \frac{\pi}{2}(1 + \alpha \frac{e_n(t)}{e_s})]) - \sin(r[w_s t - \frac{\pi}{2}(1 + \beta \frac{e_n(t)}{e_s})]) \right\} / r$$

where $e_o(t)$ is the instantaneous encoder output voltage,
 V_s is the supply rail voltage (+ V_s & - V_s),
 $e(t)$ is the encoder input voltage,
 e_s is the peak to peak sampling wave voltage,
 w_s is the sampling wave angular frequency,
 α is the proportion of positive slope, in each period of the triangular sampling wave, and
 $\beta = 1 - \alpha$.

The expression can be derived directly from those given by Bennet, Fitch, and Kretzmer or it may be derived using the theory in Appendix A 3.1.1 in a similar way to the description derived in Appendix A 3.1.2a.

E

E 1.1 Low Frequency Components of Two Levelled Waves Controlled by Linear Natural Sampling

The low frequency component of the switching wave, that described by $e_{in}(t) * (2V_s/e_s)$ in the expression, was compared with the encoder input signal during these measurements. Both d.c. and a.c. input signals were used.

The first measurements were of the d.c. input-output characteristic. These were plotted and the linearity of the system measured. Sources of nonlinearity of the d.c. characteristic were isolated and corrected as much as possible. The second stage of the experiment was the measurement of a.c. signal input-output characteristics. Initially direct measurements of harmonic amplitudes were attempted but these were abandoned in favour of the balance technique outlined in section E 7.1.

The range of parameters measured are listed below.

<u>parameter</u>	<u>range</u>
d.c. component of output	full range (saturation to saturation)
a.c. component of output	full range
input waveform shape	Sine, square, and triangular 1:1
sampling waveform shape	triangular with rise/fall time ratios from 1:1 to 1:9
sampling wave frequency	200Hz to 50khz
input waveform frequency	d.c., and from 20hz to .85 sampling frequency

For the range of conditions outlined above the d.c. and a.c. input-output characteristics matched very closely. For low sampling rates the difference was of the order of 0.05%. This difference was of the order of stray capacitive and inductive couplings between input and

output of the amplifier. For higher sampling rates and input signal frequencies the few micro seconds delay in the switching wave steps due to excessive forward bias of the output stage was a major cause of error between input and output. Compensation or adjustment of measurements to cancel the effect of the delay based upon the observed physical delay reduced the effective error to the noise level.

For the range of parameters measured it appears from these measurements that an amplifier using natural sampling can accurately match the input signal with one component of the switching wave. The constancy of the characteristic with variation in signal parameters suggests good isolation of the basic principle of operation from any undesirable, that is unpredictable effects. The constancy of input-output characteristic is observed for both linear and nonlinear characteristics suggesting the input-output relationship is set purely by the sampling waveshape in the absence of comparator and switching stage errors or deficiencies. For the experimental amplifier such deficiencies cause a nonlinearity of less than 0.1% of the maximum output provided the delay mentioned above is not considered as a nonlinearity. Most of this nonlinearity was due to the comparator which exhibited a change in triggering level for signals with short times between positive and negative going steps.

E

E 1.2 Harmonics and Sidebands of Two Levelled Waves Controlled by Linear Natural Sampling

The aim of the experimental work was to compare measurements of switching wave components other than the low frequency component with values estimated from the expression. The evaluation process followed the lines indicated in chapter IV, section 4.2. In order to minimise repeditive calculation computer program C 2.1.1 was used to tabulate estimates of sideband and harmonic amplitudes and phases for the full field of experimental measurements.

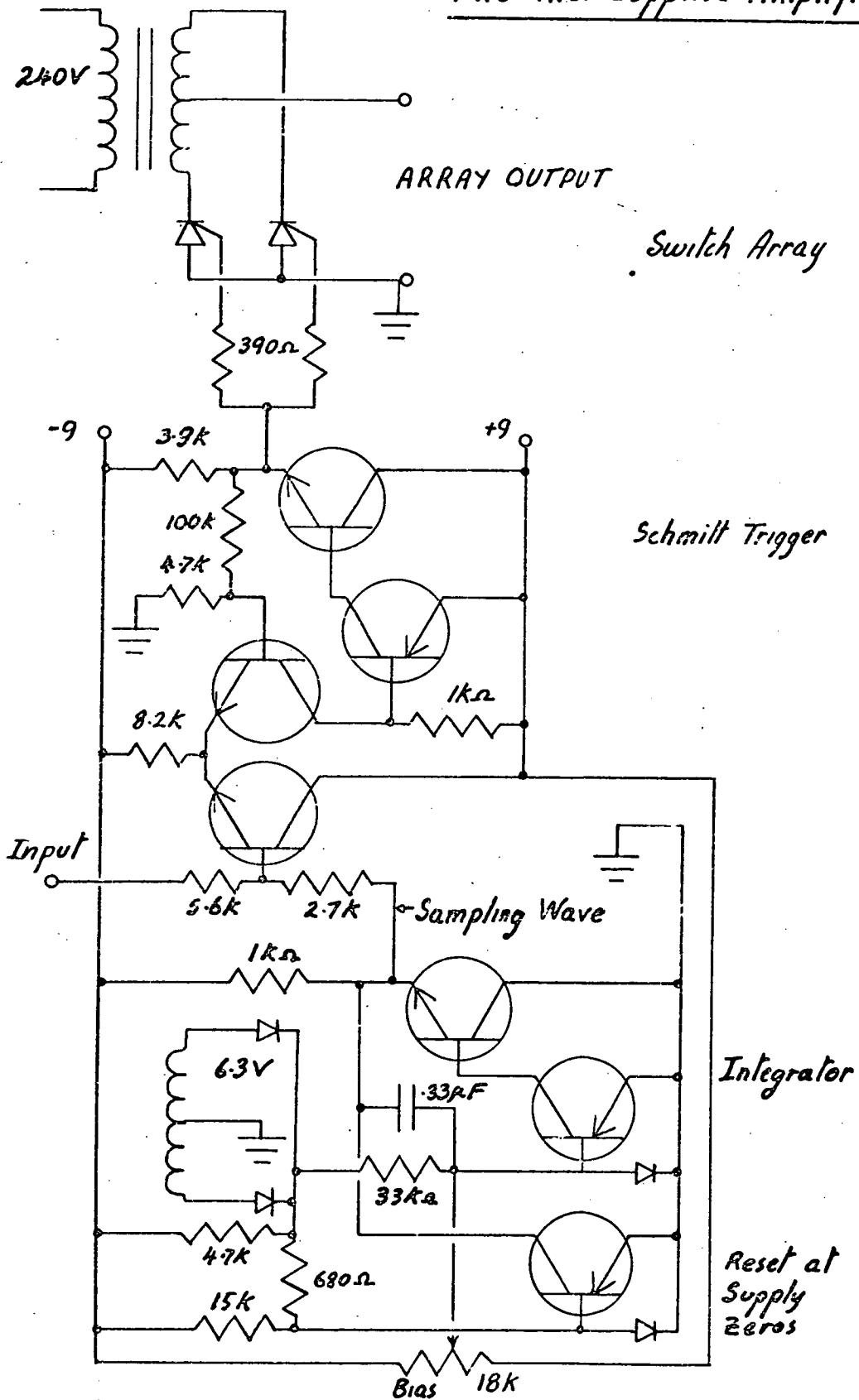
The range of conditions for which measurements were made are outlined below.

<u>parameter</u>	<u>range</u>
d.c. component of output	full range between saturation levels
a.c. component of output	full range
input waveform shape	sinewave and pairs of non-commensurate sinewaves
sampling waveform shape	triangular with rise:fall time ratios from 1:1 to 1:5
input waveform frequency	0-1khz for single sinewaves 0-500hz for pairs
sampling waveform frequency	1khz to 2khz

Individual sidebands were measured and tracked through a band of frequencies as both modulation and sampling frequencies were changed. Profiles of sideband amplitude variation with d.c. and a.c. components of the modulation were measured for the first eight sidebands of the first and second harmonics of the switching wave. Selected sidebands of harmonics up to the 15th were also tracked and measured.

240 : 18

The A.C. Supplied Amplifier



E2.0 a

E

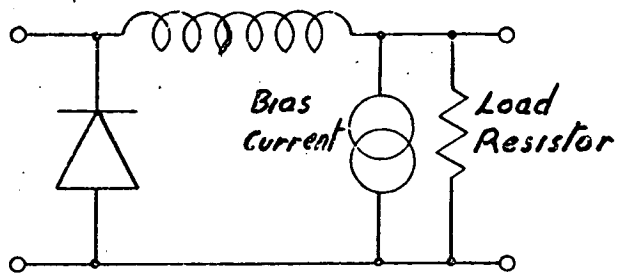
Experimental results varied in accuracy with the quality of filtering and proximity to the measurement frequency of unwanted sidebands. For this reason the accuracy of measurement varied from 1% for strong well spaced sidebands to 50% for closely spaced or very weak sidebands. In all cases the experimental results were consistent with computed amplitudes to within the tolerance of the experimental measurements.

E 2.0 Measurements of a "Linear" Thyristor Amplifier

The waveforms produced by a linear thyristor amplifier were compared with algebraic descriptions computed using the methods outlined in chapter III. The introduction below describes the equipment used and the types of waveform measured. The ranges of measurement parameters and the accuracy of their match with algebraic descriptions are described in sections 2.1 and 2.2; the former concerns the low frequency waveform components, the latter the high frequency components.

The circuit of the amplifier is shown in figure E 2.0a. This circuit allows the initiation of thyristor conduction to be varied in phase from one supply waveform zero to the next. It is thus capable of controlling waveforms with or without diode clamping of the array. Resistive loads were coupled to the array via inductors to give circuits of the form shown in figure E 2.0b. The amplifier operation is outlined below.

A sampling wave is formed by integrating the voltage waveform produced by fullwave rectification of a 6.3 volt output from the mains transformer. During each half cycle of the mains supply the integrator output swings negative but is reset to zero as the supply waveform passes through zero at the end of the half cycle.



An unclamped load is achieved by omitting the diode.

Loads For Thyristor Amplifiers

E 2.0 b

E

The sampling wave and the amplifier input signal are summed at the comparator input. Once each half cycle of the supply waveform the comparator input signal passes the comparator threshold from positive to negative and causes the output signal to initiate thyristor turn on. At the end of each half cycle the resetting of the sampling wave causes a positive going transition through the comparator threshold and removes the gate drive from the thyristors.

For the sinewave supply used the sampling wave is a cosine segment so that as the input signal is varied positively away from the comparator threshold the phase of thyristor turnon varies from 0° to 180° and the average value of the resulting switching wave varies linearly with the input signal. This ideal is attained only if the load circuit causes a negligible change in thyristor conduction voltage over each half cycle. This is partially facilitated by the current source indicated as part of the load. This is set to a current greater than the negative peak of the filter input ripple current so that the thyristors are always biased on.

E 2.1 Low Frequency Measurements

The objectives of the low frequency component measurements were first, to establish the degree of and sources of nonlinearity in the input-output characteristic, and second, to measure any variation of the input-output characteristic as the control signal frequency was increased to a significant fraction of the sampling frequency. Nonlinearities of the characteristic were measured using the balance technique outlined in section E 7.1. The calibration and measurement sequence adopted is described below.

E

E 2.2 Harmonics and Sidebands

Comparisons were made of measured and calculated sideband and harmonic amplitudes for sine-wave input signals. The ranges of conditions observed are outlined below.

<u>parameter</u>	<u>range of parameter</u>
input signal frequency	0 to 60hz
amplitude	0 to saturation
d.c. offset	0 to saturation
switching wave frequency	100hz constant.

Sidebands were measured and tracked through a range of frequencies as input signal frequency was varied. Profiles of sideband amplitude as functions of both d.c. and a.c. components of modulation were measured for the first 5 sidebands above and below harmonics 1 to 6.

The comparison of measured sidebands with those calculated for ideal waveforms by programs C 2.1.4 and C 2.1.5 showed some differences greater than the experimental error of measurement. In each case the difference was consistent with the difference between ideal and observed waveshapes. This latter difference was entirely consistent with the voltage drops on the switch array elements due to load currents.

E 3. Supply Rejection of a Modified Natural Sampler

A theoretical model of a modified natural sampling encoder which enables supply ripple to be rejected from the output signal was proposed in section 3.1.4. This experiment was intended as a necessary but not sufficient test of the major features indicated by the analysis presented in Appendix A 3.1.4.

The circuit of Figure E 1.0 was modified by placing a low impedance transformer winding in series with the supply to the switching stage. The sampling wave was modified in the manner outlined in section 3.1.4.1, with the aid of an analogue multiplier, to reject ripple injected by the transformer.

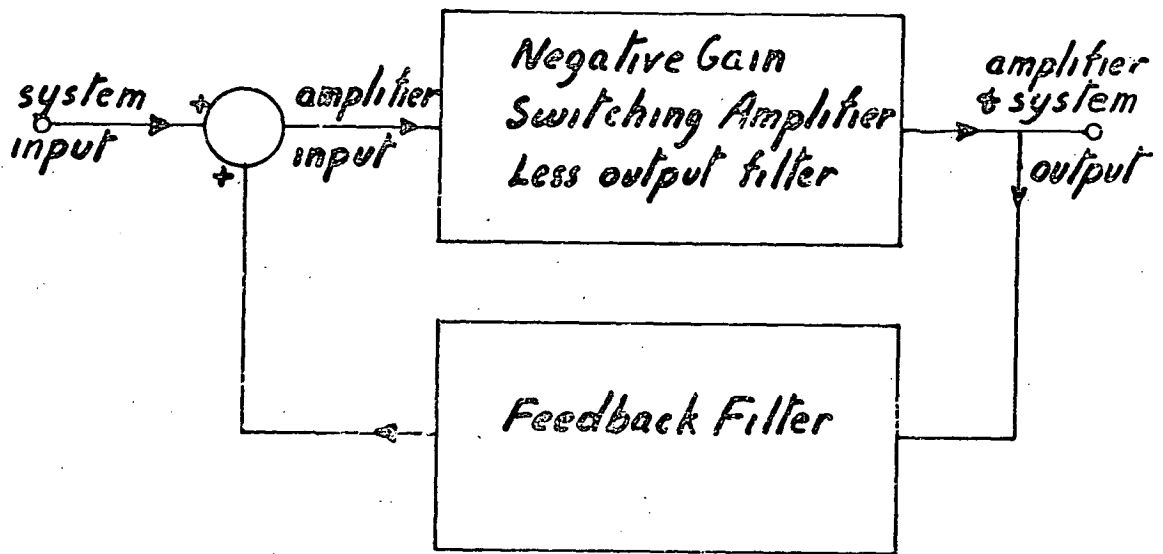
The range of conditions examined are outlined below.

<u>parameter</u>	<u>range or value of parameter</u>
injected ripple amplitude	0 to 60% of d.c. supply voltage
frequency	50hz sinewave
input signal waveform	sinewave with d.c. offset
frequency	0 to 50% sampling frequency
amplitude	0 to saturation for a.c. and d.c. components
sampling frequency	.5 to 2khz
waveshape	symmetrical triangular (for no ripple)

Three aspects of the switching waveform were measured, the residual ripple at 50hz and its harmonics, the 50hz and input signal sideband amplitudes of the first two harmonics of the sampling frequency, and the modulation of the output component corresponding to the input signal by the 50hz ripple.

The residual ripple at maximum unsaturated d.c. output was 55db below the level on the supply rail. The residual component was at the level produced by capacitive and other coupling of the supply rail to the comparator input. No sidebands of the input signal due to intermodulation with the 50hz ripple were detectable, that is they were at least 60db below the output signal level.

The model predicts (see Appendix A 3.1.4b) that the harmonics and sidebands will be modulated by the 50hz supply ripple. Comparisons were made between the measured and predicted amplitudes of this modulation. Difficulties in calculating the theoretical amplitudes limited these comparisons to situations with d.c. input signals and small supply perturbations. Within these restrictions excellent agreement was obtained. The largest difference between measured and predicted amplitudes was 5% of the measured amplitude, a value consistent with the uncertainty of measurement arising from the close proximity of the sidebands to their parent harmonics.



Arrangement for Feedback Measurements

E4.0

E 4.0 Measurements of Linearity with Feedback

The effects of feedback ripple on both d.c. and a.c. supplied amplifiers were investigated by placing these within the feedback loop outlined in figure E 4.0. The d.c. input-output characteristics of both the switching amplifier and the entire system were plotted as the input of the system was used to scan the output between saturation levels. In order to minimise the effects of load dependent features of the amplifiers light resistive loads and simulated filters based on RC networks or combinations of these with op. amps. were used.

The measurements so obtained were compared, where applicable, with estimates computed on the basis of the model described in chapter 5. Programs C 4.1 and C 4.2 generated these estimates. The feedback filters used were first and second order low pass filters with variable gain and variable pole positions.

E 4.1 A d.c. Supplied Amplifier

The amplifier used was that of figure E 1.0. The ranges of filter parameters and sampling waves are outlined below.

<u>parameter</u>	<u>range investigated</u>
pole positions	0 to 0.8 of sampling rate
damping	1 to 5 (for second order systems)
gain	0 to that giving oscillation at subharmonics for small d.c. offsets
sampling waveshape	triangular with proportions from 1:1 to 1:20

For the range of conditions outlined the experimental results matched computed values to within 3% of the total deviation from linearity. This accuracy was consistent with the accuracy of output measurement for small deviations from linearity and with the accuracy of filter gain and pole positions for larger deviations from linearity.

E 4.2 An a.c. Supplied Amplifier

The amplifier used was that of figure E 2.0a. The sampling waveshape was held fixed at that required for a linear amplifier. Only two filter responses were examined; these are listed below.

$$G(s) = G_0 / (1 + s/0.5)$$

$$\text{and } G(s) = G_0 / (1 + 3(s/0.5) + (s/0.5)^2).$$

where G_0 was varied from zero to a value sufficient to cause subharmonic jitter.

For the light load used the openloop non-linearity of the amplifier was small. The error between experimental measurements and values estimated by the model was less than 5% of the deviation from linearity. The main source of this error appeared to be poor estimates of loop gain associated with loading effects which were neglected at the time of measurement. Two single spot measurements at a later date when this effect was considered matched computed values to within 1.5%.

E 4.3 Critical Gain Estimates

The previous two experiments showed that for a given filter there was a maximum loop gain below which stable conditions apply and above which oscillation of one form or another took place. In some cases these critical gains can be estimated and plotted as functions of the d.c. output of the switching amplifier. Where the critical gain is associated with phase saturation the model of chapter V gives an accurate estimate but other conditions were not predictable either on the basis of this model or that using describing functions. Insufficient measurements were taken to determine the exact nature of these limits to open loop gain.

E

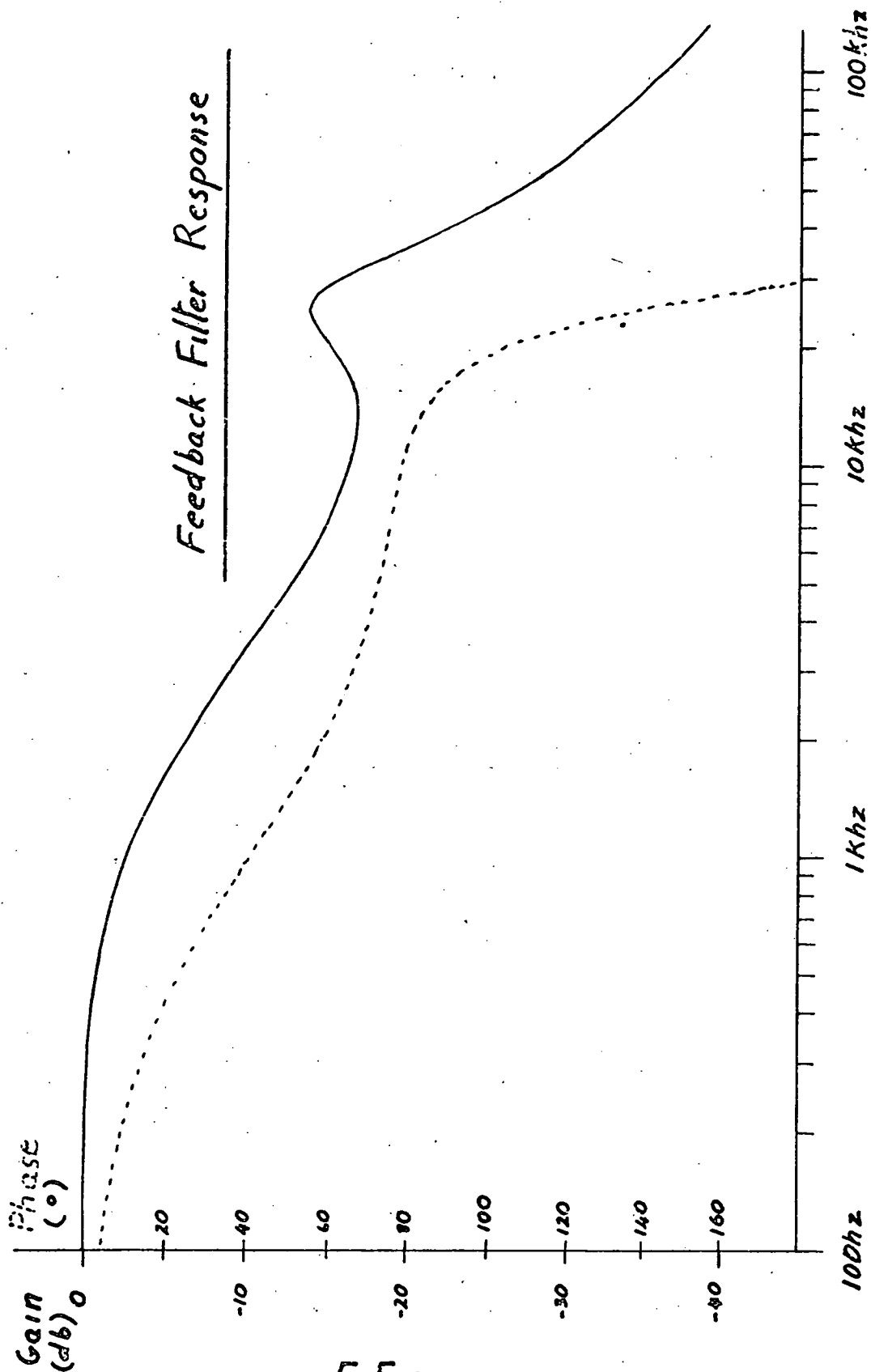
- frequency of oscillation - variation with d.c. input voltage, apparent value for a.c. input, apparent value with both d.c. and a.c. input.
- sideband amplitudes - presence and absence noted for two values of d.c. input and a range of values of a.c. input.
- phase lock - observed to occur but no numerical data taken.

The characteristics for d.c. performance, both input-output characteristics and frequency of oscillation, were then established on a theoretical basis and checked immediately by more accurate measurements. The conditions for phase lock were established theoretically and tested at a later date.

The circuit based on figure E 1.0 was used to check the a.c. performance, the form of the switching wave sidebands, and the model for phase lock. The results were those discussed in chapter VI. This second check was made to test the model on a system with higher frequencies of oscillation, 50khz rather than the 0.5khz of the analogue computer simulation.

The high Q filter used for the third experimental system had the response shown in figure E 5a. Input-output responses for the d.c. amplifier characteristics were measured for a range of filter gains between .5 and .05.

The central half of these input-output characteristics matched the predicted sinewave to within 0.5%. Over this range the frequency of oscillation varied by 5% but immediately outside this range sub-harmonic oscillations occurred. At each change in the mode of self oscillation steps in the input-output



E 5 a

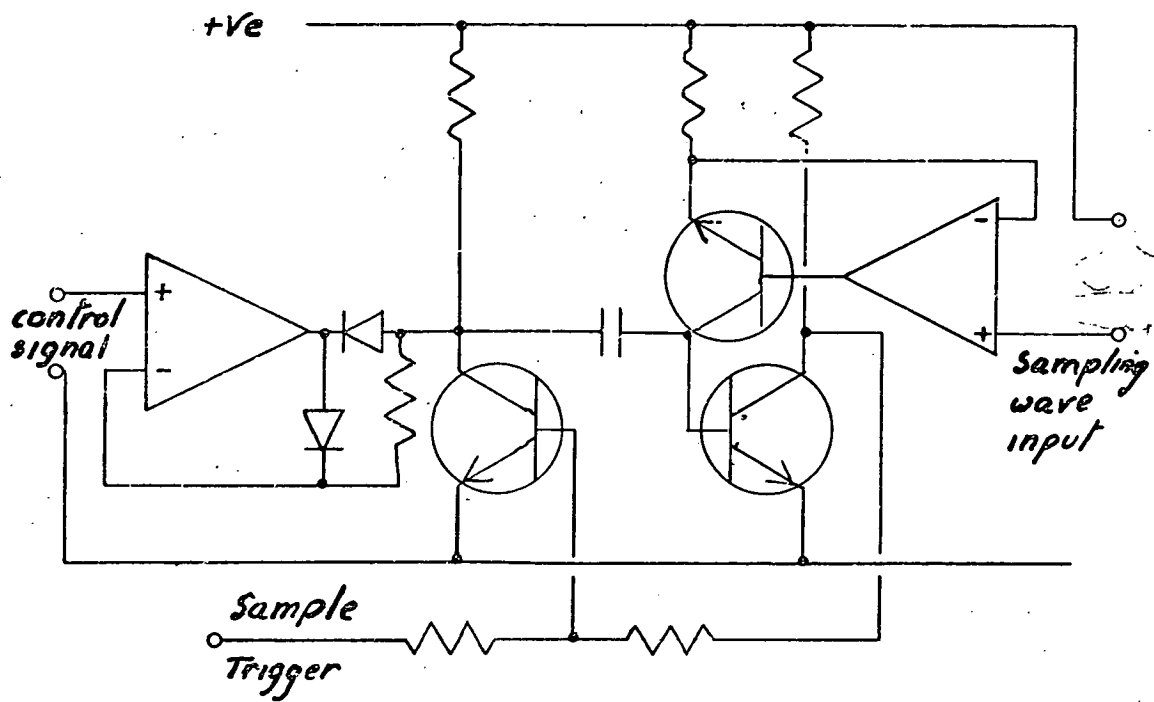
E 5 Self Oscillating Amplifier Measurements

The measurements described here were undertaken to establish the accuracy of the data in the literature and to check the computation methods described in chapter 6 as applied to the two examples detailed in appendix A 6.2. This passage describes the equipment used and the measurements taken. The comparisons made with the models of chapter 6, and the conclusions reached concerning the accuracy of the models are presented in chapter 6.

In order to take these measurements three separate circuits were used to produce switching amplifier encoders of the form shown in figure E 5.0. Initially the constant area sampler was simulated on the analogue computer. Later the encoder shown in figure E 1.0 was modified, first by the addition of an integrator to produce a constant area sampler, and later by replacing the integrator with a high Q filter.

The initial analogue computer simulation provided an outline of the constant area sampler performance which stimulated the development of the theory for the calculation of oscillation frequency and phase lock boundaries. The features examined with this system are listed below.

- | | |
|---------------------|---|
| d.c. characteristic | - linearity of input-output characteristic. |
| a.c. performance | - variation of output component with frequency, variation of harmonic amplitudes with frequency, variation of harmonic amplitudes and gain with input signal amplitude. |



A Class of Controlled Monostable Used For

Regular Sampling

E 6.0

characteristic occur but the overall form is still sinusoidal. The overall system response is substantially linear for the filter used since the ripple amplitude is small compared to the feedback signal.

No attempt was made to measure the a.c. input-output characteristic of this system or to investigate potential phase lock modes.

E 6. Regular Sampling

d.c. levelled waves with one modulated edge

Section 3.2 of chapter 3 describes an encoder model from which are derived the waveform descriptions of appendix A 3.2. The purpose of the measurements described below was to check the predictions of waveform spectra derived from these descriptions. The waveform components measured corresponded (in frequency) to the sinewave input signals, their harmonics, and their intermodulation products.

The circuit used to generate the switching waves is shown in E 6.0. Essentially, it is a monostable multivibrator. A periodic reset causes the monostable to leave its stable state for a period determined by the input signal at the reset instant, and by the charge injected into the capacitor subsequently. The capacitor charge waveform is controlled by the current generator. This requires a d.c. control for a linear sampler and a periodic waveform synchronous with the reset signal for a nonlinear sampler.

E

These measurements were made for the range of conditions outlined below.

<u>parameter</u>	<u>range of parameter</u>
input signal - d.c. component	saturation to saturation
single a.c. component	amplitude 0 to saturation frequency 0 to 0.4 sampling rate
a pair a.c. components with d.c. component at mid range amplitude	amplitudes 0 to saturation frequencies 0.1 and 0 to 0.4 sampling rate.

Measurements of the waveform components corresponding in frequency with the input signals, their harmonics, and their intermodulation products were made using the techniques outlined in E 7.2. The accuracy of measurement of relative component magnitudes was approximately $\pm 2\%$ for signals well isolated in frequency from other waveform components.

Since the differences between measured signal amplitudes and those predicted by appendix A 3.2 matched to within the experimental tolerances outlined above it can be concluded that the model predicts the low frequency components of waves formed by regular sampling. Because the synthesis which yields the low frequency component simultaneously yields the high frequency component and any error in one will cause an error in the other, it may be inferred from the experimental measurements that the high frequency components are correct also.

E 7.0 Some Measurement Techniques

The measurement of switching wave components by direct methods such as tuned filters is not suited to highly accurate results. By resorting to zero beat techniques higher precision can be attained. By using zero beat techniques in conjunction with balanced bridges high resolution can be achieved.

E 7.1 Measurement of Amplifier Gain

For the measurement of amplifier gain negative gain variants of the amplifier are used. Input and output may then be summed by resistive networks to give a null component at the frequency of the input. The proportions of the resistive divider then define the amplifier gain. By adopting suitable techniques the null can be detected with good accuracy even in the presence of switching wave components with frequencies near those of the signal of interest.

E 7.2 Measurement of Filter Phase and Gain Response

The procedure adopted is identical to that above except that the summing network included a capacitor in parallel or series with either input or output resistor branch so that cancellation of the phase component can occur. The response is then the ratio of the two branch impedances.

EIO

Facilities and Equipment Mentioned in Text
Laboratory Equipment.

CRO: Tektronix Type 317.

Function Generators: (i) Beckman 9010
 (ii) Feedback TWG500
 (iii) Feedback TWG501
 (iv) BWD Model 112

X/Y Recorder: H/P 7035 B

Signal Analysers: (i) Muirhead - Pametrada
 Type D-489-EM
 (ii) General Radio -
 Type 736-A

d.c. Power Supplies: H/P 60123A, 12V, 1A

Other Facilities

Analogue Computer: EAI TR10, TR20
with locally added analogue
multipliers

Digital Computer: Elliot 503
with Algol Compiler, 8K
mainstore, 16K backstore.

Appendix R.

References

- R1 Books
 - 1.1 Mathematics
 - 1.2 General references
 - 1.3 Thesis
- R2 Periodicals in Publication Order
- R3 Alphabetic Author Cross-Reference

R1.1 Mathematics

- 1.1.1 Introduction to Mathematical Statistics
 Paul G. Hoel
- 1.1.2 Handbook of Series for Scientists and Engineers
 Mangulis
- 1.1.3 Tables of Transcendental Functions
 Flügge
- 1.1.4 A Short Table of Integrals
 Pierce and Foster
- 1.1.5 Numerical Methods for Scientists and Engineers
 Hamming
- 1.1.6 Tables of Integrals and other Mathematical Data
 Dwight
- 1.1.7 Bessel Functions for Engineers
 McLachlan

R 1.2 General References

1.2.1

H. S. Black "Modulation Theory"

N.J.: Van Nostrand 1953 PP 263-281

1.2.2

J. Millman, H. Taub "Pulse Digital, and Switching Waveforms"

McGraw-Hill N.Y. 1965

1.2.3

F. F. Kuo "Network Analysis and Synthesis"

Wiley & Sons, Inc. N.Y. 1965

1.2.4

S. M. Shinnars "Control Systems Design"

Wiley & Sons, Inc. N.Y. 1964

R 1.3 Thesis

1.3.1

S. G. Furmage "Subharmonic Instability in Closed Loop Control Systems with Pulse Width Modulation"

Honours Thesis in Electrical Engineering, Uni. Tas.

March 1969

R 2 Periodical References Publication Order

2.1

Bennet "New Results in the Calculation of Modulation Products"

Bell System Tech. Journal Vol. 12

April 1933

PP 228-243

2.2

E. Fitch "The Spectrum of Modulated Pulses"

J. IEE Vol. 94 PT 3A

1947

PP 556-564

2.3

E.R. Kretzmer "Distortion in Pulse Duration Modulation"
Proc. IRE Vol. 35 November 1947 PP 1230-1235

2.4

E.F.W. Alexanderson "Control Applications of the Transistor"
Proc. IRE Vol. 40 November 1952 PP 1508-1511

2.5

A.G. Milnes "Transistor Power Amplifiers with Switched
mode of Operation"
Trans. AIEE Vol. 75 Pt.1. 1956 PP 368-372

2.6

G.T. Flesher "Transistor Pulse Width Control Amplifier
with Reactive Load"
Proc. NEC Vol. 14 1953 PP 454-463

2.7

Andeen "Analysis of Pulse Duration Sampled Data Systems
with Linear Elements"
IRE Trans on Aut. Control September 1960

2.8

R.A. Schaefer "A New Pulse Modulator for Accurate d.c.
Amplification....."
IRE Trans on Instrumentation
September 1962 PP 34-47

2.9

D.R. Brit "Modulated Pulse Audio Frequency Amplifiers"
Wireless World Vol. 69 No. 2.
February 1963 PP 76-83

2.10

K.C. Johnson "Pulse Modulated Audio Frequency Amplifiers"
Wireless World Vol. 69 No. 3.
March 1963 PP 135-136

2.11

C.H. Miller "High Efficiency Amplification Using
Width Modulated Pulses"

Proc.IREE (Australia) Vol.May 1964 PP 314-323

2.12

A.G. Bose "A Two State Modulation System"

Electrotechnology Vol. 74 No. 2

August 1964 PP 42-47

2.13

G.F. Turnbull, J.M. Townsend "A Feedback Pulse Width
Modulated Audio Amp."

Wireless World Vol. 71 No. 4

April 1965 PP 160-168

2.14

E.C. Bell, T. Sergeant "Distortion and Power Output of
P.D. Modulated Amp."

Electronic Engineering Vol. 37

August 1965 PP 540-542

2.15

J. Das, P.D. Sharma "Rectangular Wave Modulation -
A P.L.M.-FM System"

Electronic Letters Vol. 2 No. 1

January 1966 PP 7-9

2.16

F.G. Turnbull "Carrier Frequency Gating Circuit"

IEEE Trans Mag. 2 No. 1 March 1966 PP 14-17

2.17

B. Mokrytzki "Pulse Width Modulated Inverters for
a.c. Motor Drives"

IEEE Internat. Con. Rec. IGA-8

March 1966 PP 8-23

2.18

S.P. Jackson, H.R. Weed "The Differential Saturable Transformer as the Basic Component of a Controlled High-Efficiency Power Supply"

IEEE Internat. Con. Rec. IGA-2 No. 5

September/October 1966

PP 378-383

2.19

E.S. McVey, R.E. Russel "The Design of a Simple Single Phase SCR Regulator"

IEEE Internat. Con. Rec. IGA-8

March 1966

PP 68-73

2.20

C.J. Amato "An Equivalent Circuit for a Cycloconverter"

IEEE Trans IGA-2 No. 5 September 1966

PP 358-362

2.21

H.R. Camenzind "Modulated Pulse Audio Power Amplifiers for I.C.S."

IEEE Trans Vol. AU-14 No. 3

September 1966

PP 136-140

2.22

P. Ramirez "The Design of Modular High Frequency Converters"

Proc. NEC Vol. 22

1966

PP 1035-1040

2.23

F. Fallside, A.R. Farmer "Ripple Instability in Closed Loop Control Systems."

Proc. IEE Vol. 114

March 1967

PP 139-152

2.24

G.F. Turnbull, J.M. Townsend "Efficiency Considerations in a Class D Amp."

Wireless World Vol. 73 No. 4,5

April, May 1967

P 154, P 214

2.25

Yuan Yu, T.G. Wilson, Et Al "Static d.c. to Sinusoid
a.c. Inverter"

IEEE Trans Mag-3 No. 3 September 1967 PP 250-256

2.26

J.E. Murray "Analogue Simulation Simplifies Static
Power Inverter Design"

Electrotechnology Vol. 80 No. 6

December 1967

PP 36-41

2.27

F. Fallside "Ripple Instability in Closed-loop Pulse
Modulation Systems including Inverter Drives"

Proc. IEEE. Vol. 115 1968

P 218

2.28

P.F. Pitman, R.J. Ravas, R.W. Briggs "Staggered Phase
Technique"

Electrotechnology Vol. 83 No. 6

June 1968

PP 55-58

2.29

J.N. Strettor-Downes "Thyristors in Motor Control"

Electrical Review 19 July 1968

P 87

2.30

G.W. Graham "Chopper Circuits for Traction Vehicles"

English Electric Journal Vol. 23 No. 4

August 1968

PP 32-36

2.31

L. Malesini "Improved Delay Circuit for Thyristor
Linear Power Control"

Electronic Engineering January 1969

PP 84-89

2.32

R.A. Stevens "Three Phase Point-on-a-Cycle Switch"

Electronic Engineering Vol. 41 No. 491

January 1969

PP 82-84

2.33

T.H. Barton, R.S. Birch "A 5kw Low Frequency Power
Amplifier"

IEEE Internat. Con. Rec. PT 9-12 No. 10 PP 146-153

2.34

S.B. Dewan Et Al "Harmonic Analysis of a.c.-a.c.
Frequency Converter"

IEEE Trans IGA-5 No. 1 February 1969

PP 29-33

2.35

I.D. Landau "Practical Converter Systems for Squirrel
Cage Motors"

IEEE Trans IGA-5 No. 1 February 1969

PP 53-59

2.36

K. Heumann "Development of Inverters with Forced
Commutation for Motor Speed Control up to the
Megawatt Range"

IEEE Trans IGA-5 No. 1 February 1969

PP 61-67

2.37

W.J. Chudobiak, D.F. Page "Frequency and Power
Limitations of Class D"

IEEE Trans Vol. SC-4 No. 1

February 1969

PP 25-37

2.38

R.H. Masterman "Cycle Converter Amplifier"

Electronics Letters Vol. 5 No. 14

July 1969

PP 306-308

2.39

E.S. McVey, P.F. Chen "Improvements of Position and
Velocity Detecting Accuracy by Signal Perturbation"

IEEE Trans Vol. IECI-16 July 1969 PP 94-98

2.40

C.J. Amato "Latent Losses in 'Electric Lissies"

IEEE Trans IGA-5 No. 5 September 1969 PP 558-565

2.41

F.J. Evans "A Linear Thyristor Power Stage with Self
Limiting Firing Circuits"

IEEE Trans Vol. IECI-17 No. 1

February 1970

PP 25-33

2.42

P.F. Chen "Optimal Signal Perturbation Waveform for
Sensing Arrays"

IEEE Trans Vol. IM-19 May 1970 PP 135-139

2.43

S.B. Dewan, M.D. Kankam "A Method for Harmonic
Analysis of Cycloconverters"

IEEE Trans IGA-6 No. 5 September 1970 PP 455-462

2.44

S.B. Dewan, R.S. Segsworth, P.P. Biringer "Input
Filter Design with Static Power Converters"

IEEE Trans IGA-6 No. 4 July 1970 PP 378-383

2.45

R.E. Bedford, V.D. Nene "Analysis and Performance of
a Three Phase Ring Inverter"

IEEE Trans IGA-6 No. 5 September 1970 PP 488-496

2.46

N. Vutz "PWM Inverter Induction Motor Transit Car Drives"

IEEE Trans IA-8 No. 1 January/February 1972

2.47

E.A. Parrish, J.W. Stoughton "Achieving Improved Position Detection Using a Modified Triangular Perturbation Signal"

IEEE Trans IM-21 No. 1 February 1972

2.48

J.J. Pollack "Advanced Pulse Width Modulator Inverter Techniques"

IEEE Trans IA-8 No. 2 March/April 1972 PP 145-154

2.49

K. Tachibana Et Al "Harmonic Currents in Catenary Systems from Chopper Control"

IEEE Trans IA-8 No. 2 March/April 1972

R 3 Alphabetic Cross-reference.

Author Name		Publication Details
Alexanderson	E.F.W.	2.4
Amato	C.J.	2.20, 2.40
Andeen	R.E.	2.7
Babaa	I.M.H.	2.25
Barton	T.H.	2.33
Bedford	R.E.	2.45
Bell	E.C.	2.14
Bendzsak	G.J.	2.34
Bennet		2.1
Birch	R.S.	2.33
Biringer	P.P.	2.34, 2.44
Black	H.S.	1.2.1
Bose	A.G.	2.12
Briggs	R.W.	2.28
Brit	D.R.	2.9
Camenzind	H.R.	2.21
Chen	P.F.	2.39, 2.42
Chudobiak	W.J.	2.37
Das	J.	2.15
Dewan	S.B.	2.34, 2.43, 2.44
Dwight		1.1.6
Evans	F.J.	2.41
Fallside	F.	2.23, 2.27
Farmer	A.R.	2.23
Feng	S.Y.M.	2.25
Fitch	E.	2.2
Flesher	G.T.	2.6
Flugge		1.1.3
Foster		1.1.4
Furmage	S.G.	1.3.1
Graham	G.W.	2.3
Hamming		1.1.5
Heuman	K.	2.36
Hoel	P.G.	1.1.1
Jackson	S.P.	2.18
Johnson	K.C.	2.10
Kankam	M.D.	2.43
Kariya	S	2.49
Kretzmer	E.R.	2.3
Kuo	F.F.	1.2.3
Landau	I.D.	2.35

Malesini	L.	2.31
Mangulis		1.1.2
Masterman	R.H.	2.38
McLachlan		1.1.7
McVey	E.S.	2.19, 2.39
Miller	C.H.	2.11
Millman	J.	1.2.2
Milnes		2.5
Mokrytzki	B.	2.17
Moore	E.	2.25
Murray	J.E.	2.26
Nene	V.D.	2.45
Page	D.F.	2.37
Parrish	E.A.	2.47
Pierce		1.1.4
Pitman	P.F.	2.28
Pollack	J.J.	2.48
Ramirez	P.	2.22
Ravas	R.J.	2.28
Russel	R.E.	2.19
Schaefer	R.A.	2.8
Segsworth	R.S.	2.44
Sergent	T.	2.14
Sharma	P.D.	2.15
Shinners		1.2.4
Stevens	R.A.	2.32
Stoughton	J.W.	2.47
Strettor-Downes	J.N.	2.29
Tachibana	K.	2.49
Taub	H.	1.2.2
Townsend	J.M.	2.13, 2.24
Turnbull	F.G.	2.16
Turnbull	G.F.	2.13, 2.24
Tsuboi	T.	2.49
Vutz	N.	2.46
Weed	H.R.	2.18
Wilson	T.G.	2.25
Yu	Yuan	2.25